RADIOLOGY AND ONCOLOGY

vol.48 no.2
june 2014

Halaven®
eribulin

NOVA SMER DO PODALJŠANJA CELOKUPNEGA PREŽIVETJA

Eisai

Prva in edina samostojna kemoterapija,
ki v primerjavi z ostalimi možnostmi zdravljenja
z enim zdravilom, pri bolnicah s predhodno že
večkratno zdravljenim metastatskim rakom dojke,
dokazano značilno podaljša celokupno preživetje.[1,2]

- **Halaven** (eribulin): ne-taksanski zaviralec dinamike mikrotubulov, prvo zdravilo iz nove skupine kemoterapevtikov, imenovanih *halihondrini*.
- Monoterapija z zdravilom HALAVEN je indicirana za zdravljenje bolnic z lokalno napredovalim ali metastatskim rakom dojke, ki je napredoval po vsaj dveh režimih kemoterapije za napredovalo bolezen. Predhodna zdravljenja morajo vključevati antraciklin in taksan, razen če to zdravljenje za bolnice ni bilo primerno.[1]
- Priporočeni odmerek 1,23 mg/m^2, intravensko, v obliki 2- do 5-minutne infuzije, 1. in 8. dan vsakega 21-dnevnega cikla.
- Ena 2 ml viala vsebuje 0,88 mg eribulina.
- Raztopina, pripravljena za uporabo, redčenje ni potrebno.

SKRAJŠAN POVZETEK GLAVNIH ZNAČILNOSTI ZDRAVILA

HALAVEN 0,44 mg/ml raztopina za injiciranje (eribulin)
TERAPEVTSKE INDIKACIJE: Zdravljenje lokalno napredovalega ali metastatskega raka dojke, ki je napredoval po vsaj dveh režimih kemoterapije za napredovalo bolezen vključno z antraciklinom in taksanom, razen če to ni bilo primerno. **ODMERJANJE IN NAČIN UPORABE:** Halaven se daje v enotah, specializiranih za dajanje citotoksične kemoterapije, in le pod nadzorom usposobljenega zdravnika z izkušnjami v uporabi citotoksičnih zdravil. **ODMERJANJE:** Priporočeni odmerek eribulina v obliki raztopine je 1,23 mg/m^2 i. v. obliki 2- do 5- minutne infuzije 1. in 8. dan vsakega 21-dnevnega cikla. Bolnikom je lahko slabo ali bruhajo. Treba je razmisliti o antiemetični profilaksi, vključno s kortikosteroidi. **Preložitev odmerka med zdravljenjem:** Dajanje Halavena je treba preložiti, če se pojavi kaj od naslednjega: absolutno število nevtrofilcev (ANC) < 1 x 10^9/l, trombociti < 75 x 10^9/l ali nehematološki neželeni učinki 3. ali 4. stopnje. **Zmanjšanje odmerka med zdravljenjem:** Za priporočila za zmanjšanje odmerka ob pojavu hematoloških ali nehematoloških neželenih učinkov glejte celoten povzetek glavnih značilnosti zdravila. **Okvara jeter zaradi zasevkov:** Priporočeni odmerek pri blagi okvari jeter (stopnje A po Child-Pughu) je 0,97 mg/m^2 v obliki 2- do 5- minutne i. v. infuzije 1. in 8. dan 21-dnevnega cikla. Priporočeni odmerek pri zmerni okvari jeter (stopnje B po Child-Pughu) je 0,62 mg/m^2 v obliki 2- do 5- minutne i. v. infuzije 1. in 8. dan 21-dnevnega cikla. Pri hudi okvari jeter (stopnje C) se pričakuje, da je treba dati še manjši odmerek eribulina. **Okvara jeter zaradi ciroze:** Zgornje odmerke se lahko uporabi za blago do zmerno okvaro, vendar se priporoča skrbno nadziranje, saj bo odmerke morda treba ponovno prilagoditi. **Okvara ledvic:** Pri hudi okvari ledvic (očistek kreatinina <40 ml/min) bo morda treba odmerek zmanjšati. Priporoča se skrbno nadziranje varnosti. **NAČIN UPORABE:** Odmerek se lahko razredči z do 100 ml 0,9 % natrijevega klorida (9 mg/ml) za injiciranje. Ne sme se ga redčiti v 5 % infuzijski raztopini glukoze. Pred dajanjem glejte navodila glede redčenja zdravila v celotnem povzetku glavnih značilnosti zdravila ter se prepričajte, da obstaja dober periferni venski dostop ali prehodna centralna linija. Ni znakov, da bi eribulin povzročal mehurje ali dražil. V primeru ekstravazacije mora biti zdravljenje simptomatsko. **KONTRAINDIKACIJE:** Preobčutljivost na zdravilno učinkovino ali katerokoli pomožno snov. Dojenje. **POSEBNA OPOZORILA IN PREVIDNOSTNI UKREPI:** Mielosupresija je odvisna od odmerka in se kaže kot nevtropenija. Pred vsakim odmerkom eribulina je treba opraviti pregled celotne krvne slike. Zdravljenje z eribulinom se lahko uvede le pri bolnikih z vrednostmi ANC ≥ 1,5 x 10^9/l in s trombociti > 100 x 10^9/l. Bolnike, pri katerih se pojavijo febrilna nevtropenija, huda nevtropenija ali trombocitopenija, je treba zdraviti v skladu s priporočili v celotnem povzetku glavnih značilnosti zdravila. Hudo nevtropenijo se lahko zdravi z uporabo G-CSF ali enakovrednim zdravilom v skladu s smernicami. Bolnike je treba skrbno nadzirati za znake periferne motorične in senzorične nevropatije. Pri razvoju hude periferne nevrotoksičnosti je treba odmerek prestaviti ali zmanjšati. Če začnemo zdravljenje pri bolnikih s kongestivnim srčnim popuščanjem, z bradiaritmijami, z zdravili, za katera je znano, da podaljšujejo interval QT, vključno z antiaritmiki razreda Ia in III, in z elektrolitskimi motnjami, je priporočljivo spremljanje EKG. Pred začetkom zdravljenja s Halavenom je treba popraviti hipokaliemijo in hipomagneziemijo in te elektrolite je treba občasno kontrolirati med zdravljenjem. Halavena ne smemo dajati bolnikom s prirojenim sindromom dolgega intervala QT. To zdravilo vsebuje majhne količine etanola (alkohola), manj kot 100 mg na odmerek. Eribulin je pri podganah embriotoksičen, fetotoksičen in teratogen. Halavena se ne sme uporabljati med nosečnostjo, razen kadar je to nujno potrebno. Ženske v rodni dobi naj ne zanosijo v času, ko same ali njihov moški partner dobivajo Halaven, in naj med zdravljenjem in še do 3 mesece po njem uporabljajo učinkovito kontracepcijo. Moški naj se pred zdravljenjem posvetujejo o shranjevanju sperme zaradi možnosti nepopravljive neplodnosti. **INTERAKCIJE:** Eribulin se izloča do 70 % prek žolča. Sočasna uporaba učinkovin, ki zavirajo jetrne transportne beljakovine, kot so beljakovine za prenos organskih anionov, P-glikoprotein, beljakovine, odporne na številna zdravila, z eribulinom se ne priporoča (npr. ciklosporin, ritonavir, sakvinavir, lopinavir in nekateri drugi zaviralci proteaze, efavirenz, emtricitabin, verapamil, klaritromicin, kinin, kinidin, dizopiramid itd). Sočasno zdravljenje z indukcijskimi učinkovinami, kot so rifampicin, karbamazepin, fenitoin, šentjanževka lahko povzroči znižanje koncentracij eribulina v plazmi, zato je ob sočasni uporabi induktorjev potrebna previdnost. Eribulin lahko zavira encim CYP3A4. Pri sočasni uporabi z učinkovinami, ki jih v glavnem presnavlja encim CYP3A4, se priporoča skrbno spremljanje zaradi povečanih koncentracij sočasno uporabljene učinkovine v plazmi. Če ima učinkovina ozek terapevtski razpon, je ne uporabljajte sočasno. **NEŽELENI UČINKI:** *Zelo pogosti (≥1/10):* nevtropenija (54,5 %), (3./4. stopnje: 48,3 %), levkopenija (22,1 %), (3./4. stopnje: 14 %), anemija (20,3 %), (3./4. stopnje: 1,4 %), zmanjšan apetit, periferna nevropatija (32,0 %), (3./4. stopnje: 6,9 %), glavobol, slabost (35,1 %), (3./4. stopnje: 1,1 %), zaprtost, driska, bruhanje, alopecija, artralgija in mialgija, utrujenost/astenija (52,8 %), (3./4. stopnje: 8,4 %), pireksija. *Pogosti (≥1/100 do <1/10):* okužba sečil, ustna kandidiaza, okužba zgornjih dihal, nazofaringitis, rinitis, febrilna nevtropenija (4,7 %), (3./4. stopnje: 4,6 %), trombocitopenija, limfopenija, hipokaliemija, hipomagneziemija, dehidracija, hiperglikemija, hipofosfatemija, nespečnost, depresija, disgevzija, omotičnost, hipoestezija, letargija, nevrotoksičnost, obilnejše solzenje, konjunktivitis, vrtoglavica, tahikardija, vročinski valovi, dispnea, kašelj, orofaringealna bolečina, epistaksa, rinoreja, bolečina v trebuhu, stomatitis, suha usta, dispepsija, gastroezofagealna refluksna bolezen, razjede v ustih, napihnjenost želodca, zvišanje alanin aminotransferaze (3,0 %), (3./4. stopnje: 1,1 %) in aspartat aminotransferaze, izpuščaj, pruritus, bolezni nohtov, nočno potenje, palmarno-plantarna eritrodisestezija, suha koža, eritem, hiperhidroza, bolečina v okončinah, mišični spazmi, mišično-skeletna bolečina in mišično-skeletna bolečina v prsih, mišična oslabelost, bolečina v kosteh, bolečina v hrbtu, vnetje sluznice (9,8 %), (3./4. stopnje: 1,3 %), periferni edem, bolečina, mrzlica, gripi podobna bolezen, bolečina v prsih, zmanjšanje telesne mase. *Občasni (≥1/1.000 do <1/100):* pljučnica, nevtropenična sepsa, ustni herpes, herpes zoster, tinitus, globoka venska tromboza, pljučna embolija, intersticijska pljučna bolezen, hiperbilirubinemija, angioedem, disurija, hematurija, proteinurija, odpoved ledvic. *Redki (≥1/10.000 do <1/1.000):* pankreatitis. Za popoln opis neželenih učinkov glejte celoten povzetek glavnih značilnosti zdravila. **Vrsta ovojnine in vsebina:** viala z 2 ml raztopine. **Režim izdaje:** H. **Imetnik dovoljenja za promet:** Eisai Europe Ltd, Mosquito Way, Hatfield, Hertfordshire, AL10 9SN, Velika Britanija. HAL-161112

Pred predpisovanjem in uporabo zdravila prosimo preberite celoten povzetek glavnih značilnosti zdravila!

Viri: (1) Povzetek glavnih značilnosti zdravila Halaven, november 2012; (2) Cortes J *et al. Lancet* 2011; 377: 914–23

PharmaSwiss
Choose More Life

Odgovoren za trženje v Sloveniji:
PharmaSwiss d.o.o., Dolenjska cesta 242c, 1000 Ljubljana
telefon: +386 1 236 47 00, faks: +386 1 283 38 10

HAL 0113-01, januar 2013

RADIOLOGY AND ONCOLOGY

June 2014
Vol. 48 No. 2
Pages 99-218
ISSN 1318-2099
UDC 616-006
CODEN: RONCEM

Publisher
Association of Radiology and Oncology

Affiliated with
Slovenian Medical Association – Slovenian Association of Radiology, Nuclear Medicine Society,
Slovenian Society for Radiotherapy and Oncology, and Slovenian Cancer Society
Croatian Medical Association – Croatian Society of Radiology
Societas Radiologorum Hungarorum
Friuli-Venezia Giulia regional groups of S.I.R.M.
Italian Society of Medical Radiology

Aims and scope
Radiology and Oncology is a journal devoted to publication of original contributions in diagnostic and interventional radiology, computerized tomography, ultrasound, magnetic resonance, nuclear medicine, radiotherapy, clinical and experimental oncology, radiobiology, radiophysics and radiation protection.

Editorial office

Radiology and Oncology
Zaloška cesta 2
P. O. Box 2217
SI-1000 Ljubljana
Slovenia
Phone: +386 1 5879 369
Phone/Fax: +386 1 5879 434
E-mail: gsersa@onko-i.si

Reader for English

Vida Kološa

Secretary

Mira Klemenčič

Zvezdana Vukmirović

Design

Monika Fink-Serša, Samo Rovan, Ivana Ljubanović

Layout

Matjaž Lužar

Printed by

Tiskarna Ozimek, Slovenia

Published quarterly in 400 copies

Beneficiary name: DRUŠTVO RADIOLOGIJE IN ONKOLOGIJE
Zaloška cesta 2
1000 Ljubljana
Slovenia

Beneficiary bank account number: SI56 02010-0090006751
IBAN: SI56 0201 0009 0006 751
Our bank name: Nova Ljubljanska banka, d.d.,
Ljubljana, Trg republike 2,
1520 Ljubljana; Slovenia

SWIFT: LJBASI2X

Subscription fee for institutions EUR 100, individuals EUR 50

The publication of this journal is subsidized by the Slovenian Research Agency.

Indexed and abstracted by:
Science Citation Index Expanded (SciSearch®)
Journal Citation Reports/Science Edition
Scopus
PubMed
PubMed Central
EMBASE/Excerpta Medica
DOAJ
Open J-gate
Chemical Abstracts
Biomedicina Slovenica
Summon by Serial Solutions (ProQuest)

This journal is printed on acid- free paper

On the web: ISSN 1581-3207
http://www.degruyter.com/view/j/raon
http://www.radioloncol.com

contents

clinical oncology

Radiology and Oncology is covered in Science Citation Index Expanded (SciSearch®),Journal Citation Reports/Science Edition, Scopus, PubMed, PubMed Central, DOAJ, EMBASE/Excerpta Medica, Open J-gate, Chemical Abstracts, Biomedicina Slovenica, Summon by Serial Solutions (ProQuest)

review

Prevalence and malignancy risk of focal colorectal incidental uptake detected by ^{18}F-FDG-PET or PET/CT: a meta-analysis

Giorgio Treglia[1], Silvia Taralli[2], Marco Salsano[3], Barbara Muoio[4], Ramin Sadeghi[5], Luca Giovanella[1]

[1] Department of Nuclear Medicine and PET/CT Center, Oncology Institute of Southern Switzerland, Bellinzona, Switzerland
[2] Institute of Nuclear Medicine, Catholic University of the Sacred Heart, Rome, Italy
[3] Institute of Radiology, Catholic University of the Sacred Heart, Rome, Italy
[4] School of Medicine, Catholic University of the Sacred Heart, Rome, Italy
[5] Nuclear Medicine Research Center, Mashhad University of Medical Sciences, Mashhad, Iran

Radiol Oncol 2014; 48(2): 99-104.

Received 18 December 2012
Accepted 1 May 2013

Correspondence to: Giorgio Treglia, M.D., Department of Nuclear Medicine and PET/CT Center, Oncology Institute of Southern Switzerland, Via Ospedale 12, CH-6500 Bellinzona, Switzerland. Telephone: +41918118919; Fax: +41918118250; E-mail: giorgiomednuc@libero.it

Disclosure: No potential conflicts of interest were disclosed.

Background. The aim of the study was to meta-analyze published data about prevalence and malignancy risk of focal colorectal incidentalomas (FCIs) detected by Fluorine-18-Fluorodeoxyglucose positron emission tomography or positron emission tomography/computed tomography (^{18}F-FDG-PET or PET/CT).

Methods. A comprehensive computer literature search of studies published through July 31st 2012 regarding FCIs detected by ^{18}F-FDG-PET or PET/CT was performed. Pooled prevalence of patients with FCIs and risk of malignant or premalignant FCIs after colonoscopy or histopathology verification were calculated. Furthermore, separate calculations for geographic areas were performed. Finally, average standardized uptake values (SUV) in malignant, premalignant and benign FCIs were reported.

Results. Thirty-two studies comprising 89,061 patients evaluated by ^{18}F-FDG-PET or PET/CT were included. The pooled prevalence of FCIs detected by ^{18}F-FDG-PET or PET/CT was 3.6% (95% confidence interval [95% CI]: 2.6-4.7%). Overall, 1,044 FCIs detected by ^{18}F-FDG-PET or PET/CT underwent colonoscopy or histopathology evaluation. Pooled risk of malignant or premalignant lesions was 68% (95% CI: 60-75%). Risk of malignant and premalignant FCIs in Asia-Oceania was lower compared to that of Europe and America. A significant overlap in average SUV was found between malignant, premalignant and benign FCIs.

Conclusions. FCIs are observed in a not negligible number of patients who undergo ^{18}F-FDG-PET or PET/CT studies with a high risk of malignant or premalignant lesions. SUV is not reliable as a tool to differentiate between malignant, premalignant and benign FCIs. Further investigation is warranted whenever FCIs are detected by ^{18}F-FDG-PET or PET/CT.

Key words: PET/CT; fluorodeoxyglucose; colonic uptake; incidentaloma; focal uptake; colorectal cancer

Introduction

Colorectal incidentalomas (CIs) are defined as unexpected colorectal findings that are discovered on an imaging study unrelated to the large bowel. CIs represent a challenge for the clinicians: some of these findings are benign but the risk of malignancy in CIs might be significant.[1]

As Fluorine-18-Fluorodeoxyglucose positron emission tomography or positron emission tomography/computed tomography (^{18}F-FDG-PET or PET/CT) are increasingly used, especially for oncologic patients, incidental uptake detected by these functional imaging methods are also increasing. ^{18}F-FDG-PET or PET/CT may sometimes reveal an unexpected area of increased radiopharmaceutical

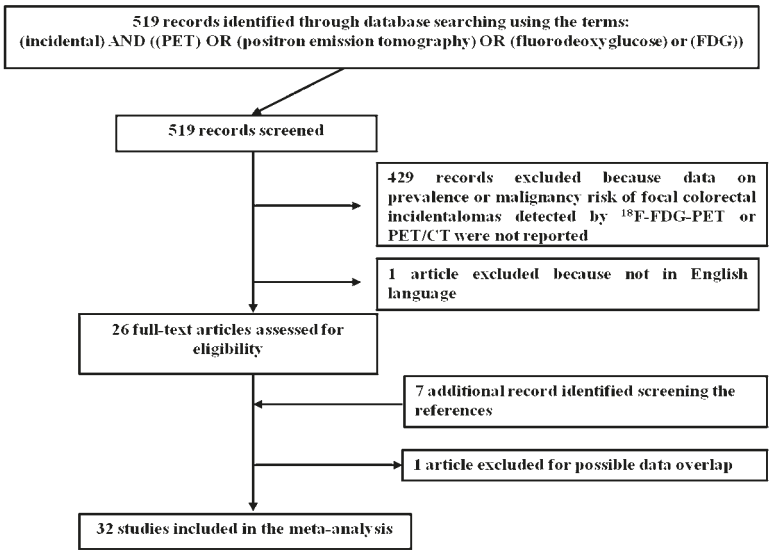

FIGURE 1. Flow chart of the search for eligible studies on the prevalence or malignancy risk of focal colorectal incidental uptake detected by ^{18}F-FDG-PET or PET/CT.

uptake within the large bowel in patients referred for other diseases and this finding is defined as CI.[1,2]

Both focal, segmental and diffuse unexpected ^{18}F-FDG uptake in the large bowel were reported. Segmental and diffuse increased uptake of ^{18}F-FDG in the large bowel are considered at low risk of malignancy, being more likely associated with inflammation, physiological uptake or radiopharmaceutical excretion. Conversely, unexpected focal ^{18}F-FDG uptake in the large bowel is of greater concern since it may represent both benign, premalignant (*i.e.* colonic adenomas) or malignant lesions (*i.e.* primary colorectal cancer or metastatic lesions).[1,2]

Several articles have reported data about the prevalence and the malignancy risk of focal colorectal incidental uptake (FCIs) detected by ^{18}F-FDG-PET or PET/CT with discordant results. A systematic review about this topic and a meta-analysis providing pooled estimates of prevalence and malignancy risk of FCIs detected by ^{18}F-FDG-PET or PET/CT are still lacking. Therefore, the objective of our article is to meta-analyze published data about prevalence and malignancy risk of FCIs detected by ^{18}F-FDG-PET or PET/CT, in order to derive more robust estimates in this regard.

Methods

Search strategy

A comprehensive computer literature search of the PubMed/MEDLINE and Scopus databases was conducted to find relevant published articles on the prevalence and malignancy risk of FCIs detected by ^{18}F-FDG-PET or PET/CT. We used a search algorithm that was based on a combination of the terms: "incidental" AND "PET" OR "positron emission tomography" OR "fluorodeoxyglucose" OR "FDG". No beginning date limit was used; the search was updated until July 31st, 2012. Only articles in English language were selected. To expand our search, references of the retrieved articles were also screened for additional studies.

Study selection

Original articles investigating both the prevalence and the malignancy risk of FCIs detected by ^{18}F-FDG-PET or PET/CT were eligible for inclusion. The exclusion criteria were: a) articles not providing information about prevalence or malignancy risk of FCIs detected by ^{18}F-FDG-PET or PET/CT; b) articles not in English language; c) overlap in patient data (in this case the most complete article was included). Three researchers independently reviewed the titles and abstracts of the retrieved articles, applying the inclusion and exclusion criteria mentioned above. Articles were rejected if they were clearly ineligible. The same three researchers then independently reviewed the full-text version of the remaining articles to determine their eligibility for inclusion.

Data extraction

For each included study, information was collected concerning basic study data (authors, year of publication, country), instrumentation used (PET or PET/CT), number of patients evaluated with PET or PET/CT, number of FCIs detected by PET or PET/CT, number of FCIs verified by colonoscopy or histology, final diagnosis of FCIs, average standardized uptake values (SUV) in malignant, premalignant and benign FCIs.

Statistical analysis

The prevalence of patients with FCIs who underwent PET or PET/CT was obtained from individual studies using this formula: prevalence of FCIs = number of patients with FCIs / number of patients evaluated with PET or PET/CT x100.

The risk of malignant or premalignant FCIs detected by PET or PET/CT was obtained from individual studies using this formula: risk of malignant or premalignant FCIs = number of malignant or

premalignant lesions found between FCIs / number of FCIs revealed by PET or PET/CT and verified by colonoscopy or histology x100.

Patients with a history of colorectal cancer were excluded from the analysis.

A random-effects model was used for statistical pooling of the data; pooled data were presented with 95% confidence intervals (95% CI) and displayed using forest plots. A I-square statistic was also performed to test for heterogeneity between studies. A sub-analysis of the risk of malignant and premalignant FCIs taking into account different geographic areas was carried out. Statistical analyses were performed using StatsDirect statistical software version 2.7.9 (StatsDirect Limited, UK).

Results

The comprehensive computer literature search from PubMed/MEDLINE and Scopus databases revealed 519 articles. Reviewing titles and abstracts, 492 articles were excluded because they did not report any data on prevalence neither on malignancy risk of FCIs detected by ^{18}F-FDG-PET or PET/CT. One article was excluded because not in English language.[3]

Twenty-six articles were selected and retrieved in full-text version; seven additional studies were found screening the references of these articles. Out of these 33 articles potentially eligible for inclusion, after reviewing the full-text article, one article was excluded due to possible data overlap.[4] Finally, 32 studies including 89,061 patients met all inclusion and exclusion criteria, and they were included in our meta-analysis (Figure 1) [2,5-35]; 18 studies had data to calculate the pooled prevalence of FCIs and 31 studies had data to calculate the pooled risk of malignant of premalignant FCIs. The characteristics of the included studies are presented in Table 1.

Overall, the pooled prevalence of FCIs detected by ^{18}F-FDG-PET or PET/CT in the included studies was 3.6% (95% CI: 2.6-4.7%), ranging from 0.4% to 16.3% (Figure 2). Overall, 1,044 FCIs detected by ^{18}F-FDG-PET or PET/CT underwent colonoscopy or histology verification. Pooled risk of malignant or premalignant lesions between FCIs was 68% (95% CI: 60-75%), ranging from 16% to 100% in the included studies (Figure 3). The included studies were statistically heterogeneous (I-square: > 75%) both for prevalence and risk of malignant or premalignant FCIs.

Concerning geographic distribution, the pooled risk of malignant or premalignant lesions in FCIs

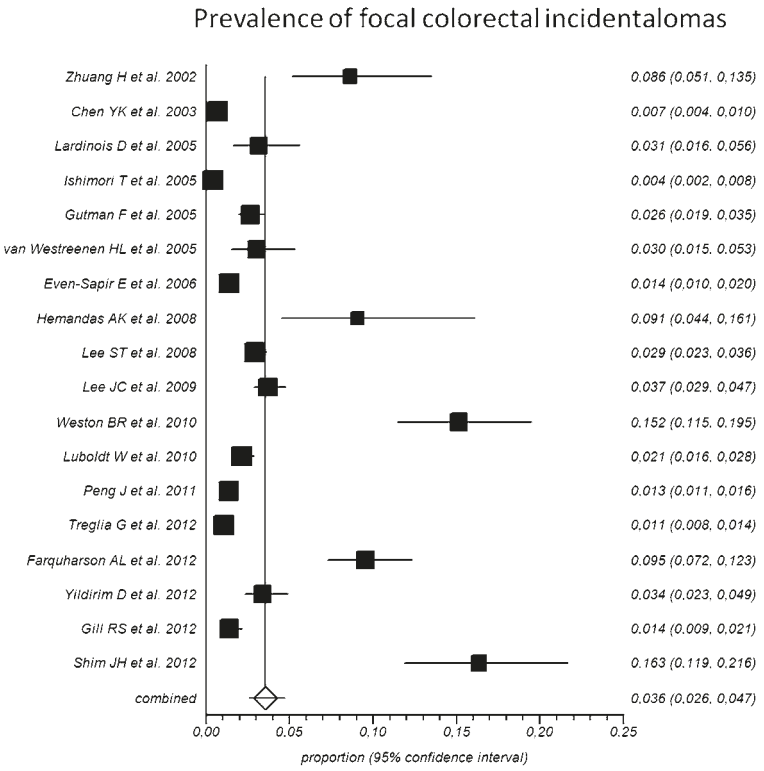

FIGURE 2. Plot of individual studies and pooled prevalence of patients with focal colorectal incidental uptake detected by ^{18}F-FDG-PET or PET/CT, including 95% confidence intervals (95%CI). Prevalence of patients with focal colorectal incidental uptake ranged from 0.4% to 16.3%, with pooled estimate of 3.6% (95%CI: 2.6-4.7%). The included studies were statistically heterogeneous (I-square: > 75%).

was lower in Asia-Oceania (62%; 95% CI: 43-79%) compared to America (70%; 95% CI: 61-79%) and Europe (70%; 95% CI: 65-74%).

A statistically significant difference in average SUV between malignant, premalignant and benign FCIs was reported in some articles; nevertheless, a significant overlap about SUV was found between these three groups (Table 1).

Discussion

The increasing use of ^{18}F-FDG-PET and PET/CT is associated with a concomitant increase in the number of patients with FCIs. The major difference between PET/CT and other imaging studies is that PET/CT provides both anatomic and metabolic information about incidental lesions found in the large bowel. The pattern of ^{18}F-FDG uptake in the large bowel on PET imaging influences the likelihood of malignancy. Diffuse and segmental increased uptake detected at ^{18}F-FDG-PET or PET/CT in the large bowel are usually associated with benign conditions [1,2]: such cases were not covered

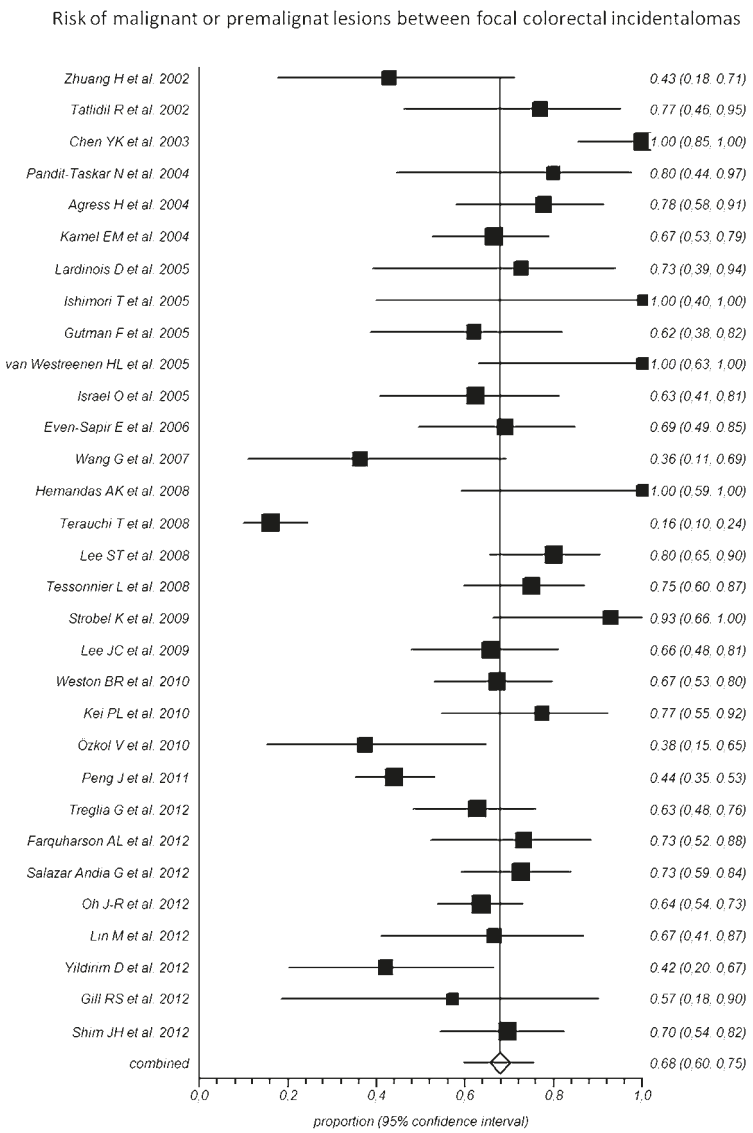

FIGURE 3. Plot of individual studies and pooled risk of malignant or premalignant lesions between focal colorectal incidental uptake detected by ^{18}F-FDG-PET or PET/CT, including 95% confidence intervals (95%CI). The risk of malignant or premalignant lesions ranged from 16% to 100%, with pooled estimate of 68% (95%CI: 60-75%). The included studies were statistically heterogeneous (I-square: > 75%).

by this meta-analysis. We focused our analysis on FCIs because they can be associated with malignant or premalignant conditions in a significant number of cases.[1,2]

Several single-center studies have reported the prevalence of FCIs and risk of malignant and premalignant lesions between FCIs detected by ^{18}F-FDG-PET or PET/CT with discordant findings.[2,5-35] In order to derive more robust estimates and obtain evidence-based data about this topic, we performed a meta-analysis pooling published data.

Pooled results of our meta-analysis indicate that FCIs are observed in about 3.6% of patients performing ^{18}F-FDG-PET or PET/CT. Moreover, in our pooled analysis FCIs were associated with a high risk of malignant or premalignant lesions (68%), considering colonoscopy or histology confirmation as reference standard. Therefore, whenever a focal hot spot is detected within the large bowel, the ^{18}F-FDG-PET or PET/CT report should suggest further investigation, such as colonoscopy, in order to exclude a malignant or premalignant lesions.[1,2]

In the calculation of pooled malignancy risk, we considered premalignant lesions together with malignant lesions because colonic adenomas can transform from adenoma to carcinoma and progress insidiously in asymptomatic patients.

Performing a sub-analysis for geographic areas we found that the risk of malignant or premalignant lesions between FCIs was higher in America and Europe compared to Asia and Oceania. A possible explanation of this finding is that the prevalence of colorectal cancer is superior in these geographic areas.[36]

A significant difference in average SUV between malignant, premalignant and benign FCIs was reported in some articles (Table 1). Nevertheless, a significant overlap about SUV was found between these three groups. Therefore, SUV alone should not be used to differentiate between malignant, premalignant and benign FCIs. Indeed, it is well known that SUV is influenced by several factors, related to the patient as well as to technical aspects and procedures. Any calculation of a pooled SUV obtained by different studies - acquired with different tomographs, scan protocols, ^{18}F-FDG injected activity, and patient characteristics - is in our opinion inappropriate, and therefore we decided not to meta-analyze data about SUV.

The present study has some limitations, related to the included articles, such as the selection bias in the calculation of malignancy risk and the heterogeneity between studies. Indeed, only a percentage of FCIs detected by ^{18}F-FDG-PET or PET/CT underwent colonoscopy or histopathology confirmation in the included studies and this may represent a selection bias in the calculation of the risk of malignant or premalignant lesions. Furthermore, the included studies were statistically heterogeneous in their estimates of prevalence of FCIs and risk of malignant or premalignant lesions. This heterogeneity is likely to stem from diversity in methodological aspects between different studies. The baseline differences between the patients performing PET or PET/CT in the included studies may have

TABLE 1. Characteristics of the included studies about focal colorectal incidental uptake detected by ^{18}F-FDG PET or PET/CT

Authors	Year	Country	Device used	No. of patients evaluated	No. of patients with FCIs	No. of FCIs	No. of FCIs verified by colonoscopy or histology	Final diagnosis of FCIs				Average SUV in FCIs		
								Malignant	Pre-malignant	Benign	No lesions identified	Malignant FCIS	Pre-malignant FCIs	Benign FCIs
Zhuang H et al.	2002	USA/Brazil	PET	197	17	17	14	5	1	8		n.a.	n.a.	n.a.
Tatlidil R et al.	2002	USA	PET	3000	n.a.	n.a.	13	6	4	3	0	n.a.	n.a.	n.a.
Chen YK et al.	2003	Taiwan	PET	3210	22	23	23	6	17	0	0	5.74 ± 2.26*	3.56 ± 0.68*	n.a.
Pandit-Taskar N et al.	2004	USA	PET	1000	n.a	n.a.	10	1	7	0	2	13.6	7.0 ± 3.0	n.a.
Agress H et al.	2004	USA	PET	1750	n.a.	n.a.	27	3	18	3	3	n.a	n.a	n.a.
Kamel EM et al.	2004	Switzerland	PET/CT	3281	n.a.	n.a.	54	9	27	9	9	n.a	n.a	n.a.
Lardinois D et al.	2005	Switzerland/ Russia	PET/CT	350	11	11	11	0	8	3	0	n.a.	n.a	n.a.
Ishimori T et al.	2005	USA	PET/CT	1912	8	8	4	4	0	0	0	n.a.	n.a.	n.a.
Gutman F et al.	2005	France	PET/CT	1716	45	n.a.	21	3	10	1	7	15 ± 11.6	12.0±3.7	25
van Westreenen HL et al.	2005	The Netherlands	PET	366	11	11	8	2	6	0	0	n.a.	n.a.	n.a.
Israel O et al.	2005	Israel	PET/CT	4390	n.a.	n.a.	24	6	9	3	6	n.a.	14.0 ± 10.5	n.a.
Even-Sapir E et al.	2006	Israel	PET/CT	2360	33	39	29	13	7	5	4	n.a	n.a	n.a.
Wang G et al.	2007	China/ Australia	PET/CT	1727	n.a.	n.a.	11	1	3	4	3	n.a.	n.a.	n.a.
Hemandas AK et al.	2008	UK	PET/CT	110	10	10	7	0	7	0	0	n.a.	n.a.	n.a.
Terauchi T et al.	2008	Japan	PET	2911	n.a.	111	111	7	11	9	84	8.31	n.a.	n.a.
Lee ST et al.	2008	Australia	PET/CT	2916	85	95	45	12	24	2	7	n.a.	n.a.	n.a.
Tessonnier L et al.	2008	France	PET/CT	4033	n.a.	n.a.	44	8	25	4	7	12.3 ± 5	9.8 ± 6.1	8.2±2.1
Strobel K et al.	2009	Switzerland	PET/CT	598	n.a.	14	14	5	8	0	1	n.a.	n.a.	n.a.
Lee JC et al.	2009	Australia	PET/CT	1665	62	70	35	11	12	5	7	n.a.	n.a.	n.a.
Weston BR et al.	2010	USA	PET/CT	330	50	52	52	10	25	2	15	17.2*	14.2 ± 7.2*	n.a.
Kei PL et al.	2010	USA/ Singapore/ Hong Kong	PET/CT	2250	n.a.	n.a.	22	4	13	1	4	n.a.	20.7 ± 11.3*	12.0*
Özkol V et al.	2010	Turkey	PET/CT	2370	n.a	n.a.	16	3	3	7	3	n.a.	n.a.	n.a.
Luboldt W et al.	2010	Germany	PET/CT	2338	50	n.a.	n.a.	n.a.	n.a.	n.a.	n.a.	n.a.	n.a.	n.a.
Peng J et al.	2011	China	PET/CT	10978	148	n.a.	125	32	23	5	65	9.7*	8.2*	6.1*
Treglia G et al.	2012	Italy	PET/CT	6000	64	n.a.	51	13	19	8	11	9.6 ± 4.7	8.5 ± 5.2	6.5 ± 3.6
Farquharson AL et al.	2012	UK	PET/CT	555	53	n.a.	26	2	17	3	4	n.a.	n.a.	n.a.
Salazar Andia G et al.	2012	Spain	PET/CT	2220	n.a.	n.a.	55	13	27	10	5	n.a.	n.a.	n.a.
Oh J-R et al.	2012	Republic of Korea	PET/CT	21317	n.a.	296	102	32	43	13	14	13.6 ± 4.9*	8.4 ± 4.5*	6.8*
Lin M et al.	2012	Australia	PET/CT	649	n.a.	n.a.	18	3	9	4	2	6.0	10.4	5.8
Yildirim D et al.	2012	Turkey	PET/CT	823	28	28	19	6	2	1	10	n.a	n.a	n.a.
Gill RS et al.	2012	Canada	PET or PET/CT	1500	21	21	7	2	2	1	2	7.4	n.a.	4.1
Shim JH et al.	2012	South Korea	PET/CT	239	39	46	46	8	24	14		8.9	5.5	n.a.

FCIs = focal colorectal incidental uptake; pts = patients; n.a. = not available; *significant statistical difference

contributed to the observed heterogeneity too. However, such variability was accounted for in a random-effects model.

Lastly, we did not perform a sub-analysis taking into account the device used (PET vs. PET/CT) or the site of FCIs (rectum and different colonic segments) because sufficient data in this regard could not be retrieved from the included studies.

Conclusions

FCIs are observed in a not negligible number of patients who undergo ^{18}F-FDG-PET or PET/CT studies with a high risk to be malignant or premalignant lesions. SUV is not reliable as a tool to differentiate between malignant, premalignant and benign FCIs. Further investigation, such as colonoscopy, is warranted whenever FCIs are detected by ^{18}F-FDG-PET or PET/CT in order to exclude malignant or premalignant lesions.

References

1. Lin M, Koo JH, Abi-Hanna D. Management of patients following detection of unsuspected colon lesions by PET imaging. *Clin Gastroenterol Hepatol* 2011; **9:** 1025-32.
2. Treglia G, Calcagni ML, Rufini V, Leccisotti L, Meduri GM, Spitilli MG, et al. Clinical significance of incidental focal colorectal (18)F-fluorodeoxyglucose uptake: our experience and a review of the literature. *Colorectal Dis* 2012; **14:** 174-80.

3. Isobe K, Hata Y, Sakaguchi S, Takai Y, Shibuya K, Takagi K, et al. The role of positron emission tomography in the detection of incidental gastrointestinal tract lesions in patients examined for lung cancer. *Nihon Kokyuki Gakkai Zasshi* 2010; **48:** 482-87.
4. Chopra A, Ford A, De Noronha R, Matthews S. Incidental findings on positron emission tomography/CT scans performed in the investigation of lung cancer. *Br J Radiol* 2012; **85:** e229-37.
5. Zhuang H, Hickeson M, Chacko TK, Duarte PS, Nakhoda KZ, Feng Q, Alavi A. Incidental detection of colon cancer by FDG positron emission tomography in patients examined for pulmonary nodules. *Clin Nucl Med* 2002; **27:** 628-32.
6. Tatlidil R, Jadvar H, Bading JR, Conti PS. Incidental colonic fluorodeoxyglucose uptake: correlation with colonoscopic and histopathologic findings. *Radiology* 2002; **224:** 783-87.
7. Chen YK, Kao CH, Liao AC, Shen YY, Su CT. Colorectal cancer screening in asymptomatic adults: the role of FDG PET scan. *Anticancer Res* 2003; **23:** 4357-61.
8. Pandit-Taskar N, Schöder H, Gonen M, Larson SM, Yeung HW. Clinical significance of unexplained abnormal focal FDG uptake in the abdomen during whole-body PET. *Am J Roentgenol* 2004; **183:** 1143-47.
9. Agress H Jr, Cooper BZ. Detection of clinically unexpected malignant and premalignant tumors with whole-body FDG PET: histopathologic comparison. *Radiology* 2004; **230:** 417-22.
10. Kamel EM, Thumshirn M, Truninger K, Schiesser M, Fried M, Padberg B, et al. Significance of incidental 18F-FDG accumulations in the gastrointestinal tract in PET/CT: correlation with endoscopic and histopathologic results. *J Nucl Med* 2004; **45:** 1804-10.
11. Lardinois D, Weder W, Roudas M, von Schulthess GK, Tutic M, Moch H, et al. Etiology of solitary extrapulmonary positron emission tomography and computed tomography findings in patients with lung cancer. *J Clin Oncol* 2005; **23:** 6846-53.
12. Ishimori T, Patel PV, Wahl RL. Detection of unexpected additional primary malignancies with PET/CT. *J Nucl Med* 2005; **46:** 752-57.
13. Gutman F, Alberini JL, Wartski M, Vilain D, Le Stanc E, Sarandi F, et al. Incidental colonic focal lesions detected by FDG PET/CT. *Am J Roentgenol* 2005; **185:** 495-500.
14. van Westreenen HL, Westerterp M, Jager PL, van Dullemen HM, Sloof GW, Comans EF, et al. Synchronous primary neoplasms detected on 18F-FDG PET in staging of patients with esophageal cancer. *J Nucl Med.* 2005; **46:** 1321-25.
15. Israel O, Yefremov N, Bar-Shalom R, Kagana O, Frenkel A, Keidar Z, et al. PET/CT detection of unexpected gastrointestinal foci of 18F-FDG uptake: incidence, localization patterns, and clinical significance. *J Nucl Med* 2005; **46:** 758-62.
16. Even-Sapir E, Lerman H, Gutman M, Lievshitz G, Zuriel L, Polliack A, et al. The presentation of malignant tumours and pre-malignant lesions incidentally found on PET-CT. *Eur J Nucl Med Mol Imaging* 2006; **33:** 541-52.
17. Wang G, Lau EW, Shakher R, Rischin D, Ware RE, Hong E, et al. How do oncologists deal with incidental abnormalities on whole-body fluorine-18 fluorodeoxyglucose PET/CT? *Cancer* 2007; **109:** 117-24.
18. Hemandas AK, Robson NK, Hickish T, Talbot RW. Colorectal tubulovillous adenomas identified on fluoro-2-deoxy-D glucose positron emission tomography/computed tomography scans. *Colorectal Dis* 2008; **10:** 386-89.
19. Terauchi T, Murano T, Daisaki H, Kanou D, Shoda H, Kakinuma R, et al. Evaluation of whole-body cancer screening using 18F-2-deoxy-2-fluoro-D-glucose positron emission tomography: a preliminary report. *Ann Nucl Med* 2008; **22:** 379-85.
20. Lee ST, Tan T, Poon AM, Toh HB, Gill S, Berlangieri SU, et al. Role of low-dose, noncontrast computed tomography from integrated positron emission tomography/computed tomography in evaluating incidental 2-deoxy-2-[F-18] fluoro-D-glucose-avid colon lesions. *Mol Imaging Biol* 2008; **10:** 48-53.
21. Tessonnier L, Gonfrier S, Carrier P, Valerio L, Mouroux J, Benisvy D, et al. Unexpected focal bowel 18-FDG uptake sites: should they be systematically investigated? *Bull Cancer* 2008; **95:** 1083-87.
22. Strobel K, Haerle SK, Stoeckli SJ, Schrank M, Soyka JD, Veit-Haibach P, et al. Head and neck squamous cell carcinoma (HNSCC) - detection of synchronous primaries with (18)F-FDG-PET/CT. *Eur J Nucl Med Mol Imaging* 2009; **36:** 919-27.
23. Lee JC, Hartnett GF, Hughes BG, Ravi Kumar AS. The segmental distribution and clinical significance of colorectal fluorodeoxyglucose uptake incidentally detected on PET-CT. *Nucl Med Commun* 2009; **30:** 333-37.
24. Weston BR, Iyer RB, Qiao W, Lee JH, Bresalier RS, Ross WA. Ability of integrated positron emission and computed tomography to detect significant colonic pathology: the experience of a tertiary cancer center. *Cancer* 2010; **116:** 1454-61.
25. Kei PL, Vikram R, Yeung HW, Stroehlein JR, Macapinlac HA. Incidental finding of focal FDG uptake in the bowel during PET/CT: CT features and correlation with histopathologic results. *Am J Roentgenol* 2010; **194:** W401-06.
26. Ozkol V, Alper E, Aydin N, Ozkol HF, Topal NB, Akpinar AT. The clinical value of incidental 18F-fluorodeoxyglucose-avid foci detected on positron emission tomography/computed tomography. *Nucl Med Commun* 2010; **31:** 128-36.
27. Luboldt W, Volker T, Wiedemann B, Wehrmann U, Koch A, Toussaint T, et al. Detection of relevant colonic neoplasms with PET/CT: promising accuracy with minimal CT dose and a standardised PET cut-off. *Eur Radiol* 2010; **20:** 2274-85.
28. Peng J, He Y, Xu J, Sheng J, Cai S, Zhang Z. Detection of incidental colorectal tumours with 18F-labelled 2-fluoro-2-deoxyglucose positron emission tomography/computed tomography scans: results of a prospective study. *Colorectal Dis* 2011; **13:** e374-78.
29. Farquharson AL, Chopra A, Ford A, Matthews S, Amin SN, De Noronha R. Incidental focal colonic lesions found on (18)Fluorodeoxyglucose positron emission tomography/computed tomography scan: further support for a national guideline on definitive management. *Colorectal Dis* 2012; **14:** e56-63.
30. Salazar Andía G, Prieto Soriano A, Ortega Candil A, Cabrera Martín MN, González Roiz C, Ortiz Zapata JJ, et al. Clinical relevance of incidental finding of focal uptakes in the colon during 18F-FDG PET/CT studies in oncology patients without known colorectal carcinoma and evaluation of the impact on management. *Rev Esp Med Nucl* 2012; **31:** 15-21.
31. Oh JR, Min JJ, Song HC, Chong A, Kim GE, Choi C, et al. A stepwise approach using metabolic volume and SUVmax to differentiate malignancy and dysplasia from benign colonic uptakes on 18F-FDG PET/CT. *Clin Nucl Med* 2012; **37:** e134-40.
32. Lin M, Ambati C. The management impact of clinically significant incidental lesions detected on staging FDG PET-CT in patients with non-small cell lung cancer (NSCLC): an analysis of 649 cases. *Lung Cancer* 2012; **76:** 344-9.
33. Yildirim D, Tamam MO, Sahin M, Ekci B, Gurses B. Differentiation of incidental intestinal activities at PET/CT examinations with a new sign: Peristaltic segment sign. *Rev Esp Med Nucl Imagen Mol.* 2013; **32:** 86-91.
34. Gill RS, Perry T, Abele JT, Bédard EL, Schiller D. The clinical significance of incidental intra-abdominal findings on positron emission tomography performed to investigate pulmonary nodules. *World J Surg Oncol* 2012; **10:** 25.
35. Shim JH, O JH, Oh SI, Yoo HM, Jeon HM, Park CH, et al. Clinical Significance of Incidental Colonic (18)F-FDG Uptake on PET/CT Images in Patients with Gastric Adenocarcinoma. *J Gastrointest Surg* 2012; **16:** 1847-53.
36. Jemal A, Bray F, Center MM, Ferlay J, Ward E, Forman D. Global cancer statistics. *CA Cancer J Clin* 2011; **61:** 69-90.

review

Cardiotoxicity of concomitant radiotherapy and trastuzumab for early breast cancer

Tanja Marinko[1], Jure Dolenc[2], Cvetka Bilban-Jakopin[3]

[1] Department of Radiotherapy, Institute of Oncology Ljubljana, Ljubljana, Slovenia
[2] Department of Cardiology, University Medical Centre Ljubljana, Ljubljana, Slovenia
[3] Institute of Oncology Ljubljana, Ljubljana, Slovenia

Radiol Oncol 2014; 48(2): 105-112.

Received 15 March 2013
Accepted 12 April 2013

Correspondence to: Tanja Marinko, M.D., Department of Radiotherapy, Institute of Oncology Ljubljana, Zaloska 2, 1000 Ljubljana, Slovenia. Phone: +386 1 5879 505; Fax: +386 1 5879 400; E-mail: tmarinko@onko-i.si

Disclosure: No potential conflicts of interest were disclosed.

Background. Trastuzumab therapy given in combination with one of several chemotherapy regimens is currently considered the standard of care for the treatment of early-stage, human epidermal growth factor receptor-2 (HER2) -positive breast cancer. The treatment with trastuzumab is due to a significant impact on the survival part of the standard adjuvant treatment of patients with HER2-positive breast cancer. Patients treated with postoperative breast or chest wall irradiation receive trastuzumab concomitant with radiotherapy. In a small proportion of patients trastuzumab causes cardiotoxicity. Preclinical findings indicate a radiosensibilizing effect of trastuzumab in breast cancer cells, but it is not yet clear whether it radiosensibilizes cells of healthy tissues too.

Conclusions. Special attention is required when left breast or left thoracic wall is irradiated in patient receiving trastuzumab, because long-term effects of the concurrent treatment with trastuzumab and radiotherapy are not yet known. In an era where more patients are surviving a diagnosis of breast cancer, better understanding and earlier detection of therapy-induced cardiac toxicity will be of paramount importance.

Key words: radiotherapy; cardiotoxicity; trastuzumab; early breast cancer

Introduction

Trastuzumab (Herceptin®) is a humanised monoclonal antibody that binds to the extracellular domain of the HER2 receptor, transmembrane glycoprotein and thereby inhibits cell growth and reproduction. The exact mechanism of action that leads to the clinical efficacy of trastuzumab is not yet entirely clear, although its antitumor effect *in vitro* has already been shown before 20 years. Trastuzumab was approved by the US Food and Drug Administration in September 1998 for the treatment of metastatic breast cancer. Nowadays it is widely used in the metastatic and adjuvant systemic treatment for breast cancer.

HER2-positive (HER2 over-expression of the receptor) is 15–25% of breast cancers.[1-3] If untreated, they have a worse prognosis than HER2 negative tumours.[4] Within the adjuvant treatment of patients with HER2-positive breast cancer, a therapy with trastuzumab improves the survival, which is confirmed by the four major international studies: Herceptin Adjuvant Trial (HERA), National Surgical Adjuvant Breast and Bowel Project (NSABP) B-31, North Central Cancer Treatment Group (NCCTG) N9831 and BCIRG Breast Cancer International Research Group (BCIRG) 006th. Among four major adjuvant trials more than 13.000 women with HER2-positive early breast cancer were enrolled.[5] All four studies report on the extension of time to disease recurrence and the overall survival if one year of the treatment with trastuzumab is added to the standard chemotherapy (CT).[3,6,7] As an adjuvant treatment of breast cancer in these studies patients firstly received anthracyclines and then taxanes, as monotherapy or concomitantly with trastuzumab, which was then given with total one year.[5]

The meta analysis, published in Cohrane Database in April 2012, which included eight studies involving 11.991 patients, found that the combined hazard ratios (HR) for the overall survival and disease-free survival significantly favoured the trastuzumab-containing regiments (HR 0.66, 95% confidence interval [CI] 0.57–0.77, P < 0.00001; and HR 0.60, 95% CI 0.50 to 0.71, P < 0.00001) used in the treatment for early and locally advanced breast cancer.[4] Benefit of trastuzumab is higher if it is introduced as soon as possible in the course of the treatment and simultaneously with CT.[8,9]

Clinical guidelines based on these findings, therefore, recommended the introduction of trastuzumab before postoperative radiotherapy and after the treatment with anthracyclines.[10] Because the half-life of trastuzumab is long (four weeks) and washout period is 20 weeks, it is usually administered concomitantly with radiotherapy.[11]

Cardiotoxicity of trastuzumab and anthracyclins

The treatment with trastuzumab is well tolerated by most patients. In a small proportion of patients treatment may be necessarily temporary or permanently discontinued due to the resulting damage to the heart.[2,9,12] In a large randomized clinical trials, where patients received trastuzumab as a part of the adjuvant treatment (after completing anthracycline CT), the reported incidence of severe heart failure and cardiac death was from 0.6% (study HERA) to 4% (NSABP-B31). The most common cardiovascular event reported was an asymptomatic decrease in left ventricular ejection fraction (LVEF). It was shown that the risk of developing heart failure was significantly higher in patients who had previously received anthracyclines.[13] In the above mentioned Cochran's meta-analysis published in 2012 it was reported, that trastuzumab significantly increased the risk of congestive heart failure (CHF) (risk ratio [RR] 5.11, 90% CI 3.00–8.72, P < 0.0001) and LVEF decline (RR 1.83; 90% CI 1.36 to 2.47, P = 0.0008).

Anthracyclines, which are received by most patients with early breast cancer during the adjuvant treatment with CT, may cause cardiotoxicity type I.[14] They induce injury to myocites, probably caused by the resulting toxic oxygen free radicals. The injury is the result of oxidative stress and leads to irreversible damage of myocites (necrosis and apoptosis), which are eventually replaced by connective tissue.[15] The rate of heart failure is dependent on the cumulative dose of medication.[14]

Trastuzumab could cause cardiotoxicity type II.[14] The occurrence of cardiotoxicity isn't dose-dependent. Whether asymptomatic or symptomatic heart failure, if it is caused by trastuzumab, it should be reversible. Ewer *et al*. report on the reversibility of trastuzumab-induced reduction in LVEF after discontinuation of therapy.[16] In the heart biopsy only benign ultrastructural changes can be found.[14]

So far there is very little known about the long-term significance of asymptomatic LVEF reductions. Cardiologists warn that it is necessary to monitor these patients annually even after the treatment with trastuzumab.[15,17] The mechanism of heart damage caused by trastuzumab is not yet fully understood. HER2 receptors are normally present on the myocites and they are important for the normal development and function of the heart. Preclinical studies indicate that the direct blockade of the HER2 receptor on myocites has at least partially an important impact on cardiotoxicity of trastuzumab.[18,19] Among the drugs used for the treatment of patients with cancer there are some other well-known substances, that cause mild, chronic, partially reversible, but clinically silent cardiotoxic side effects, that in the opinion of the cardiologists needs a long term attention.[20]

Cardiotoxicity of radiation therapy

Irradiation of the heart may be associated with multiple effects on the heart; the result could be acute or chronic pericarditis, pericardial effusion, constrictive pericarditis, coronary vascular disease, restrictive cardiomyopathy, valvular heart disease or malfunction of the conductive system of the heart. The development of these defects depends mainly on the dose received by the heart and the proportion of the heart, which is exposed to radiation.[14] Another important factor for the development of heart damage, is the age. According to the literature, young people (< 20 years) have the highest risk of subsequent heart damage because the organism is still developing and cells multiply rapidly, which makes them more susceptible to damage of the DNA molecules.[21] Heart damage due to radiation is caused by microvascular lesions, as well as direct apoptosis of damaged cells. The final outcome is fibrosis that develops over the years, after the completion of radiotherapy.[22]

Cardiotoxicity of adjuvant radiotherapy in patients with breast cancer is the subject of many studies.[23,24] In the EBCTCG meta-analysis in 2005, which included 42 000 women in 78 randomised trials, it was shown that the use of radiation ther-

apy significantly improves the disease-specific survival for patients with an early stage breast cancer.[23] But the same analysis, comparing the trials with radiotherapy *versus* not, also reported that there was, at least with some of the older radiotherapy regimens, a significant excess mortality from heart disease (RR 1.27, standard error [SE] 0.07, 2p = 0.0001). It was slight during the first five years, but continued after year 15.

Meta-analysis, which allows the identification and abstraction of critical information from different randomized, controlled trials[25], analysed long term mortality from heart disease after radiotherapy for an early breast cancer of about 300 000 women in United States (US) Surveillance, Epidemiology and End Results (SEER) cancer registries. It was found that for women diagnosed during 1973–82 and irradiated, the cardiac mortality ratio (left versus right tumour laterality) was 1.20 (95% CI 1.04–1.38) less than 10 years afterwards, 1.42 (1.11–1.82) 10–14 years afterwards, and 1.58 (1.29–1.95) after 15 years or more (trend: 2p = 0.03), respectivelly.[26] For women diagnosed during 1983-92 and irradiated, the cardiac mortality ratio was 1.04 (0.91–1.18) less than 10 years afterwards and 1.27 (0.99–1.63) 10 or more years afterwards. For women diagnosed 1993-2001 and irradiated the cardiac mortality ratio was 0.96 (0.82–1.12) with none yet followed for 10 years. According to the author's interpretation of the results, since the early 1980s, improvements in radiotherapy planning should have reduced mortality from heart disease in women received radiotherapy.

Older radiotherapy techniques (two-dimensional (2D) radiotherapy) and irradiation devices (telecobalt machine), which were used in the past for the treatment of patients with a breast cancer did not allow for as good protection of the heart as it is possible with newer radiotherapy techniques (three-dimensional (3D) conformal radiotherapy) and modern irradiation devices (linear accelerator) (Figure 1). In the future, it is reasonable to expect better outcomes of such studies and less cardiotoxicity.

Despite progress in radiotherapy for the patients with breast cancer, there is still some risk of a cardiac damage due to irradiation. The reason for the damage is the anatomical position of the heart, which lies just below the breast or chest wall, which is irradiated with the therapeutic dose.

Cardiotoxicity of concomitant radiotherapy and trastuzumab

Preclinical *in vitro* and *in vivo* studies have shown that the cascade of events through the HER2 receptor is involved in tumour radiosensibility[27], application of trastuzumab concurrently with radiation thus increases the antitumor effect of radiation. There are same clinical evidences in the literature that trastuzumab also radiosensibilizes human healthy tissues and in this way it could increase the toxicity of the treatment.[28]

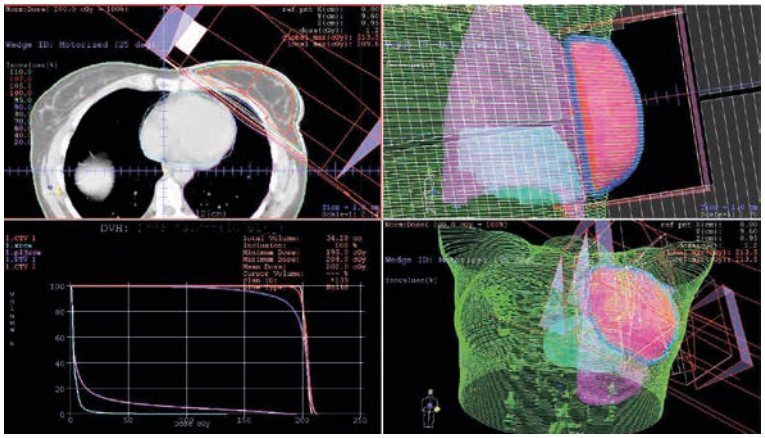

FIGURE 1. Treatment plan for postoperative irradiation of the left breast in patient with early breast cancer - Three dimensional conformal radiation therapy (3DCRT).

Currently the most important question remains whether the concomitant therapy with trastuzumab and radiotherapy increases cardiotoxicity of the treatment. In the literature, there are limited data about the safety of concomitant therapy with radiotherapy and trastuzumab. The observation period in the studies was short, the longest reported median observation period after the completion of concomitant treatment with radiotherapy and trastuzumab was 3.7 years.[29]

In the study which included a retrospective series of 218 patients with advanced breast cancer at MD Anderson, a significantly higher rate of cardiovascular events was identified in patients who have completed left breast irradiation, as it was found in patients after irradiation of the right breast (26% *vs.* 7%).[30] In the multivariate analysis radiation wasn't shown as an important risk factor for cardiotoxicity, which was observed after the treatment with trastuzumab.

In the monocentric prospective study from the Institute Curie in Paris acceptable skin toxicity and cardiac toxicity was reported after a median observation period of 13 months after the completion of the adjuvant treatment with trastuzumab and concomitant radiotherapy.[11] In this trial 83% of patients received irradiation not only to the breast or thoracic wall but also to the parasternal lymph nodes. The study involved 106 patients

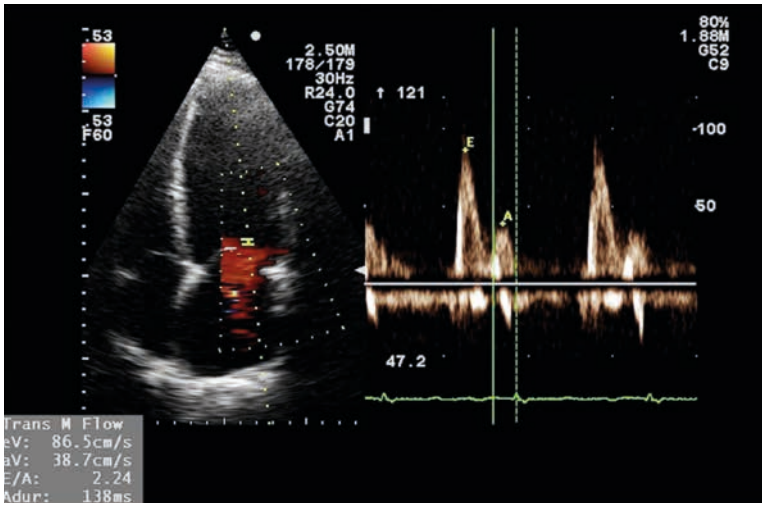

FIGURE 2. Pulsed wave Doppler measurement of flow velocities through the mitral valve annulus showing normal left ventricular filling pattern. (E = early diastolic flow velocity, A = atrial contraction flow velocity).

treated between June 2006 and March 2007. Four % of patients developed symptomatic heart failure of whom 2% experienced serious complications related to the heart. Researchers didn't find significant differences in the effect of the treatment on the skin between the two compered groups of patients (concomitant treatment with trastuzumab and radiotherapy *vs.* only radiotherapy).

NSABP-B31 study did not allow radiotherapy of parasternal lymph nodes. It included 1503 patients and did not show any differences in the incidence of cardiovascular events, regardless of whether the patients were irradiated to the left or right breast/thoracic wall.[31]

Sub-analysis of NCCTG N9831 study has included 1286 patients, of whom in the adjuvant treatment 908 patients received concomitant trastuzumab and radiotherapy and 378 patients received only trastuzumab.[29] Trastuzumab was administered after the completion of CT with anthracyclines and taxanes. The study shows no significant difference in the frequency of clinically manifest cardiovascular events between the two groups (irradiated *vs.* non-irradiated patients), and there were no significant differences in comparison with the irradiated side.

The Canadian study included 59 patients, of whom 44 were treated with concomitant trastuzumab and radiotherapy.[32] Median absolute decrease in LVEF after irradiation was 4% between groups (left breast/right breast and with/without parasternal lymph nodes included in the irradiated field), but the study did not show significant differences.

In the HERA study[3], where there were fewer cardiovascular events than in the NSABP-B31 and NCCTG N9831 trials, the treatment with trastuzumab was started after the completion of CT and radiotherapy, in contrast with the previously mentioned studies, in which trastuzumab was administered concurrently, firstly with CT (except in one study group of NSABP-B31 trial) and then concurrently with radiotherapy.

Methods for evaluation of cardiotoxicity

The optimal method, duration and frequency of cardiac monitoring for patients receiving trastuzumab combined with radiotherapy have not yet been established. The role of careful history, physical examination, electrocardiograph and chest radiograph is crucial.[33] Different biomarkers and imaging techniques and their potential role in cardiotoxicity diagnosis have been evaluated in numerous trials. Cardiac troponins and brain natriuretic peptide (BNP) seem to be the most appropriate biomarkers for cardiotoxicity evaluation[34], while echocardiography and radionuclide ventriculography are imaging techniques that are being most widely used in this setting for the assessment of left ventricular ejection fraction (LVEF). LVEF is the golden standard for monitoring cardiac function in patients receiving cardiotoxic therapy.[35] The diagnostic importance of other biomarkers such as endothelin-1 or atrial natriuretic peptide[36-38], other imaging techniques such as magnetic resonance imaging[39] and invasive diagnostic tools such as classical ventriculography with endomyocardial biopsy is limited and are not widely accepted.[37,40]

Cardiac troponins I and T are early, highly specific and sensitive markers of myocardial injury.[35,37] Their role in the acute coronary syndrome diagnosis and prognosis is crucial. Elevated levels of troponins can be detected 4-12 hours after the myocardial injury and can persist elevated up to 10 days.[41] Elevated serum troponins can be detected in variety of other clinical settings such as advanced heart failure, pulmonary embolism, myocarditis, sepsis, arrhythmias, renal failure and also in chemotherapy induced cardiomyopathies. In breast carcinoma patients receiving high doses of anthracyclins, elevated troponins after drug application were related to reduction of LVEF and development of symptomatic heart failure later on.[40] Those patients were also less likely to recover from heart failure.[42] On the other hand, the role of troponins in the long-term follow up of these patients

is limited because elevated levels do not persist late after the myocardial injury.

BNP is a member of natriuretic hormones family. Their effect is vasodilatative, natriuretic, diuretic and hypotensive. They inhibit renin-angiotensin system and enhance neurohormonal activation in heart failure patients.[37] BNP is synthesized in the brain and in the ventricles in response to volume overload and consequent ventricular wall distension. After being synthesized, its inactive form proBNP is then cleaved into active BNP and inactive N terminal proBNP (NT-proBNP). Both molecules are being used in heart failure diagnosis, but NT-proBNP is more widely accepted because it is more stable in the serum than active BNP. Also, NT-proBNP levels are higher than BNP levels in heart failure patients comparing to healthy individuals.[43] NT-proBNP is a sensitive biomarker of both systolic and diastolic heart failure not just as a diagnostic tool but also as a prognostic tool.[37] Elevated levels can be detected early in the asymptomatic stage of the disease or in patients with the preserved ejection fraction.[34] Higher levels of NT-proBNP can be detected in patients with low body mass index, women, elderly patients and patients with renal failure or anemia.[37] Numerous trials tested BNP or NT-proBNP as a diagnostic and prognostic tool for the evaluation of carditoxicity of cancer chemotherapy and radiation therapy. Both hormones proved to be early and sensitive biomarkers of such cardiotoxicity. Patients with elevated NT-proBNP had a higher possibility for asymptomatic LVEF reduction or to develop a symptomatic heart failure later on. Because changes in NT-proBNP are usually earlier than changes in LVEF, its elevated level exposes patients at higher risk. Also in a patient with already developed cardiotoxic effects, the reduction in NT-proBNP carries good prognosis for the improvement in cardiac function. For these reasons NT-proBNP is already widely used as a marker in the evaluation of cardiotoxicity in cancer patients.[35]

Standard transthoracic two-dimensional echocardiography is already a golden standard in the evaluation of carditoxicity in cancer patients.[39,44] It provides useful morphologic and haemodynamic information and not just LVEF alone.[33,37] Measurements of heart chambers and great vessels dimensions, estimation of ventricular systolic and diastolic function, assessment of ventricular wall contraction abnormalities, valvular anatomy and function and diagnosis of pericardial disease are a standard part of echocardiographic exam (Figure 2,3). The limiting factor of echocardiography as a diagnostic tool is its relatively low reproducibility due to high inter- and intraobserver variability.[37,40,44] For that reason it is highly recommended for patients that are being followed up for a longer period of time, that serial examinations are performed on the same device by the same echocardiographist. Traditionally, LVEF reduction was the only marker of cardiotoxicity in cancer patients. Recently it has been proved that reduction in LVEF is not as sensitive and occurs later than left ventricular diastolic dysfunction.[45-47] Patients with left ventricular diastolic dysfunction before the initiation of the treatment with trastuzumab are at higher risk for developing trastuzumab related cardiotoxicity.[47] For these reasons a detection of different degrees of left ventricular diastolic dysfunction is of crucial role in early cardiotoxicity diagnosis, especially because some patients never develop ventricular systolic dysfunction (patients with heart failure with preserved ejection fraction). In patients with atrial fibrillation or mitral regurgitation the assessment of ventricular diastolic function can be difficult. In obese patients or in patients after chest irradiation the quality of LVEF measurements can be poor due to suboptimal chest echotranslucency. In these settings tissue Doppler imaging (TDI), a Doppler derived echocardiographic technique measuring myocardial contraction velocities offers additional information regarding left ventricular systolic and diastolic dysfunction (Figure 4). For that reason, many investigators already propose that serial TDI measurements should be a part of a routine echocardiographic examination in cancer patients receiving a cardiotoxic therapy.[39,48,49]

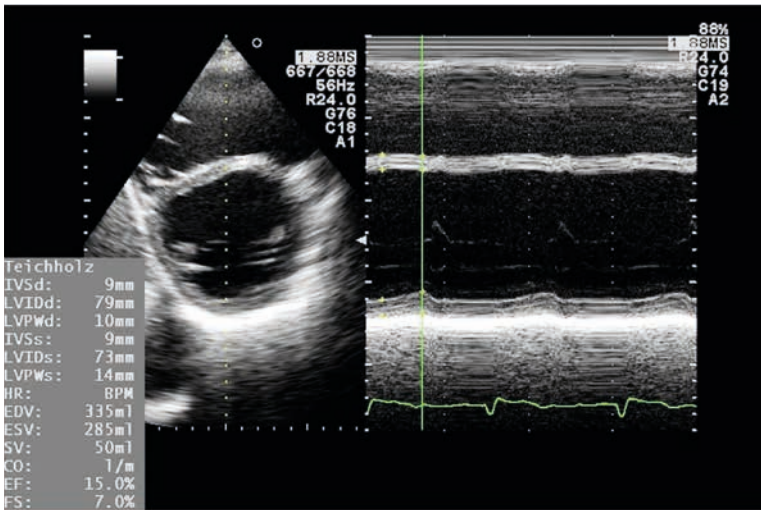

FIGURE 3. M mode measurement of left ventricular ejection fraction (LVEF) using the Teichholz method from the parasternal short axis view showing extremely enlarged left ventricle with severely reduced LVEF.

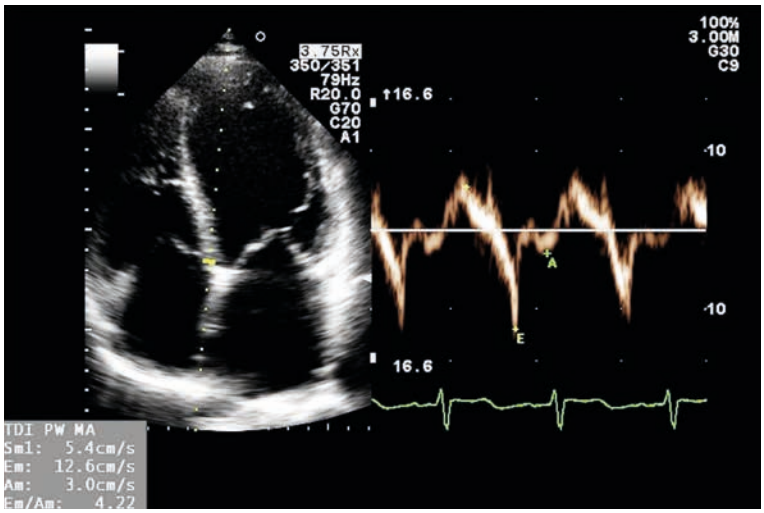

FIGURE 4. Measurement of tissue Doppler velocities on the mitral annulus from the apical four chamber view showing depressed left ventricular systolic function. (x = systolic velocity, x E = early diastolic velocity, x A = atrial contraction velocity).

Another useful diagnostic tool in the evaluation of cardiotoxicity is radionuclide ventriculography. This radionuclear technique uses *in vivo* technetium-99m labelled red blood cells and observes their intracardiac accumulation during different stages of the heart cycle with gamma camera in a standard left anterior oblique view.[47] It provides highly reproducible and observer independent calculation of LVEF and the assessment of left ventricular diastolic function.[37,40] This method is especially appropriate in conditions mentioned earlier where echocardiography provides less accurate measurements.[44] That is why some investigators promote radionuclide ventriculography as a golden standard and as a diagnostic method superior to echocardiography in serial evaluation of cardiotoxicity in cancer patients.[38,47] However, comparing to echocardiography radionuclide ventriculography provides solely the information regarding the left ventricular function and no information regarding chamber dimensions, heart valves and pericardium. Its diagnostic role is additionally limited because of the risks related to additional radiation of the patient, especially in the paediatric population.[40]

Perspectives for the future

Data from the studies published so far indicate that the concomitant therapy with radiation and trastuzumab is likely safety; irradiation should not have a significant additional effect on cardiotoxicity detected after the treatment with trastuzumab. However, so far only data obtained solely some years after the treatment are published. Currently there is no evidence that such therapy is safe even after a long observation period. In the previously mentioned studies biomarker NT-proBNP wasn't measured, which could possibly earlier than the measurement of LVEF show a significant difference in cardiac toxicity between the two compared groups of patients (concomitant trastuzumab and irradiation to the left/right breast or thoracic wall).

Because we know that trastuzumab in terms of cardiotoxicity in most patients causes only asymptomatic decrease in LVEF[33] and clinically expressed cardiovascular events do not often occur, there is a need for the trial which would observe heart function after the completion of the treatment with trastuzumab, particularly in combination with radiation, more precisely, as it is only by measuring LVEF. In addition, it is known that 50% of patients with impaired left ventricular function are asymptomatic.[50] In this group of patients on the basis of clinical symptoms and signs the heart failure or other cardiovascular events cannot be defined, but the treatment success rate of heart failure in this patient group is significantly better.[51]

As yet there are no guidelines for the follow-up of the patients after the treatment with trastuzumab. Perhaps particularly young patients would need a regular follow-up by the cardiologist after the treatment.

Since the new target drugs from the group of HER2 inhibitors (lapatinib, pertuzumab) have been used alone or in combination with trastuzumab, the question of co-toxicity of trastuzumab and radiation is even more important.

Conclusions

Because the prognosis of patients with HER2-positive early breast cancer, which is considered a more aggressive type of breast cancer, with new types of treatment is improving and their expected lifespan is extending, the determination of the toxicity of treatment has an increasing importance.

References

1. Slamon DJ, Clark GM, Wong SG, Levin WJ, Ullrich A, McGuire WL. Human breast cancer: correlation of relapse and survival with amplification of the HER-2/neu oncogene. *Science* 1987; **235:** 177-82.

2. Romond EH, Perez EA, Bryant J, Suman VJ, Geyer CE Jr, Davidson NE, et al. Trastuzumab plus adjuvant chemotherapy for operable HER2-positive breast cancer. *N Engl J Med* 2005; **353:** 1673-84.

3. Smith I, Procter M, Gelber RD, Guillaume S, Feyereislova A, Dowsett M, et al. 2-year follow-up of trastuzumab after adjuvant chemotherapy in HER2-positive breast cancer: a randomised controlled trial. *Lancet* 2007; **369:** 29-36.
4. Moja L, Tagliabue L, Balduzzi S, Parmelli E, Pistotti V, Guarneli V, et al. Trastuzumab containing regiments for early breast cancer. *Cochrane Database Syst Rev* 2012; **4:** CD006243.
5. Matos E. [Treatment of HER2 positive breast cancer patients]. [Slovenian]. *Zdrav Vestn* 2012; **81:** 236-45.
6. Perez EA, Romond EH, Suman VJ, Jeong JH, Davidson NE, Geyer Jr CE et al. Four-year follow-up of trastuzumab plus adjuvant chemotherapy for operable human epidermal growth factor receptor 2-positive breast cancer: joint analysis of data from NCCTG N9831 and NSABP B-31. *J Clin Oncol* 2011; **29:** 3366-73.
7. Slamon D, Eiermann W, Robert N, Pienkowski T, Martin M, Rolski J, et al. Phase III Randomized trial comparing doxorubicin and cyclophosphamide followed by docetaxel (AC -> T) with doxorubicin and cyclophosphamide followed by docetaxel and trastuzumab (AC -> TH) with docetaxel, carboplatin and trastuzumab (TCH) in Her2neu positive early breast cancer patients: BCIRG 006 Study. [Abstract]. *Cancer Res* 2009; **69:** 500S.
8. Joensuu H, Kellokumpu-Lehtinen PL, Bono P, Alanko T, Kataja V, Asola R, et al. Adjuvant docetaxel or vinorelbine with or without trastuzumab for breast cancer. *N Engl J Med* 2006; **354:** 809-20.
9. Slamon DJ, Leyland-Jones B, Shak S, Fuchs H, Paton V, Bajamonde A, et al. Use of chemotherapy plus a monoclonal antibody against HER2 for metastatic breast cancer that overexpresses HER2. *N Engl J Med* 2001; **344:** 783-92.
10. National Comprehensive Cancer network. NCCN guidelines. Avaiable 10th March, 2013: http://www.nccn.org/index.asp
11. Caussa L, Kirova YM, Gault N, Pierga JY, Savignoni A, Campana F, et al. The acute skin and heart toxicity of a concurrent association of trastuzumab and locoregional breast radiotherapy including internal mammary chain: a single-institution study. *Eur J Cancer* 2011; **47:** 65-73.
12. Piccart-Gebhart MJ, Procter M, Leyland-Jones B, Goldhirsch A, Untch M, Smith I, et al. Traastuzumab after adjuvant chemotherapy in HER-2 positive breast cancer. *N Engl J Med* 2005; **353:** 1659-72.
13. Lefrak EA, Pitha J, Rosenheim S, Gottlieb JA. A clinicopathologic analysis of adriamycin cardiotoxicity. *Cancer* 1973; **32:** 302-14.
14. Ewer MS, Ewer SM. Cardiotoxicity of anticancer treatments: what the cardiologist needs to know. *Nat Rev Cardiol* 2010; **7:** 564-75.
15. Chien AJ, Rugo HS. The cardiac safety of trastuzumab in the treatment of breast cancer. *Expert Opin Drug Saf* 2010; **9:** 335-46.
16. Ewer MS, Tan-Chiu E. Reversibility of trastuzumab cardiotoxicity: is the concept alive and well? *J Clin Oncol* 2007; **25:** 5532-3. Author reply: 5533-4.
17. Steinherz LJ, Steihherz PG, Tan CT, Heller G, Murphy ML. Cardiac toxicity 4-20 years after completing anthracycline therapy. *JAMA* 1991; **266:** 1672-7.
18. Klein PM, Dybdal N. Trastuzumab and cardiac dysfunction: update on preclinical studies. *Semin Oncol* 2003; **30(5 Suppl 16):** 49-53.
19. Schneider JW, Chang AY, Rocco TP. Cardiotoxicity in signal transduction therapeutics: erbB2 antibodies and the heart. *Semin Oncol* 2001; **28(5 Suppl 16):** 18-26.
20. Koželj M, Zver S, Zadnik V. Long term follow-up report of cardiac toxicity in patients with multiple myeloma treated with tandem autologous hematopoetic stem cell transplantation. *Radiol Oncol* 2013; **47:** 161-5.
21. Hancock SL, Tucker MA, Hoppe RT. Factors affecting late mortality from heart disease after treatment of Hodgkin s disease. *JAMA* 1993; **270:** 1949-55.
22. Schultz-Hector S. Radiation-induced heart disease: review of experimental data on dose response and pathogenesis. *Int J Radiat Biol* 1992; **61:** 149-60.
23. Clarke M, Collins R, Darby S, Davies C, Elphinstone P, Evans E, et al. Effects of radiotherapy and of differences in the extent of surgery for early breast cancer on local recurrence and 15-year survival: an overview of the randomised trials. *Lancet* 2005; **366:** 2087-106.
24. Favourable and unfavourable effects on long-term survival of radiotherapy for early breast cancer: an overview of the randomised trials. Early Breast Cancer Trialists' Collaborative Group. *Lancet* 2000; **355:** 1757-70.
25. Kovac V, Smrdel U. Meta-analyses of clinical trials in patients with non-small cell lung cancer. Minireview. *Neoplasma* 2004; **51:** 334-40.
26. Darby SC, McGale P, Taylor CW, Peto R. Long-term mortality from heart disease and lung cancer after radiotherapy for early breast cancer: prospective cohort study of about 300 000 women in US SEER cancer registries. *Lancet Oncol* 2005; **6:** 557-65.
27. Pietras RJ, Poen JC, Gallardo D, Wongvipat PN, Lee HJ, Slamon DJ. Monoclonal antibody to HER-2/neu receptor modulates repair of radiation–induced DNA damage and enhances radiosensitivity of human breast cancer cells overexpressing this oncogene. *Cancer Res* 1999; **59:** 1347-55.
28. Law AB, Evans T, Hayward RL, Higgins GS, Murray KL, Summers D, et al. Possible radiation sensitisation by trastuzumab leading to radiation-induced myelitis. *Breast Care (Basel)* 2009; **4:** 40-2.
29. Halyard MY, Pisansky TM, Dueck AC, Suman V, Pierce L, Solin L, et al. Radiotherapy and adjuvant trastuzumab in operable breast cancer: tolerability and adverse event data from the NCCTG Phase III Trial N9831. *J Clin Oncol* 2009; **27:** 2638-44.
30. Guarneri V, Lenihan DJ, Valero V, Durand JB, Broglio K, Hess KR, et al. Long-term cardiac tolerability of trastuzumab in metastatic breast cancer: the M.D. Anderson Cancer Center experience. *J Clin Oncol* 2006; **24:** 4107.
31. Tan-Chiu E, Yothers G, Romond E, Geyer CE Jr, Ewer M, Keefe D, et al. Assessement of cardiac dysfunction in a randomized trial comparing doxorubicin and cyclophosphamyde followed by paclitaxel, with or without trastuzumab as adjuvant therapy in node positive, human epidermal growth factor receptor 2-overexpressing breast cancer: NSABP B-31. *J Clin Oncol* 2005; **23:** 7811-19.
32. Shaffer R, Tyldesley S, Rolles M, Chia S, Mohamed I. Acute cardiotoxicity with concurrent trastuzumab and radiotherapy including internal mammary chain nodes: a retrospective single-institution study. *Radiother Oncol* 2009; **90:** 122-6.
33. Carver JR. Management of trastuzumab-related cardiac dysfunction. *Prog Cardiovasc Dis* 2010; **53:** 130-9.
34. Goel S, Simes RJ, Beith JM. Exploratory analysis of cardiac biomarkers in women with normal cardiac function receiving trastuzumab for breast cancer. *Asia Pac J Clin Oncol* 2011; **7:** 276-80.
35. Fiuza M. Cardiotoxicitiy associated with trastuzumabTreatment of HER2+ breast cancer. *Adv Ther* 2009: **26(Suppl 1):** S9- 17.
36. Wondergem J, Strootman EG, Frölich M, Leer JWH, Noordijk EM. Circulating atrial natriuretic peptide plasma levels as a marker for cardiac damage after radiotherapy. *Radiother Oncol* 2001; **58:** 295-301.
37. Geiger S, Lang V, Suhl P, Heinemann V, Stemmler HJ. Anticancer therapy induced cardiotoxicity: review of the literature. *Anticancer Drugs* 2010, **21:** 578-90.
38. Feola M, Garrone O, Occelli M, Francini A, Biggi A, Visconti G, et al. Cardiotoxicity after anthracycline chemotherapy in breast carcinoma: effects on left ventricular ejection fraction, troponin I and brain natriuretic peptide. *Int J Cardiol* 2011; **148:** 194-8.
39. Zeglinski M, Ludke A, Jassal DS, Singal PK. Trastuzumab-induced cardiac dysfunction: a 'dual-hit'. *Exp Clin Cardiol* 2011; **16:** 70-4.
40. Ng R, Better N, Green MD. Anticancer agents and cardiotoxicity. *Semin Oncol* 2006; **33:** 2-14.
41. Antman EM. Decision making with cardiac troponin tests. *N Engl J Med* 2002; **346:** 2079-82.
42. Cardinale D, Colombo A, Torrisi R, Sandri MT, Civelli M, Salvatici M, et al. Trastuzumab-induced cardiotoxicity: clinical and progonostic implications of troponin I evaluation. *J Clin Oncol* 2010; **28:** 3910-6.
43. Seino Y, Ogawa A. Application of NT-proBNP and BNP measurements in cardiac care: a more discerning marker for the detection and evaluation of heart failure. *Eur J Heart Fail* 2004; **6:** 295-300.
44. Sengupta PP, Northfelt DW, Gentile F, Zamorano JL, Khandheria BK. Trastuzumab-induced cardiotoxicity: Heart failure at the crossroads. *Mayo Clin Proc* 2008; **83:** 197-203.
45. Gianizzi P, Temporelli PL, Bosimini E, Silva P, Imparato A, Corra U, et al. Independent and incremental prognostic value of Doppler-derived mitral deceleration time of early filling in both symptomatic and asymptomatic patients with left ventricular dysfunction. *J Am Coll Cardiol* 1996; **28:** 383-90.

46. Suzuki J, Yanagisawa A, Shigejama T, Tsubota J, Yasumura T, Shimoyama K, et al. Early detection of anthracycline-induced cardiotoxicity by radionuclide angiocardiography. *Angiology* 1999; **50:** 37-45.

47. Cochet A, Quilichini G, Dygai-Cochet I, Touzery C, Toubeau M, Berriolo-Riedinger A, et al. Baseline diastolic dysfunction as a predictive factor of trastuzumab-mediated cardiotoxicity after adjuvant anthracycline therapy in breast cancer. *Breast Cancer Res Treat* 2011; **130:** 845-54.

48. Gulati VK, Katz WE, Follansbee WP, Gorcsan J. Mitral annular descent velocity by tissue Doppler echocardiography as an index of global left ventricular function. *Am J Cardiol* 1996; **77:** 979-84.

49. Benvenuto GM, Ometto R, Fontanelli A, Fortunato A, Ruffini PA, Fosser V, et al. Chemotherapy related cardiotoxicity: new diagnostic and preventive strategies. *Ital Heart J* 2003; **4:** 655-67.

50. Redfield MM, Jacobsen SJ, Burnett JC Jr, Mahoney DW, Bailey KR, Rodeheffer RJ. Burden of systolic and diastolic ventricular dysfunction in the community: appreciating the scope of the heart failure epidemic. *JAMA* 2003; **289:** 194-202.

51. Effect of enalapril on mortality and the development of heart failure in asymptomatic patients with reduced left ventricular ejection fractions. The SOLVD Investigators. *N Engl J Med* 1992; **327:** 685-91.

research article

Lung scintigraphy in the diagnosis of pulmonary embolism: current methods and interpretation criteria in clinical practice

Ajda Skarlovnik[1], Damjana Hrastnik[2], Jure Fettich[3], Marko Grmek[3]

[1] Department for Vascular Diseases, Ljubljana University Medical Centre, Ljubljana, Slovenia
[2] Department for Nuclear Medicine, Celje General Hospital, Celje, Slovenia
[3] Department for Nuclear Medicine, Ljubljana University Medical Centre, Ljubljana, Slovenia

Radiol Oncol 2014; 48(2): 113-119.

Received: 3 April 2013
Accepted: 18 August 2013

Correspondence to: Assist. Prof. Marko Grmek, M.D., Ph.D., Department for Nuclear Medicine, University Medical Centre Ljubljana, Zaloška 2, 1000 Ljubljana, Slovenia. E-mail: marko.grmek@kclj.si

Disclosure: No potential conflicts of interest were disclosed.

Background. In current clinical practice lung scintigraphy is mainly used to exclude pulmonary embolism (PE). Modified diagnostic criteria for planar lung scintigraphy are considered, as newer scitigraphic methods, especially single photon emission computed tomography (SPECT) are becoming more popular.

Patients and methods. Data of 98 outpatients who underwent planar ventilation/perfusion (V/Q) scintigraphy and 49 outpatients who underwent V/Q SPECT from the emergency department (ED) were retrospectively collected. Planar V/Q images were interpreted according to 0.5 segment mismatch criteria and revised PIOPED II criteria and perfusion scans according to PISA-PED criteria. V/Q SPECT images were interpreted according to the criteria suggested in EANM guidelines. Final diagnosis of PE was based on the clinical decision of an attending physician and evaluation of a 12 months follow-up period.

Results. Using 0.5 segment mismatch criteria and revised PIOPED II, planar V/Q scans were diagnostic in 93% and 84% of cases, respectively. Among the diagnostic planar scans readings specificity for 0.5 segment mismatch criteria was 98%, and 99% for revised PIOPED II criteria. V/Q SPECT showed a sensitivity of 100% and a specificity of 98%, without any non-diagnostic cases. In patients with low pretest probability for PE, planar V/Q scans assessed by 0.5 segment mismatch criteria were diagnostic in 92%, and in 85% using revised PIOPED II criteria, while perfusion scintigraphy without ventilation scans was diagnostic in 80%.

Conclusions. Lung scintigraphy yielded diagnostically definitive results and is reliable in ruling out PE in patients from ED. V/Q SPECT has excellent specificity and sensitivity without any non-diagnostic results. Percentage of non-diagnostic results in planar lung scintigraphy is considerably smaller when 0.5 segment mismatch criteria instead of revised PIOPED II criteria are used. Diagnostic value of perfusion scintigraphy according to PISA-PED criteria is inferior to combined V/Q scintigraphy; the difference is evident especially in patients with low pretest probability for PE.

Key words: pulmonary embolism; lung scintigraphy; interpretation criteria; 0.5 segment mismatch criteria

Introduction

Pulmonary embolism (PE) remains a diagnostic challenge. With the development of modern diagnostic methods, the role of lung scintigraphy in the work up of patients with suspected PE has also changed. In current clinical practice lung scintigraphy is mainly used to exclude PE.[1,2] Recently developments in scintigraphic methods have been made, as well as modified criteria for the interpretation of scans.

For many years, chest radiographs and ventilation/perfusion (V/Q) scintigraphy have been the primary imaging modalities used in the evaluation of patients with suspected acute PE. The revised PIOPED criteria for V/Q scintigraphy currently in

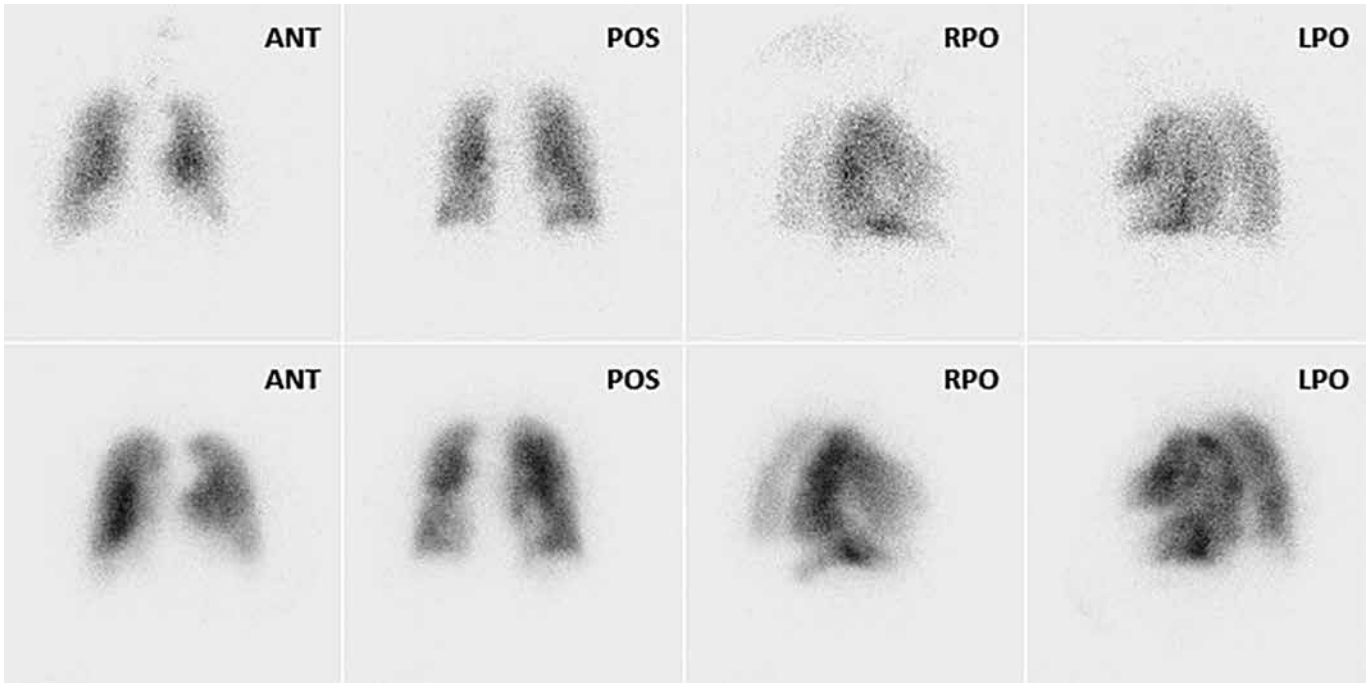

FIGURE 1. Planar perfusion scintigrams (lower row) with abnormalities, partly matched with abnormalities on planar ventilation scintigrams (upper row) are presented in the picture. The case was assessed as PE negative according to 0,5 segment mismatch criteria, and as non-diagnostic when PIOPED criteria were used. Using PISA-PED criteria the study was assessed as PE positive. (ANT = anterior, POS = posterior, RPO = right posterior oblique, LPO = left posterior oblique). After 12 month follow up the case was closed as PE negative.

use have a reported sensitivity of 41% and a specificity of 97%.[3] A major problem in clinical practice is the large percentage of scans falling in the category of intermediate (indeterminate) probability of PE.[3,4]

Advances in computed tomographic pulmonary angiography (CTPA) have enabled the direct visualization of PE. This technique has emerged as an important diagnostic tool in the evaluation of patients with suspected PE, almost completely replacing scintigraphy in clinical practice in some hospitals.[5-8] However, the suitability of CTPA as a primary diagnostic modality is questionable primarly because of the radiation exposure, certain contraindications and significant percentage of false positive results. In a group of patients with low pretest probability of PE, CTPA gave false positives in as many as 42% of cases.[9]

In 1995 the PISA–PED (Prospective Investigative Study of Acute Pulmonary Embolism Diagnosis) study re-evaluated the role of perfusion scintigraphy alone. According to PISA-PED criteria the perfusion scans were classified into normal, abnormal compatible with PE and abnormal not compatible with PE.[10] A sensitivity of 92% and a specificity of 87% was reported. In retrospective analysis of data from PIOPED II, perfusion scintigraphy assessed according to PISA-PED criteria, and combined with chest radiography had a sensitivity of 80% and specificity of 96%, none of the study were non-diagnostic.[11]

In 2007 Howarth *et al.* suggested that a more than 0.5 segment V/Q mismatch is sufficient for diagnosis of PE and that such a simplified approach could also reduce the percentage of non-diagnostic scans.[12]

The 2009 European Association for Nuclear Medicine (EANM) guidelines for V/Q lung scintigraphy strongly support the use of Single Photon Emission Computed Tomography (SPECT) V/Q scintigraphy.[13,14] Studies have shown that SPECT has a greater sensitivity and specificity, and a lower number of inconclusive results in the detection of pulmonary embolism compared to planar scans. However, there are several challenges that must be overcome for V/Q SPECT to be successful, including shortening of the acquisition time and a different approach in image reporting.[15,16]

The objective of this study was to assess the diagnostic value of lung scintigraphy in outpatients with suspected acute PE using 0.5 segment V/Q mismatch criteria, revised PIOPED II criteria, PISA-PED criteria and V/Q SPECT.

Our aim was: 1. to evaluate the role of V/Q SPECT in the diagnostic algorithm of acute PE; 2.

TABLE 1. Criteria used for planar lung scans interpretation in patients with suspicion of acute pulmonary embolism: 0.5 segment mismatch criteria, revised PIOPED II criteria and PISA-PED criteria. (* prominent hilum, cardiomegaly, elevated diaphragm, linear atelectasis or costophrenic angle effusion)

	0.5 segment mismatch criteria	Revised PIOPED II criteria	PISA-PED criteria
PE positive	≥2 segments of V/Q mismatch ≥3 V/Q mismatch defects >50% of segment	≥2 segments of V/Q mismatch	≥1 wedge-shaped Q defect(s) corresponding to anatomic regions of the lung
PE negative	Nonsegmental perfusion abnormalities* Q defect smaller than corresponding radiographic lesion 1 V/Q mismatch defect ≤50% of segment Stripe sign	Nonsegmental perfusion abnormalities* Q defect smaller than corresponding radiographic lesion ≥2 matched V/Q defects with regionally normal chest radiograph 1-3 small segmental perfusion defects (<25% of segment) Solitary triple matched defect in the mid or upper lung zone confined to a single segment Stripe sign Large pleural effusion	Other than wedge shaped Q defects Presence of impressions caused by enlarged heart, hila or mediastinum on an otherwise normal scan No Q defects
Nondiagnostic	All other findings	All other findings	All other findings

PE = pulmonary embolism; V/Q = ventilation / perfusion

to assess the use of new simplified criteria based on >0.5 segment V/Q mismatch and 3. to assess the value of planar perfusion lung scintigraphy (without ventilation scans) in excluding PE, especially in patients with low pretest probability.

Patients and methods

The study was retrospective and approved by the National Medical Ethics Committee.

Patients

Two groups of patients were included in this study. The first group consisted of 98 randomly selected outpatients who were presented in 2010 to the Internistic Emergency Department (IPP) of University Medical Centre in Ljubljana with suspicion of acute PE. In all of the patients a planar V/Q scintigraphy was performed at the Department for Nuclear Medicine in Ljubljana. The second group consisted of 49 randomly selected outpatients who presented in 2010 to IPP of the General Hospital in Celje with suspicion of acute PE and had a V/Q SPECT performed in the Department for Nuclear Medicine in Celje.

Patients with technically inadequate scans, younger than 18 years, on anticoagulant therapy, pregnant women and patients who could not be followed up for 12 months were not included in the study.

Pretest probability was assessed according to Wells' criteria. D-dimer values were obtained when possible. All patients also had a chest X-ray at the time of presentation.

Lung scintigraphy

Planar ventilation study. Technegas was used for ventilation studies. Images were acquired in the sitting position if possible, in at least four standard projections: posterior, anterior, left and right posterior oblique. The camera was equipped with a low-energy high-resolution (LEHR) collimator. A 256 x 256 pixel matrix was used. The predefined total image acquisition time was 90 seconds, in rare cases it was prolonged (up to 180 seconds).

Planar perfusion study. 99mTc - Macro Aggregated Albumin (99mTc-MAA) in activity 120–200 MBq was administered intravenously to patients in the supine position. Images were acquired in the sitting position if possible, in at least four standard projections: posterior, anterior, left and right posterior oblique. The camera was equipped with a LEHR collimator. A 256 x 256 pixel matrix was selected for accumulation of at least 600 000 counts per image.

V/Q SPECT. Inhalation of Technegas (approximately 20 – 40 MBq accumulated in the lung) and in-

TABLE 2. Number and percentage of PE negative, non - diagnostic and PE positive readings when lung scans were interpreted using 0.5 segment mismatch criteria, revised PIOPED II criteria or PISA-PED criteria and V/Q SPECT

Reading criteria (method)	N	PE negative readings	Non-diagnostic readings	PE positive readings
0.5 segment mismatch (planar V/Q scintigraphy)	98	84 (86%)	7 (7%)	7 (7%)
Revised PIOPED II (planar V/Q scintigraphy)	98	78 (80%)	16 (16%)	4 (4%)
PISA-PED (planar Q scintigraphy)	98	68 (69%)	21 (22%)	9 (9%)
V/Q SPECT	49	39 (80%)	0 (0%)	10 (20%)

PE = pulmonary embolism; V/Q = ventilation / perfusion

jection of 99mTc-MAA (activity 100–125 MBq) were administered to patient in the supine position. A dual head gamma camera was used, with a total acquisition time of 20 min. 128 projections (64/head) were acquired. The camera was equipped with a LEHR collimator and a 64 x 64 pixel matrix was used.

Interpretation criteria. Planar lung scans were interpreted independently by 2 qualified nuclear medicine physicians. First, the perfusion scans were interpreted according to PISA-PED criteria with the chest X-ray available but without knowledge of the ventilation data.[10] This was followed by addition of ventilation data analysis using revised PIOPED criteria.[4] Separately, V/Q scans were then again interpreted according to 0.5 segment mismatch criteria (Table 1, Figure 1).

V/Q SPECT images were interpreted strictly according to the criteria from EANM guidelines.[13,14] The total extent of perfusion abnormalities compatible with PE was calculated and reported in per cent.

Final diagnosis

Patient's final diagnosis was a composite diagnosis based on the clinical decision of the attending physician and evaluation of the 12 months follow-up period when results of all performed investigations (for example CTPA) were taken in consideration.

Results

Pretest probability and PE prevalence estimated by final diagnosis

In the first group of 98 outpatients (median age 71 years) who underwent planar V/Q scintigraphy, 4 patients (4%) had high, 32 patients (33%) moderate and 62 patients (63%) low pretest probability for PE. 8 patients (8%) had a final diagnosis of acute PE. 7 patients were given anticoagulant therapy by their attending physician and 1 patient was diagnosed with deep venous thrombosis and PE (on CTPA) in the next two weeks, and was subsequently given anticoagulant therapy. 90 patients (92%) did not have a final diagnosis of acute PE and did not receive anticoagulant therapy within the follow-up period.

In the second group of 49 patients (median age 72 years) who underwent V/Q SPECT, 2 patients (4%) had high, 14 patients (29%) moderate and 33 patients (67%) low pretest probability. 9 patients (18%) had a final diagnosis of acute PE and were given anticoagulant therapy. 40 patients (82%) did not have a final diagnosis of acute PE and did not receive anticoagulant therapy within the follow-up period.

Lung scintigraphy

The results of scans readings using 0.5 segment mismatch criteria, revised PIOPED II criteria, PISA-PED criteria or V/Q SPECT are presented in Table 2. When assessing planar V/Q scans according to 0.5 segment mismatch criteria, 84 scans (86%) were read as PE negative, 7 scans (7%) were read as PE positive and 7 scans (7%) were non-diagnostic. When assessing planar V/Q scans according to PIOPED criteria, 78 scans (80%) were read as PE negative, 4 scans (4%) were read as PE positive and 16 scans (16%) were non-diagnostic. When assessing planar perfusion scans according to PISA-PED criteria, 68 scans (69%) were read as PE negative, 9 scans (9%) were read as PE positive and 21 scans (22%) were non-diagnostic. When assessing V/Q SPECT scans according to EANM guidelines, 39 scans (80%) were read as PE negative, 10 scans (20%) were read as PE positive and none of the investigation was non-diagnostic.

Diagnostic value of lung scintigraphy using different interpretative criteria

Positive predictive value (PPV) and negative predictive value (NPV) for lung scintigraphy are pre-

TABLE 3. Positive predictive value (PPV) and negative predictive value (NPV) for 0.5 segment mismatch criteria, revised PIOPED II criteria, PISA-PED criteria and V/Q SPECT in lung scans interpretations are presented in the table

Reading criteria (method)	Diagnostic readings	PPV	NPV
0.5 segment mismatch (planar V/Q scintigraphy)	93% (91/98)	71% (5/7)	99% (83/84)
Revised PIOPED II (planar V/Q scintigraphy)	84% (82/98)	75% (3/4)	99% (77/78)
PISA-PED (planar Q scintigraphy)	78% (77/98)	56% (5/9)	99% (67/68)
V/Q SPECT	49/49 (100%)	90% (9/10)	100% (39/39)

PE = pulmonary embolism; V/Q = ventilation / perfusion

TABLE 4. Number and percentage of PE negative, non- diagnostic and PE positive studies in patients with low pretest probability for PE when lung scans were interpreted according to 0.5 segment mismatch criteria, revised PIOPED II criteria or PISA-PED criteria

Reading criteria (method)	N	PE negative readings	Non-diagnostic readings	PE positive readings
0.5 segment mismatch (planar V/Q scintigraphy)	62	55 (89%)	5 (8%)	2 (3%)
Revised PIOPED II (planar V/Q scintigraphy)	62	51 (82%)	9 (15%)	2 (3%)
PISA-PED (planar Q scintigraphy)	62	43 (70%)	13 (20%)	6 (10%)

PE = pulmonary embolism; V/Q = ventilation / perfusion

sented in Table 3. When assessing planar V/Q scans according to 0.5 segment mismatch criteria, 91 patients (93%) had diagnostic (PE positive or PE negative) result, the PPV was 71% (5/7), while the NPV was 99% (83/84). If only diagnostic scans readings were taken into consideration the sensitivity was 83% and the specificity 98%. When assessing planar V/Q scans according to revised PIOPED II criteria, 82 patients (84%) had diagnostic result, the PPV was 75% (3/4), while the NPV was 99% (77/78). If only diagnostic scans readings were taken into consideration the sensitivity was 75% and the specificity 99%. When assessing planar perfusion scans according to PISA-PED criteria, 77 patients (78%) had diagnostic result, the PPV was 56% (5/9), while the NPV was 99% (67/71). If only diagnostic scans readings were taken into consideration the sensitivity was 83% and the specificity 94%. When using V/Q SPECT, all patients had diagnostic (PE positive or PE negative) result. The sensitivity was 100%, specificity 98%, PPV 90% and NPV 100%.

Sensitivity of PE positive scan readings and specificity of PE negative scan readings in patients with low pretest probability for PE

In the subgroup of 62 patients with low pretest probability for PE only two patients had PE. Planar scans assessed according to 0.5 segment mismatch, revised PIOPED II and PISA-PED criteria gave definitive readings in 57 patients (92%), 53 patients (85%) and 49 patients (80%), respectively (Table 4). Among patients with definitive scan readings, the sensitivity of PE positive scan findings was 100% with all reading criteria, but PPV for PISA-PED criteria was only 33% (2/6). The specificity of PE negative scan findings was 100%, 100% and 91% (43/47), respectively.

Discussion

Our study population consisted of outpatients with a predominantly low pretest probability for PE. Therefore it is not surprising that the prevalence of PE in the group of 98 patients who underwent planar scintigraphy was low (9%) and was comparable to that in the population studied by Howarth (13%).[12] In the group of 49 patients who underwent V/Q SPECT the prevalence of PE was similar to that in the PIOPED II study (19%).[17]

Two thirds of patients had a low pretest probability and 4% had a high pretest probability according to Wells' criteria, while in PIOPED II study 56% of the patients included had low and 6% had high pretest probability.[18]

Diagnostic value of planar V/Q scintigraphy

We found out that specificity and NPV of planar V/Q scintigraphy using 0.5 segment mismatch or

revised PIOPED II criteria were very good. The results were comparable to the results of PIOPED II and other planar V/Q studies.[3,17,19,20,21] In our study only one patient with PE negative scan reading according to 0.5 segment mismatch criteria and revised PIOPED criteria was later diagnosed with PE. This patient had a high pretest probability – discrepancy between the clinical probability and imaging results was present.

The percentage of non-diagnostic V/Q planar studies in our study (assessed by revised PIOPED criteria) was considerably lower than in the PIOPED II study (16% *vs.* 26.5%), where the studied population was already heavily weighted towards outpatients. When we used 0.5 segment mismatch criteria, the number of non-diagnostic scans was further reduced and did not exceed 8%. This represents a significant improvement in comparison to PIOPED criteria (16% of non-diagnostic scans).

V/Q SPECT

In our study, V/Q SPECT showed excellent sensitivity, specificity and NPV, comparable to results from other studies, where sensitivities ranged from 80% – 100% and specificities from 93% - 100%.[22,23] V/Q SPECT enables better detection of perfusion defects on the subsegmental level, especially in medial parts of lung. Several studies show better sensitivity and significantly less non-diagnostic results with SPECT than with planar scintigraphy but similar specificity.[14,22,23,24]

Total acquisition times for V/Q SPECT have now decreased to 20-30 minutes for dual head cameras and to 14-20 min for triple head cameras.[25,26] A further option in the workup for acute PE could be use of perfusion SPECT imaging without ventilation. In certain subgroups of patients, *i.e.* in patients with a low pretest probability and normal chest radiographs or pregnant women, ventilation scintigraphy could be performed on following day when needed.

Perfusion scintigraphy without ventilation

Our results of planar perfusion lung scans readings by PISA-PED criteria were non-diagnostic in a considerably larger percentage compared to V/Q scintigraphy interpreted either by PIOPED or 0.5 segment mismatch criteria (22% *vs.* 16% and 7%, respectively). The percentage of non-diagnostic results was also larger than in the PISA-PED study and retrospective analysis of perfusion scans from PIOPED II study.[17]

Lung scintigraphy in patients with low pretest probability for PE

Using 0.5 segment mismatch criteria for V/Q scan interpretation 8% of cases were non-diagnostic, and 15% if revised PIOPED II criteria were used. So we recommend the use of 0.5 segment mismatch criteria for scans readings in patients with low pretest probability PE. By using perfusion scintigraphy according to PISA-PED, 20% of investigations were non-diagnostic. There were also 4 false positive results when only lung perfusion scintigraphy was used and none using V/Q scintigraphy. Therefore, our results do not support routine use of only perfusion scintigraphy in patients with low pretest clinical probability. Results based on only perfusion scintigraphy could possibly be improved by gaining more experience with the PISA-PED methodology. Recently, a Chinese multicenter study including 544 patients was published[27], in which perfusion scintigraphy assessed according to PISA PED criteria showed no non-diagnostic results, with a sensitivity of 86% and a specificity of 81%.

Lung scintigraphy and the diagnostic algorithm for acute PE in outpatients

In all patients with suspected acute PE, assessment of pretest probability according to Wells' criteria is strongly recommended.[28] Depending on clinical probability, especially D-dimer, further diagnostic imaging is indicated. Echocardiography and Duplex examination of lower extremity veins are now standard and easily accessible in an ED clinical setting.

According to our results, planar V/Q scintigraphy can reliably rule out PE. Its results are not inferior to CTA[9] and could be recommended as the imaging test of choice first of all in patients with a low clinical probability. Use of planar perfusion scintigraphy alone might be considered in patients who cannot ventilate adequately and those with normal findings on plain chest radiograph.[29,30] Excellent diagnostic accuracy of V/Q SPECT and reduction of the acquisition time make this method clinically useful for diagnosis of acute PE in an ED setting also in patients with higher clinical probability.[31]

Additional workup is necessary when the clinical probability is inconsistent with the imaging results regardless of used modality.

Conclusions

In the outpatient population of an emergency department PE can be reliably ruled out using planar V/Q lung scintigraphy or V/Q SPECT.

V/Q SPECT has excellent sensitivity and specificity without non-diagnostic results.

Percentage of non-diagnostic results in planar lung scintigraphy is considerably smaller when 0.5 segment mismatch criteria instead of revised PIOPED II criteria are used.

Diagnostic value of perfusion scintigraphy according to PISA-PED criteria is inferior to combined V/Q scintigraphy; the difference is evident especially in patients with low pretest probability for PE.

References

1. British Thoracic Society Standards of Care Committee Pulmonary Embolism Guideline Development Group. British Thoracic Society guidelines for the management of suspected acute PE. *Thorax* 2003; **58:** 470-83.
2. Kluetz PG, White CS. Acute Pulmonary embolism: imaging in the emergency department. *Rad Clin N Am* 2006; **44:** 259-71.
3. The PIOPED Investigators. Value of the ventilation/perfusion scan in acute pulmonary embolism. Results of the prospective investigation of pulmonary embolism diagnosis (PIOPED). *JAMA* 1990; **263:** 2753-9.
4. Stein PD, Woodard PK, Weg JG, Wakefield TW, Tapson VF, Sostman HD, et. al. PIOPED II investigators. Diagnostic pathways in acute pulmonary embolism: reccomendations of the PIOPED II investigators. *Am J Med* 2006; **119:** 1048-55.
5. Stein PD, Sostman HD, Bounameaux H, Buller HR, Chenevert TL, Dalen JE, et al. Challenges in the diagnosis acute pulmonary embolism. *Am J Med* 2008; **121:** 565-71.
6. Musset D, Parent F, Meyer G, Maitre S, Girard P, Leroyer C, et al. Diagnostic strategy for patients with suspected pulmonary embolism: a prospective multicentre outcome study. *The Lancet* 2002; **360:** 1914-20.
7. Van Rossum AB, Pattynama PM, Ton ER, Treurniet FE, Arndt JW, van Eck B, et al. Pulmonary embolism: validation of spiral CT angiography in 149 patients. *Radiology* 1996; **201:** 467-70.
8. Bešlić Š, Dalagija F, Đurović V. Multislice computed tomography of pulmonary embolism: spectrum of findings. *Radiol Oncol* 2005; **39:** 101-14.
9. Stein PD, Fowler SE, Goodman LR, Gottschalk A, Hales CA, Hull RD, et al. Multidetector computed tomography for acute pulmonary embolism. *N Engl J Med* 2006; **22:** 2317-27.
10. Miniati M, Pistolesi M, Marini C, Di Ricco G, Formichi B, Prediletto R, et al. Value of perfusion lung scan in the diagnosis of pulmonary embolism: results of the prospective investigative study of acute pulmonary embolism diagnosis (PISA-PED). *Am J Respir Crit Care Med* 1996; **154:** 1387-93.
11. Miniati M, Sostman HD, Gottschalk A, Monti S, Pistolesi M. Perfusion lung scintigraphy for the diagnosis of pulmonary embolism: a reappraisal and review of the prospective investigative study of acute pulmonary embolism diagnosis methods. *Sem Nucl Med* 2008; **38:** 450-61.
12. Howarth DM, Booker JA, Voutnis DD. Diagnosis of pulmonary embolus using ventilation/perfusion lung scintigraphy: more than 0,5 segment of ventilation/perfusion V/Q mismatch is sufficient. *Intern Med J* 2006; **36:** 281-8
13. Bajc M, Neilly JB, Miniati M, Schuemichen C, Meignan M, Jonson B. EANM guidelines for ventilation/perfusion scintigraphy Part 1. Pulmonary imaging with ventilation/perfusion single photon emission tomography. *Eur J Nucl Med Mol Imaging* 2009; **36:** 1356-70.
14. Bajc M, Neilly JB, Miniati M, Schuemichen C, Meignan M, Jonson B. EANM guidelines for ventilation/perfusion scintigraphy Part 2. Algorithms and clinical considerations for diagnosis of pulmonary emboli with V/P SPECT and MDCT. *Eur J Nucl Med Mol Imaging* 2009; **36:** 1528-38.
15. Reinartz P, Wildberger JE, Schaefer W, Nowak B, Mahnken AH, Buell U. Tomographic imaging in the diagnosis of pulmonary embolism: a comparison between V/Q lung scintigraphy in SPECT technique and multislice spiral CT. *J Nucl Med* 2004; **45:** 1501-8.
16. Jögi J, Jonson B, Ekberg M, Bajc M. V/P SPECT with ^{99}Tc-DTPA versus Technegas: a head-to-head study in obstructive and nonobstructive disease. *J Nucl Med* 2010; **5:** 735-41.
17. Sostman HD, Miniati M, Gottschalk A, Matta F, Stein PD, Pistolesi M. Sensitivity and specificity of perfusion scintigraphy combined with chest radiography for acute pulmonary embolism in PIOPED II. *J Nucl Med* 2008; **49:** 1741-48.
18. Stein PD, Beemath A, Matta F, Weg JG, Yusen RD, Hales CA, et al. Clinical characteristics of patients with acute pulmonary embolism: data from PIOPED II. *Am J Med* 2007; **120:** 871-9.
19. Sostman HD, Stein PD, Gottschalk A, Matta F, Hull R, Goodman L. Acute pulmonary embolism: sensitivity and specificity of ventilation-perfusion scintigraphy in PIOPED II study. *Radiology* 2008; **246:** 941-6.
20. Anderson DR, Kahn SR, Rodger MA, Kovacs MJ, Morris T, Hirsch A. Computed tomographic pulmonary angiography vs ventilation–perfusion lung scanning in patients with suspected pulmonary embolism. *JAMA* 2007; **298:** 2743-53.
21. Stein PD, Henry JW, Gottschalk A. Mismatched vascular defects. An easy alternative to mismatched segmental equivalent defects for the interpretation of ventilation/perfusion lung scans in pulmonary embolism. *Chest* 1993; **104:** 1468-72.
22. Collart JP, Roelants V, Vanpee D, Lacrosse M, Trigaux JP, Delaunois L, et al. Is a lung perfusion scan obtained by using single photon emission computed tomography able to improve the radionuclide diagnosis of pulmonary embolism? *Nucl Med Commun* 2002; **23:** 1107-13.
23. Stein PD, Freeman LM, Sostman HD, Goodman LR, Woodard PK, Naidich DP, et al. SPECT in acute pulmonary embolism. *J Nucl Med* 2009; **50:** 1999-2007.
24. Bajc M. Value of ventilation/perfusion SPECT detecting extensive pulmonary embolism in patient with pneumonia. *Thromb Haemost* 2005; **93:** 993-4.
25. Stein PD, Goodman LR, Hull RD, Dalen JE, Matta F. Diagnosis and management of isolated subsegmental pulmonary embolism: review and assessment of the options. *Clin App Thromb Haem* 2012; **18:** 20-6.
26. Reinartz P, Schirp U, Zimny M, Sabri O, Nowak B, Schäfer W, et al. Optimizing ventilation-perfusion lung scintigraphy: parting with planar imaging. *Nuklearmedizin* 2001; **40:** 38-43.
27. He J, Wang F, Dai HJ, Li M, Wang Q, Yao Z, et al. Chinese multi-center study of lung scintigraphy and CT pulmonary angiography for the diagnosis of pulmonary embolism. *Int J Cardiovasc Imaging* 2012; **28:** 1799-805.
28. Miniati M, Bottai M, Monti S. Comparison of three clinical models for predicting the probability of pulmonary embolism. *Medicine (Baltimore)* 2005; **84:** 107-14.
29. Stein PD, Sostman HD, Dalen JE, Bailey DL, Bajc M, Goldhaber SZ. Controversies in diagnosis of pulmonary embolism. *Clin App Thromb Haem* 2011; **17:** 140-9.
30. Glaser JE, Chamarthy M, Haramati LB, Esses D, Freeman LM. Successful and safe implementation of a trinary interpretation and reporting strategy for V/Q lung scintigraphy. *J Nucl Med* 2011; **52:** 1508-12.
31. Sostman HD, Pistolesi M. Scintigraphy for pulmonary embolism: too old to rock'n roll, too young to die? *J Nucl Med* 2011; **52:** 1505-7.

research article

Detection of neuroendocrine tumours in the small intestines using contrast-enhanced multiphase Ga-68 DOTATOC PET/CT: the potential role of arterial hyperperfusion

Nils F. Schreiter[1], Martin Maurer[2], Ulrich-Frank Pape[3], Bernd Hamm[2], Winfried Brenner[1], Vera Froeling[2]

[1] Department of Nuclear Medicine, Charité, Berlin, Germany
[2] Department of Radiology, Charité, Berlin, Germany
[3] Department of Gastroenterology, Charité, Berlin, Germany

Radiol Oncol 2014; 48(2): 120-126.

Received: 27 August 2013
Accepted: 24 October 2013

Correspondence to: Nils F. Schreiter M.D., Department of Nuclear Medicine, Charité, Augustenburger Platz 1, 13353 Berlin, Germany. Phone: +49 30 450 657 299; E-mail: nils.schreiter@charite.de

Disclosure: No potential conflicts of interest were disclosed.

Background. Interpretation of small intestinal neuroendocrine tumours (NETs) by Ga-68 DOTATOC PET/CT can be difficult. The potential benefit of arterial hyperperfusion for the detection of NETs was evaluated.

Methods. Between 2006 and 2009, 320 consecutive Ga-68 DOTATOC PET/CT examinations, performed for NETs, revealed 40 lesions suggesting intestinal NETs in 25 patients. Two groups of lesions were distinguished: epigastric lesions evaluable in the arterial and venous CT scan (Group 1) and hypogastrial lesions evaluable in the venous CT scan only (Group 2). Lesions were jointly rated by two radiologists and a nuclear medicine physician. Maximum standard uptake values (SUVmax) of lesions and background were assessed. The reference standard was histology (available for 28 lesions) or follow-up (for a mean of 22.9 months).

Results. PET detected all suspicious lesions but was false positive in 3 lesions. In Group 1 the arterial scan performed significantly better than the venous scan ($p = 0.008$). Diagnostic performance was better in Group 1 than in Group 2 ($p < 0.001$). SUVmax of true positive lesions were significantly higher than background SUVmax ($p < 0.001$) and SUVmax of false positive lesions ($p = 0.005$).

Conclusions. The arterial phase of multiphase Ga-68 DOTATOC PET/CT might improve the localization of intestinal NETs and, thereby, improve the overall diagnostic accuracy of this modality in the assessment of intestinal NETs by adding information about lesion perfusion not available when only venous CT is performed.

Key words: Ga-68 DOTATOC PET/CT; small intestine; neuroendocrine tumors; arterial phase CT

Introduction

Neuroendocrine tumours (NETs) are a heterogeneous group of neoplasms of neuroendocrine origin.[1] The annual incidence is low at 1-2/100 000 people.[2] Two thirds of all NETs are found in the gastrointestinal tract including the pancreas and the hepatobiliary system (very rare).[3] An increasing incidence of these tumours has been detected over the last 20 years, which is partially attributable to advances in diagnostic modalities.[4,5] A promising approach for diagnosis and therapy is somatostatin receptor targeting.

Ga-68-DOTA(0)-Phe(1)-Tyr(3)-octreotide (Ga-68 DOTATOC) is a somatostatin analogue with affinity for somatostatin receptor 2 (SSTR-2) and has a higher sensitivity and specificity than the current gold standard, single photon emission computed tomography (SPECT) with the somatostatin analogue In-111 diethylene triamine pentaacetic

acid octreotide (In-111 DTPA octreotide).[6] Ga-68 DOTATOC positron emission tomography (PET) has been found to detect significantly more lesions than In-111 DTPA octreotide SPECT.[7] A major advantage of Ga-68 DOTATOC PET/CT is that it combines somatostatin receptor imaging with a full contrast-enhanced multiphase computed tomography (CT) scan. While somatostatin receptor imaging has high specificity, the CT scan provides good image resolution and enables a dynamic evaluation following contrast medium administration, which improves the detection of small NETs.[8,9] A drawback of CT is that it relies on lesion size and enhancement characteristics for lesion characterization, which has low specificity.[10]

Ruf *et al.* have shown that multiphase Ga-68 DOTATOC PET/CT has a significant impact on the patient's management with PET and CT providing complementary information.[11] Other authors also report an impact on the patient's management.[12,13] In the study by Ruf *et al*., CT was significantly superior to PET in detecting the small number of 17 intestinal NETs, which the authors attributed to the difficulty in differentiating between physiologic intestinal accumulation of Ga-68 DOTATOC and abnormal accumulation of this tracer in intestinal NETs.[11] For liver metastases of NETs and for NET primaries in the pancreas the value of multiphase CT has already been described.[14-20] As far as we know the value of arterial hyperperfusion of NETs in the small intestines and how it can be exploited in diagnostic imaging has never been investigated before.

The aim of the present study is to investigate whether contrast-enhanced multiphase PET/CT in general, and the arterial phase in particular, have an added benefit for the detection of NETs in the small intestines.

Patients and methods

We retrospectively analyzed the records of 320 Ga-68 DOTATOC PET/CT examinations performed at our department from 2006 to 2009 for the diagnostic evaluation of patients with NETs. An experienced specialist in nuclear medicine identified 25 patients (12 males, 13 females; age range: 35-79 years; mean: 56.5 years, median: 56 years) with 40 findings suggesting primary NETs in the small intestine. There were 16 patients with cancer of unknown primary (CUP) in whom the examination was performed to search for the primary tumour and 9 patients who underwent PET/CT for staging. Only one examination per patient was included in this study.

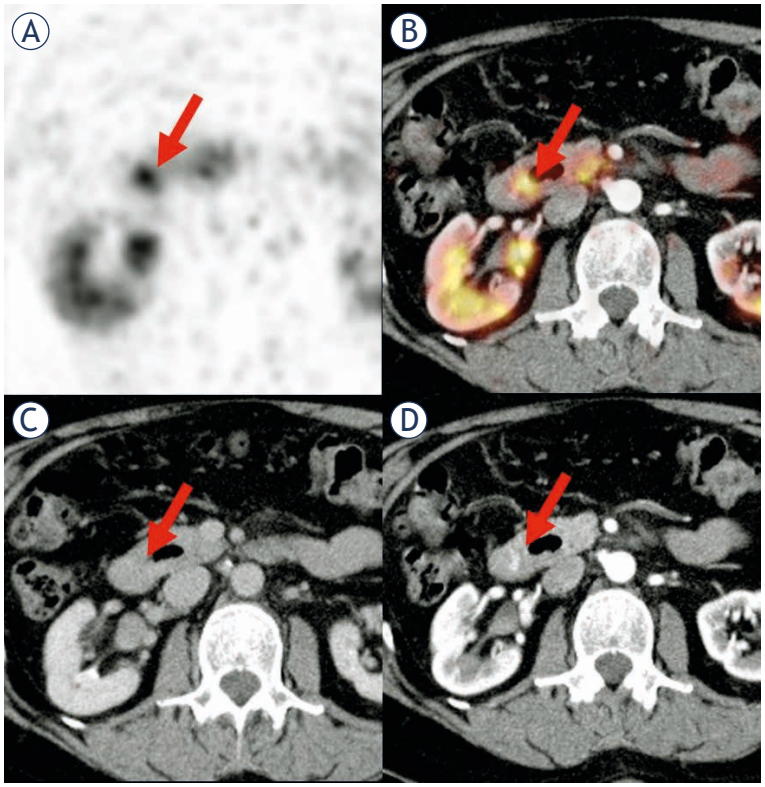

FIGURE 1. Suspicious Ga-68-DOTATOC PET lesion (#2) **(A)** located in the duodenum **(B)** without a clear correlate in the venous-phase CT **(C)**, but arterial hyperperfusion **(D)**.

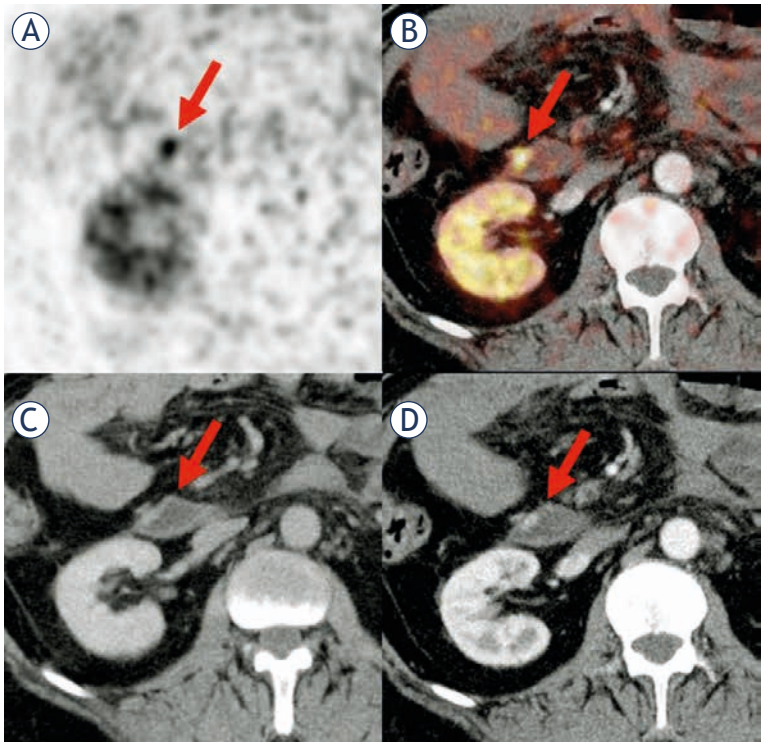

FIGURE 2. Another suspicious Ga-68-DOTATOC PET lesion (#11) **(A)** located in the duodenum **(B)** without a clear correlate in the venous-phase CT **(C)**, but arterial hyperperfusion **(D)**.

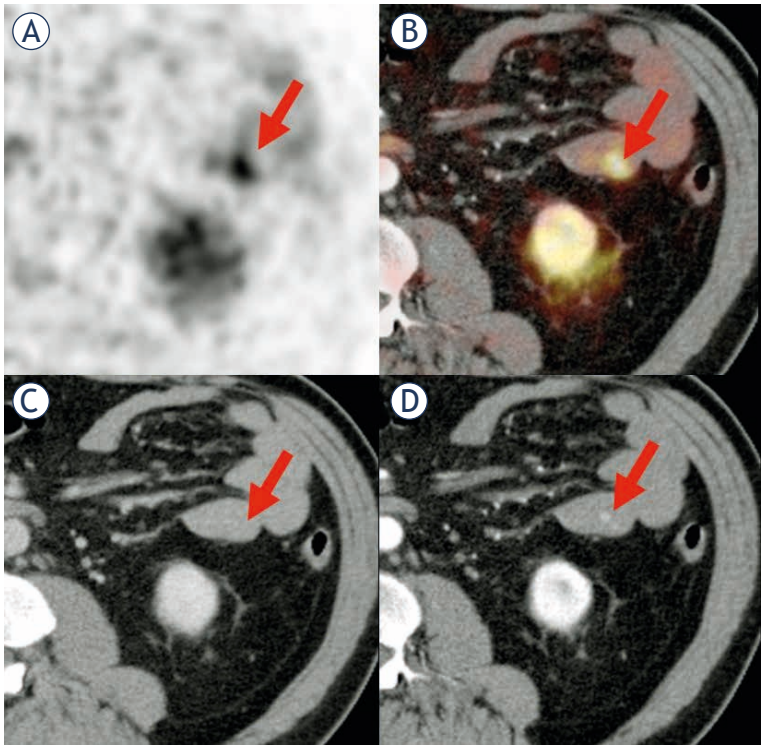

FIGURE 3. Patient with biopsy-proven NET liver metastases. The Ga-68-DOTATOC focus (#7a) **(A)** in the jejunum **(B)** has no correlation in the venous-phase CT **(C)**, while a lesion is clearly detectable in the arterial-phase CT **(D)**.

Ga-68 DOTATOC was prepared by our radiochemist as described by Zhernosekov *et al*.[21] The PET scans were acquired 45 min to 60 min after injection of approximately 100–120 MBq of Ga-68 DOTATOC.

The examinations were performed on a 16-row PET/CT system (Biograph 16; Siemens AG, Erlangen, Germany). In 22 patients, CT was performed using a triple-phase protocol with CareDose4D (230 mAs eff., 120 kV) and 70-100 ml of IV contrast medium (Ultravist 370; Bayer Schering Pharma, Berlin, Germany). The delay was 24 s for the arterial bolus and 45 s for the portal-venous phase, both obtained with bolus tracking. During each phase, an upper abdominal scan with a slice thickness of 16 x 0.75 mm was acquired. For the venous phase, the delay was 70 s and 16 x 1.25 mm slice thickness was acquired. In 3 examinations, CT was performed as a low-dose CT without contrast medium (40 mAs eff/120 kV).

The PET scans were acquired over 5-6 bed positions of 3 minutes each, covering the area from the base of the skull to the upper thigh. PET images derived from a 168 x 168 matrix acquisition were iteratively reconstructed with scatter correction using the ordered subset expectation maximization technique (5 iterations, 8 subsets). Attenuation correction was based on an attenuation map generated from the whole-body venous-phase CT scan or the low-dose CT scan. No radiopaque oral contrast medium was given as it may degrade PET images.[22]

Two experienced radiologists and one nuclear medicine physician first interpreted PET and CT alone and then simultaneously. Lesions were classified into three categories: suspicious, nonsuspicious, and suspicious in conjunction with PET (hyperperfusion). The 3 PET/CT examinations without contrast medium administration were excluded from this analysis. The remaining lesions were assigned to one of two groups: lesions evaluable in the venous and arterial CT scan (Group 1) and lesions evaluable in the venous CT scan only (Group 2).

Maximum standard uptake values (SUVmax) were calculated at a Leonardo workstation (Siemens AG, Erlangen, Germany). A region of interest (ROI) was drawn around the suspicious lesion to assess its SUVmax. An approximate average background SUVmax was calculated as the mean of 5 ROIs placed in bowel segments not suspicious for NET.

The histopathologic diagnosis (available for 28 lesions) or the results of another diagnostic modality such as endoscopy and/or follow-up imaging (for 12 lesions) for a mean of 22.9 months (median 14.5; range: 6-52 months) were used as the standard of reference.

Statistical analysis

Data were collected using Excel (Microsoft®, Windows®XP). The statistical analysis was performed with PASW 18 (IBM, USA). The Wilcoxon rank-sum test was used to assess the level of significance for the differences between lesion SUVmax and background SUVmax.

A p-value < 0.05 was considered significant. Differences between SUVmax and the SUVmax lesion-to-background ratio of true positive and false positive lesions were analysed using the Mann-Whitney U-test. A receiver operating characteristic **(**ROC**)** analysis of SUVmax and SUVmax lesion-to-background ratio was performed. The difference between no lesion correlate (nonsuspicious) and a lesion correlate (suspicious + suspicious in conjunction with PET) in Group 1 was assessed by the McNemar test, and the differences between the overall diagnostic performance in Group 1 and Group 2 by the Fisher`s exact test.

The institutional ethics review board approved this retrospective study.

Results

Seven of 25 patients with suspected NETs of the small intestines had multifocal lesions, resulting in a total of 40 suspected intestinal NETs. An overview of all lesions is presented in Table 1. Three lesions (in 2 patients) of the 40 suspicious lesions were subsequently classified as false-positive based on the reference standard. There were no CT abnormalities in either the arterial or venous phase in these cases. In Group 1, 14 (in 13 patients) of the PET-positive lesions could be evaluated on both arterial and venous CT scans (Figures 1-4). The results are summarized in Table 2. The arterial CT scans detected 3 lesions (21.4%) when interpreted alone and 8 lesions (57.1%) in conjunction with PET, while 3 lesions (21.4%) could not be detected at all. The venous CT scan detected only 3 lesions (21.4%), while 11 lesions (78.6%) were rated as non-suspicious. The venous CT in conjunction with PET did not offer any new information about lesions. In conjunction with PET the arterial CT scan was significantly superior to the venous CT scan (p-value = 0.008). In Group 2, 17 of the PET-positive lesions (in 7 patients) could only be evaluated on venous-phase CT scans: only 2 (11.8%) of the 17 lesions were suspicious at venous-phase CT, the remaining lesions appeared normal (n = 15, 88.2%). The patient group with evaluable lesions in the arterial and venous CT scan (Group 1) was significantly superior to the group with evaluable lesions in the venous CT only (Group 2) regarding the sensitivity (p-value > 0.001) for NET lesions. Only 6 PET-positive lesions (in 3 patients) could be judged in the low-dose CT scan none of them had a correlate in the low-dose scan.

The mean SUVmax of true positive lesions (n = 37) was 18.48 (median: 14.9; range: 5.5-64.6). The mean SUVmax lesion-to-background ratio for 23 patients was 3.32 (median: 3.2; range: 1.7-5.1). The false positive lesions (n = 3) had SUVmax of 7.5, 3.6, and 4.5. The lesion SUVmax and background SUVmax were significantly different (p-value > 0.001). The SUVmax and the lesion-to-background SUVmax ratio lesion/background of true positive lesions and false positive lesions were also significantly different (p-value = 0.005 and 0.011). In ROC analysis the area under the curve (AUC) of lesion SUVmax was 0.946 and the AUC of lesion-to-background SUVmax was 0.919 (Figure 5).

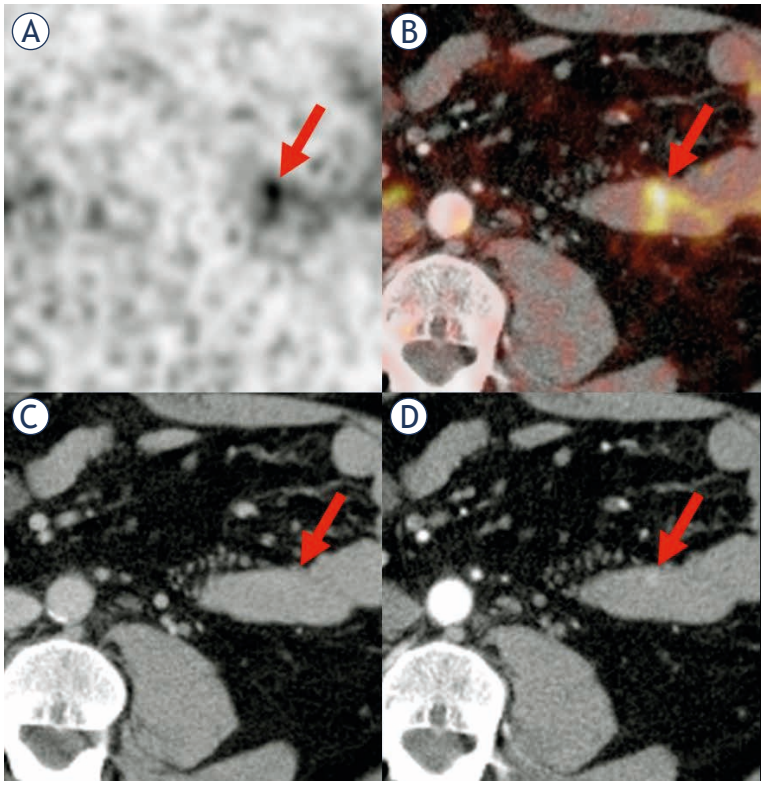

FIGURE 4. The same patient as in Figure 3 had another Ga-68-DOTATOC-positive focus (#7b) **(A)** more distal in the jejunum without a correlate in the venous-phase CT **(C)** but matching a lesion visible in the arterial-phase CT **(D)**. This lesion was not detected during surgery; however, it was definitely confirmed by histopathology.

Discussion

Our results suggest that many primary NETs in the small intestines display not only an increased expression of somatostatin receptors, which was shown to be very effective for the diagnosis of intestinal NETs, but also frequently arterial hyperperfusion. The arterial phase and not the venous phase appears to be beneficial in detecting NETs of the small intestines using multiphase Ga-68 DOTATOC PET/CT.

Arterial hyperperfusion has been reported to characterize both metastasis from NETs and primary NETs.[18-20] In our patient population, only a few NETs were identified in venous-phase CT; this applies to both hypogastric NETs that could be evaluated in the venous phase only and epigastric NETs that could be evaluated in arterial and venous phases. While venous-phase CT mainly relies on lesion size, the arterial phase can add information on perfusion. A study by Versari *et al*. investigated the detection of duodenopancreatic NETs using endoscopic ultrasound (EUS), Ga-68 DOTATOC

TABLE 1. Overview of all suspicious lesions of the small intestine (n = 40/25 patients)

n=40	Number of evaluable lesions	TP	TN	FP	FN
PET	40	37	0	3	0
CT, multiphase	16	See Table 2	2	0	See Table 2
CT, ven. phase only	18	2	1	0	15
CT low dose	6	0	0	0	6

FN = false negative; FP = false positive; TN = true negative; TP = true positive

TABLE 2. Comparison of the performances of PET and arterial- and venous-phase CT

N = 14	#1	#2	#3	#4	#5	#6	#7a	#7b	#8	#9	#10	#11	#12	#13
PET	+	+	+	+	+	+	+	+	+	+	+	+	+	+
CT, art. phase	-	c	c	c	c	+	c	c	+	-	c	c	+	-
CT, ven. phase	-	-	-	-	-	+	-	-	+	-	-	-	+	-
SUVmax	23.4	43.6	5.9	43.7	31.5	6.2	9.0	5.5	64.6	9.5	10.3	11.3	58.0	14.1
Localisation	ile	duo	ile	duo	duo	duo	jej	jej	duo	duo	jej	duo	ile	duo
Proceeding after PET/CT	OP	OP	FU 36m	FU 37m	OP	OP	OP	OP	OP	OP	FU 14m	OP	OP	FU 52m

+ = suspicious lesion; - = nonsuspicious lesion; c = suspicious CT lesion in combination with PET (hyperperfusion) for true positive NET lesions (n = 14/13 patients) according to the reference standard; duo = duodenum; FU = follow-up; ile = ileum; jej = jejunum; m = months; OP = operation

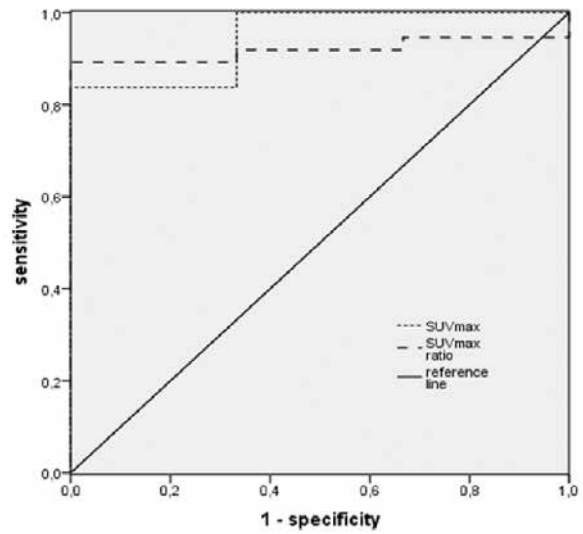

FIGURE 5. ROC analysis of lesion SUVmax and lesion-to-background SUVmax ratios.

PET, and CT. They report a comparable accuracy for each of these modalities alone, concluding that their combination may allow an optimal preoperative diagnosis.[23] While the 23 NETs in 19 patients investigated by Versari *et al*. also included pancreatic lesions, we only investigated lesions in the small intestines. Moreover, Versari *et al*. did not analyze arterial and venous CT scans separately. In a study evaluating the role of Ga-68 DOTATOC with a triple-phase CT protocol Ruf *et al*. detected gastrointestinal lesions with PET only.[24] Regarding gastrointestinal lesions a drawback of this study is that only 2 NET lesions were analyzed. Our finding that PET appears to be more appropriate than CT for the detection of intestinal NETs is in disagreement with another study of Ruf *et al*. which investigated the role of Ga-68 DOTATOC PET/CT for the therapy management.[11] In most of our cases, arterial hyperperfusion can be seen in conjunction with PET reading only, because the lesions are very small and the enhanced area is hard to differentiate from the inhomogeneous appearance of bowel loops. However, PET requires CT for correct localization and characterization of intestinal lesions.

Reliable characterization of NETs of the small intestines is difficult on the basis of abnormal Ga-68 DOTATOC PET findings alone.[11] This situation is mainly attributable to physiologic Ga-68 DOTATOC accumulation in the intestine and the fact that the tracer typically shows an inhomogeneous distribution. For these reasons, findings in organs with physiologic tracer accumulation should be interpreted with caution.[8] Our results suggest that the SUVmax can help to decide whether a le-

sion is malignant or benign. Nevertheless, we think that caution is in order in suggesting a threshold. Our statistical analysis relies on only 3 false positive lesions and the background SUVmax is only an approximation averaged over 5 ROIs. SUVmax in normal intestinal tissue may be much higher than an averaged background SUVmax. Another reason for using background SUVmax with caution is that the AUC of lesion SUVmax is slightly higher than the AUC of the lesion-to-background SUVmax ratio. However, very high SUVmax are strong clues for NETs.

Our patient population is biased towards small lesions. Larger NETs of the small intestines are easier to detect and have typically been identified by other diagnostic tests such as endoscopy or CT before PET/CT is performed. In contrast, most of the patients we investigated here had CUP, which means that primary intestinal tumours are very small and have not been detected by other diagnostic modalities before. Detection of a Ga-68 DOTATOC positive lesion is of course easier when the target-to-background ratio is high as opposed to a low ratio as is typical in a small lesion against a heterogeneous background.

Mainly in case of inhomogeneous tracer distribution contrast-enhanced multiphase CT can help to overcome the limitations of the diagnostic performance of Ga-68 DOTATOC PET. The combination of hyperperfusion and increased somatostatin receptor expression increases the detection of NETs of the intestine and should improve diagnostic confidence. A reader who notices a Ga-68 DOTATOC focus that he or she cannot classify with confidence can additionally look at the arterial phase CT images. Conversely, a hyperperfused lesion at CT can be verified by checking the corresponding PET scan. PET/CT, therefore, should increase both accuracy and diagnostic confidence.

Normal intestinal motility may make it difficult to match a nuclide focus with the correct intestinal loop on CT. Here, arterial hyperperfusion may also be helpful and improve localization with endoscopy in case the imaging result is clear and no further testing is required for surgical resection. Studies have reported promising results for somatostatin PET/CT.[7,11,13,25] An optimized PET/CT protocol including an intestinal scan during arterial enhancement might improve the detection of primary NETs in this location even further. The protocol for detecting intestinal NETs may be further improved by a negative oral contrast agent such as water and butylscopolamine administration for reducing intestinal motility.

Conclusions

Our results indicate that a considerable number of intestinal NETs may demonstrate arterial hyperperfusion. A Ga-68 DOTATOC PET/CT protocol for the evaluation of intestinal NETs should include an arterial phase CT scan of the bowel loops, especially when it is used to search for primary tumours in patients with CUP. Together with foci of high SUVmax, visual interpretation of arterial hyperperfusion is a strong clue for NET lesions in the small intestines and can be helpful for image interpretation and lesion localization.

References

1. Kocha W, Maroun J, Kennecke H, Law C, Metrakos P, Ouellet JF, et al. Consensus recommendations for the diagnosis and management of well-differentiated gastroenterohepatic neuroendocrine tumours: a revised statement from a Canadian National Expert Group. *Curr Oncol* 2010; **17:** 49-64.
2. Modlin IM, Lye KD, Kidd M. A 5-decade analysis of 13,715 carcinoid tumors. *Cancer* 2003; **97:** 934-59.
3. Modlin IM, Latich I, Zikusoka M, Kidd M, Eick G, Chan AK. Gastrointestinal carcinoids: the evolution of diagnostic strategies. *J Clin Gastroenterol* 2006; **40:** 572-82.
4. Bornschein J, Kidd M, Malfertheiner P, Modlin IM. Gastrointestinal neuroendocrine tumors. *Dtsch Med Wochenschr* 2008; **133:** 1505-10.
5. Slavec ZZ, Gaberscek S, Slavec K. The development of nuclear medicine in Slovenia and Ljubljana: half a century of nuclear medicine in Slovenia. *Radiol Oncol* 2012; **46:** 81-8.
6. Kowalski J, Henze M, Schuhmacher J, Macke HR, Hofmann M, Haberkorn U. Evaluation of positron emission tomography imaging using [68Ga]-DOTA-D Phe(1)-Tyr(3)-Octreotide in comparison to [111In]-DTPAOC SPECT. First results in patients with neuroendocrine tumors. *Mol Imaging Biol* 2003; **5:** 42-8.
7. Buchmann I, Henze M, Engelbrecht S, Eisenhut M, Runz A, Schafer M, et al. Comparison of 68Ga-DOTATOC PET and 111In-DTPAOC (Octreoscan) SPECT in patients with neuroendocrine tumours. *Eur J Nucl Med Mol Imaging* 2007; **34:** 1617-26.
8. Gabriel M, Decristoforo C, Kendler D, Dobrozemsky G, Heute D, Uprimny C, et al. 68Ga-DOTA-Tyr3-octreotide PET in neuroendocrine tumors: comparison with somatostatin receptor scintigraphy and CT. *J Nucl Med* 2007; **48:** 508-18.
9. Horton KM, Fishman EK. The current status of multidetector row CT and three-dimensional imaging of the small bowel. *Radiol Clin North Am* 2003; **41:** 199-212.
10. Gabriel M, Hausler F, Bale R, Moncayo R, Decristoforo C, Kovacs P, et al. Image fusion analysis of (99m)Tc-HYNIC-Tyr(3)-octreotide SPECT and diagnostic CT using an immobilisation device with external markers in patients with endocrine tumours. *Eur J Nucl Med Mol Imaging* 2005; **32:** 1440-51.
11. Ruf J, Heuck F, Schiefer J, Denecke T, Elgeti F, Pascher A, et al. Impact of Multiphase 68Ga-DOTATOC-PET/CT on therapy management in patients with neuroendocrine tumors. *Neuroendocrinology* 2010; **91:** 101-9.
12. Van Riet J, Rattat D, Verbruggen A, Mortelmans L, Mottaghy FM. Ga-68 DOTATOC PET/CT changed the therapeutic course of a patient with the sudden onset of vision problems. *Clin Nucl Med* 2009; **34:** 27-8.
13. Frilling A, Sotiropoulos GC, Radtke A, Malago M, Bockisch A, Kuehl H, et al. The impact of 68Ga-DOTATOC positron emission tomography/computed tomography on the multimodal management of patients with neuroendocrine tumors. *Ann Surg* 2010; **252:** 850-86.

14. Van Hoe L, Gryspeerdt S, Marchal G, Baert AL, Mertens L. Helical CT for the preoperative localization of islet cell tumors of the pancreas: value of arterial and parenchymal phase images. *Am J Roentgenol* 1995; **165:** 1437-9.

15. Stafford-Johnson DB, Francis IR, Eckhauser FE, Knol JA, Chang AE. Dual-phase helical CT of nonfunctioning islet cell tumors. *J Comput Assist Tomogr* 1998; **22:** 335-9.

16. Chung MJ, Choi BI, Han JK, Chung JW, Han MC, Bae SH. Functioning islet cell tumor of the pancreas. Localization with dynamic spiral CT. *Acta Radiol* 1997; **38:** 135-8.

17. Schreiter NF, Nogami M, Steffen I, Pape UF, Hamm B, Brenner W, et al. Evaluation of the potential of PET-MRI fusion for detection of liver metastases in patients with neuroendocrine tumours. *Eur Radiol* 2012; **22:** 458-67.

18. Andersson T, Eriksson B, Hemmingsson A, Lindgren PG, Oberg K. Angiography, computed tomography, magnetic resonance imaging and ultrasonography in detection of liver metastases from endocrine gastrointestinal tumours. *Acta Radiol* 1987; **28:** 535-9.

19. Wallace S, Ajani JA, Charnsangavej C, DuBrow R, Yang DJ, Chuang VP, et al. Carcinoid tumors: imaging procedures and interventional radiology. *World J Surg* 1996; **20:** 147-56.

20. Ricke J, Hanninen EL, Amthauer H, Lemke A, Felix R. Assessment of the vascularization of neuroendocrine tumors by stimulated acoustic emission of SH U 508A ultrasound contrast agent and color or power Doppler sonography. *Invest Radiol* 2000; **35:** 253-9.

21. Zhernosekov KP, Filosofov DV, Baum RP, Aschoff P, Bihl H, Razbash AA, et al. Processing of generator-produced 68Ga for medical application. *J Nucl Med* 2007; **48:** 1741-8.

22. Prabhakar HB, Sahani DV, Fischman AJ, Mueller PR, Blake MA. Bowel hot spots at PET-CT. *Radiographics* 2007; **27:** 145-59.

23. Versari A, Camellini L, Carlinfante G, Frasoldati A, Nicoli F, Grassi E, et al. Ga-68 DOTATOC PET, endoscopic ultrasonography, and multidetector CT in the diagnosis of duodenopancreatic neuroendocrine tumors: a single-centre retrospective study. *Clin Nucl Med* 2010; **35:** 321-8.

24. Ruf J, Schiefer J, Furth C, Kosiek O, Kropf S, Heuck F, et al. 68Ga-DOTATOC PET/CT of neuroendocrine tumors: spotlight on the CT phases of a triple-phase protocol. *J Nucl Med* 2011; **52:** 697-704.

25. Prasad V, Ambrosini V, Hommann M, Hoersch D, Fanti S, Baum RP. Detection of unknown primary neuroendocrine tumours (CUP-NET) using (68)Ga-DOTA-NOC receptor PET/CT. *Eur J Nucl Med Mol Imaging* 2010; **37:** 67-77.

research article

Global diffusion tensor imaging derived metrics differentiate glioblastoma multiforme vs. normal brains by using discriminant analysis: introduction of a novel whole-brain approach

Ernesto Roldan-Valadez[1], Camilo Rios[2], David Cortez-Conradis[1], Rafael Favila[3], Sergio Moreno-Jimenez[4]

[1] Magnetic Resonance Unit, Medica Sur Clinic & Foundation, Mexico City, Mexico
[2] Department of Neurochemistry, National Institute of Neurology and Neurosurgery, Mexico City, Mexico
[3] GE Healthcare, Mexico city, Mexico
[4] Radioneurosurgery Unit, National Institute of Neurology and Neurosurgery, Mexico City, Mexico

Radiol Oncol 2014; 48(2): 127-136.

Received 15 October 2013
Accepted 21 December 2013

Correspondence to: Ernesto Roldan-Valadez, Coordination of Research & Innovation, Magnetic Resonance Unit, Medica Sur Clinic & Foundation, Puente de Piedra 150, Toriello Guerra, Tlalpan, CP 14050, Mexico City, Mexico. E-mail: ernest.roldan@usa.net

Disclosure: No potential conflicts of interest were disclosed.

Background. Histological behavior of glioblastoma multiforme suggests it would benefit more from a global rather than regional evaluation. A global (whole-brain) calculation of diffusion tensor imaging (DTI) derived tensor metrics offers a valid method to detect the integrity of white matter structures without missing infiltrated brain areas not seen in conventional sequences. In this study we calculated a predictive model of brain infiltration in patients with glioblastoma using global tensor metrics.

Methods. Retrospective, case and control study; 11 global DTI-derived tensor metrics were calculated in 27 patients with glioblastoma multiforme and 34 controls: mean diffusivity, fractional anisotropy, pure isotropic diffusion, pure anisotropic diffusion, the total magnitude of the diffusion tensor, linear tensor, planar tensor, spherical tensor, relative anisotropy, axial diffusivity and radial diffusivity. The multivariate discriminant analysis of these variables (including age) with a diagnostic test evaluation was performed.

Results. The simultaneous analysis of 732 measures from 12 continuous variables in 61 subjects revealed one discriminant model that significantly differentiated normal brains and brains with glioblastoma: Wilks' $\lambda = 0.324$, χ^2 (3) = 38.907, $p < .001$. The overall predictive accuracy was 92.7%.

Conclusions. We present a phase II study introducing a novel global approach using DTI-derived biomarkers of brain impairment. The final predictive model selected only three metrics: axial diffusivity, spherical tensor and linear tensor. These metrics might be clinically applied for diagnosis, follow-up, and the study of other neurological diseases.

Key words: brain neoplasms; diffusion tensor imaging; discriminant analysis; magnetic resonance imaging; predictive value of tests

Introduction

Some pathologic and magnetic resonance (MR) imaging characteristics of astrocytomas grades II to IV (highest degree known as glioblastoma multiforme, GBM) suggest these tumors would benefit from the use of a global measurement of brain impairment.[1]

The first imaging approaches to characterize high-grade glial lesions, especially GBM, were fraught with pitfalls resulting from the marked heterogeneity of both glial-infiltrated and normal brains.[2,3] These tumors frequently contain multiple areas of variable histologic features, so that a sampling error in a biopsy may mean that the degree of

malignancy seen by the neuropathologist may not reflect the degree of malignancy present elsewhere in the tumor, resulting in significant undergrading of some lesions.[2] Thus, even when all radiologically visible portions of a tumor have been excised, the surgical margins may not be "clean", and further neoplastic growth can (and usually does) occur in the adjacent brain tissue, leading from microscopic residual to gross recurrence.[4] Therefore, none of the MR protocols for GBM in every day practice should be only morphologic.[3,5,6] As a consequence, surgery usually only reduces the tumor; this information is relevant as recent evidence has proved gross total resection (surgical margin status) significantly correlates with progression-free, recurrence pattern and overall survival in patients with GBM.[7,8]

GBM is considered a whole brain disease. Radiotherapy and chemotherapy follow surgery.

Although MR perfusion and spectroscopy[9], and sometimes diffusion tensor imaging (DTI)[10] are routinely used methods to locate parts of the tumor-GBM with high malignancy that should be biopsied, the development of specific and sensitive biomarkers remains a critical unmet need.[11]

Our purpose in this study was to explore the diagnostic ability of a *global* (whole brain) assessment of DTI-derived tensor metrics in normal and infiltrated brains with GBM. We used the multivariate technique of linear discriminant analysis (DA), previously reported in MRI diagnosis[12], to classify the study participants into groups, describe group differences and to assess the relative importance of DTI variables for discriminating between groups. This analysis might unveil findings and associations that cannot, in a partial-regional assessment, be recognized at surgery, neurologic, MRI and/or pathologic examination. Considering there is still scarce information in the medical literature about the global calculation of tensor metrics[13,14], a predictive discriminating model may offer an innovative diagnostic approach to the surgical-neuro-oncology team.

Subjects and methods

Subjects

This was a case-control study. We included patients with suspected diagnosis and later pathological confirmation of primary GBM who had undergone preoperative brain MR examinations between January 2010 and September 2012. Exclusion criteria were corticosteroid or antibiotic treatment, lesions with areas related to calcification and/or hemorrhage and previous brain surgery. A control group included young and elderly healthy volunteers recruited from the enrolled interns and medical residents of the hospital, and elderly subjects from our Geriatrics unit. All volunteers received detailed health examinations; exclusion criteria were major neurological, psychiatric, or cardiovascular diseases. A radiologist interpreted the MR images blinded to the patient's history and MRI examinations with other structural abnormalities were excluded. The local institutional review board approved the study (Project #2011-EXT-05).

Brain image acquisition

MR sequences included conventional axial T2-weighted imaging, axial Fluid-Attenuated Inversion Recovery (FLAIR), axial Spoiled Gradient Echo (SPGR), DWI and axial T1-weighted imaging, using 0.1 mmol/kg of body weight of gadopentetate dimeglumine (Magnevist; Schering, Berlin, Germany). Healthy volunteers did not receive endogenous contrast. DTI was performed using a single-shot SE EPI sequence. Diffusion gradients were applied in 25 directions with b-values of 1000 s/mm^2 and an image without diffusion weighting with b-value of 0 s/mm^2. DTI sequences were acquired in the axial plane with 44 contiguous sections, 2.4 mm section thickness, no intersection gap; TR/TE of 17,000/80 ms, with parallel imaging to reduce off-resonance artifacts (PI factor was 2); 25 x 25 cm FOV; and 128 x 128 matrix/pixel size. MR was performed on a single occasion using a 3T unit (Signa HDxt, GE Healthcare, Waukesha, WI, USA); and a high-resolution eight-channel head coil (Invivo, Gainesville, FL, USA).

Image postprocessing and data analysis

We used the software dcm2nii[15] and the FMRIB Software Library (FSL) v. 4.1.9.[16] DTI images were extracted using the *Brain Extraction Tool (BET)* v. 2.1.[17] Eddy currents were corrected using the *FMRIB's Diffusion Toolbox v. 2.0;* the *Reconstruct Diffusion Tensor* (*DTIFIT)* and the *fslmaths tool* generated the eigenvector and eigenvalue maps for each tensor metric. The *fslstats tool* calculated the scalar measures (mean values) of each whole-brain calculation. The apparent diffusion coefficient (ADC) value, a simple index calculated from diffusion-weighted images[18], was considered equivalent to the MD (mean diffusivity) metric, as it was obtained from the DTI sequence.[19] DTI-derived tensor

TABLE 1. Correlations of tensor metrics, controlled for the effect of diagnosis, age and gender

Tensor metric											
		Cs									
FA	Pearson´s R	-.552	**FA**								
	p-value	< .001									
RA	Pearson´s R	-1.000	.557	**RA**							
	p-value	< .001	< .001								
Cp	Pearson´s R	-.937	.584	.912	**Cp**						
	p-value	< .001	< .001	< .001							
Cl	Pearson´s R	-.898	.541	.943	.673	**Cl**					
	p-value	< .001	< .001	< .001	< .001						
L	Pearson´s R	.211	.075	-.175	-.191	< .001	**L**				
	p-value	.165	.596	.256	.213	.999					
p	Pearson´s R	.195	-.079	-.183	-.194	.006	.890	**p**			
	p-value	.205	.580	.240	.214	.972	< .001				
AD	Pearson´s R	.034	.209	-.008	-.002	.106	.882	.880	**AD**		
	p-value	.826	.137	.958	.989	.508	< .001	< .001			
MD	Pearson´s R	.195	-.078	-.183	-.193	.007	.892	1.000	.881	**MD**	
	p-value	.206	.589	.241	.214	.968	< .001	< .001	< .001		
RD	Pearson´s R	.213	-.226	-.209	-.149	-.105	.815	.973	.779	.973	**RD**
	p-value	.151	.103	.163	.316	.502	< .001	< .001	< .001	< .001	
q	Pearson´s R	-.306	.804	.310	.339	.328	.403	.281	.627	.284	.214
	p-value	.031	< .001	.030	.016	.026	.003	.046	< .001	.044	.116

AD = axial diffusivity; Cl = linear tensor; Cp = planar tensor; Cs = spherical tensor; FA = fractional anisotropy; L = the total magnitude of the diffusion tensor; MD = mean diffusivity; p = pure isotropic diffusion; q = pure anisotropic diffusion; RA = relative anisotropy; RD = radial diffusivity

metrics formulas using the major (λ1), intermediate (λ2), and minor (λ3) eigenvalues allowed the calculation of the eleven most common tensor metrics for brain imaging: mean diffusivity (MD), fractional anisotropy (FA), pure isotropic diffusion (p), pure anisotropic diffusion (q), the total magnitude of the diffusion tensor (L), linear tensor (Cl), planar tensor (Cp), spherical tensor (Cs), relative anisotropy (RA), axial diffusivity (AD) and radial diffusivity (RD)[10]; each one representing a single global measure of the whole-brain. Figure 1A shows the algorithm for measuring the DTI-derived tensor metrics.

Statistical analysis

Study design

The study was considered a Phase II aimed to determine the capacity of DTI-derived biomarkers to distinguish between people with cancer and those without.[20]

Sample size

Considering our predictive model to discriminate between normal brains *vs*. brains infiltrated with GBM underwent a diagnostic performance assessment, the adequacy of the sample size to expect validity from our results was based on matching this phase with the summarized list of computed sample sizes needed for an exploratory retrospective study reported by Obuchowski *et al*.[21], at least 10 diseased patients and 10 control patients were required to maintain statistical validation in a diagnostic test evaluation where the type I error rate was set at 0.05, type II error rate was ≤ 0.10, and power ≥ 0.90. Our study included 27 patients and 34 controls.

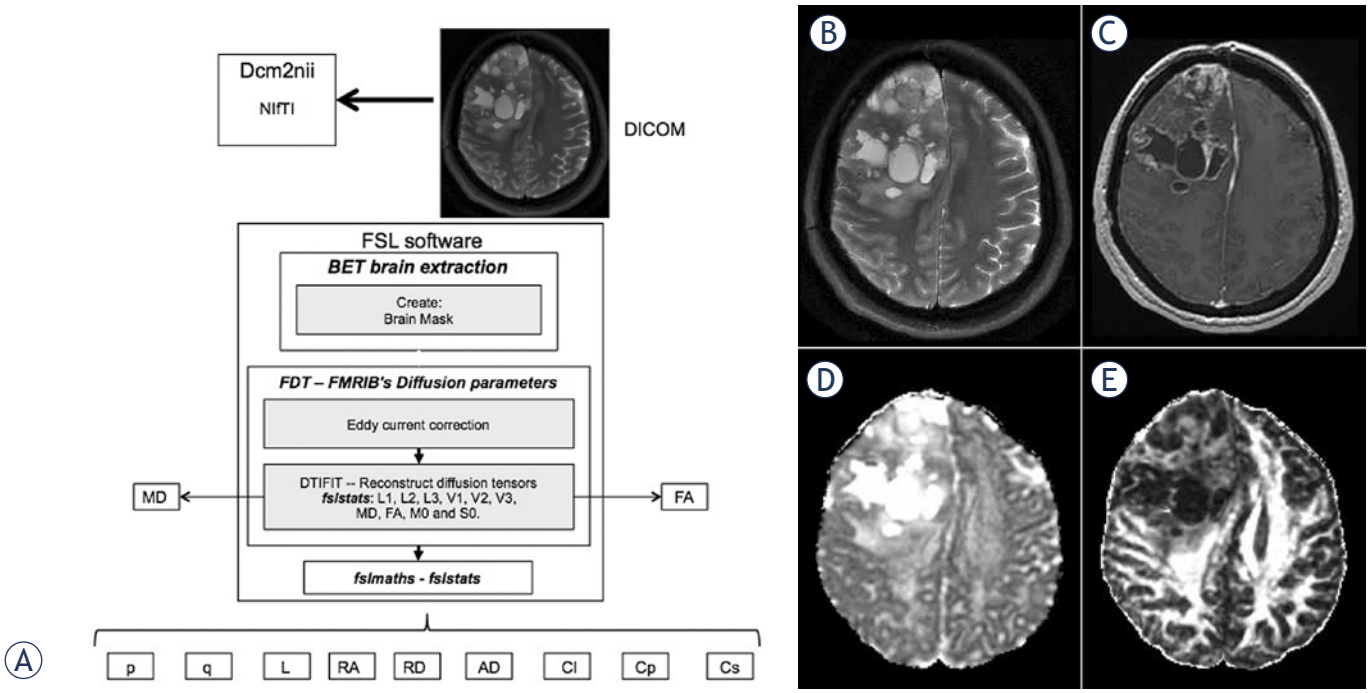

FIGURE 1. (A), FSL software algorithm used in the image postprocessing and data analyses. (**B-E)**, Examples of acquired sequences in a patient with GBM and the tensor-metric maps generated for the data analyses: **(B)**, axial T2-weighted; **(C)**, post contrast axial T1-weighted; **(D)**, axial diffusivity (AD) tensor map; and **(E)**, fractional anisotropy (FA) tensor map. Notice how it might not be possible to perform an imaging diagnosis based only on a visual inspection of these maps.

Multivariate DA

We ran a DA, which was optimal under the same conditions where Manova was optimal; then attempted to detect any deviation from Manova assumptions that might distort the tests of statistical significance.[22] We assessed the normality of the distribution of the DTI-derived scores using the Kolmogorov–Smirnov´s and Shapiro-Wilk normality tests[23]; eliminated significant outliers, evaluated multivariate normality and linearity, and tested the homogeneity of variance-covariance matrices using the Box´s M test.[24] Considering the similarity of the tensor-metric formulae, we ran scatterplots and correlations to check the strength of correlations among the dependent variables in order to detect the presence of multicollinearity and singularity (Table 1). Partial correlation analyses were carried out to calculate the Pearson´s correlation coefficient (r) controlling for the effect of age, gender and clinical diagnosis. The strength of the linear relationship corresponding to each correlation coefficient value was interpreted as very strong (at least of 0.8), moderately strong (0.6 up to 0.8), fair (0.3 up to 0.6) and poor (less than 0.3). A squared r value represented the coefficient of determination, the proportion of variance that each two compared variables had in common.[25]

We applied the stepwise method in *DA*, it considered the value of Wilk´s lambda and changing criteria: minimum partial F to enter of 3.84 and minimum partial F to remove of 2.71.[22] Continuous variables were included with the predictive aim to identify specific tensor-metric attributes in GBM and normal brains. The dependent variable (DV) used in the DA was the clinical diagnosis, which classified subjects as patients or controls. The independent variables (IVs) included 11 DTI-derived tensor metrics: MD, FA, p, q, L, Cl, Cp, Cs, RA, RD and AD, and the patients' age (in years). The effect-size measure for discriminant analysis was calculated using the squared canonical correlation as the equivalent of the R^2 in regression.[26] By convention, effect sizes of 0.02, 0.15, and 0.35 are termed small, medium, and large, respectively.[27] For all analyses, statistical significance was indicated by a *p-value* < 0.05.

Diagnostic model evaluation

The cross-validated contingency Table generated by the DA was used to evaluate the diagnostic performance of the DA model. We reported values of sensitivity, specificity, positive and negative likelihood ratios, and positive and negative predictive values, with their corresponding confidence in-

TABLE 2. Multivariate analysis (between-groups) of diffusion tensor imaging (DTI)-derived tensor metrics and age showing the statistical differences between means of normal-brain and brain-with- as glioblastoma multiforme (GBM) groups for the independent variables included in the analysis

Variable	Healthy brains		Brains with GBM		Wilks' Lambda	F test	p-value
	Mean	SD	Mean	SD			
Cs (spherical tensor)	.747091	.026938	.768395	.042299	.915	3.341	.076
FA (fractional anisotropy)	.287029	.011517	.254082	.026761	.607	23.341	< .001
RA (relative anisotropy)	.233436	.025491	.209370	.033559	.855	6.088	.018
Cp (planar tensor)	.138366	.013823	.136635	.036218	.999	.036	.850
Cl (linear tensor)	.114543	.013991	.098463	.011930	.711	14.621	.001
L (total magnitude of the diffusion tensor)	.002277	.000087	.002117	.000147	.691	16.077	< .001
p (pure isotropic diffusion)	.002107	.000077	.001959	.000134	.681	16.893	< .001
AD (axial diffusivity)	.001548	.000044	.001399	.000087	.461	42.052	< .001
MD (mean diffusivity)	.001217	.000044	.001132	.000078	.685	16.526	< .001
RD (radial diffusivity)	.001051	.000050	.000997	.000078	.852	6.237	.017
q (pure anisotropic diffusion)	.000452	.000036	.000367	.000047	.483	38.529	< .001
Age	40.333	21.502	47.150	15.187	.965	1.294	.263

SD = standard deviation

tervals (CI). Evaluation of the diagnostic tests followed the Standards for Reporting of Diagnostic Accuracy (STARD) initiative.[28]

Software

All analyses were carried out using the IBM® SPSS® Statistics software (version 22.0.0.0 IBM Corporation; Armonk, NY, USA). Diagnostic performance was assessed using MedCalc® (version 12.3.0.0 MedCalc Software bvba, Mariakerke, Belgium).

Results

Subjects and MRI acquisition

The study was conducted in 61 subjects; 27 patients: 13 females (mean age 50.0 ± 15.400 years, range 31–73 years) and 14 males (mean age 46.93 ± 15.403 years, range 18–78 years); and 34 controls: 26 females (mean age 41.04 ± 22.37 years, range 21–80 years) and 8 males (mean age 42.88 ± 21.89 years, range 24–72 years). The eleven DTI tensor-maps plus the age (per subject) added up 732 measurements included in the analyses. Figure 1 B-E shows examples of some of the MR sequences and tensor-metric maps used in the data analyses.

Partial correlation analyses

A scatterplot showed no serious violation of the assumptions of linearity, homoscedasticity, and outliers. Among 55 pairs of bivariate correlations, we found only 15 with a significantly very strong (at least 0.8) r value: Cs⇔RA (-), Cs⇔Cp (-), Cs⇔L (-), FA⇔q (+), RA⇔Cp (+), RA⇔Cl (+), L⇔p (+), L⇔AD (+), L⇔MD (+), L⇔RD (+), p⇔AD (+), p⇔MD (+), p⇔RD (+), AD⇔MD (+), and MD⇔RD (+). Table 1 and Figure 2 depict correlation values and the scatterplot of the eleven tensor-metrics.

Discriminant analysis

Although some r values were calculated at > 0.8, we included all variables in the DA, as we found evidence the stepwise variant of this method protects against multicollinearity and singularity;[29] a brief explanation is presented in the discussion section. The assumption of homogeneity of variance-covariance matrices was interpreted as significant (Box´s M value = 35.110, F = 5.317, df (6, 9087.738), p = < .001). In the stepwise statistics, at each step, the best variable that minimized the overall Wilks' Lambda was entered: AD was entered at Step 1, F = 42.052 (1, 36) p < .001; Cl entered at Step 2, F = 29.609 (2, 35) p < .001; and Cs entered at Step 3, F = 23.672 (3, 34) p < .001.

DA revealed one discriminant function that significantly differentiated the normal brains and GBM brains: Wilks' λ = 0.324, $\chi 2$ (3) = 38.907, p < .001. By indicating the significance of the discriminant function, Wilks' lambda provided a moderate proportion of total variability not explained by the model of 10.49%. A canonical correlation of 0.822

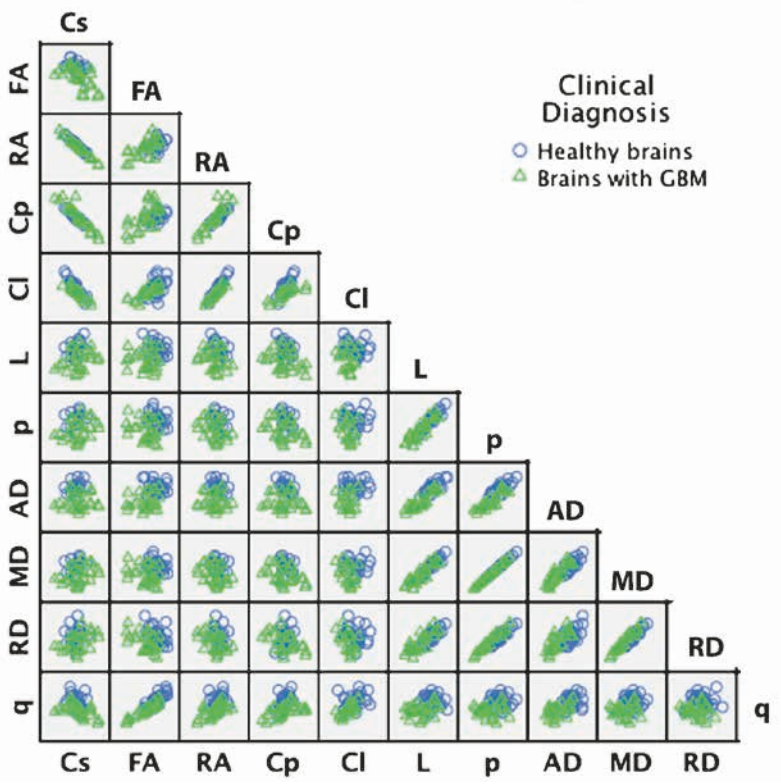

FIGURE 2. Scatter matrix of the data variables grouped by diagnosis.

suggested the model explains 67.56% of the variation in the grouping variable.

Summary of discriminant functions

The tests of equality of group means provided statistical evidence of significant differences between means of normal brains and brains with GBM in 9 of the IVs, with AD producing the highest F's value; Table 2 depicts the means, standard deviations (SD) and F´s tests values (between-groups multivariate analysis).

Standardized canonical discriminant function coefficients showed an index of the importance of each predictor for diagnosis with the sign indicating the direction of the relationship. A significant increase in values of Cs (spherical tensor), Cl (linear tensor) and AD (axial diffusivity) were the strongest diagnostic predictors. The variable coefficients stood out (for these data) as those that strongly predicted allocation to the normal-brain or tumor-brain group. The coefficient score decrement was proportional to less successful diagnostic predictors (Table 3A).

Structure Matrix Data provided another way of indicating the relative importance of the diagnostic predictors by showing the correlations (Pearson coefficients) of each variable with each discriminate function. Many researchers consider the structure matrix correlations more accurate than the standardized canonical discriminant function coefficients.[26] By identifying the largest loadings for each discriminate function, different patterns of loading variables can be seen. We found AD, MD, p, q, Cl, RD and FA, as the functions that best discriminate between normal brains and brains with tumor. A value of 0.30 was considered as the cut-off between important and less important variables (Table 3B).[30]

The canonical discriminant function coefficients Table showed the unstandardized coefficients (b) that were used to create the discriminant function (equation), they operated just like a regression equation, allowing us to build a predictive model of brain status:

Brain status (normal brain vs. tumor infiltration) = -48.295 +11,443.557 (axial diffusivity, AD) +105.124 (longitudinal tensor, Cl) +26.804 (spherical tensor, Cs)

The discriminant function coefficients (b) indicated the partial contribution of each variable to the discriminate function controlling all other variables in the equation (Table 3C).

The group centroids values described each group in terms of its profile, using the group means of the predictor variables called centroids. The cut-off value was defined as the mean of the two centroids; if the discriminant score of the function of a new case was less than or equal to the cut-off, the case was classed as 1 (brain with tumor), whereas if it was above the cut-off, it was classed as 0 (normal brain). In our study, normal brains had a mean of 1.483 while brains with GBM produced a mean of −1.334; the cut-off for the function at group centroids showed a calculated value of 0.149.

For the final part of the DA we performed a classification phase using the cross-validated set of data to present the power of the discriminant function. These results revealed that 92.7% of patients were classified correctly into "normal brain" or "brain with GBM" groups, this value corresponded to the overall predictive accuracy of the discriminant function. Additional results of diagnostic tests performance including the 95% confidence intervals (C.I.) showed: sensitivity = 100.00 (80.49 – 100.00); specificity = 87.50 (67.64 – 97.34); (+) likelihood ratio = 8.00 (82.78 – 23.06); (-) likelihood ratio = 0.00 (-); (+) predictive value = 85.00 (62.11 – 96.79); and (-) predictive value = 100.00 (83.89 – 100.00).

The average discriminant (D) scores for each group and the group centroids were used as visual demonstrations of the effectiveness of the dis-

TABLE 3. Independent variables included in the discriminant analysis. A, ordered by their Standardized Canonical Discriminant Function Coefficients (variables with larger coefficients stand out as those that strongly predict allocation to each diagnosis). B, Within-groups correlation matrix depicts the participant variables ordered by absolute size of correlation (Pearson coefficients) within function. The largest loadings for each discriminate function (AD was the largest) suggest the preference of diffusivity values that discriminates between normal- and brain-tumor groups. A value of 0.30 is considered as the cut-off between important and less important variables, notice that variables with (*) were not used in the analysis. C, unstandardized coefficients used to create a discriminant function operating just like a regression equation. Coefficients indicate the partial contribution of each variable to the discriminate function controlling for all other variables in the equation

A		B		C	
Standardized Canonical Discriminant Function Coefficients		**Structure Matrix**		**Canonical Discriminant Function Coefficients**	
Variable	**Function**	**Variable**	**Function**	**Variable**	**Function**
	1		**1**		**1**
Cl (linear tensor)	1.361	AD (axial diffusivity)	.748	AD (axial diffusivity)	11443.557
Cs (spherical tensor)	.962	MD (mean diffusivity)*	.568	Cl (linear tensor)	105.124
AD (axial diffusivity)	.806	p (pure isotropic diffusion)*	.566	Cs (spherical tensor)	26.804
		L (total magnitude of the diffusion tensor)*	.553	(Constant)	- 48.295
		q (pure anisotropic diffusion)*	.533		
		Cl (linear tensor)	.441		
		RD (radial diffusivity)*	.427		
		FA (fractional anisotropy)	.320		
		RA (relative anisotropy)*	.278		
		Cs (spherical tensor)	- .211		
		Age*	.124		
		Cp (planar tensor)*	.020		

criminant function. Histograms and box plots of the average D scores for each group were used as graphical demonstrations of the effectiveness of the discriminant function, the absence of overlap of the plots revealed an excellent discrimination (Figure 3 A-B).

Discussion

The lack of consensus regarding which DTI-derived tensor metrics are the most meaningful[31], and the scarce information about their diagnostic abilities, compelled us to evaluate whether a *global* approach might have clinical applicability. We consider our study an introduction to the method and proof-of-principle that a *global* approach using selected DTI-derived tensor metrics can differentiate normal brains from brains infiltrated with GBM, the selected metrics may function as biomarkers assembling a predictive model of tumor infiltration.

The relevant findings in our study showed that a multivariate DA of global measurements excluded the pair-wise comparisons from conventional tumor-region evaluations; the assembled statistically significant discriminant model of tumor brain impairment (for these data) needed only three *global* DTI-derived metrics: AD, Cl, and Cs.

Some advantages of a global approach using DTI metrics need to be mentioned: it decreases the bias associated with manual placement of a region of interest encompassing tumor regions; the tumor and edema regions are implicitly included in the evaluation; lesions not perceived by the radiologist´s eye on conventional sequences would be included in a global assessment; it may avoid problems associated with partial volume effects, and inaccurate image coregistrations; DTI biomarkers can be applied to other tumors/neurological diseases; its acquisition does not need contrast, and its post processing method can be semiautomatic; these facts broad the clinical applicability with no significant increase in the cost of MRI examinations.

The selected biomarkers in our final model deserve a brief explanation: AD depicted the main influence (larger value of its b unstandardized coefficient); it represents the directional diffusivity describing the microscopic water movement parallel to axonal tracts. AD is one of the best biomarkers in the diagnosis of enhancing rim in GBM, but not for other tumor regions[10]; (this fact provides evidence

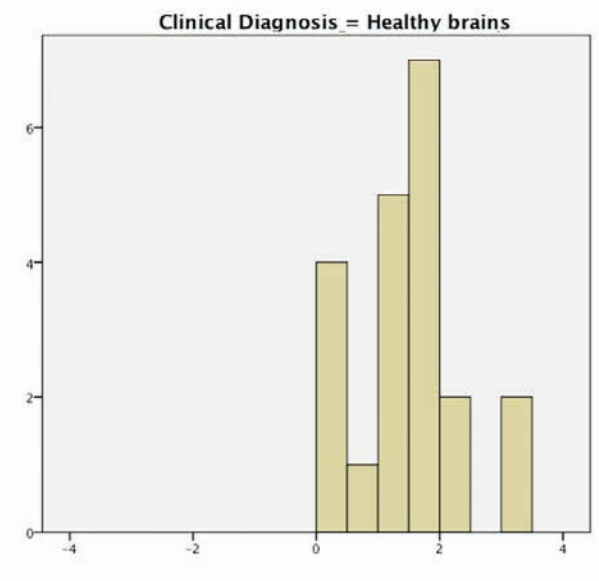

A

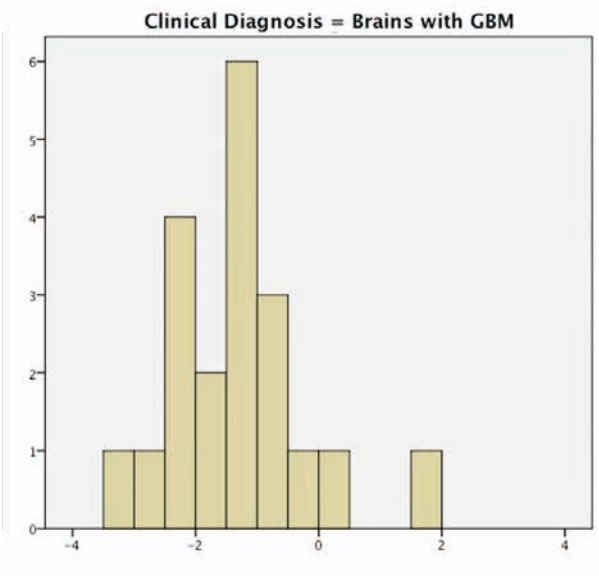

B

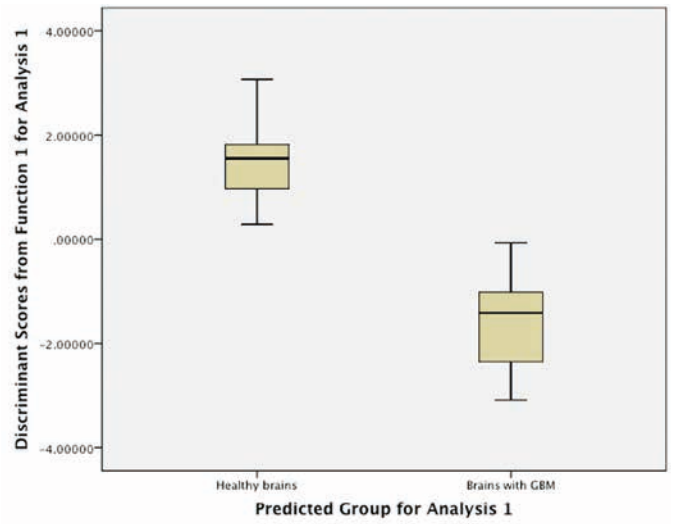

C

that a *regional* measurements may not be the most effective way to use DTI metrics in brain tumor imaging).[14] AD has been studied in animal models of encephalomyelitis of the spinal cord[32,33], in unfixed *ex vivo* human brains with multiple sclerosis[34], in a model of axonal injury caused by stroke[35], and in optic neuritis. Cl and Cs on the other hand, along with FA, have been reported among the biomarkers with best overall performance in differentiating the cystic cavity in abscess from GBM.[13] They show best diagnostic performance in the detection of normal-appearance white matter (NAWM) and the cystic cavity in brains with GBM.[10] Cs represents spherical normalized coordinates of a non-orthogonal DTI-derived tensor for each voxel, and Cl corresponds to the linear case.[36]

Several limitations in this study need to be addressed: because there have not been studies investigating a whole set of tensor metrics (not only FA and ADC) in a global approach[1,37,38], it is difficult to compare our results with others in the literature. Further studies might include comparisons with other brain tumors, the influence of variables like radiation necrosis, inflammatory and demyelinating diseases; and tumor infiltration categories such as post-surgery and post-radiotherapy; all of them were beyond the scope of this study. A concern of using DTI-metric values with high correlations (correlations up 0.8 or 0.9), as we observed in our data, might be raised because in those situations one variable is a near-linear combination of the other variable (the variable provides information that is redundant to the information available in one or more of the others, making matrix inversion unreliable).[29] The usual solution is a deletion of the redundant variable, however, because we have a compelling theoretical reason to retain all variables in this study (to evaluate the simultaneous discriminant ability of 11 global tensor metrics), the IBM® SPSS® Statistics software protects against multicollinearity and singularity through computation of pooled within-cell tolerance (1-squared multiple correlation, SMC) for each variable. SMC is the squared multiple correlation of a variable where it serves as the dependent variable (DV) with the rest

FIGURE 3. Visual demonstration of the effectiveness of the discriminant function. **(A)**, histograms showing the distribution of discriminant scores for normal- and tumor-brains. **(B)**, box plots of the average D scores. Both kinds of plots illustrate the distribution of the discriminant function scores for each group. The box-plots depict a visual demonstration of the excellent discrimination of the model by showing no overlap between groups.

as independent variables (IV) in multiple correlation. Variables with insufficient tolerance are deleted from the analysis; this procedure is a part of the stepwise method in DA.[22] Our discriminant model was able to explain a significant proportion of the variability in the data (67.56%), but may still have some errors in predicting individual diagnosis, so model validation should be done in subsequent studies. We acknowledge the linking of tensormetric values with the axonal-integrity status represents an oversimplification with respect to what is happening in brains with GBM, where complex tissue changes occur and affect water diffusivity: density of fiber, average diameters, degree of myelination, directional similarity, cellularity, viscosity, permeability, and histologic architecture; the DTI-tensor values are the effects of the summation of all these microstructural barriers.[13]

Several questions remain unanswered, for example, what is the relation of these tumor-DTI biomarkers with those of MR perfusion and spectroscopy? What is the association of DTI-biomarkers with the pattern of relapse and extension of resection in GBM? So far, only one study, to the best of our knowledge, has correlated a few *regional* DTI-tensor metrics with the survival of patients with GBM[39]; thus the clinical value of global DTI-metrics in predicting the overall survival has yet to be determined. As a phase II study, our research line will look for a sequel, applying the proven concepts in the follow-up of tumor-infiltration categories (post-surgery, post-radiotherapy, etc.) and in differential diagnoses (primary brain tumors vs. metastasis vs. demyelinating diseases).

Conclusions

Although we cannot affirm the superiority of global vs. regional DTI-derived tensor metrics in the evaluation of GBM yet, we can ascertain with certainty that there is an immediate clinical applicability of these biomarkers in assembling statistically significant predictive models able to announce the conversion of normal tissue to tumor infiltrated tissue before the conventional MR sequences show conspicuous findings. These principles could easily be extended to other neurological diseases. A first step in the advanced evaluation of brain tumors might include a global measurement of DTI-biomarkers able to pick up major infiltration zones. Due to the large number of variables (qualitative and quantitative) that must be analyzed in contemporary brain MRI by radiologists and neuroscientists conducting research on novel imaging biomarkers; multivariate techniques, like DA, may help in the generalization of knowledge beyond one setting.

References

1. Zolal A, Hejcl A, Malucelli A, Novakova M, Vachata P, Bartos R, et al. Distant white-matter diffusion changes caused by tumor growth. *J Neuroradiol* 2013; **40:** 71-80.
2. Rees JH, Smirniotopoulos JG, Jones RV, Wong K. Glioblastoma multiforme: radiologic-pathologic correlation. *Radiographics* 1996; **16:** 1413-38.
3. Watanabe M, Tanaka R, Takeda N. Magnetic resonance imaging and histopathology of cerebral gliomas. *Neuroradiology* 1992; **34:** 463-9.
4. Zimmerman RA. Imaging of adult central nervous system primary malignant gliomas. Staging and follow-up. *Cancer* 1991; **67:** 1278-83.
5. Johnson PC, Hunt SJ, Drayer BP. Human cerebral gliomas: correlation of postmortem MR imaging and neuropathologic findings. *Radiology* 1989; **170:** 211-7.
6. DeAngelis LM. Brain tumors. *N Engl J Med* 2001; **344:** 114-23.
7. Smets T, Lawson TM, Grandin C, Jankovski A, Raftopoulos C. Immediate post-operative MRI suggestive of the site and timing of glioblastoma recurrence after gross total resection: a retrospective longitudinal preliminary study. *Eur Radiol* 2013; **23:** 1467-77.
8. De Bonis P, Anile C, Pompucci A, Fiorentino A, Balducci M, Chiesa S, et al. The influence of surgery on recurrence pattern of glioblastoma. *Clin Neurol Neurosurg* 2013; **115:** 37-43.
9. Young GS. Advanced MRI of adult brain tumors. *Neurol Clin* 2007; **25:** 947-73.
10. Cortez-Conradis D, Favila R, Isaac-Olive K, Martinez-Lopez M, Rios C, Roldan-Valadez E. Diagnostic performance of regional DTI-derived tensor metrics in glioblastoma multiforme: simultaneous evaluation of p, q, L, Cl, Cp, Cs, RA, RD, AD, mean diffusivity and fractional anisotropy. *Eur Radiol* 2013; **23:** 1112-21.
11. Chaudhry NS, Shah AH, Ferraro N, Snelling BM, Bregy A, Madhavan K, et al. Predictors of long-term survival in patients with glioblastoma multiforme: advancements from the last quarter century. *Cancer Invest* 2013; **31:** 287-308.
12. Lopez-Acevedo ML, Martinez-Lopez M, Favila R, Roldan-Valadez E. Secondary MRI-findings, volumetric and spectroscopic measurements in mesial temporal sclerosis: a multivariate discriminant analysis. *Swiss Med Wkly* 2012; **142:** w13549.
13. Toh CH, Wei KC, Ng SH, Wan YL, Lin CP, Castillo M. Differentiation of brain abscesses from necrotic glioblastomas and cystic metastatic brain tumors with diffusion tensor imaging. *Am J Neuroradiol* 2011; **32:** 1646-51.
14. Wang W, Steward CE, Desmond PM. Diffusion tensor imaging in glioblastoma multiforme and brain metastases: the role of p, q, L, and fractional anisotropy. *Am J Neuroradiol* 2009; **30:** 203-8.
15. Rorden C, Karnath HO, Bonilha L. MRIcron dicom to nifti converter. In: *Neuroimaging Informatics Tools and Resources Clearinghouse (NITRC).* Available from: http://www.mccauslandcenter.sc.edu/mricro/mricron/dcm2nii.html, Accessed on June 07, 2012.
16. Smith SM, Jenkinson M, Woolrich MW, Beckmann CF, Behrens TE, Johansen-Berg H, et al. Advances in functional and structural MR image analysis and implementation as FSL. *Neuroimage* 2004: **23:** 208-21.
17. Smith SM. Fast robust automated brain extraction. *Hum Brain Mapping* 2002; **17:** 143-55.
18. Moseley ME, Cohen Y, Kucharczyk J, Mintorovitch J, Asgari HS, Wendland MF, et al. Diffusion-weighted MR imaging of anisotropic water diffusion in cat central nervous system. *Radiology* 1990; **176:** 439-45.
19. Le Bihan D, Mangin JF, Poupon C, Clark CA, Pappata S, Molko N, et al. Diffusion tensor imaging: concepts and applications. *J Magn Reson Imaging* 2001; **13:** 534-46.

20. Brown SR, Gregory WM, Twelves CJ, Buyse M, Collinson F, Parmar M, et al. Designing phase II trials in cancer: a systematic review and guidance. *Br J Cancer* 2011; **105:** 194-9.

21. Obuchowski NA, McClish DK. Sample size determination for diagnostic accuracy studies involving binormal ROC curve indices. *Stat Med* 1997; **16:** 1529-42.

22. Tabachnik BG, Fidell SL. Discriminant analysis. In: Tabachnik BG, Fidell SL, editors. *Using multivariate statistics*. Boston: Pearson Education Inc.; 2013. p. 377-438.

23. Pallant J. Assesing normality. In: Pallant J, editor. *SPSS survival manual*. Crows Nest: Allen & Unwin; 2011. p. 59-64.

24. Pallant J. Multivariate analysis of variance. In: Pallant J, editor. *SPSS survival manual*. Crows Nest: Allen & Unwin; 2011. p. 283-96.

25. Chan YH. Biostatistics 104: correlational analysis. *Singapore Med J* 2003; **44:** 614-9.

26. Field A. Output from the discriminant analysis. In: Field A, editor. *Discovering statistics using SPSS*. London: SAGE Publications Ltd; 2009. p. 618-21.

27. Cohen JW. *Statistical power analysis for the behavioral sciences.* 2nd edition. Hillsdale: Lawrence Erlbaum Associates; 1988.

28. Bossuyt PM, Reitsma JB, Bruns DE, Gatsonis CA, Glasziou PP, Irwig LM, et al. The STARD statement for reporting studies of diagnostic accuracy: explanation and elaboration. *Ann Int Med* 2003; **138**: W1-12.

29. Tabachnik BG, Fidell SL. Multicollinearity and singularity. In: Tabachnik BG, Fidell SL, editors. *Using multivariate statistics*. Boston: Pearson Education Inc.; 2013. p. 88-91.

30. Field A. Discriminant function variates. In: Field A, editor. *Discovering statistics using SPSS*. London: SAGE Publications Inc.; 2009. p. 599-624.

31. Pena A, Green HA, Carpenter TA, Price SJ, Pickard JD, Gillard JH. Enhanced visualization and quantification of magnetic resonance diffusion tensor imaging using the p:q tensor decomposition. *Br J Radiol* 2006; **79:** 101-9.

32. Budde MD, Xie M, Cross AH, Song SK. Axial diffusivity is the primary correlate of axonal injury in the experimental autoimmune encephalomyelitis spinal cord: a quantitative pixelwise analysis. *J Neurosci* 2009; **29:** 2805-13.

33. Feng S, Hong Y, Zhou Z, Jinsong Z, Xiaofeng D, Zaizhong W, et al. Monitoring of acute axonal injury in the swine spinal cord with EAE by diffusion tensor imaging. *J Magn Reson Imaging* 2009; **30:** 277-85.

34. Schmierer K, Wheeler-Kingshott CA, Boulby PA, Scaravilli F, Altmann DR, Barker GJ, et al. Diffusion tensor imaging of post mortem multiple sclerosis brain. *Neuroimage* 2007; **35:** 467-77.

35. Song SK, Yoshino J, Le TQ, Lin SJ, Sun SW, Cross AH, et al. Demyelination increases radial diffusivity in corpus callosum of mouse brain. *Neuroimage* 2005; **26:** 132-40.

36. Westin CF, Maier SE, Mamata H, Nabavi A, Jolesz FA, Kikinis R. Processing and visualization for diffusion tensor MRI. *Med Image Anal* 2002; **6:** 93-108.

37. Woodworth DC, Pope WB, Liau LM, Kim HJ, Lai A, Nghiemphu PL, et al. Nonlinear distortion correction of diffusion MR images improves quantitative DTI measurements in glioblastoma. *J Neurooncol* 2013. 2014; **116:** 551-8.

38. Saksena S, Jain R, Schultz L, Jiang Q, Soltanian-Zadeh H, Scarpace L, et al. The corpus callosum Wallerian degeneration in the unilateral brain tumors: evaluation with diffusion tensor imaging (DTI). *J Clin Diagn Res* 2013; **7:** 320-5.

39. Saksena S, Jain R, Narang J, Scarpace L, Schultz LR, Lehman NL, et al. Predicting survival in glioblastomas using diffusion tensor imaging metrics. *J Magn Reson Imaging* 2010; **32:** 788-95.

case report

Magnetic resonance spectroscopy (MRS) of vertebral column - an additional tool for evaluation of aggressiveness of vertebral haemangioma like lesion

Miran Jeromel, Janez Podobnik

Clinical Institute of Radiology, University Medical Centre Ljubljana, Ljubljana, Slovenia

Radiol Oncol 2014; 48(2): 137-141.

Received 08 June 2012
Accepted 16 December 2012

Correspondence to: Miran Jeromel, M.D., Clinical Institute of Radiology, University Medical Centre Ljubljana, Zaloska cesta 7, Ljubljana, Slovenia. Phone: +386 1 522 3054; Fax: +386 40 32 66 90; E-mail: miran.jeromel@gmail.com

Disclosure: No potential conflicts of interest were disclosed.

Background. Most vertebral haemangioma are asymptomatic and discovered incidentally. Sometimes the symptomatic lesions present with radiological signs of aggressiveness and their appearance resemble other aggressive lesions (e.g. solitary plasmacytoma).

Case report. We present a patient with large symptomatic aggressive haemangioma like lesion in 12th thoracic vertebra in which a magnetic resonance spectroscopy (MRS) was used to analyse fat content within the lesion. The lesion in affected vertebrae showed low fat content with 33% of fat fraction (%FF). The fat content in non-affected (1st lumbar) vertebra was as expected for patient's age (68%). Based on MRS data, the lesion was characterized as an aggressive haemangioma. The diagnosis was confirmed with biopsy, performed during the treatment – percutaneous vertebroplasty.

Conclusions. The presented case shows that MRS can be used as an additional tool for evaluation of aggressiveness of vertebral haemangioma like lesions.

Key words: aggressive vertebral haemangioma; magnetic resonance spectroscopy; percutaneous vertebroplasty

Introduction

Vascular lesions of the musculoskeletal system are relatively common. Haemangioma is by far the most common benign tumour of the axial skeleton, occurring in 11% of spines at autopsy.[1,2] The histological pattern of osseous haemangioma is characterized by the proliferation of anomalous thin – walled blood vessels and sinuses lined by endothelium between the thickened, vertically oriented trabeculae of bone.[3,4]

Most vertebral haemangioma (VH) are asymptomatic and discovered incidentally. However, the lesions sometimes present with radiological signs of aggressiveness, clinically manifested as local pain and neurologic deficit. Symptomatic VH occur in 0.9 to 1.2% of patients.[5,6] The term aggressive or active haemangioma is used for those lesions. The differentiation of aggressive VH lesions from some other tumour lesions of vertebral column could be challenging.

Imaging characteristics of aggressive VH are: occupancy of the entire vertebral body, extension into the neural arch, expansion of osseous margins, and presence of a soft tissue component.[7] The lesions typically contain less fat and more vascular stroma thereby producing a low signal on T1 weighted magnetic resonance (MR) images.[4,5,8] Marked post-contrast enhancement is another characteristic. However, the lesion can resemble a solitary vertebral plasmacytoma on computer tomography (CT), as well as on MR images. Epitheloid haemangioen-

dothelioma is another although rare vertebral lesion that must be encountered in the differential diagnosis.

MR spectroscopy (MRS) as advanced MR imaging modality has the potential to quantify vertebral tissue components (*i.e.* bone and marrow). Data about vertebral fat content in healthy individuals were published previously.[9,10] Spectral analysis of fat content in VH is useful as it can clear out the diagnosis as well as aggressiveness of the lesion. On the basis of MRS data, the lesions that need to be treated could be selected.

Authors present a case report of a patient with symptomatic aggressive haemangioma like lesion in whom a MRS was used to analyse fat content. On the basis of MRS, the decision for biopsy and early treatment with the goal of stabilization (percutaneous vertebroplasty) was made.

Case report

A 61 year old otherwise healthy female patient presented with progressive low back pain. MR examination revealed pathologic lesion in 12th thoracic vertebra. The lesion filled majority of the vertebral body with extension into a left pedicle. Signal characteristics of the lesion were as follows: hyperintense on fat suppressed (STIR) MR image, homogeneously hypointense on pre-contrast *T1 w* SE MR image, homogeneously hyperintense on *T2 w* TSE MR image and very hyperintense on post-contrast *T1 w* SE MR image. Subtle disruption of the posterior vertebral wall was seen on pre-contrast MR scan. Post-contrast images confirmed homogenously enhancing (vascularized) haemangioma like tumour. The aggressiveness of the lesion was confirmed with signs of cortical bone disruption seen on CT (Figure 1).

However, the lesion lacked typical thickened trabeculae what brought a diagnosis of haemangioma into a question. A "mini brain" pattern that was partially recognized on CT raised a possibility of a plasmacytoma in the differential diagnosis. The PET scan showed no activity of the lesion. Therefore clear distinction between possible plasmacytoma was not possible with standard CT and MR imaging.

Additional MR examination with MRS was used to define fat content in order to clear out the diagnosis and confirm the aggressiveness of the lesion.

The examination was performed on Philips Achieva 1.5 T NOVA 16 channel MR scanner equipped with High Performed gradients with peak amplitude of 33 mT/m and slew rate 180 mT/m/ms. The SENSE 15 elements phased array Spine coil was used. MR imaging protocol consists of *T2 w* TSE, *T1 w* SE and STIR in sagittal plane, *T2 w* TSE, *T1 w* TSE in axial plane. After the use of the gadolinium contrast media *T1 w* sequences in sagittal and axial plane were repeated. Single Voxel (SV) spectroscopy data were acquired with STEAM (Stimulated Echo Acquisition Mode) sequence because it has several advantages compared to PRESS (Point Resolved Spectroscopy) in spine region.[10] Parameters of SV STEAM sequences were: TR 2000 ms, TE 8.7 ms, TM (Mixing Time) 12 ms, voxel size of 19 mm x 26 mm x 17 mm, NSA (Number of Signal Averaging) 128. Water suppression was disabled and to define optimal cubic target volume PB (Pencil Beam) volume shimming was utilized. To suppress unwanted signals from adjacent structures three REST (REgional Saturation Technique) slabs were applied. The voxel of first measurement was placed in the lesion (12th thoracic vertebral body) and the second in lower healthy (1st lumbar) vertebral body. The data were processed on a Philips – Extended MR WorkSpace with

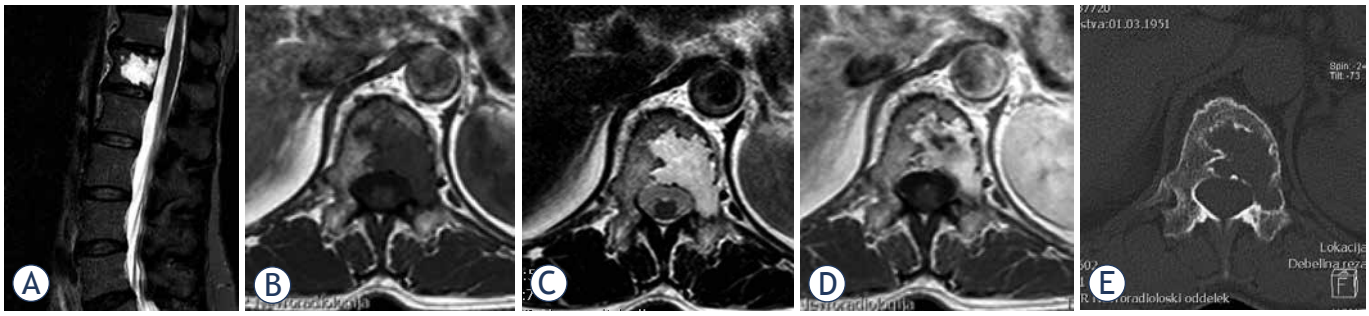

FIGURE 1. MR and CT images of the patient. The pathologic lesion in 12th thoracic vertebra that fills the majority of the vertebral body is seen as a hyperintense lesion on sagittal fat suppressed (STIR) MR image (A). The lesion appeared homogeneously hypointense on pre-contrast axial *T1 w* SE MR image (B) and homogeneously hyperintense on axial *T2 w* TSE MR image (C). Post-contrast axial *T1 w* SE MR image shows marked enhancement of the lesion that extends to the left pedicle (D). The aggressiveness of the lesion was confirmed with subtle signs of cortical bone disruption seen on CT (E). However, the lesion lacked typical thickened trabeculae what brought a diagnosis of haemangioma into a question.

SpectroView software. Special script for processing data was formed; only peaks from water and lipids were selected.

Peak lipid-water ratio (LWR), calculated as lipid peak/water peak was derived for each voxel. Another parameter – percent fat fraction (%FF) was used. %FF was derived from LWR as follows: LWR/(LWR+1) x 100.[10]

MRS was successfully performed in both (12th thoracic and 1st lumbar) vertebral bodies. Two major signals (water and lipid) separated by 3.1 ppm were identified in both spectres. A difference between lipid peaks in both vertebral bodies was noticed, as expected (Figure 2). Peak LWR in affected 12th thoracic and adjacent 1st lumbar vertebral body were 0.49 and 2.15, respectively. The lesion in affected vertebra showed lower fat content (33%FF) than normal adjacent vertebra (68%FF). On the basis of % FF we speculated that the amount of fat could be more a feature of haemangioma than plasmacytoma.

Based on MRS data, the lesion was therefore characterized as an aggressive haemangioma.

The diagnosis of haemangioma was confirmed with biopsy, performed during the therapeutic procedure - percutaneous vertebroplasty.

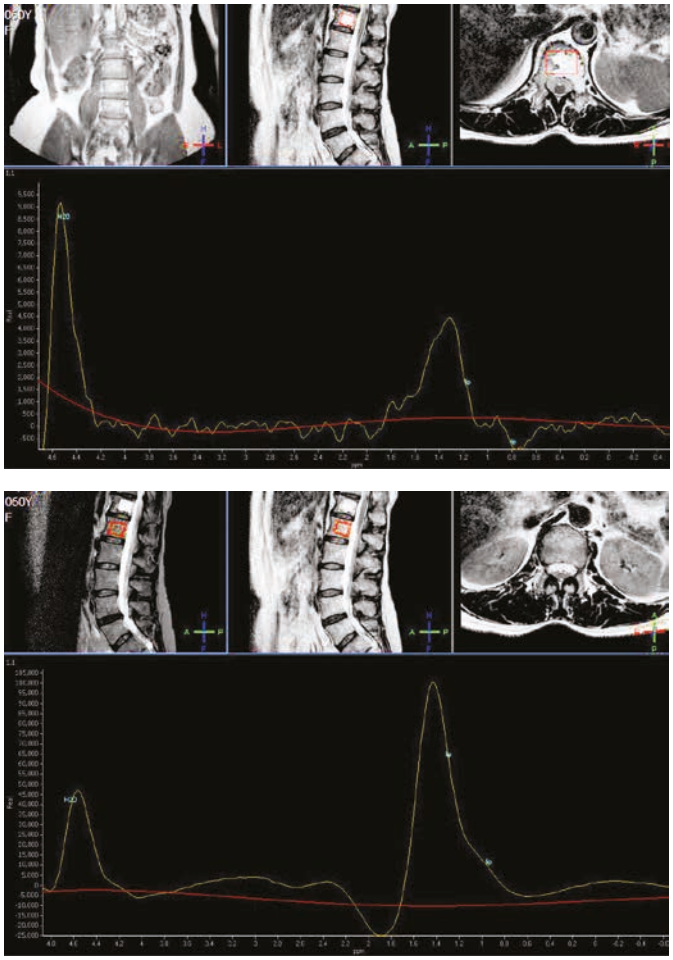

FIGURE 2. MR spectroscopy of the affected (12th thoracic) and adjacent healthy (1st lumbar) vertebra. Two major signals (water and lipid) separated by 3.1 ppm are clearly seen in both specters. The lipid peak in pathologic lesion (A) is much lower than in non-affected vertebral body (B). Lipid-water ratio (LWR), calculated as lipid peak/water peak in affected and adjacent vertebral body were 0.49 and 2.15, respectively. The fat content, expressed as percentage fat fraction (%FF, derived from LWR/ (LWR +1) x 100) was lower in affected (33 %FF) than in normal adjacent vertebra (68 %FF). On the basis of fat content we speculated that the amount of fat could be more a feature of aggressive haemangioma.

Discussion

Vertebral haemangioma are common lesions and usually considered benign.

Both, CT and MR are important imaging modalities to help differentiate between benign and malignant lesions.[11,12] It is also used to evaluate VH. The lesion shows typical pattern on CT. Multiple dots (polka-dot appearance) represent a cross-section of reinforced trabeculae.[13] The presence of high signal intensity on T1- and T2-weighted MR images is related to the amount of adipocytes or vessels and interstitial oedema, respectively.[14] Fatty VH may represent inactive forms of this lesion, whereas low signal intensity at MR imaging (less fat content) may indicate more active lesion with the potential to compress the spinal cord.[4,5,8,13]

Other radiological signs of aggressiveness are: location between Th3 and Th9, involvement of the entire vertebral body, extension to the neural arch, expanded cortex with indistinct margins, irregular honeycomb pattern, and soft-tissue mass.[7]

Determination of aggressiveness is an important part of imaging evaluation, as it influences the decision about the treatment. According to Deramond, considering radiological signs of aggressiveness, VH can be classified into four groups:
1 - Asymptomatic VH, without radiological signs;
2 - Asymptomatic VH, with radiological signs;
3 - Symptomatic VH, without radiological signs;
4 - Symptomatic VH, with radiological signs (13).
Patients in group 1 require no treatment. Patient from all other groups need some kind of intervention.[15]

Aggressive VH could closely resemble solitary plasmacytoma. Lytic appearance on CT is characteristic for both lesions. Low signal on T1 and high signal on T2 images as well as marked enhancement on MR are also common features. A characteristic "mini brain" appearance on MR images is

described to be a typical finding in plasmacytoma. Rare vertebral epitheloid haemangioendothelioma is another lytic lesion that could be very similar to aggressive haemangioma on CT and MR imaging.

Our patient presented with symptomatic VH like lesion that showed some radiological characteristics of aggressiveness (low fat content on standard MR imaging, extension to the neural arch, and expanded cortex with indistinct margins). Therefore the lesion could be classified into group 4 (according to Deramond).[15]

However, fat content, as important factor that determines VH and its behaviour (aggressiveness), could be evaluated only qualitatively on standard MR images. High signal on STIR sequence and particularly low signal on T1 sequence are features of aggressive VH. More accurate quantitative assessment of fat content could be very useful in some cases. This is especially important with lesions that do not present with typical imaging characteristics of haemangioma and in those haemangioma with some characteristics of aggressiveness. The later was true in our case.

MRS enables quantitative evaluation of biological tissue. Namely, the method has the ability to transform bulk MR imaging data (derived from examined tissue) to distinct components. Technique applied in our case (proton MR spectroscopy) uses the signal from hydrogen protons to determine the concentration of metabolites. Bone marrow is composed mainly of water and lipid. Accurate determination of these two key fractions can be achieved with spectral analysis using MRS.[10,16] The method was used early to determine vertebral fat content in healthy individuals.[9,10]

We were able to perform a MRS in our patient and on the basis of collected data a spectral analysis of two vertebral bodies (affected and normal adjacent) was performed. MRS data from healthy lumbar vertebral body showed high lipid peak (high fat content) as expected for the patient's age (68%FF). Our data were in concordance with data published by other authors.[17] The analysis of age differences in the proton spectrum of vertebral bone marrow showed an increase in %FF with increasing age, from 24% in the age group of 11 to 20 years to 54% in the group aged 61 years or older.[17] Specter from pathological lesion within the 12th thoracic body was completely different, as expected. The water content was comparable to healthy vertebral body, while fat content was low, but still very obvious (33%FF).

There is another fact that must be considered analysing water content in vertebral bodies. It has been shown that the water fraction approximates the percentage volume of haematopoietic (red) marrow. It declined with age from 81-89% in the 2nd decade to 37-45% in subjects older than 70 years.[10] A hypothetic presence of a large amount of haematopoietic marrow (high water content) in the affected vertebra would result in a low %FF. According to our knowledge there are only two available reports of using vertebral body MRS in patients with multiple myeloma.[18,19] The authors reported about decreased fat content in multiple myeloma (20% *vs*. 31% and 34% in volunteers and osteoporosis).[17]

Based on our low but still significant amount of %FF (33%FF), we could speculate that a haematopoietic origin of the lesion (*i.e*. solitary plasmacytoma) was less likely**.** The result of MRS could therefore confirm the diagnosis of aggressive haemangioma.

A dilemma about the treatment modality and time to intervention rose. Due to the size of the lesion, there was an obviously need for stabilization to avoid collapse of the vertebra. A minimally invasive percutaneous vertebroplasty with biopsy at the same time was chosen. The procedure was successfully done and the biopsy confirmed the diagnosis of aggressive haemangioma.

Conclusions

The presented case shows that MRS can be used as an additional tool for diagnosis and evaluation of aggressiveness of vertebral haemangioma and haemangioma like lesions.

References

1. Bloomer CW, Ackerman A, Bhatia RG. Imaging for spine tumors and new applications. *Top Magn Reson Imaging* 2006; **17:** 69-87.
2. Schmorl G, Junghanns H. *The human spine in health and disease.* New York: Grune and Stratton; 1971.
3. Schrock WB, Wetzel RJ, Tanner SC, Khan MA. Aggressive hemangioma of the thoracic spine. *Radiol Case Rep* 2011; **5:** 7-13.
4. Laredo JD, Assouline E, Gelbert F, Wybier M, Merland JJ, Tubiana JM. Vertebral hemangiomas: fat content as a sign of aggressiveness. *Radiology* 1990; **177:** 467-72.
5. Chen HI, Heuer GG, Zaghloul K, Simon SL, Weigele JB, Grady MS. Case report. Lumbarvertebral hemangioma presenting with the acute onset of neurological symptoms. *J Neurosurg Spine* 2007; **7:** 80-5.
6. Cheung NK, Doorenbosch X, Christie JG. Rapid onset aggressive vertebral haemangioma. *Childs Nerv Syst* 2011; **27:** 469-72.
7. Laredo JD, Reizine D, Bard M, Merland JJ. Vertebral Hemangiomas: radiologic evaluation. *Radiology* 1986; **161:** 183-9.
8. Fox MW, Onofrio BM. The natural history and management of symptomatic and asymptomatic vertebral hemangiomas. *J Neurosurg* 1993; **78:** 36-45.

9. Schick F, Bongers H, Jung WI, Skalej M, Lutz O, Claussen CD. Volume-selective proton MRS in vertebral bodies. *Magn Reson Med* 1992; **26:** 207–17.

10. Schellinger D, Lin CS, Fertikh D, Lee JS, Lauerman WC, Henderson F, et al. Normal lumbar vertebrae: anatomic, age, and sex variance in subjects at proton MR spectroscopy – initial experience. *Radiology* 2000; **215:** 910-6.

11. Pavlisa1 G, Pavlisa G, Rados M. Diffusion differences between pilocytic astrocytomas and grade II ependymomas. *Radiol Oncol* 2011; **45:** 97-101.

12. Xu J, Shen J, Ding Y, Shen HY, Zeng ZP, Ma RF, et al. The clinical value of combined use of MR imaging and multi-slice spiral CT in limb salvage surgery for orthopaedic oncology patients: initial experience in nine patients. *Radiol Oncol* 2012; **46:** 189-97.

13. Rodallec MH, Feydy A, Larousserie F, Anract P, Campagna R, Babinet A, et al. Diagnostic imaging of solitary tumors of the spine: what to do and say. *Radiographics* 2008; **28:** 1019-41.

14. Baudrez V, Galant C, Van de Berg BC. Benign vertebral hemangioma: MR-histological correlation. *Skeletal Radiol* 2001; **30:** 442-6.

15. Deramond H, Depriester C, Galibert P, Le Gars D. Percutaneous vertebroplasty with polymethylmethacrylate: Technique, indications, and results. *Radiol Clin North Am* 1998; **36:** 533-46.

16. Schellinger D, Lin CS, Hatipoglu HG, Fertikh D. Potential value of vertebral proton MR spectroscopy in determining bone weakness. *Am J Neuroradiol* 2001; **22:** 1620-7.

17. Kugel H, Jung C, Schulte O, Heindel W. Age- and sex-specific differences in the 1H-spectrum of vertebral bone marrow. *J Magn Reson Imaging* 2001; **13:** 263-8.

18. Schick F, Forster J, Einsele H, Weiss B, Lutz O, Claussen CD. Magnetization transfer in hemopoietic bone marrow examined by localized proton spectroscopy. *Magn Reson Med* 1995; **34:** 792-802.

19. Layer G, Träber F, Block W, Bräucker G, Kretzer S, Flacke S, et al. 1H MR spectroscopy of the lumbar spine in diffuse osteopenia due to plasmacytoma or osteoporosis. *Rofo* 1998; **169:** 596-600.

research article

Proteomic analysis of effects by x-rays and heavy ion in HeLa cells

Zhitong Bing[1]*, Guanghui Yang[1,2]*, Yanan Zhang[1], Fengling Wang[3], Caiyong Ye[1], Jintu Sun[1], Guangming Zhou[1], Lei Yang[1]

[1] Institute of Modern Physics, Chinese Academy of Sciences, Lanzhou, China
[2] Graduate School of Chinese Academy of Sciences, Beijing, China
[3] Biochemistry and Molecular Laboratory, Medical College of Henan University, Henan, China

Radiol Oncol 2014; 48(2): 142-154.

Received 4 July 2013
Accepted 19 October 2013

Correspondence to: Lei Yang, Institute of Modern Physics, Chinese Academy of Sciences, Lanzhou 730000, China. E-mail: lyang@impcas.ac.cn and Guangming Zhou, Institute of Modern Physics, Chinese Academy of Sciences, Lanzhou 730000, China. E-mail: zhougm@impcas.ac.cn

* These authors contributed equally to this work.

Disclosure: The authors declare no competing financial interests.

Background. Carbon ion therapy may be better against cancer than the effects of a photon beam. To investigate a biological advantage of carbon ion beam over X-rays, the radioresistant cell line HeLa cells were used. Radiation-induced changes in the biological processes were investigated post-irradiation at 1 h by a clinically relevant radiation dose (2 Gy X-ray and 2 Gy carbon beam). The differential expression proteins were collected for analysing biological effects.

Materials and methods. The radioresistant cell line Hela cells were used. In our study, the stable isotope labelling with amino acids (SILAC) method coupled with 2D-LC-LTQ Orbitrap mass spectrometry was applied to identity and quantify the differentially expressed proteins after irradiation. The Western blotting experiment was used to validate the data.

Results. A total of 123 and 155 significantly changed proteins were evaluated with treatment of 2 Gy carbon and X-rays after radiation 1 h, respectively. These deregulated proteins were found to be mainly involved in several kinds of metabolism processes through Gene Ontology (GO) enrichment analysis. The two groups perform different response to different types of irradiation.

Conclusions. The radioresistance of the cancer cells treated with 2 Gy X-rays irradiation may be largely due to glycolysis enhancement, while the greater killing effect of 2 Gy carbon may be due to unchanged glycolysis and decreased amino acid metabolism.

Key words: X-rays; Carbon ion; 2D-LC-MS/MS; SILAC; Gene Ontology enrichment

Introduction

Radiotherapy is one of the most important treatments for many human cancers. The statistics showed that at least 50 percent of patients who suffered from cancer received radiotherapy during the course of their therapy. X-rays and carbon beams have been widely applied in radiotherapy. Although X-rays treatment is an effective modality for variety of human cancers, in certain cases it can provide poor results.[1] Some studies report that heavy ion beam have obvious advantages over other radiotherapy mainly due to the spread out Bragg's peaks (SOBP), which can cover tumors with biological equivalent dose distribution.[2,3] Besides, heavy ion can also reduce oxygen enhancement ratio, decrease cell-cycle-dependent radiosensitivity, and induce more DNA double strand breaks that are not easily repaired.[4-6] Although many studies focused on the different biological effects between heavy ion and X-rays, few have revealed the mechanism of their difference on the systems level. Therefore, understanding the mechanisms of radiation effect on cancer cells will contribute

to the development of powerful therapeutics for treatment of cancer. In recent years, the tendency of researches on exploring the difference between low-LET (X-ray and gamma ray) and carbon beam are increasing in clinical application.[7,8]

In fact, radiation biological effectiveness (RBE) means not only the response of different DNA damage to different types of radiation, but also the combined effects of protein interaction regulation and protein differential expression. So, proteomic analysis will provide more information as well as novel insight into understanding the difference of the two types of radiation therapies. In this study, our aim is to provide systems level insight into understanding molecular mechanism of the cancer cells exposure to different types of radiation. Therefore, a precise quantitative measurement, stable isotope labelling with amino acids in cell culture (SILAC) in combination with two-dimensional liquid chromatography-tandem mass spectrometry (2D-LC-MS/MS) shotgun proteomics[9-12], was employed to investigate the response of HeLa cells exposed to different types of 2 Gy radiation. And it has been widely accepted that quantitative proteomic analysis was a powerful tool for investigating the radiation effect.[13-16]

By Gene Ontology (GO) term enrichment analysis and Ingenuity Pathway Analysis (IPA), we found that the therapeutic differences between X-ray and heavy ion beam on killing effects, DNA damage and survival fraction in cancer cells might be largely due to their different metabolism processes.

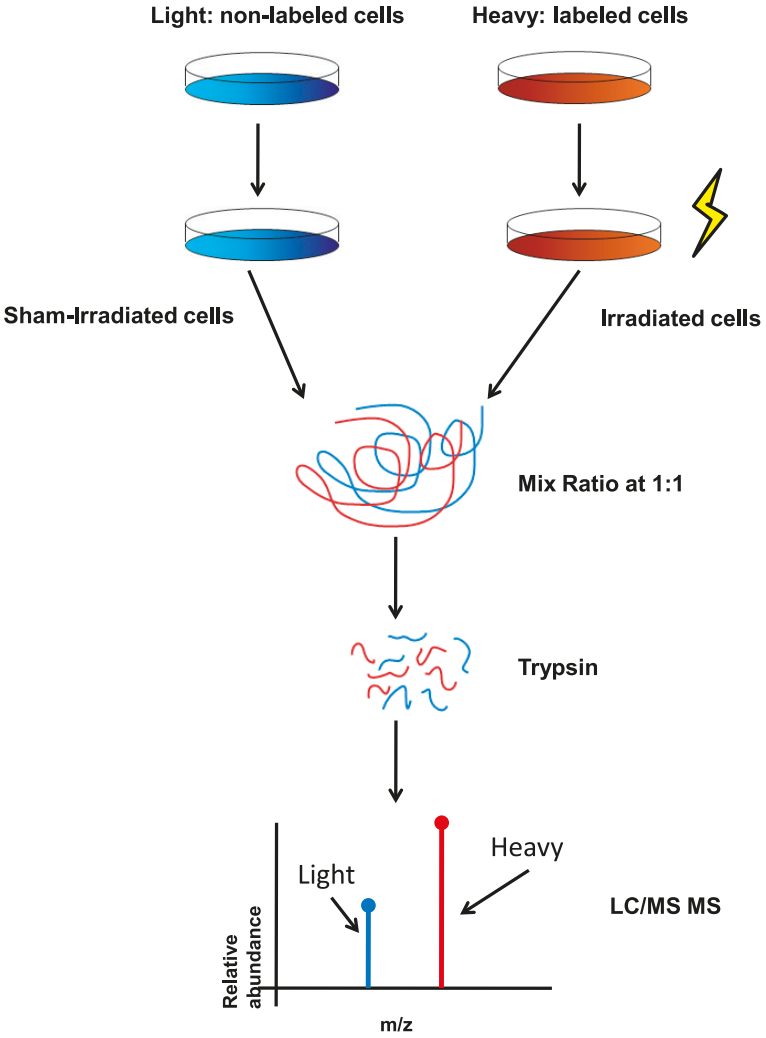

FIGURE 1. Brief SILAC experiment workflow. For the SILAC experiment, the HeLa cells were culture in DMEM containing "heavy" $^{13}C_6{}^{15}N_4$ L-arginine , $^{13}C_6{}^{15}N_2$ L-lysine and "light" $^{12}C_6{}^{14}N_4$ L-arginine and $^{12}C_6{}^{14}N_2$ L-lysine. After 100% label incorporation, heavy cells were irradiated and harvested after 1 h. Then, the cells were digested and mixed (treated *vs.* control) at 1:1 for mass spectrometric analysis.

Materials and methods

Sample preparation

Human cervical carcinoma HeLa cells (ATCC, CCL-2) were maintained in DMEM (Gibco) at 37°C in the 5% CO_2 air-humidified incubator. Cells in control group were prepared by supplementing the growth medium with light $^{12}C_6{}^{14}N_4$ L-arginine and $^{12}C_6{}^{14}N_2$ L-lysine. Cells irradiated were maintained in heavy $^{13}C_6{}^{15}N_4$ L-arginine and $^{13}C_6{}^{15}N_2$ L-lysine supplemented medium. At least 7 subcultures were performed to obtain efficiently labelled cell populations. We separated the heavy labelled cells into 2 groups to be exposed to carbon ion and X-rays irradiation.

Irradiation

HeLa cells were trypsinized, counted and seeded in 25 cm^2 flasks at a density of 5×10^5 cells/flask. After 48 h of incubation, sample 1 was irradiated at room temperature with 2 Gy of high-LET carbon beam with original energy of 165 MeV/u generated by the Heavy Ion Research Facility at Lanzhou (HIRFL, Institute of Modern Physics, Chinese Academy of Science). Sample 2 was irradiated at room temperature using RX650 X-Ray irradiator (Faxitron, Lincolnshire, IL, USA) at a dose of 2 Gy. The X-Ray generator at 200 kVp and 20 mA with 0.5 mm AI and 0.5 Cu filters. The dose rate was 1 Gy/min. Cells were returned to the incubator for further incubation.

Trypsin digestion

All protein samples were extracted for MS analysis. Cells were scraped into 6 M urea and sonicated

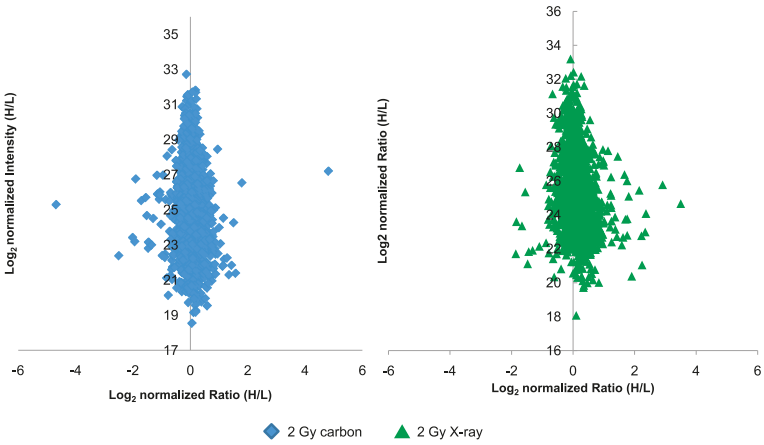

FIGURE 2. Distribution of log_2 transformed protein expression ratios of two irradiation types. The proteins represented by data points lying close to the y-axis (y-axis=1) did not show any expression changes. Outliers were considered as proteins with significantly differential expression only if they had a p-value≤0.05 and were identified with a minimum of 2 unique peptides.

for 10 min at 4°C. After centrifugation for 30 min at 20,000g, the supernatants were collected and stored at -80°C. Protein concentrations were measured using the Bradford method.

Extracted protein samples from irradiated cells and control cells were combined at a 1:1 ratio. In short, 100 μg of protein mixture was dissolved in 6 M urea and 25 mM NH_4HCO_3 and reduced with 10 mM DTT for 1 h room at temperature. Samples were alkylated by 40 mM iodacetamide in the dark for 1 h at room temperature, and then 40 mM DTT was added to quench the iodacetamide for 1 h at room temperature. After diluting 8 M urea with 25 mM NH_4HCO_3 to 0.6 M, subsequently trypsin was added at a ratio of 1:40 and digested at 37°C for overnight. In order to completely fragmentate proteins, trypsin was added to at a ratio of 1:40 again and digested at 37°C for 8 h. At last, trypsin digestion was stopped by adding 1% formic acid.[17]

2D-LC-MS/MS analysis

The tryptic peptide mixtures were analyzed by 2D-LC coupled to a linear ion trap mass spectrometer LTQ-Orbitrap (Thermo Electron, San Jose, CA, USA). For each experiment, the peptide mixtures (from about 100 μg proteins) were pressure-loaded onto a biphasic silica capillary column (250 um id) packed with 3 cm of reverse phase C18 resin (SP-120-3-ODS-A, 3 mm, the Great Eur-Asia Sci&Tech Devolopment, Beijing, China) and 3 cm of strong cation exchange resin (Luma 5 um SCX 100A, Phenomenex, Torrance, CA, USA). The buffers used were 0.1% FA (buffer A), 80% ACN/0.1% FA (buffer B), and 600 mM ammonium acetate/5% ACN/0.1% FA (buffer C). After sample loading, the biphasic column was first desalted with buffer A and then eluted using a 10-step salt gradient ranging from 0 to 600 mM ammonium acetate. After each salt gradient, a gradient of buffer B ranging from 0 to 100% was applied. Step 1 consisted of a 100-min gradient from 0 to 100% buffer B. For steps 2–9, after equilibrating with buffer A for the first 3 min, X% buffer C was applied for 5 min, and peptides were eluted using a linear gradient as follows: 0–10% buffer B in 5 min, 10–45% buffer B in 77 min, 45–100% buffer B in 10 min and 100% buffer B for 10 min, followed by re-equilibration with buffer A for 10 min. The 5-min buffer C percentages (X) were 5, 10, 15, 20, 25, 35, 50, 75%. The gradient used in the final step contained 3 min of 100% buffer A, 20 min of 100% buffer C, a 5-min gradient from 0 to 10% buffer B, a 72-min gradient from 10 to 55% buffer B and a 5-min gradient from 55 to100% buffer B. Then 100% buffer B was applied for 5 min, followed by a 5-min elution with buffer A and another 10-min elution with buffer B. The effluent of the biphasic column in each case was directed into an in-house-packed 10 cm C18 analytical column (100 um id, SP-120-3-ODS-A, 3 mm) with a 3- to 5-um spray tip. The flow rate at the tip was maintained at about 500 nL/min. Nano-electrospray ionization was performed at a spray voltage of 1.9 kV and a heated capillary temperature of 170°C. The MS instrument was set to the data-dependent acquisition mode with dynamic exclusion turned on, and maximum ion injection time was set to 100 ms. One MS survey scan, with mass range 400–2000 m/z, was followed by five MS/MS scans.[18] All tandem mass spectra were collected using a normalized collision energy (a setting of 35%), an isolation window of 2 Da, and 1 micro-scan. The XCalibur data system (ThermoElectron, Waltham, MA, USA) was used to control the HPLC solvent gradients and the application of MS scanning functions.

Data analysis and bioinformatics

Peptides were identified using the MaxQuant software package[19], version 1.3.0.5. MS/MS spectra were searched against the human international Protein Index (IPI) database (version 3.87), which was released on Sep 27,2011, and contains 91,464 protein sequences. Precursor mass tolerance was set to 20 ppm for the first search. For the main search, a 6ppm precursor mass tolerance was used. The maximum precursor ion charge state used for searching was 7. D2-carbamidomethylation of

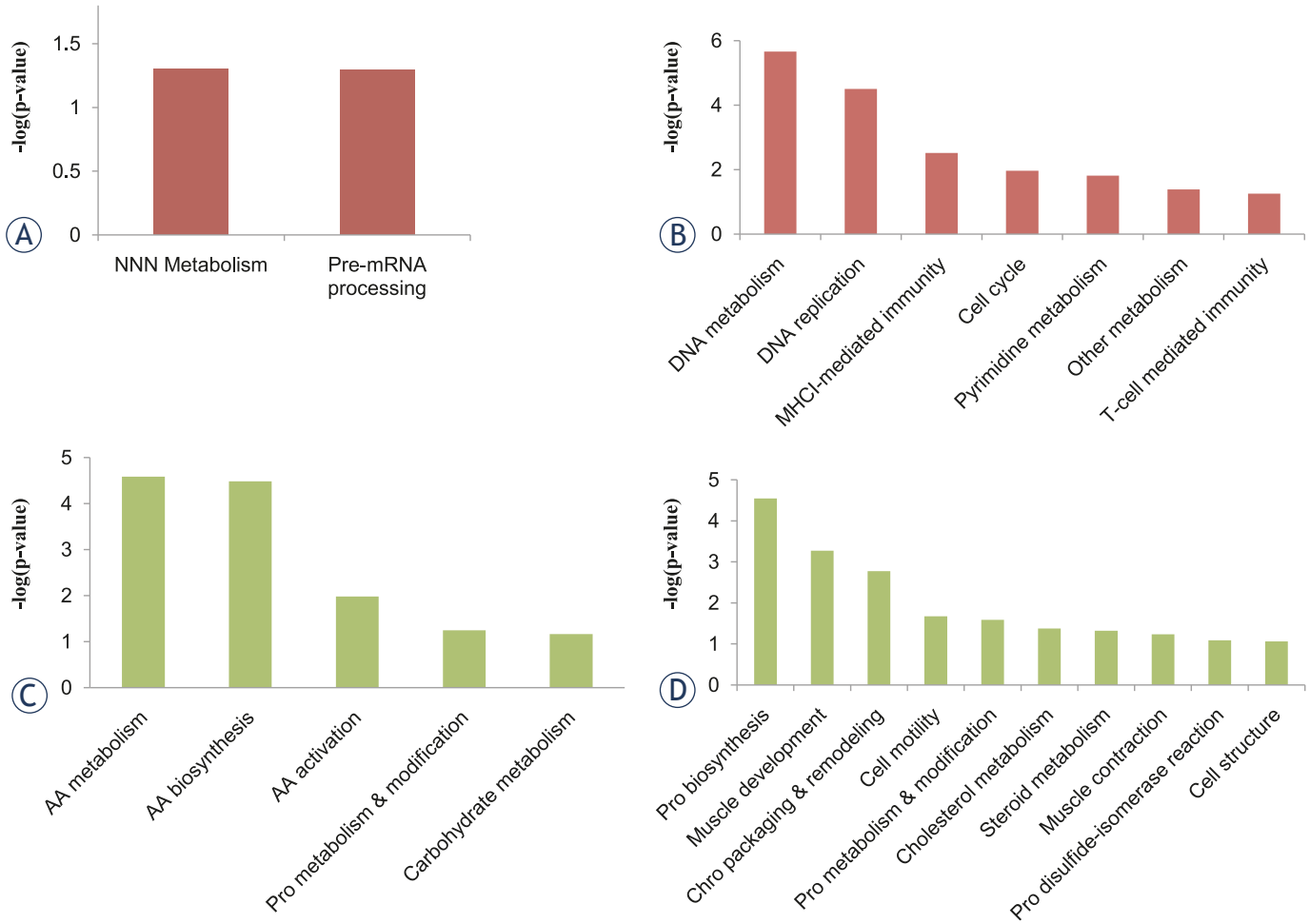

FIGURE3. The biological process analysis for 2 Gy carbon and 2 Gy X-ray deregulated proteins. **(A)** the biological process distribution of up-regulated proteins in 2 Gy carbon irradiation(NNN, Nucleoside, nucleotide and nucleic acid). **(B)** The biological process distribution of up-regulated proteins in 2 Gy X-ray. C The biological process distribution of down-regulated proteins in 2 Gy carbon irradiation (AA, Amino acids; Pro, Protein;). **(D)** The biological process distribution of down-regulated proteins in 2 Gy X-ray (Chro, Chromatin; Pro, Protein).

cysteines (59.0340 delta mass) was searched as a fixed modification and oxidation of methionines (15.999 delta mass), heavy L-arginine (10.0083 delta mass) and heavy L-lysine (8.0142 delta mass) were search as variable modifications. Enzyme specificity was set to trypsin and a maximum of two missed cleavages was allowed for searching. The target-decoy- based false discovery rate (FDR) for peptide and protein identification was set to 1% for peptides and proteins.[20] Unmodified, oxidized methionine, deamidated asparagines, and N-terminally acetylated peptides were utilized for protein quantification.

Protein level information was obtained from the MaxQuant Protein Groups table. The proteins that identified as reverse or contaminants were removed from the result. All reported proteins were identified by two or more unique peptides and quantified with two or more ratio counts. Then, the data analysis was using the MaxQuant software program to generate an average normalized heavy/light ratio over three biological replicates, and significance B values were calculated using Perseus software.[21] To determine significance, we used the cutoff of a significant B score of less than 0.05.

In this study, Ingenuity Pathway Analysis (IPA) (Ingenuity® Systems, www.ingenuity.com) was applied to obtain information of relationship, biological mechanism, functions, and pathways of differentially regulated proteins. The fold change with $\log_2$ ratio and IPI accession number of deregulated proteins were submitted to IPA.

The DAVID Bioinformatics resource and Protein Analysis Through Evolution Relationships (PANTHER)[22] classification system were used to identify enriched gene ontology (GO) terms in our dataset.[23,24] GO terms assigned a Benjamini-Hochberg adjusted p-value of less than 0.05 by DAVID were deemed to be enriched over the background gene set.

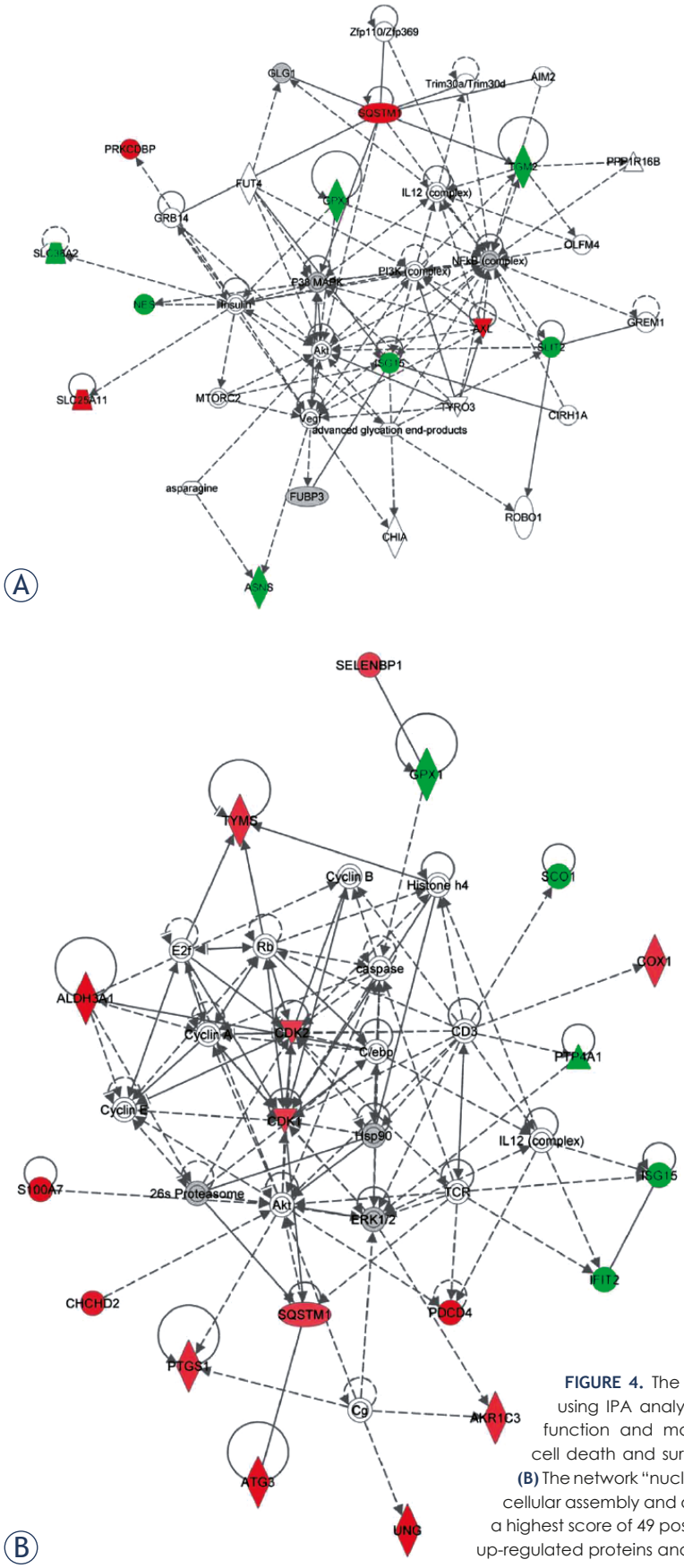

Western Blot analysis

Antibodies to lactate dehydrogenase A (LDHA) (sc-27230) were purchased from Santa Cruz Biotechnology and Anti-SCO1 (54653) antibody was purchased from Anaspec. Antibodies to AKT (9272) antibodies were purchased from Cell Signaling Technology.

Cells were collected and lysed in appropriate amounts of lysis buffer (Biyuntian, Nanjing, China). Samples were centrifuged at 10,000 g, 4°C for 15 min and the concentration of total protein was determined from the supernatants using BCA protein assay kit (Pierce, Rockford, IL, USA). Thereafter, samples were mixed with sample buffer (250 mM Tris HCl, 5% β-mercaptoethanol, 50% glycerol, 10% SDS, 0.5% bromophenol blue), boiled for 5 min and equal amounts of protein (30 μg) were separated with 10% SDS-PAGE gels (Bio-Rad, Tokyo, Japan). PVDF membranes (GE healthcare, Beijing, China) were rinsed in 100% methanol for 10 s and subsequently placed in transfer buffer (48 mM Tris, 39 mM Glycine, 0.037% SDS, 20% methanol) for 5 min. Blotting was performed at 120V for 1.5 h in a wet transfer instrument (Bio-Rad, Hercules, CA). The membranes were blocked for 1 h in blocking buffer (5% skim milk) and incubated with primary antibodies for 2 h. The membranes were then washed three times with PBS containing 0.1% Tween20 and incubated with secondary antibody for 1 h. Finally, following washing the membranes, protein bands were visualized using the enhanced chemiluminescence system (Amersham-Buchler, Braunschweig, Germany) and exposed to X-ray medical film (Kodak, Tokyo, Japan). The image analysis of western blots were using Photoshop CS5 software (Adobe).

Colony formation assay

Cell survival was determined by conventional colony-formation assay. The irradiated cells were collected by trypsinization and resuspended in RPMI-1640 medium complemented with 10% FBS. Cell concentration was determined with a cell counter (Coulter, model Z1 with a 100 μm aperture tube). Cells were diluted with medium and seeded

FIGURE 4. The highest score network post-irradiation by 2 Gy carbon and X-ray using IPA analysis. **(A)** The network "Cellular assembly and organization, cellular function and maintenance, post-translational modification, protein folding and cell death and survival" had a highest score of 29 post-irradiation by 2 Gy carbon. **(B)** The network "nucleic acid metabolism, small molecule biochemistry, lipid metabolism, cellular assembly and organization, and DNA replication, recombination, and repair" had a highest score of 49 post-irradiation by 2 Gy X-ray. The shade of red represented significant up-regulated proteins and shade of green represented down-regulated proteins.

in 60-mm Petri dishes (3002 Falcon) to provide 10-100 colonies per dish. Dishes were incubated for 2 Gy X-ray and 2 Gy carbon for HeLa cell line respectively, then fixed with 10% formalin and stained with 1% methylene blue.[25]

ATP level measurements

Following irradiation and subsequent incubation for 1 h at 37°C, cells were washed thoroughly with 0.9% sodium chloride solution, harvested by centrifugation, resuspended in distilled water and then lysed in ice water using an ultrasonic cell disrupter (Sonics, Newtown, CT, USA). Sonication was performed 4 times for 10 s each time with a 30 s pause between sonication bursts. Then, the lysate was boiled for 10 min in a boiling water bath, cell debris was removed by centrifugation at 4000 rpm for 10 min, and the ATP levels in the supernatant were measured using an ATP determination kit (Nanjing Jiancheng, Nanjing, China). The total protein concentration in the cell lysates was assayed using a BCA protein assay kit (Pierce, Rockford, IL, USA).

Lactic acid level measurements

Lactate production was measured using an enzymatic kit (Nanjing Jiancheng) by following the manufacturer's instruction. These results were normalized by cell counts. Briefly, NAD^+ was added to media and stoichiometrically converted to NADH by lactate in the media. The levels of NADH were then quantified colorimetrically, as described by the manufacturer.

Results

Protein identification and quantification

HeLa cells were irradiated by 2 Gy carbon and X-rays respectively and then submitted to SILAC assay. The brief workflow was shown in Figure 1.

The analysis of three biological SILAC replicates was carried out upon two types of irradiation (2 Gy carbon and 2 Gy X-rays) at 1 h. In these samples, 1658 and 1627 proteins were quantified in 2 Gy carbon and 2 Gy X-ray, respectively. Of these, 123 and 155 proteins were significantly changed. In Figure 2, normalized protein ratios of all identified proteins by SILAC were plotted against summed peptide intensities. The data points lying close to the y-axis did not show any expression changes. Outliers were considered as proteins with differential expression only if they had significance B value ≤ 0.05 (the significance B score calculation see methods) and were identified with a minimum of 2 unique peptides. The fold changed threshold was set at ±1.3 and significance B value ≤ 0.05.

In this study, 123 and 155 deregulated proteins were quantified in 2 Gy carbon and 2 Gy X-rays,

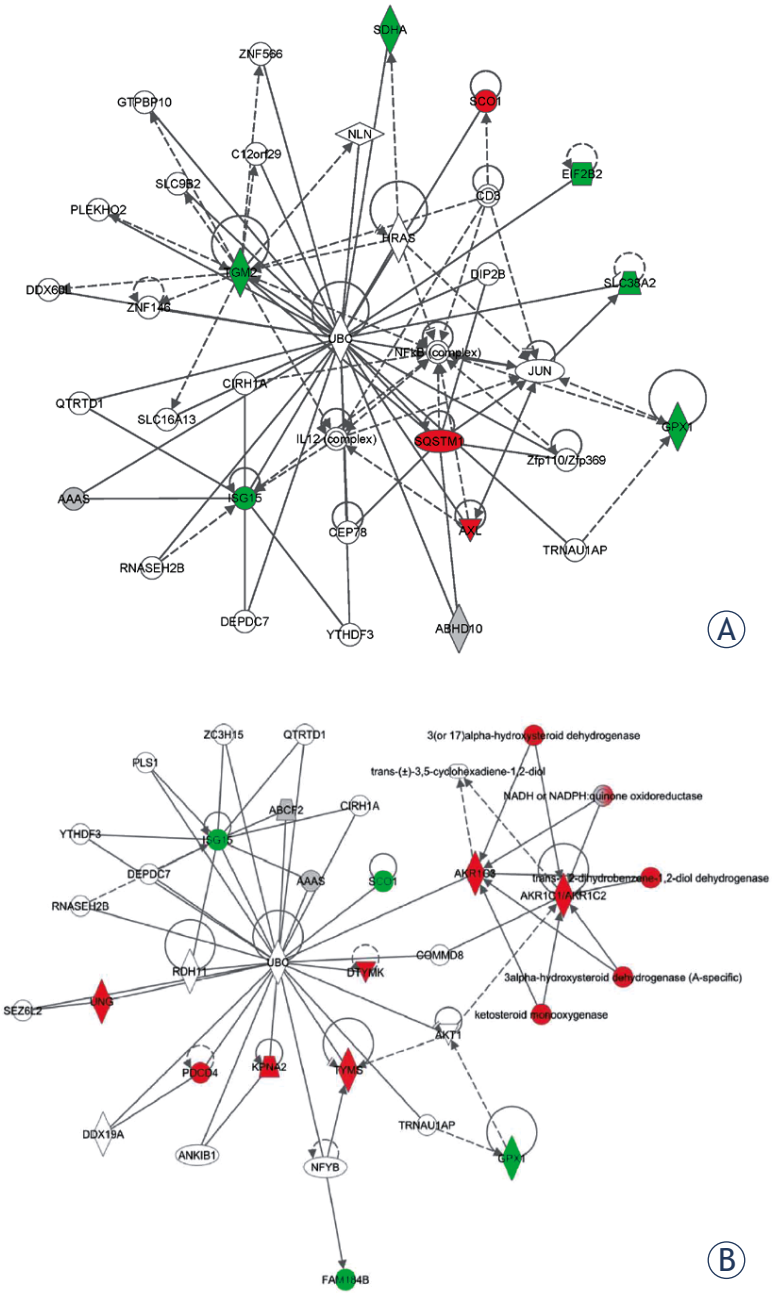

FIGURE 5. The highest score network of overlap deregulated proteins underlying 2 Gy carbon and X-ray using IPA analysis. **(A)** The overlap proteins with significant changes underlying 2 Gy carbon. The network "cellular assembly and organization, cellular function and maintenance, amino acid metabolism" had a highest score of 26. **(B)** The overlap proteins with significant changes underlying 2 Gy carbon. The network "lipid metabolism, small molecule biochemistry, nucleic acid metabolism" had a highest score of 32. (red: up-regulated; green: down-regulated).

TABLE 1. List of deregulated proteins in the highest score network after 2 Gy carbon irradiation

Gene name	Protein name	IPI Acc	Log ratio
SQSTM1	Sequestosome1	IPI00179473	1.799
PRKCDBP	Protein kinase C delta-binding protein	IPI00056334	1.582
SCO1	SCO cytochrome oxidase deficient homolog 1	IPI00027233	1.438
AXL	Tyrosine-protein kinase receptor UFO	IPI00296992	1.349
SLC25A11	**Mitochondrial 2-oxoglutarate/malate carrier protein**	IPI00219729	1.285
SLIT2	Slit homolog 2 protein	IPI00006288	-4.676
SDHA	Succinate dehydrogenase flavoprotein subunit, mitochondrial	IPI00305166	-2.494
SLC38A2	Sodium-coupled neutral amino acid transporter 2	IPI00410034	-2.012
EIF2B2	Translation initiation factor eIF-2B subunit beta	IPI00028083	-1.933
ISG15	Ubiquitin-like protein ISG15	IPI00375631	-1.903
NES	Nestin	IPI00010800	-1.700
FAM184B	Protein FAM184B	IPI00297208	-1.548
TGM2	Protein-glutamine gamma-glutamyltransferase2	IPI00218251	-1.513
PCNX	Pecanex-like protein 1	IPI00102678	-1.454
GPX1	Glutathione peroxidise 1	IPI00927606	-1.348

respectively (Supplementary File 1). A "Christmas tree" model representing normalised protein ratios of all identified proteins by SILAC plotted against summed peptide intensities is shown in Figure 2. In 2 Gy carbon group, 63 proteins were up-regulated and 60 were down-regulated. And in 2 Gy X-rays group, 76 proteins were up-regulated and 79 were down-regulated.

The GO enrichment and Network analysis

The Gene Ontology (GO) enrichment of biological processes in two groups was done by searching database using PANTHER system. The analysis revealed some radiation-induced biological processes (see Supplementary File 2). The result of PANTHER system analysis indicated that the process catalogues of the deregulated proteins in two groups were very similar. Then, the up-regulated proteins and down-regulated proteins in two groups were respectively submitted to DAVID database for biological process detail analysis (Figure 3). Surprisingly, most of the proteins regulated biological processes from 2 Gy carbon group were quite different from 2 Gy X-rays.

In 2 Gy carbon, the up-regulated proteins were mainly involved in nucleotide metabolism and pre-mRNA processing. While in 2 Gy X-ray, the up-regulated proteins were mainly involved in several kinds of metabolism, DNA repair and immunity. The distribution of up-regulated proteins in two groups indicated that HeLa cells might respond to irradiation through enhancing DNA metabolism. However, among the down-regulated proteins, it was found the distribution of down-regulated proteins in 2 Gy carbon was mainly involved in amino acid metabolism, which was a primary biological process with carbon beam irradiation. The down-regulated proteins in 2 Gy X-ray were involved in many biological processes.

To deeply understand the radiation response between the two groups, the protein interaction networks and pathway analysis were applied. The differentially expressed proteins of 2 Gy carbon and 2 Gy X-ray were submitted to IPA system respectively.

In 2 Gy carbon, the highest score network mainly involved in cellular functions of "Cellular Assembly and Organization, Cellular Function and Maintenance, Post-Translational Modification, Protein Folding and cell Death and Survival". The network and proteins were showed in Table 1 and Figure 4A.

In 2 Gy X-ray, the deregulated proteins were involved in four protein networks. The most significant one with a score of 49 was involved in "nucleic acid metabolism, small molecule biochemistry, lipid metabolism, cellular assembly and organization, and DNA replication, recombination, and repair" (Figure 4B). These proteins involved in the network were indicated with their IPA names and log-ratio in Table 2.

TABLE 2. List of deregulated proteins found in the highest score network after 2 Gy X-ray irradiation

Gene name	Protein name	IPI Acc	Log ratio
STK38l	Serine/threonine-protein kinase 38-like	IPI00237011	3.499
DTYMK	Thymidylate kinase	IPI00013862	2.371
SDHC	Succinate dehydrogenase cytochrome b560 subunit, mitochondrial	IPI00016968	2.346
ALDH3A1	Aldehyde dehydrogenase, dimeric NADP-preferring	IPI00296183	2.244
S100A7	Protein S100-7	IPI00219806	2.222
UNG	Uracil-DNA glycosylase	IPI00011069	1.907
PDCD4	Programmed cell death protein4	IPI00240675	1.807
ADI1	1,2-dihydroxy-3-keto-5-methylthiopentene dioxygenase	IPI00470791	1.762
KPNA2	Importin subunit alpha-2	IPI00002214	1.758
ATG3	Ubiquitin-like-conjugating enzyme ATG3	IPI00022254	1.756
DHX36	Probable ATP-dependent RNA helicase DHX36	IPI00027415	-1.863
NCSTN	Nicastrin	IPI00021983	-1.843
ISG15	**Ubiquitin-like protein ISG15**	IPI00375631	-1.734
IFIT2	Interferon-induce protein with tetratricopeptide repeats 2	IPI00018298	-1.664
FAM184B	Protein FAM184B	IPI00297208	-1.557
PTP4A1	Protein tyrosine phosphatise type IVA 1	IPI00020164	-1.479
SCO1	Protein SCO1 homolog, mitochondrial	IPI00027233	-1.441
GPX1	Glutathione peroxidise 1	IPI00927606	-1.318

To further understand the differential responses of two irradiation types, the overlapped proteins within two groups were separately submitted to IPA. Although the overlapped shared many common deregulated proteins, the distinction still existed between carbon beam and X-ray. In 2 Gy carbon, deregulated proteins network (Figure 5A) contained biological processes of "cellular assembly and organization, cellular function and maintenance, amino acid metabolism", which might play a dominant role in response to carbon beam with a score of 26. As far as 2 Gy X-ray was concerned, the processes were mainly involved in "lipid metabolism, small molecule biochemistry, nucleic acid metabolism" with a score of 32 Figure 5B.

Biological and function assay

To further validate the alternation of energy pathway by different types of irradiation, we assayed the survival fraction, ATP level and lactic acid level (Figure 6). As shown in Figure 6A, HeLa cells with 2 Gy X-ray had greater colony than the cells with 2 Gy carbon beam. The plating efficiency of HeLa cells were 0.279 ± 0.020 and 0.095 ± 0.003 respectively in 2 Gy X-ray and 2 Gy carbon. The Figure 6B showed that the ATP levels with two treatments were both up-regulated. Thus, the Figure 6C showed that the cells with 2 Gy X-ray treatment had higher lactic acid level than 2 Gy carbon beam.

The MS data verification by Western Blotting

We found that the two types of radiation could activate different metabolism pathways. LDHA and SCO1 proteins represented glycolysis activation and oxidative phosphorylation activation respectively.[26,27] So the two proteins were selected to verify MS data. The SILAC ratio of SCO1 was

TABLE 3. The Ratio comparison of SILAC and Western Blotting

Gene name	SILAC Ratio (H/L)		Normalized Ratio (Western blot)	
	2 Gy Carbon	2 Gy X-ray	2 Gy Carbon	2 Gy X-ray
LDHA	1.025 ± 0.13	1.829 ± 0.16*	1.030 ± 0.11	3.412 ± 0.82*
SCO1	1.438 ± 0.18*	0.368 ± 0.25*	3.513 ± 0.15*	0.760 ± 0.27*

*p-value≤0.05

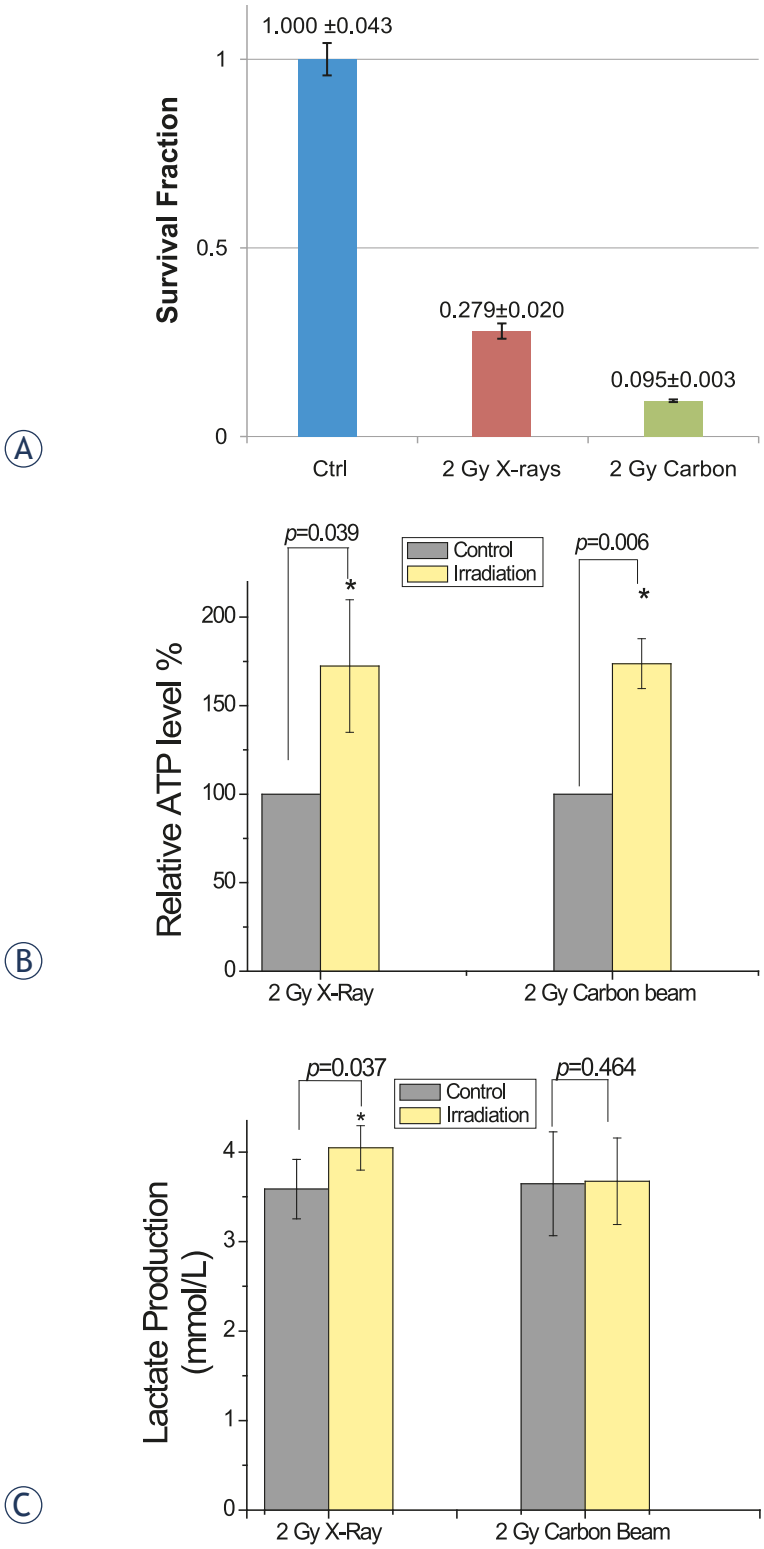

FIGURE 6. Biological and function assays for 2 Gy X-ray and carbon beam. **(A)** Survival fraction of HeLa cells after 2 Gy X-ray (red) or carbon beam (green) exposure. The plating efficiency of HeLa cells were 0.279±0.020 and 0.095±0.003 respectively in 2 Gy X-ray and 2 Gy carbon. **(B)** Changes in ATP levels between cells exposed to different irradiation and sham control (*, $p < 0.05$, t-test was one-tailed). **(C)** Differences in lactic acid levels between sham control and irradiated cells (*, $p < 0.05$, t-test was one-tailed).

increased in 2 Gy carbon while decreased in 2 Gy X-rays. The SILAC ratio of LDHA was insignificantly changed in 2 Gy carbon but significantly elevated in 2 Gy X-rays. The expression changes of SCO1 and LDHA were confirmed by western blot analysis (Figure 7), which showed that the changes were basically identical with SILAC (Table 3).

Discussion

In this study, we aimed to reveal the different cellular responses to the exposure of two irradiation types. In the previous study, it has been found that the survival fraction of cancer cells with carbon beam was lower than that of X-rays with same does, indicating that the carbon beam may have advantages over X-rays in radiotherapy.[2,3,28] Although many studies have reported the changes of phenotype underlying different types of radiation, the molecular mechanism is still pending to be clarified to improve radiotherapy.

From deregulated proteins analysis, we found the two different irradiation types of 2 Gy carbon and 2 Gy X-ray demonstrated significant differences in cellular response (Figure 3). In 2 Gy carbon group, the result of IPA network analysis showed that the irradiation induced cell death and inhibiting cell growth. The up-regulated proteins Sequestosome1 (SQSTM1) and Protein kinase C delta-binding protein (PRKCDBP) were involved in promoting apoptosis.[29,30] Although the up-regulated protein SCO1 was not directly involved in the regulated network (Figure 4A), the recent research has reported that SCO1 caused apoptosis by inducing reactive oxygen species in mitochondria.[31] Furthermore, up-regulated mitochondrial proteins (SCO1, SLC25A11) and down-regulated GPX1 might indicate that the cancer cells were suffered from oxidation stress induced by 2 Gy carbon irradiation. Among down-regulated proteins, ASNS and SLC38A2 were closely associated with amino acid metabolism. ASNS was involved in asparagines synthesis and SLC38A2 was function as a sodium-dependent amino acid transporter.[32,33] Other down-regulated proteins of IPA network such as GPX1, NES, TGM2 and SLIT2 were mainly involved in response to external stimulus and radiation by DAVID analysis (Supplementary File 3). The down-regulated protein ISG15 is an ubiquitin-like protein that involved in many biological processes. And we found ISG15 is regulated by many regulators from IPA analysis (Figure 4A). These down-regulated proteins indicated that the

protein synthesis and response to radiation might be decreased. Additionally, some up-regulated proteins (SQSTM1, PRKCDBP and SCO1) were mainly involved in the apoptotic promotion. Many researchers reported the killing effect of heavy ion was stronger than X-ray due to DNA double strand breaks but hardly repair,[34,35] which might be closely associated with many down-regulated proteins involved in amino acid metabolism process in 2 Gy carbon. Rapid accumulation of biomass is necessary for cancer cell growth. When cancer cells are damaged by irradiation, the cells must generate enough energy and acquire or synthesize biomolecules at a sufficient rate to meet the demands of repair. Although we found ATP level increased (Figure 6B) in this study, the amino acid metabolism was not increased. As well known, amino acid metabolism plays an important role in biomass synthesis and most biomass are glycolytic intermediate production.[36] Many enzymes down-regulated post-irradiation with 2 Gy carbon might lead to less biomass production and poor outcome of survival fraction. Thus, we inferred that the cancer cells might be more seriously damaged by 2 Gy carbon than 2 Gy X-ray.

In 2 Gy X-ray group, significant alternations were seen in the metabolic processes and DNA repair process (Figure 3 and Figure 6). Recent studies have reported that glycolysis and glucose utilisation were increased by radiation or oxidative stress.[37-39] For example, glucose-6-phosphate dehydrogenase (G6PD), (pyruvate carboxylase) PC and (L-lactate dehydrogenase A) LDHA were up-regulated post-irradiation 1 h from mass spectrometry (see Supplement Table1). In 2 Gy X-rays group, the up-regulated proteins in nucleic acid metabolism (Figure 3 and Figure 5B) were key proteins in the process of DNA damage repair. The results indicated that 2 Gy X-rays can enhance cell abilities of the DNA repair. Besides, in this study, we assayed the ATP level and lactic acid level increasing with 2 Gy X-ray. The increasing ATP level and lactic acid level indicated that the cells with 2 Gy X-ray generated energy mainly depending glycolysis. It has been reported that high level glycolysis would enhance capacity of radioresistance in cancer cells[40,41], and the lactate from high level glycolysis might contribute to radioresistance. Because lactate production relies on reducing the pyruvate and this process recycles NADH back to NAD^+, which would reduce the

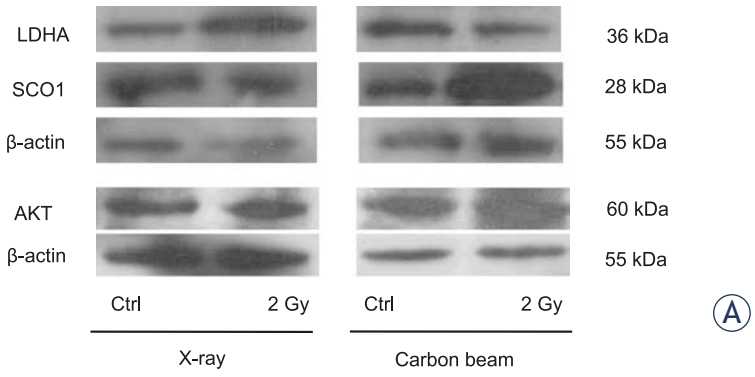

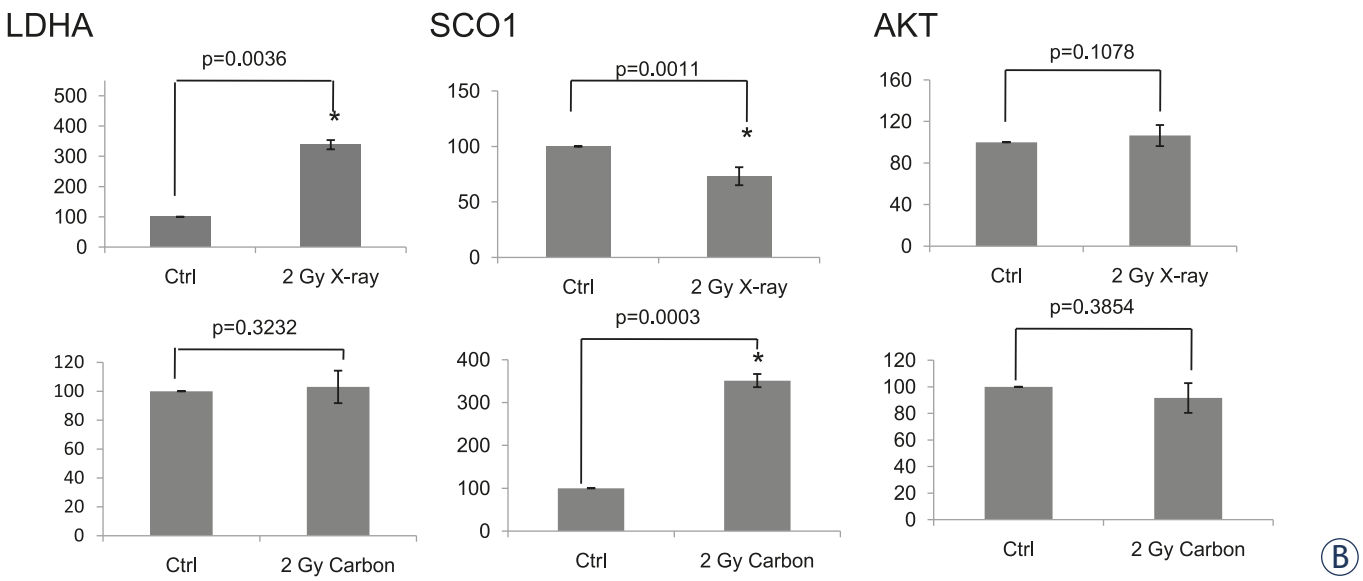

FIGURE 7. The western blotting for analysis of LDHA, SCO1 and Akt. **(A)** The images of western blot. **(B)** Fold changes between treated samples and control were analyzed by gray-values.

oxidative stress of irradiated cancer cells.[42,43] That study also provide evidence that the poor outcome for patients with high lactate malignancies at least partially due to glycolysis-mediated resistance to radiotherapy.[42] From IPA network results of 2 Gy X-ray, "nucleic acid metabolism, small molecule biochemistry, lipid metabolism, cellular assembly and organization, and DNA replication, recombination, and repair" were the most influenced biological pathway. From DAVID analysis of GO enrichment, among the up-regulated proteins, AKR1C3, COX1, PTGS1 and ALDH3A1were mainly involved in oxidation reduction. Besides, CDK1, CDK2, PDCD4, TYMS and UNG were mainly involved in cell cycle and response to DNA damage stimulus (Supplementary File 3). Other up-regulated proteins such as S100A7, CHCHD2, SELENBP1, ATG3 and SQSTM1 were not classified by DAVID. But we found S100A7, CHCHD2 and SQSTM1 directly interacted with Akt that plays a vital role in signalling pathway of cancer cells (Figure 4B). Previous study also found that ionizing radiation induced Akt activation in glioblastoma multiform, and the PI3K-Akt signalling pathway has been correlated with radioresistance. Among the down-regulated proteins, the function of GPX1 and ISG15 were similar to 2 Gy carbon treatment. The rest down-regulated proteins SCO1, PTP4A1 and IFIT2 were associated with cell growth and apoptosis.[44,45] In specific, down-regulation of SCO1 also indicated that oxidative phosphorylation process was decreased.

From the subsequent analysis of overlapped proteins network, we found metabolism process might play a vital role in irradiation treatment. Although the same proteins with differential expression were submitted to IPA, the network displayed distinct function modules. The Figure 5A showed that the regulation network of 2 Gy carbon treatment was mainly regulated by key nodal UBC, NF-κB complex, IL12 complex and JUN. Previous studies reported that NF-κB, IL12 and JUN were closely associated with ionizing radiation response.[46-48] And Figure 5B showed that the regulation network of 2 Gy X-ray treatment was consisted of two modules that regulated by nodal UBC and AKR1C1/AKR1C2. The two modules connected with nodal Akt, COMMD8 and AKR1C3. AKR1C1/AKR1C2 and AKR1C3 were involved in lipid metabolism. Akt is a key regulator for regulating many cell events and considered as a regulator of radioresistance.[49]

From the result of IPA network analysis (Figure 4 and Figure 5) and previous publication, increased energy metabolism might promote radioresistance and decreased amino acid might enhance radiosensitivity. We found that the different metabolism processes in response to irradiation might be associated with their survival fraction. Interestingly, we also found two networks with highest scores shared two regulators serine/threonine-specific protein kinase (Akt) and polyubiquitin-C (UBC). In this study, Akt and UBC proteins were not identified due to their very low abundance. Recent reports indicated that PTEN-PI3K/AKT pathway could regulate the cell death and cell cycle by ionizing radiation.[50,51] Besides, Akt can also regulate energy metabolism.[52,53] In this study, we assayed the Akt level with 2 Gy X-ray and 2 Gy carbon respectively. But we found that the Akt level was not significantly changed with two types of radiation treatment (Figure 7). In fact, different phosphorylation site of Akt would perform different function to regulate cell event. The regulation process of PI3K-Akt and phosphorylation site need further study. To a great extent, the functions of UBC protein are decided by the different Lys residue modifications. In addition, the target proteins conjugating different sites of UBC might show distinct roles in biological processes. Therefore, the specific regulation mechanism of UBC protein was comparatively difficult to explore underling two irradiation types.

From above, we came to the conclusion that cancer cells in response to different types of radiation performed differently not only in DNA repair, but also in many other biological processes. Activation of the glycolysis, DNA metabolism and DNA repair process were seemed as key mechanisms for radioresistance of X-ray. Furthermore, previous study about metabolism of HeLa cells exposed to radiation reported some similar results with this study. Early in 1993, Karu *et al*. found ATP level of HeLa cells increased post-irradiation.[54] And they provided four possibilities for explaining the reason of increasing ATP. But these possibilities have not been verified by experiment. In 2001, Grande *et al*. found that lactate of HeLa cells was increased 48 h after irradiation with high dose of gamma ray.[55] Until recent years, with development of proteomic and genetic methods, the relationship between radiation and metabolism received more and more attention. Recent researches report that alternation of metabolism induced by radiation might be associated with cell damage and repair demand.[39] And the result of distinct metabolism pathway induced by different types of radiation might provide some novel insight into improving clinical radiotherapy. At present, fluorine 18 fluorodeoxyglucose (FDG) positron emission tomography (PET) has been widely used for diagnosis, initial staging, and restaging of

many kinds of cancer.[56] The method could monitor glycolytic activity in malignant cells. And the distinct metabolism induced by radiation could be investigated by FDG-PET. We inferred that our finding integrating with FDG-PET could evaluate the effect of radiotherapy.

Supplementary files

Supplementary file 1. List of all deregulated proteins underlying 2 Gy carbon and X-ray. The sheet 1 is table of 123 deregulated proteins underlying 2 Gy carbon beam. The sheet 2 is table of 155 deregulated proteins underlying 2 Gy X-ray. Available from: http://www.degruyter.com/view/j/raon.2014.48.issue-2/raon-2013-0087/suppl/raon-2013-0087_supp1.pdf

Supplementary file 2. Biological analysis of deregulated proteins by PANTHER system. Associated biological process of proteins found to be deregulated by 2 Gy carbon and 2 Gy X-ray irradiation. The differential expression proteins with significance were analyzed for biological processes using PANTHER classification system. Available from: http://www.degruyter.com/view/j/raon.2014.48.issue-2/raon-2013-0087/suppl/raon-2013-0087_supp2.pdf

Supplementary file 3. GO enrichment of deregulated proteins from IPA network. Many deregulated proteins that are not part of the results in 2 Gy carbon and 2 Gy X-ray are listed by GO enrichment from DAVID analysis. Available from: http://www.degruyter.com/view/j/raon.2014.48.issue-2/raon-2013-0087/suppl/raon-2013-0087_supp3.pdf

Acknowledgements

We give our great gratitude to the HIRFL-CSR crew for providing the carbon ion beam. This work was also supported by grants from the "Strategic Priority Research Program" of the Chinese Academy of Sciences (No. XDA01040411 & XDA01020304), the National Natural Science Foundations of China awarded to Guangming Zhou (No. 10979062) and the Foundation for Young Talents of Gansu (No.1208RJYA013).

References

1. Takahashi A, Ota I, Tamamoto T, Asakawa I, Nagata Y, Nakagawa H, et al. p53-dependent hyperthermic enhancement of tumour growth inhibition by X-ray or carbon-ion beam irradiation. *Int J Hyperther* 2003; **19:** 145-53.
2. Yamamoto N, Ikeda C, Yakushiji T, Nomura T, Katakura A, Shibahara T, et al. Genetic effects of X-ray and carbon ion irradiation in head and neck carcinoma cell lines. *Bull Tokyo Dent Coll* 2007; **48:** 177-85.
3. Cui X, Oonishi K, Tsujii H, Yasuda T, Matsumoto Y, Furusawa Y, et al. Effects of Carbon Ion Beam on Putative Colon Cancer Stem Cells and Its Comparison with X-rays. *Cancer Res* 2011; **71:** 3676-87.
4. Suit H, Urie M. Proton beams in radiation therapy. *J Natl Cancer I* 1992; **84:** 155-64.
5. Okayasu R, Okada M, Okabe A, Noguchi M, Takakura K, Takahashi S. Repair of DNA damage induced by accelerated heavy ions in mammalian cells proficient and deficient in the non-homologous end-joining pathway. *Radiat Res* 2006; **165:** 59-67.
6. Zhao J, Guo Z, Zhang H, Wang Z, Song L, Ma J, et al. The potential value of the neutral comet assay and γH2AX foci assay in assessing the radiosensitivity of carbon beam in human tumor cell lines. *Radiol Oncol* 2013; **47:** 15-25.
7. Ghosh S, Narang H, Sarma A, Krishna M. DNA damage response signaling in lung adenocarcinoma A549 cells following gamma and carbon beam irradiation. *Mutation Research/Fundamental and Molecular Mechanisms of Mutagenesis* 2011; **716:** 10-19.
8. Oonishi K, Cui X, Hirakawa H, Fujimori A, Kamijo T, Yamada S, et al. Different effects of carbon ion beams and X-rays on clonogenic survival and DNA repair in human pancreatic cancer stem-like cells. *Radiother Oncol* 2012; **105:** 258-65.
9. Ong SE, Blagoev B, Kratchmarova I, Kristensen DB, Steen H, Pandey A, et al. Stable isotope labeling by amino acids in cell culture, SILAC, as a simple and accurate approach to expression proteomics. *Mol Cell Proteomics* 2002; **1:** 376-86.
10. Ong SE, Mann M. Mass spectrometry-based proteomics turns quantitative. *Nat Chem Biol* 2005; **1:** 252-62.
11. Mann M. Functional and quantitative proteomics using SILAC. *Nat Rev Mol Cell Bio* 2006; **7:** 952-58.
12. Chen EI, Yates JR. Cancer proteomics by quantitative shotgun proteomics. *Molecular Oncology* 2007; **1:** 144-59.
13. Lin R-X, Zhao H-B, Li C-R, Sun Y-N, Qian X-H, Wang S-Q. Proteomic Analysis of Ionizing Radiation-Induced Proteins at the Subcellular Level. *J Proteome Res* 2008; **8:** 390-99.
14. Wang F, Bing Z, Zhang Y, Ao B, Zhang S, Ye C, et al. Quantitative proteomic analysis for radiation-induced cell cycle suspension in 92-1 melanoma cell line. *J Radiat Res* 2013; **54:** 649-62.
15. Cui J, Cai J, Gao F, Li B. Proteomic analysis of proteins related to radiation-induced carcinogenesis. *Chinese J Cancer* 2007; **26:** 1157.
16. Berglund SR, Santana AR, Li D, Rice RH, Rocke DM, Goldberg Z. Proteomic analysis of low dose arsenic and ionizing radiation exposure on keratinocytes. *Proteomics* 2009; **9:** 1925-38.
17. Cui ZY, Chen XL, Lu BW, Park SK, Xu T, Xie ZS, et al. Preliminary quantitative profile of differential protein expression between rat L6 myoblasts and myotubes by stable isotope labeling with amino acids in cell culture. *Proteomics* 2009; **9:** 1274-92.
18. Li J, Cai T, Wu P, Cui Z, Chen X, Hou J, et al. Proteomic analysis of mitochondria from Caenorhabditis elegans. *Proteomics* 2009; **9:** 4539-53.
19. Cox J, Mann M. MaxQuant enables high peptide identification rates, individualized p.p.b.-range mass accuracies and proteome-wide protein quantification. *Nat Biotech* 2008; **26:** 1367-72.
20. Elias JE, Gygi SP. Target-decoy search strategy for increased confidence in large-scale protein identifications by mass spectrometry. *Nat Meth* 2007; **4:** 207-14.
21. Cox J, Mann M. Quantitative, High-Resolution Proteomics for Data-Driven Systems Biology. *Annu Rev Biochem* 2011; **80:** 273-99.
22. Thomas PD, Kejariwal A, Campbell MJ, Mi H, Diemer K, Guo N, et al. PANTHER: a browsable database of gene products organized by biological function, using curated protein family and subfamily classification. *Nucleic Acids Res* 2003; **31:** 334-41.
23. Huang DW, Sherman BT, Lempicki RA. Systematic and integrative analysis of large gene lists using DAVID bioinformatics resources. *Nat Protocols* 2008; **4:** 44-57.

24. Huang DW, Sherman BT, Lempicki RA. Bioinformatics enrichment tools: paths toward the comprehensive functional analysis of large gene lists. *Nucleic Acids Res* 2009; **37:** 1-13.

25. He JP, Li JH, Ye CY, Zhou LB, Zhu JY, Wang JF, et al. Cell cycle suspension A novel process lurking in G(2) arrest. *Cell Cycle* 2011; **10:** 1468-76.

26. Fantin VR, St-Pierre J, Leder P. Attenuation of LDH-A expression uncovers a link between glycolysis, mitochondrial physiology, and tumor maintenance. *Cancer Cell* 2006; **9:** 425-34.

27. Leary SC, Cobine PA, Kaufman BA, Guercin G-H, Mattman A, Palaty J, et al. The human cytochrome c oxidase assembly factors SCO1 and SCO2 have regulatory roles in the maintenance of cellular copper homeostasis. *Cell Metab* 2007; **5:** 9-20.

28. Iwadate Y, Mizoe J-E, Osaka Y, Yamaura A, Tsujii H. High linear energy transfer carbon radiation effectively kills cultured glioma cells with either mutant or wild-type p53. *Int J Radiat Oncol Biol Phys* 2001; **50:** 803-08.

29. Long J, Garner TP, Pandya MJ, Craven CJ, Chen P, Shaw B, et al. Dimerisation of the UBA domain of p62 inhibits ubiquitin binding and regulates NF-κB signalling. *J Mol Biol* 2010; **396:** 178-94.

30. Lee J-H, Kang M-J, Han H-Y, Lee M-G, Jeong S-I, Ryu B-K, et al. Epigenetic alteration of PRKCDBP in colorectal cancers and its implication in tumor cell resistance to TNFα-induced apoptosis. *Clin Cancer Res* 2011; **17:** 7551-62.

31. Monticone M, Bisio A, Daga A, Giannoni P, Giaretti W, Maffei M, et al. Demethyl fruticulin A (SCO-1) causes apoptosis by inducing reactive oxygen species in mitochondria. *J Cell Biochem* 2010; **111:** 1149-59.

32. Hatanaka T, Huang W, Wang H, Sugawara M, Prasad PD, Leibach FH, et al. Primary structure, functional characteristics and tissue expression pattern of human ATA2, a subtype of amino acid transport system A. *Biochim Biophys Acta (BBA) - Biomembranes* 2000; **1467:** 1-6.

33. Zhang YP, Lambert MA, Cairney AEL, Wills D, Ray PN, Andrulis IL. Molecular structure of the human asparagine synthetase gene. *Genomics* 1989; **4:** 259-65.

34. Goodwin E, Blakely E, Ivery G, Tobias C. Repair and misrepair of heavy-ion-induced chromosomal damage. *Adv Space Res* 1989; **9:** 83-9.

35. Okayasu R, Okada M, Okabe A, Noguchi M, Takakura K, Takahashi S. Repair of DNA Damage Induced by Accelerated Heavy Ions in Mammalian Cells Proficient and Deficient in the Non-homologous End-Joining Pathway. *Radiat Res* 2006; **165:** 59-67.

36. Jones RG, Thompson CB. Tumor suppressors and cell metabolism: a recipe for cancer growth. *Gene Dev* 2009; **23:** 537-48.

37. Ralser M, Wamelink M, Kowald A, Gerisch B, Heeren G, Struys E, et al. Dynamic rerouting of the carbohydrate flux is key to counteracting oxidative stress. *J Biol* 2007; **6:** 10.

38. Grant C. Metabolic reconfiguration is a regulated response to oxidative stress. *J Biol* 2008; **7:** 1.

39. Sriharshan A, Boldt K, Sarioglu H, Barjaktarovic Z, Azimzadeh O, Hieber L, et al. Proteomic analysis by SILAC and 2D-DIGE reveals radiation-induced endothelial response: Four key pathways. *J Proteomics* 2012; **75:** 2319-30.

40. Sattler UGA, Mueller-Klieser W. The anti-oxidant capacity of tumour glycolysis. *Int J Radiat Biol* 2009; **85:** 963-71.

41. Pitroda SP, Wakim BT, Sood RF, Beveridge MG, Beckett MA, MacDermed DM, et al. STAT1-dependent expression of energy metabolic pathways links tumour growth and radioresistance to the Warburg effect. *BMC Med* 2009; **7:**68.

42. Sattler UGA, Meyer SS, Quennet V, Hoerner C, Knoerzer H, Fabian C, et al. Glycolytic metabolism and tumour response to fractionated irradiation. *Radiother Oncol* 2010; **94:** 102-9.

43. Mathupala S, Colen C, Parajuli P, Sloan A. Lactate and malignant tumors: A therapeutic target at the end stage of glycolysis. *J Bioenerg Biomembr* 2007; **39:** 73-7.

44. Wang J, Kirby CE, Herbst R. The Tyrosine phosphatase PRL-1 localizes to the endoplasmic reticulum and the mitotic spindle and is required for normal mitosis. *J Biol Chem* 2002; **277:** 46659-68.

45. Stawowczyk M, Van Scoy S, Kumar KP, Reich NC. The Interferon Stimulated Gene 54 Promotes Apoptosis. *J Biol Chem* 2011; **286:** 7257-66.

46. Deng Z, Sui G, Rosa PM, Zhao W. Radiation-Induced c-Jun Activation Depends on MEK1-ERK1/2 Signaling Pathway in Microglial Cells. *PLoS ONE* 2012; **7:** e36739.

47. Magné N, Toillon R-A, Bottero V, Didelot C, Houtte PV, Gérard J-P, et al. NF-κB modulation and ionizing radiation: mechanisms and future directions for cancer treatment. *Cancer Lett* 2006; **231:** 158-68.

48. Chen T, Burke KA, Zhan Y, Wang X, Shibata D, Zhao Y. IL-12 Facilitates both the recovery of endogenous hematopoiesis and the engraftment of stem cells after ionizing radiation. *Exp Hematol* 2007; **35:** 203-13.

49. Li H-F, Kim J-S, Waldman T. Radiation-induced Akt activation modulates radioresistance in human glioblastoma cells. *Radiat Oncol* 2009; **4:** 43.

50. Park JK, Jung H-Y, Park SH, Kang SY, Yi M-R, Um HD, et al. Combination of PTEN and γ-ionizing radiation enhances cell death and G2/M arrest through regulation of AKT activity and p21 induction in non–small-cell lung cancer cells. *Int J Radiat Oncol Biol Phys* 2008; **70:** 1552-60.

51. Toulany M, Baumann M, Rodemann HP. Stimulated PI3K-AKT signaling mediated through ligand or radiation-induced EGFR depends indirectly, but not directly, on constitutive K-Ras activity. *Mol Cancer Res* 2007; **5:** 863-72.

52. Li X, Monks B, Ge Q, Birnbaum MJ. Akt/PKB regulates hepatic metabolism by directly inhibiting PGC-1α transcription coactivator. *Nature* 2007; **447:** 1012-6.

53. Ono H, Katagiri H, Funaki M, Anai M, Inukai K, Fukushima Y, et al. Regulation of phosphoinositide metabolism, Akt phosphorylation, and glucose transport by PTEN (phosphatase and tensin homolog deleted on chromosome 10) in 3T3-L1 adipocytes. *Mol Endocrinol* 2001; **15:** 1411-22.

54. Karu T, Piatibrat L, Kalendo G, Serebriakov N. Changes in the amount of ATP in HeLa cells under the action of He-Ne laser radiation. *Biulleten'eksperimental'noi biologii i meditsiny* 1993; **115:** 617-8.

55. Grande S, Luciani AM, Rosi A, Cherubini R, Conzato M, Guidoni L, et al. Radiation effects on soluble metabolites in cultured HeLa cells examined by 1H MRS: Changes in concentration of glutathione and of lipid catabolites induced by gamma rays and proton beams. *Int J Cancer* 2001; **96:** 27-42.

56. Kostakoglu L, Agress H, Goldsmith SJ. Clinical role of FDG PET in evaluation of cancer patients1. *Radiographics* 2003; **23:** 315-40.

research article

Clonality analysis of lymphoid proliferations using the BIOMED-2 clonality assays: a single institution experience

Ira Kokovic[1], Barbara Jezersek Novakovic[2], Petra Cerkovnik[1], Srdjan Novakovic[1]

[1] Department of Molecular Diagnostics, [2] Department of Medical Oncology, Institute of Oncology Ljubljana, Ljubljana, Slovenia

Radiol Oncol 2014; 48(2): 155-162.

Received 9 May 2013
Accepted 1 October 2013

Correspondence to: Prof. Dr. Srdjan Novaković, Institute of Oncology Ljubljana, Zaloška 2, 1000 Ljubljana, Slovenia. Tel: +386 1 5879 432; Fax: +386 1 5879 410; E-mail: snovakovic@onko-i.si

Disclosure: No potential conflicts of interest were disclosed.

Background. Clonality determination in patients with lymphoproliferative disorders can improve the final diagnosis. The aim of our study was to evaluate the applicative value of standardized BIOMED-2 gene clonality assay protocols for the analysis of clonality of lymphocytes in a group of different lymphoid proliferations.

Materials and methods. With this purpose, 121 specimens from 91 patients with suspected lymphoproliferations submitted for routine diagnostics from January to December 2011 were retrospectively analyzed. According to the final diagnosis, our series comprised 32 cases of B-cell lymphomas, 38 cases of non-Hodgkin's T-cell lymphomas and 51 cases of reactive lymphoid proliferations. Clonality testing was performed using the BIOMED-2 clonality assays.

Results. The determined sensitivity of the TCR assay was 91.9%, while the sensitivity of the IGH assay was 74.2%. The determined specificity of the IGH assay was 73.3% in the group of lymphomas and 87.2% in the group of reactive lesions. The determined specificity of the TCR assay was 62.5% in the group of lymphomas and 54.3% in the group of reactive lesions.

Conclusions. In the present study, we confirmed the utility of standardized BIOMED-2 clonality assays for the detection of clonality in a routine diagnostical setting of non-Hodgkin's lymphomas. Reactions for the detection of the complete *IGH* rearrangements and reactions for the detection of the *TCR* rearrangements are a good choice for clonality testing of a wide range of lymphoid proliferations and specimen types while the reactions for the detection of incomplete *IGH* rearrangements have not shown any additional diagnostic value.

Key words: BIOMED-2; clonality analysis; lymphomas; IGH rearrangement; TCR rearrangement

Introduction

In the majority of patients with suspected lymphoproliferations (LP), the diagnosis can be done by histomorphology or cytomorphology, supplemented with immunohistochemistry or flow cytometric immunophenotyping.[1] However, in 5-15% of patients the morphological and immunophenotypic features are not typical and the diagnosis is more complicated. In such cases, molecular clonality analysis of lymphocyte populations may contribute to the diagnosis.[1,2] Clonality analysis of lymphoid cells using the polymerase chain reaction (PCR) to amplify V-(D)-J junctional regions of immunoglobulin (*Ig*) and T-cell receptor (*TCR*) genes enables the discrimination between polyclonal, reactive processes and monoclonal, malignant tumors.[1-3] Since the introduction of PCR-based assays in the early nineties, different strategies with different primer sets have been developed and used for determination of B and T-cell clonality.[4-12] However, many of those PCR-based clonality assays were designed to cover a limited number of possible *Ig* and *TCR* gene rearrangements, resulting in false negative results.[3,13]

A comprehensive work of the European BIOMED-2 collaborative study group (now called the EuroClonality consortium) led to new stand-

ardized PCR protocols with multiple primer sets for the clonality analysis of both *Ig* and *TCR* gene rearrangements in a diagnostic setting.[14] In initial studies, novel BIOMED-2 multiplex PCR protocols were evaluated on large series of B-cell and T-cell malignancies, and histomorphologically reactive lesions.[15-17] Based on their conclusions, the BIOMED-2 clonality assays were declared as highly sensitive, specific and reproducible, and thus reliable for detection of clonality in lymphoid malignancies.[15-17] The guidelines for use of these assays in the routine clonality testing have been proposed.[3] Recommendations for correct interpretation and potential pitfalls in the Ig/TCR clonality testing were also presented.[18,19] Over the past decade, a number of studies have reported the successful application of the BIOMED-2 clonality assays in a diagnostic setting.[20-38] Some studies have evaluated subsets of BIOMED-2 primers for clonality analysis in selected specimen types - fixed and decalcified bone marrow biopsies[23], archival skin biopsy samples[24], formalin-fixed and paraffin-embedded specimens[26,29] and fine needle aspiration biopsies.[27] The others applied BIOMED-2 assays to different disease sub-categories – B-cell precursor acute lymphoblastic leukemia[21], classical Hodgkin's lymphoma[26], follicular lymphoma[28,29], cutaneous lymphoproliferations[30], anaplastic large cell lymphoma and peripheral T-cell lymphomas[32], Mycosis fungoides and inflammatory dermatoses[33], polymorphous lymphoproliferative disorders in individuals with immunodeficiency conditions[34] and granulomatous disorders.[35] Thus, the BIOMED-2 clonality assays have become the world standard for PCR-based Ig/TCR clonality testing.[39] Moreover, the EuroClonality consortium recently developed a uniform reporting system for describing results and conclusions of Ig/TCR clonality assays.[39]

The aim of our retrospective study was to evaluate the applicative value of standardized BIOMED-2 gene clonality assay protocols for the analysis of clonality of lymphocytes on a series of various diagnostic specimens (fresh and formalin-fixed) from Slovenian patients with different lymphoid proliferations.

Materials and methods

Study group

One hundred and twenty-one specimens from 91 patients with suspected non-Hodgkin's lymphoma submitted for routine diagnostics from January to December 2011 were analyzed. Among diagnostic samples, bone marrow (BM) aspirates predominated (51), followed by formalin-fixed, paraffin-embedded tissue specimens (FFPE) (31) and fine-needle aspiration specimens (FNA) (31). A minority of specimens consisted of cerebrospinal fluid (1), pleural fluid (4), imprint cytology of lymph node (1) and ascites (2). All specimens were subjected to cyto/histomorphological and immunophenotyping examination as well as to molecular clonality analysis of lymphocyte populations during routine diagnostic assessment.

DNA isolation

DNA from FFPE tissue specimens was isolated using the QIAamp FFPE tissue kit (Qiagen GmbH, Hilden, Germany). DNA from other types of specimens was isolated using High Pure PCR Template Preparation kit (Roche Applied Science, Penzberg, Germany) according to the manufacturers' protocols. The concentration and the purity of DNA (A_{260nm}/A_{280nm}) were determined using the Nanodrop spectrophotometer (ThermoScientific, Wilmington, USA).

Clonality analysis

Clonality analysis of lymphoid cells was performed using the BIOMED-2 clonality assays – ABI Fluorescence Detection (IdentiClone, *InVivo* Scribe Technologies, San Diego, CA, USA) according to the manufacturer's instructions. B-cell clonality was assessed using the IdentiClone IGH Gene clonality assay for detection of clonal rearrangements in the immunoglobulin heavy chain gene (*IGH*). The T-cell clonality was assessed using the TCRB+TCRG Gene Clonality Assay for detection of clonal rearrangements in the T-cell receptor β chain gene (*TCRB*) and the T-cell receptor γ chain gene (*TCRG*).

The DNA quality was checked for all samples using the control gene PCR (Specimen Control Size Ladder master mix). The DNA was considered of adequate quality if amplified products of ≥400 bp were obtained in a control PCR, except for the DNA from FFPE tissue, which was considered acceptable if amplified products of ≥300 bp were obtained.

The *IGH* clonality was evaluated with five different IGH multiplex PCR reactions, three reactions for detection of the complete rearrangements (V_H-J_H) and two reactions for detection of the incomplete rearrangements in the *IGH* gene (D_H-J_H)

(V – variable, D – diversity, J – joining gene segments, respectively). The *TCR* clonality was evaluated with three TCRB and two TCRG multiplex PCR reactions. In case of doubtful results, the assays were repeated. Each run included monoclonal and polyclonal control DNAs for particular primer master mix, supplied with each BIOMED-2 clonality assay, and a contamination control (no template DNA in a reaction).

The fluorescently labeled PCR products were detected by capillary gel electrophoresis using the ABI 3500 Genetic Analyzer (Applied Biosystems, Foster City, CA, USA) and analyzed by fragment analysis. Amplified products from diagnostic samples were interpreted according to the manufacturer's instructions. Samples that failed to amplify following repeated testing were reported as "not detected" (*i.e.* clonality could not be detected due to insufficient quality or quantity of DNA for analysis).

Final diagnosis

The final diagnosis of each lymphoproliferation was set upon careful examination of all available information. Malignant lymphomas were classified according to the WHO Classification of Tumours of Hematopoietic and Lymphoid Tissues.[40,41]

Sensitivity and specificity

To determine the sensitivity and the specificity of IGH/TCR clonality assays we compared the results of molecular testing with the final diagnosis of each lymphoproliferation. The sensitivity of each clonality assay was calculated using the following equation: TP/(TP+FN), in which TP represents the number of true positives and FN the number of false negatives. The specificity of each assay was calculated using the equation TN/(TN+FP), in which TN represents the number of true negatives and FP the number of false positives. The specificities of IGH and TCR assays were calculated separately for T/B-cell lymphomas and for reactive lymphoproliferations.

Results

In the period from January to December 2011 we have analyzed 121 specimens from 91 patients (96 specimens were analyzed for *IGH* and 119 specimens for *TCR* clonality). Of these, 84 specimens were analyzed for both – B and T-cell clonality.

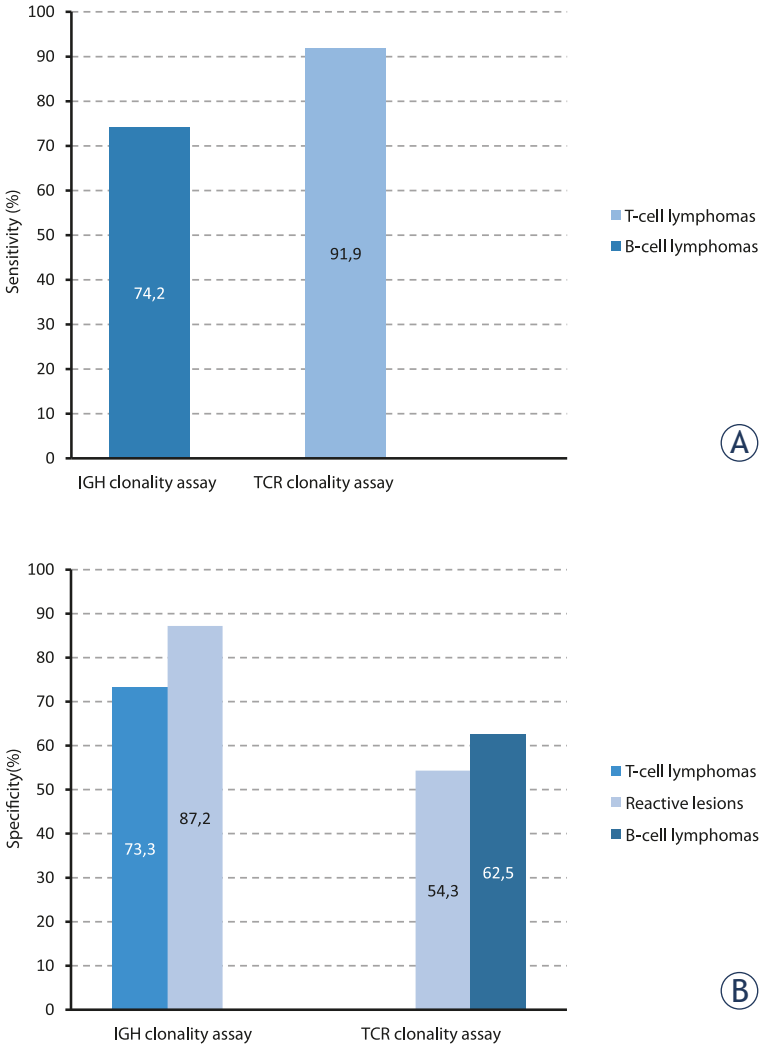

FIGURE 1. Sensitivity and specificity of the BIOMED-2 clonality assays determined in a group of T-cell lymphomas, B-cell lymphomas and reactive lesions.

To determine the sensitivity and the specificity of IGH/TCR clonality assays the results of molecular testing were compared with the final diagnosis of each lymphoproliferation.

The sensitivity of each clonality assay was calculated using the equation TP/(TP+FN); TP (true positives) – monoclonal (M) and "monoclonal in a polyclonal background" (M/P) results of the IGH clonality assay in a group of B-cell lymphomas, and M and M/P results of the TCR clonality assay in a group of T-cell lymphomas; FN (false negatives) – polyclonal (P) results of the IGH clonality assay in a group of B-cell lymphomas and P results of the TCR clonality assay in a group of T-cell lymphomas.

The specificity of the IGH clonality assay was determined separately for T-cell lymphomas and for reactive lesions. Similarly, the specificity of the TCR clonality assay was determined separately for B-cell lymphomas and for reactive lesions. The specificity of each assay was calculated using the equation TN/(TN+FP); TN (true negatives) – P results of the IGH clonality assay in a group of T-cell lymphomas or in reactive lesions, and P results of the TCR clonality assay in a group of B-cell lymphomas or in reactive lesions; FP (false positives) – M and M/P results of the IGH clonality assay in a group of T-cell lymphomas or reactive lesions, and M and M/P results of the TCR clonality assay in a group of B-cell lymphomas or in reactive lesions.

TABLE 1. Results of clonality analysis using BIOMED-2 clonality assays in suspected lymphoid proliferations

Final diagnosis (n)	IGH clonality					TCR clonality				
	M (n)	P (n)	M/P (n)	ND (n)	NP (n)	M (n)	P (n)	M/P (n)	ND (n)	NP (n)
B-NHL (32)	22	8	1	1	0	9	15	0	1	7
T-NHL (38)	4	11	0	0	23	32	3	2	1	0
Reactive (51)	6	41	0	2	2	20	25	1	0	5
TOTAL (121)	**32**	**60**	**1**	**3**	**25**	**61**	**43**	**3**	**2**	**12**

B-NHL = B-cell non-Hodgkin's lymphoma; T-NHL = T-cell non-Hodgkin's lymphoma; M = monoclonal; P = polyclonal; M/P =monoclonal in a polyclonal background; ND = not detected; NP = not performed

According to the final diagnosis, our diagnostic series comprised 32 cases of B-cell lymphomas, 38 cases of non-Hodgkin's T-cell lymphomas and 51 cases of reactive lymphoid proliferations. The results of clonality analysis using BIOMED-2 clonality assays are shown in Table 1. The calculated sensitivities and specificities of BIOMED-2 clonality assays after fragment analysis of amplified products are shown in Figure 1.

The BIOMED-2 IGH clonality assay

It was performed in 96 specimens (Table 2). In total, monoclonal *IGH* rearrangements corresponding to monoclonal B-cell proliferations were detected in 32 cases (33.3%). Polyclonal *IGH* rearrangements corresponding to polyclonal B-cell proliferations were detected in 60 cases (62.5%). One case of B-cell non-Hodgkin's lymphoma (B-NHL) was concluded as borderline ("monoclonal in a polyclonal background"). In three cases the B-cell clonality could not be determined either because of an insufficient number of B-cells in the specimen or due to the poor quality of the isolated DNA (in one case of histopathologically confirmed B-NHL and in two reactive specimens). Among B-cell lymphomas, 22 of 32 analyzed cases were monoclonal, representing "true positives" and 8 cases were polyclonal, representing "false negatives". Polyclonal *IGH* rearrangements in a group of B-cell lymphomas were detected in follicular lymphoma (FL) (3 cases), marginal zone B-cell lymphoma (MZL) (3 cases), diffuse large B-cell lymphoma (DLBCL) (1 case) and B-cell lymphoma with features intermediate between the DLBCL and Burkitt's lymphoma (BL) (1 case).

In the group of T-cell lymphomas, 11 of 15 analyzed cases were polyclonal by the IGH assay, representing "true negatives" and 4 cases were monoclonal, representing "false positives" - a case of T-cell lymphoma with monoclonal B-cell population and 3 specimens from a patient with angioimmunoblastic T-cell lymphoma (AITL) (2 FNAs and one BM aspiration). Among 51 specimens of reactive lymphoid proliferations (R), monoclonal *IGH* rearrangements were detected in 6 cases ("false positives") and polyclonal *IGH* rearrangements were detected in 41 cases ("true negatives").

Incomplete rearrangements in the *IGH* gene

Besides complete rearrangements in the *IGH* gene we also detected incomplete rearrangements (D_H-J_H) in a few cases. In total, we detected 8 incomplete rearrangements in 96 specimens of LP analyzed by the IGH assay (8.3%). Four were detected by the IGH-D reaction containing D_{H1-6} and J_H primers (one in case of T-NHL and 3 in reactive lymphoid proliferations) and four by the IGH-E reaction containing D_{H7} and J_H primers (one in case of FL, one in case of T-NHL and two in reactive specimens).

The BIOMED-2 TCR clonality assay

It was performed in 109 specimens (Table 3). In total, by using the BIOMED-2 TCR clonality assay, the T-cells with monoclonal rearrangements were detected in 61 specimens, while T-cells with polyclonal rearrangements were detected in 43 cases. Borderline results ("monoclonal in a polyclonal background") were obtained in 3 specimens (two BM specimens taken for staging/follow-up of T-cell non-Hodgkin's lymphomas (T-NHL) and one FNA specimen with reactive lymphoproliferation). The T-cell clonality was not assessed in 2 specimens due to fragmented DNA (in one case of T-NHL and in one case of B-NHL). In a group of primary T-cell lymphomas, monoclonal *TCRG* and/or *TCRB* rearrangements were detected in 32 of 38 analyzed cases, representing "true positives". Three of 38 T-NHL cases were polyclonal by the TCR assay,

TABLE 2. Detection of monoclonal *IGH* gene rearrangements in 96 specimens of lymphoid proliferations (LP)

Diagnosis	No. of monoclonal / No. of tested specimens (%)
B-NHL - Primary tumor	11/17 (64.7)
MALT lymphoma	1/2 (50.0)
Follicular lymphoma	3/4 (75.0)
Diffuse large B-cell lymphoma	1/2(50.0)
Marginal zone B-cell lymphoma	2/4 (50.0)
Lymphoplasmacytic lymphoma	2/2 (100.0)
B-NHL, unclassified	2/3 (66.7)
B-NHL - Staging/follow-up BM[a]	11/15 (73.3)
Total B-NHL	22/32 (68.8)
T-NHL	4/15 (26.7)
Reactive specimens	6/49 (12.2)
TOTAL LP	32/96 (33.3)

B-NHL = B-cell non-Hodgkin's lymphoma; T-NHL = T-cell non-Hodgkin's lymphoma; MALT lymphoma = extranodal marginal zone lymphoma of mucosa-associated tissue; LP = lymphoid proliferation

[a]Bone marrow (BM) aspirates were taken from different patients with marginal zone B-cell lymphoma (4), diffuse large B-cell lymphoma (4), follicular lymphoma (3), MALT lymphoma (1), mantle cell lymphoma (1), plasmablastic lymphoma (1) and lymphoplasmacytic lymphoma (1).

TABLE 3. Detection of monoclonal *TCR* gene rearrangements in 109 specimens of lymphoid proliferations (LP)

Diagnosis	No. of monoclonal / No. of tested specimens (%)
T-NHL – Primary tumor	22/26 (84.6)
Peripheral T-cell lymphoma, unspecified	12/15 (80.0)
Peripheral T-cell lymphoma, cutaneous	1/2 (50.0)
Angioimmunoblastic T-cell lymphoma	8/8 (100.0)
Mycosis fungoides/Sezary syndrome	1/1 (100.0)
T-NHL - Staging/follow-up BM[a]	10/12 (83.3)
Total T-NHL	32/38 (84.2)
B-NHL	9/25 (36.0)
Reactive specimens[b]	20/46 (43.5)
TOTAL LP	61/109 (56.0)

B-NHL = B-cell non-Hodgkin's lymphoma; T-NHL = T-cell non-Hodgkin's lymphoma

[a]Bone marrow (BM) aspirates were taken from patients with peripheral T-cell lymphoma, unspecified (4), angioimmunoblastic T-cell lymphoma (3), T-lymphoblastic lymphoma (3), NK/T-cell lymphoma (1) and T-cell acute lymphoblastic leukaemia (1).

[b]Reactive specimens included 20 BM aspirates, 17 FNA specimens of lymph nodes and 9 FFPE specimens.

representing "false negatives". Among T-NHLs polyclonal *TCR* rearrangements were detected in 2 cases of peripheral T-cell lymphoma, otherwise unspecified (PTCL-U) and in one case of peripheral T-cell lymphoma, cutaneous.

In the group of B-NHLs monoclonal rearrangements in *TCR* genes were detected in 9 of 25 analyzed cases ("false positives"). Fifteen cases of B-NHL had polyclonal rearrangements in *TCR* genes, as expected ("true negatives"). Among reactive lymphoid proliferations monoclonal *TCR* rearrangements were detected in 20 cases ("false positives") and polyclonal TCR rearrangements were detected in 25 cases ("true negatives").

Discussion

The aim of this study was to evaluate the application value of BIOMED-2 clonality assays for analysis of different lymphoid proliferations in the diagnostic setting. With this purpose, we analyzed 121 specimens from 91 patients with suspected lymphoproliferations. The clonality testing was performed using the BIOMED-2 clonality assays according to the guidelines proposed by the European BIOMED-2/EuroClonality group and the results of clonality testing were interpreted in the context of the final diagnosis.

BIOMED-2 IGH assay

The sensitivity as well as the specificity of the IGH assay in our diagnostic series of NHL cases was lower than expected. The sensitivity of the IGH assay in our diagnostic series was 74.2%, while the BIOMED-2/EuroClonality group reported the sensitivity of 91.0%, ranging from 85-100% depending on the disease category.[3] Similarly, the determined specificity of the IGH assay was 73.3% in our NHL cases and 87.2% in the group of reactive specimens, again lower than reported in the BIOMED-2 study, where the overall specificity of the IGH clonality assay in T-NHL was almost 91.0%.[16]

The lower sensitivity in our series may be related to a smaller number of included B-NHL cases (only 32) as well as to a rather high percentage of germinal center (GC)/post-GC lymphomas which predominated in our group of B-NHLs (28 of 32, including 14 of 15 BM aspirates taken for staging/follow-up) (Table 2). It is namely well known that somatic mutations in the *IGH* gene are frequent in GC/post-GC B-cell lymphomas, especially in FL[42], which contributes to a lower monoclonality

rate.[3,13,28,29] Indeed, all B-NHL cases with polyclonal *IGH* rearrangements in our study (8/32) were from the group of GC/post-GC lymphomas, including FL (3), marginal zone B-cell lymphoma (3), DLBCL (1) and B-cell lymphoma with features intermediate between the DLBCL and Burkitt (1).

The lower overall specificity of the IGH clonality assay in our series of NHL cases can be explained by the T-NHL entities in which monoclonal *IGH* rearrangements were detected: a case of T-cell lymphoma with monoclonal B-cell population and 3 specimens from a patient with angioimmunoblastic T-cell lymphoma (AITL). This is in concordance with the results from the BIOMED-2 study in which monoclonal *IGH* rearrangements were mostly detected in AITL (in 30.0% of cases)[16] and also with the results of other studies where the presence of monoclonal *IGH* rearrangements in AITL was reported in 17.6% of cases.[38] The fore mentioned studies have shown that monoclonal *IGH* gene rearrangements occur in 5-10% of all T-cell malignancies and represent the so-called cross-rearrangements, which sometimes occur in more immature lymphoid cells.[3,16]

Unlike in the T-NHL cases, the specificity of the IGH assay in our series of reactive lesions (87.2%) is comparable to the results from the BIOMED-2 study.[17] In our study, clearly polyclonal IGH products were determined in 41 of 49 reactive specimens (Table 1). In 6 cases, the monoclonal IGH products were detected - three BM aspirates taken for staging/follow-up of B-NHLs, two FFPE specimens suspective of lymphoma and one FNA specimen suspective of granulomatous lymphadenitis. A further pathological review of these cases did not show any cells suspective of B-cell lymphoma and were concluded as reactive lymphoproliferations. As previously stated, monoclonal results in reactive specimens must be interpreted with caution in the context of all clinical, morphological and immunophenotyping data.[1,3] Concerning this, in all 6 cases a close follow-up and the re-sampling were recommended.

An important aspect of our study was the evaluation of the utility of reactions for the detection of incomplete rearrangements in the *IGH* gene, which can be detected in ~30% of B-cell malignancies.[3] In contrast to our expectations, among B-NHL cases (32) we detected only one incomplete rearrangement by the IGH-E reaction (3.1%) - it was in case of FL, which was polyclonal in reactions targeting the complete rearrangements. Since histopathological diagnosis of this case was difficult, the detection of incomplete rearrangement might have served as an additional evidence of malignant process. The follow-up of this patient was strongly recommended. Considering the low frequency of incomplete rearrangements in all analyzed specimens of LP and the fact that only one additional monoclonal result was obtained in the group of B-NHLs we concluded that IGH-D and IGH-E reactions did not have any additional diagnostic value. Our results are in agreement with the study on 118 FFPE specimens from patients with FL, in which also no additional monoclonal results were detected with reactions targeting incomplete rearrangements (IGH-D and IGH-E).[29]

BIOMED-2 TCR clonality assay

The overall sensitivity of the TCR clonality assay in our diagnostic series was 91.9% which is in agreement with the reported sensitivity of the BIOMED-2/EuroClonality group (91.0%).[16] The TCRB clonality assay showed a higher analytical detection rate (76.3%) than the TCRG clonality assay (63.2%), which is in agreement with the results of the BIOMED-2 study.[16]

As we have previously shown for the IGH assay, the specificity of the TCR clonality assay in our study was lower than described by founders of the protocol.[3,14] The determined specificity was 62.5% in the group of B-NHLs and 54.3% in the group of reactive lymphoid proliferations. However, the detection of monoclonal rearrangements in *TCR* genes in our series of B-NHL cases and reactive lesions is consistent with the findings from other studies, which have shown that the co-existing small T-cell populations are frequently present in both, B-cell malignancies and reactive specimens.[15,17] The rearrangements in *TCR* genes occur in 10-20% of B-cell malignancies and are generally reported to be found in a single *TCR* locus.[3,15] In contrast, we have detected multiple monoclonal results in TCRB and TCRG reactions in 5 cases of B-NHL. Interestingly, 4 of 5 specimens with monoclonal rearrangements in both *TCRB* and *TCRG* loci were BM aspirates taken for staging: MZL (2), FL (1) and DLBCL (1) (results not shown). One FNA specimen of initially suspected B-NHL with monoclonal rearrangements in both *IGH* and *TCR* genes was later reclassified as the T-cell lymphoma with a monoclonal B-cell population after an additional pathological examination of pleural fluid obtained from the same patient.

The unexpectedly high frequency (43.5%) of monoclonal *TCR* rearrangements in reactive specimens in our study is difficult to explain (Table 3).

It is well known that the *TcRγ* gene has a restricted germline repertoire and a limited junctional diversity at the rearranged Vγ-Jγ region, and thus theoretically carries the risk of pseudoclonal products in samples containing small numbers of T-cells.[14] There is a possibility of detecting pseudoclonal products by the TCRG clonality assay in 4 of 20 cases, which were monoclonal by the TCRG clonality assay and polyclonal by the TCRB clonality assay. However, in 10 of 20 cases monoclonal *TCR* rearrangements were detected by both assays and can hardly be interpreted as pseudoclonal. It is of note that monoclonal *TCR* rearrangements in our cases with the final diagnosis of reactive lesions were mostly detected in BM aspirates (14/20 BM aspirates) (Table 3). The majority of BM aspirates with monoclonal *TCR* rearrangements (11/14) were taken for staging, all from patients initially suspective of having B-cell malignancies. Three specimens were taken for the assessment of minimal residual disease (MRD), the first from a patient with AITL, the second from a patient with plasmablastic lymphoma and the third from a patient with FL. All three were concluded as reactive BM specimens according to morphological and immunophenotyping data. However, it should be postulated that monoclonal *TCR* rearrangements might not always be clinically significant, since monoclonal T-cell populations can be detected in peripheral blood of the elderly, in patients with autoimmune diseases and in patients with viral infection.[43-45]

In the present study we confirmed the application value of standardized BIOMED-2 clonality assays for the detection of clonality in a routine diagnostic setting of non-Hodgkin's lymphomas. Our conclusions are that (i) three reactions for detection of complete *IGH* rearrangements and five reactions for detection of *TCR* rearrangements (targeting both *TCRB* and *TCRG* genes) are a good choice for the clonality testing in these lymphomas; (ii) reactions for the detection of incomplete *IGH* rearrangements have not shown any additional diagnostic value in our hands; (iii) due to the lower sensitivity of the IGH clonality assay in our study, we should consider the introduction of the IGK clonality assay as an additional clonality test, especially in cases of GC/post-GC B-cell malignancies; (iv) detection of monoclonal rearrangements in both *IGH* and *TCR* genes must be interpreted with caution and in the context of all clinical, morphological and immunophenotyping data, as discussed elsewhere.

We are aware that our conclusions derive from a rather small diagnostic series of 121 specimens of different lymphoid proliferations with only 32 cases of confirmed B-NHLs and 38 cases of confirmed T-NHLs. Certainly, the evaluation of larger series of B and T-cell lymphomas and reactive lesions needs to be done for firmer conclusions. Yet, we believe that our results might be useful for other laboratories aiming to introduce the standardized BIOMED-2 clonality assays in a routine laboratory practice.

References

1. Sandberg Y, van Gastel-Mol EJ, Verhaaf B, Lam KH, van Dongen JJ, Langerak AW. BIOMED-2 multiplex immunoglobulin/T-cell receptor polymerase chain reaction protocols can reliably replace Southern blot analysis in routine clonality diagnostics. *J Mol Diagn* 2005; **7:** 495-503.
2. Hoeve MA, Krol AD, Philippo K, Derksen PW, Veenendaal RA, Schuuring E, et al. Limitations of clonality analysis of B cell proliferations using CDR3 polymerase chain reaction. *J Clin Pathol Mol Pathol* 2000; **53:** 194-200.
3. van Krieken JH, Langerak AW, Macintyre EA, Kneba M, Hodges E, Garcia Sanz R, et al. Improved reliability of lymphoma diagnostics via PCR-based clonality testing: - Report of the BIOMED-2 concerted action BHM4-CT98-3936. *Leukemia* 2007; **21:** 201-6.
4. McCarthy KP, Sloane JP, Wiedemann LM. Rapid method for distinguishing clonal from polyclonal B cell populations in surgical biopsy specimens. *J Clin Pathol* 1990; **43:** 429-32.
5. Trainor KJ, Brisco MJ, Wan JH, Neoh S, Grist S, Morley AA. Gene rearrangement in B- and T-lymphoproliferative disease detected by the polymerase chain reaction. *Blood* 1991; **78:** 192-5.
6. Slack DN, McCarthy KP, Wiedemann LM, Sloane JP. Evaluation of sensitivity, specificity and reproducibility of an optimized method for detecting clonal rearrangements of immunoglobulin and T-cell receptor genes in formalin-fixed, paraffin-embedded sections. *Diagn Mol Pathol* 1993; **2:** 223-32.
7. Segal GH, Jorgensen T, Masih AS, Braylan TC. Optimal primer selection for clonality assessment by polymerase chain reaction analysis: I. Low grade B-cell lymphoproliferative disorders of nonfollicular center cell type. *Hum Pathol* 1994; **25:** 1269-75.
8. Davis TH, Courtland EY, Balk SP. Detection of clonal immunoglobulin gene rearrangements by polymerase chain reaction amplification and single-strand conformational polymorphism analysis. *Am J Pathol* 1993; **142:** 1841-47.
9. Chen YT, Whitney KD, Chen Y. Clonality analysis of B-cell lymphoma in fresh-frozen and paraffin-embedded tissues: The effects of variable polymerase chain reaction parameters. *Mod Pathol* 1994; **7:** 429-34.
10. McCarthy KP, Sloane JP, Wiedemann LM. A simplified method of detection of clonal rearrangements of the T-cell receptor g chain gene. *Diagn Mol Pathol* 1992; **1:** 173-79.
11. Theodorou I, Raphael M, Bigorgne C, Fourcade C, Lahet C, Cochet G, et al. Recombination pattern of the TCRg locus in human peripheral T-cell lymphomas. *J Pathol* 1994; **174:** 233-42.
12. Diss TC, Watts M, Pan LX, Burke M, Linch D, Isaacson PG. The polymerase chain reaction in the demonstration of monoclonality in T cell lymphomas. *J Clin Pathol* 1995; **48:** 1045-50.
13. Liu H, Bench AJ, Bacon CM, Payne K, Huang Y, Scott MA, et al. A practical strategy for the routine use of BIOMED-2 PCR assays for detection of B- and T-cell clonality in diagnostic haematopathology. *Br J Haematol* 2007; **138:** 31-43.
14. van Dongen JJ, Langerak AW, Brüggemann M, Evans PA, Hummel M, Lavender FL, et al. Design and standardization of PCR primers and protocols for detection of clonal immunoglobulin and T-cell receptore gene recombinations in suspect lymphoproliferations: report of the BIOMED-2 Concerted Action BHM4-CT98-3936. *Leukemia* 2003; **17:** 2257-317.

15. Evans PA, Pott C, Groenen PJ, Salles G, Davi F, Berger F, et al. Significantly improved PCR-based clonality testing in B-cell malignancies by use of multiple immunoglobulin gene targets. Report of the BIOMED-2 Concerted Action BHM4-CT98-3936. *Leukemia* 2007; **21:** 207-14.

16. Brüggemann M, White H, Gaulard P, Garcia-Sanz R, Gameiro P, Oeschger S, et al. Powerful strategy for polymerase chain reaction-based clonality assessment in T-cell malignancies. Report of the BIOMED-2 Concerted Action BHM4-CT98-3936. *Leukemia* 2007; **21:** 215-21.

17. Langerak AW, Molina TJ, Lavender FL, Pearson D, Flohr T, Sambade C, et al. Polymerase chain reaction-based clonality testing in tissue samples with reactive lymphoproliferations: usefulness and pitfalls. A report of the BIOMED-2 Concerted Action BHM4-CT98-3936. *Leukemia* 2007; **21:** 222-29.

18. Langerak AW, Groenen PJ, van Krieken JH, van Dongen JJ. Immunoglobulin/T-cell receptor clonality diagnostics. *Expert Opin Med Diagn* 2007; **1:** 451-61.

19. Groenen PJ, Langerak AW, van Dongen JJ, van Krieken JH. Pitfalls in TCR gene clonality testing: teaching cases. *J Hematopathol* 2008; **1:** 97-109.

20. Matthews C, Catherwood M, Morris TC, Alexander HD. Routine analysis of IgHV mutational status in CLL patients using BIOMED-2 standardized primers and protocols. *Leuk Lymphoma* 2004; **45:** 1899-904.

21. Dawidovska M, Jólkowska J, Szczepański T, Derwich K, Wachowiak J, Witt M. Implementation of the standard strategy for identification of Ig/TCR targets for minimal residual disease diagnostics in B-cell precursor ALL pediatric patients: Polish experience. *Arch Immunol Ther Exp* 2008; **56:** 409-18.

22. Chen YL, Su IJ, Cheng HY, Chang KC, Lu CC, Chow NH, et al. BIOMED-2 protocols to detect clonal immunoglobulin and T-cell receptor gene rearrangements in B- and T-cell lymphomas in southern Taiwan. *Leuk Lymphoma* 2010; **51:** 650-55.

23. Lassmann S, Gerlach UV, Technau-Ihling K, Werner M, Fisch P. Application of BIOMED-2 primers in fixed and decalcified bone marrow biopsies: analysis of immunoglobulin H receptor rearrangements in B-cell non-Hodgkin's lymphomas. *J Mol Diagn* 2005; **7:** 582-91.

24. Lukowsky A, Marchwat M, Sterry W, Gellrich S. Evaluation of B-cell clonality in archival skin biopsy samples of cutaneous B-cell lymphoma by immunoglobulin heavy chain gene polymerase chain reaction. *Leuk Lymphoma* 2006; **47:** 487-93.

25. Hebeda KM, van Altena MC, Rombout P, van Krieken JH, Groenen PJ. PCR clonality detection in Hodgkin lymphoma. *J Hematopathol* 2009;**2:**34-41.

26. Burack WR, Laughlin TS, Friedberg JW, Spence JM, Rothberg PG. PCR assays detect B-lymphocyte clonality in formalin-fixed, paraffin-embedded specimens of classical Hodgkin lymphoma without microdissection. *Am J Clin Pathol* 2010; **134:** 104-11.

27. Zhang S, Abreo F, Lowery-Nordberg M, Veillon DM, Cotelingam JD. The role of fluorescence in situ hybridization and polymerase chain reaction in the diagnosis and classification of lymphoproliferative disorders on fine-needle aspiration. *Cancer Cytopathol* 2010; **118:** 105-12.

28. Payne K, Wright P, Grant JW, Huang Y, Hamoudi J, Bacon CM, et al. BIOMED-2 PCR assays for IGK gene rearrangements are essential for B-cell clonality analysis in follicular lymphoma. *Br J Haematol* 2011; **155:** 84-92.

29. Berget E, Helgeland L, Molven A, Vintermyr OK. Detection of clonality in follicular lymphoma using formalin-fixed, paraffin-embedded tissue samples and BIOMED-2 immunoglobulin primers. *J Clin Pathol* 2011; **64:** 37-41.

30. Sandberg Y, Heule F, Lam K, Lugtenburg PJ, Wolvers-Tettero IL, van Dongen JJ, et al. Molecular immunoglobulin/T-cell receptor clonality in cutaneous lymphoproliferations. Experience with the BIOMED-2 standardized polymerase chain reaction protocol. *Haematologica* 2003; **88:** 659-70.

31. Catherwood MA, Gonzales D, Patton C; Dobbin E, Venkatraman L, Alexander HD. Improved clonality assessment in germinal centre/post germinal centre non- Hodgkin's lymphomas with high rates of somatic hypermutation. *J Clin Pathol* 2007; **60:** 524-28.

32. Tan BT, Seo K, Warnke RA, Arber DA. The frequency of immunoglobulin heavy chain gene and T-cell receptor g-chain gene rearrangements and Epstein-Barr virus in ALK+ and ALK- anaplastic large cell lymphoma and other peripheral T-cell lymphomas. *J Mol Diagn* 2008; **10:** 502-12.

33. Zhang B, Beck AH, Taube JM, Kohler S, Seo K, Zwerner J, et al. Combined use of PCR-based TCRG and TCRB clonality tests on paraffin-embedded skin tissue in the differential diagnosis of Mycosis fungoides and inflammatory dermatoses. *J Mol Diagn* 2010; **12:** 320-27.

34. Nakamichi N, Wada N, Kohara M, Fukuhara S, Sugiyama H, Ogawa H, et al. Polymorphous lymphoproliferative disorder: a clinicopathological analysis. *Virchows Arch* 2010; **456:** 269-76.

35. Dabiri S, Morales A, Ma L, Sundram U, Kim YH, Arber DA, et al. The frequency of dual TCR-PCR clonality in granulomatous disorders. *J Cutan Pathol* 2011; **38:** 704-9.

36. McClure RF, Kaur P, Pagel E, Ouillette PD, Holtegaard CE, Treptow CL, et al. Validation of immunoglobulin gene rearrangement detection by PCR using commercially available BIOMED-2 primers. *Leukemia* 2006; **20:** 176-79.

37. Patel KP, Pan Q, Wang Y, Maitta RW; Du J, Xue X, et al. Comparison of BIOMED-2 versus laboratory-developed polymerase chain reaction assays for detecting T-cell receptor-g gene rearrangements. *J Mol Diagn* 2010; **12:** 226-37.

38. Zaki MA, Wada N, Kohara M, Ikeda J, Hori Y, Fujita S, et al. Presence of B-cell clones in T-cell lymphoma. *Eur J Haematol* 2011; **86:** 412-19.

39. Langerak AW, Groenen PJ, Brüggemann M, Beldjord K, Bellan C, Bonello L, et al. EuroClonality/BIOMED-2 guidelines for interpretation and reporting of Ig/TCR clonality testing in suspected lymphoproliferations. *Leukemia* 2012; **26:** 2159-71.

40. Jaffe ES, Harris NL, Stein H and Vardiman JW: Tumours of Haematopoietic and Lymphoid Tissues. In: *World Health Organization Classification of Tumours*. Lyon: IARC Press; 2001.

41. Swerdlow SH, Campo E, Harris NL, Jaffe ES, Pileri SA, Stein H, et al. *WHO Classification of Tumors of Haematopoietic and Lymphoid Tissues*. Lyon:IARC Press; 2008.

42. Diss TC, Peng H, Wotherspoon AC, Isaacson PG, Pan L. Detection of monoclonality in low-grade B-cell lymphomas using the polymerase chain reaction is dependent on primer selection and lymphoma type. *J Pathol* 1993; **169:** 291-95.

43. Posnett DN, Sinha R, Kabak S, Russo C. Clonal populations of T cells in normal elderly humans: the T cell equivalent to "benign monoclonal gammapathy". *J Exp Med* 1994; **179:** 609-18.

44. Delfau-Larue MH, Laroche L, Wechsler J, Lepage E, Lahet C, Asso-Bonnet M, et al. Diagnostic value of dominant T-cell clones in peripheral blood in 363 patients presenting consecutively with a clinical suspicion of cutaneous lymphoma. *Blood* 2000; **96:** 2987-92.

45. Godges E, Krishna MT, Pickard C, Smith JL. Diagnostic role of test for T cell receptor (TCR) genes. *J Clin Pathol* 2003; **56:** 1-11.

research article

Polymorphisms in folate pathway and pemetrexed treatment outcome in patients with malignant pleural mesothelioma

Katja Goricar[1], Viljem Kovac[2], Vita Dolzan[1]

[1] Pharmacogenetics Laboratory, Institute of Biochemistry, Faculty of Medicine, University of Ljubljana, Ljubljana, Slovenia
[2] Institute of Oncology Ljubljana, Ljubljana, Slovenia

Radiol Oncol 2014; 48(2): 163-172.

Received 12 October 2013
Accepted 23 October 2013

Correspondence to: Prof. Vita Dolžan, Ph.D., M.D., Pharmacogenetics Laboratory, Institute of Biochemistry, Faculty of Medicine, University of Ljubljana, Vrazov trg 2, 1000 Ljubljana, Slovenia. Phone: +386 1 543 7670; Fax: +386 1 543 7641; E-mail: vita.dolzan@mf.uni-lj.si

Disclosure: No potential conflicts of interest are disclosed.

Introduction. A combination of pemetrexed and cisplatin has been shown to improve the outcome in patients with malignant pleural mesothelioma (MPM), however, there is a great heterogeneity in treatment response among patients. The aim of our study was to evaluate the influence of polymorphisms in folate pathway and transporter genes on pemetrexed treatment outcome in Slovenian patients with MPM.

Methods. MPM patients treated with pemetrexed in the course of a prospective randomized clinical trial were genotyped for nineteen polymorphisms in five genes of folate pathway and six transporter genes. Logistic regression was used to assess the influence of polymorphisms on treatment efficacy and toxicity, while Cox regression was used to determine their influence on progression-free and overall survival.

Results. Patients with at least one polymorphic *MTHFD1* rs2236225 allele had a significantly lower response rate (p = 0.005; odds ratio [OR] = 0.12; 95% confidence interval [CI] = 0.03−0.54) and shorter progression-free survival (p = 0.032; hazard ratio [HR] = 3.10; 95% CI = 1.10−8.74) than non-carriers. Polymorphisms in transporter genes did not influence survival; however, several were associated with toxicity. Liver toxicity was significantly lower in carriers of polymorphic *ABCC2* rs2273697 (p = 0.028; OR = 0.23; 95% CI = 0.06−0.85), *SLCO1B1* rs4149056 (p = 0.028; OR = 0.23; 95% CI = 0.06−0.85) and rs11045879 (p = 0.014; OR = 0.18; 95% CI = 0.05−0.71) alleles compared to non-carriers, as well as in patients with *SLCO1B1* GCAC haplotype (p = 0.048; OR = 0.17; 95% CI = 0.03−0.98). Gastrointestinal toxicity was much more common in patients with polymorphic *ABCC2* rs717620 allele (p = 0.004; OR = 10.67; 95% CI = 2.15−52.85) and *ABCC2* CAG haplotype (p = 0.006; OR = 5.67; 95% CI = 1.64−19.66).

Conclusions. *MTHFD1* polymorphism affected treatment response and survival, while polymorphisms in *ABCC2* and *SLCO1B1* transporter genes influenced the risk for toxicity. These polymorphisms could serve as potential markers of pemetrexed treatment outcome in patients with MPM.

Key words: mesothelioma; pemetrexed; polymorphism; folate pathway; toxicity

Introduction

Malignant pleural mesothelioma (MPM) is a rare but aggressive tumour of mesothelial surfaces of pleura that is mainly connected with asbestos exposure.[1] Most patients are diagnosed in later stages, often with unresectable disease, therefore the prognosis is poor and median survival time is rarely above two years.[2,3] Several clinical and genetic factors can have a prognostic value in MPM, but successful treatment remains challenging.[2] Most patients with MPM are treated with systemic chemotherapy; usually either pemetrexed (PMX) or gemcitabine combined with a platinum agent, which are often used in different oncological diseases.[4-6] Studies have shown that chemotherapy significantly improves survival of patients with MPM. Randomized clinical trial has shown that treatment with combination of PMX and cisplatin improves outcome in patients with MPM[7-9] and

TABLE 1. Clinical and treatment characteristics of patients with malignant pleural mesothelioma receiving pemetrexed (PMX) chemotherapy

Characteristic		All patients (N = 41)	PMX first line (N = 29)	PMX second line (N = 12)	p
		N (%)	N (%)	N (%)	
Gender	Male	33 (80.5)	22 (75.9)	11 (91.7)	0.398[a]
	Female	8 (19.5)	7 (24.1)	1 (8.3)	
Stage	I	3 (7.3)	3 (10.3)	0	0.578[a]
	II	12 (29.3)	9 (31.0)	3 (25.0)	
	III	12 (29.3)	9 (31.0)	3 (25.0)	
	IV	14 (34.1)	8 (27.6)	6 (50.0)	
Histological type	Epitheloid	33 (80.5)	25 (86.2)	8 (66.7)	0.267[a]
	Biphasic	3 (7.3)	1 (3.4)	2 (16.7)	
	Sarcomatoid	3 (7.3)	2 (6.9)	1 (8.3)	
	Not characterized	2 (4.9)	1 (3.4)	1 (8.3)	
ECOG performance status	0	20 (48.8)	15 (51.7)	5 (41.7)	0.499[a]
	1	18 (43.9)	11 (37.9)	7 (58.3)	
	2	3 (7.3)	3 (10.3)	0	
Response rate	CR and PR	13 (31.7)	11 (37.9)	2 (16.7)	0.140[a]
	SD	19 (46.3)	14 (48.3)	5 (41.7)	
	Progress	9 (22.0)	4 (13.8)	5 (41.7)	
Liver toxicity	Present	24 (58.5)	15 (51.7)	9 (75.0)	0.296[a]
	Absent	17 (41.5)	14 (48.3)	3 (25.0)	
GI toxicity	Present	11 (26.8)	9 (31.0)	2 (16.7)	0.457[a]
	Absent	30 (73.2)	20 (69.0)	10 (83.3)	
Haematological toxicity	Present	19 (46.3)	13 (44.8)	6 (50.0)	1.000[a]
	Absent	22 (53.7)	16 (55.2)	6 (50.0)	
Renal toxicity	Present	18 (43.9)	13 (44.8)	5 (41.7)	1.000[a]
	Absent	23 (56.1)	16 (55.2)	7(58.3)	
Overall toxicity	Present	34 (82.9)	23 (79.3)	11 (91.7)	0.419[a]
	Absent	7 (17.1)	6 (20.7)	1 (8.3)	
Overall survival	median (min-max)	12.1 (1.0-36.1)	11.9 (1.0-36.1)	14.4 (6.4-31.6)	0.558[b]
Progression-free survival	median (min-max)	6.5 (1.0-36.1)	6.7 (1.0-36.1)	6.4 (6.4-31.6)	0.431[b]
Age	median (min-max)	63 (35-79)	63 (35-79)	64 (46-78)	0.785[b]

[a]calculated using Fisher's exact test; [b]calculated using Mann-Whitney U-test; CR = complete response; PR = partial response; SD = stable disease; ECOG = Eastern Cooperative Oncology Group; GI = gastrointestinal

comparable results were obtained for treatment with gemcitabine and cisplatin.[3,4,10]

PMX is a folic acid analogue, frequently used in treatment of MPM or non-small cell lung cancer (NSCLC). It inhibits several key folate pathway enzymes, including thymidylate synthase (TYMS), thus leading to impaired DNA synthesis.[11] Several other enzymes such as *MTHFD1*, *MTHFR*, *MTR*, and *MTRR*, participate in folate metabolic pathway and may influence treatment with antifolates.[12]

The efficacy of PMX may also depend on its transport into and out of the cell. The most important for PMX uptake is reduced folate carrier (SLC19A1), but hepatic SLCO1B1 transporter is also involved in antifolate transport.[13] On the other hand, ATP-binding cassette (ABC) transporters are involved in efflux of PMX from the cells.[14,15]

Response rate to PMX treatment is up to 40% in patients with MPM[3] and toxicity of PMX may be dose limiting. Differences in response to treatment with PMX may be partly due to genetic variability of enzymes involved in its transport and metabolism. Single nucleotide polymorphisms (SNPs) in folate pathway and folate transporter genes have

been extensively studied regarding their impact on toxicity and efficacy of methotrexate, the most common antifolate used in chemotherapy. Regarding PMX, a newer antifolate agent, only a few studies of *TYMS*, *MTHFR*, and *SLC19A1* polymorphisms in NSCLC were published to date.[16,17] Very little is known about the influence of these polymorphisms on response to treatment with PMX in MPM.[18]

The aim of this study was therefore to evaluate how polymorphisms in folate pathway genes (*TYMS*, *MTHFR*, *MTHFD1*, *MTR*, *MTRR*) and transporter genes (*SLC19A1*, *SLCO1B1*, *ABCB1*, *ABCC2*, *ABCG2*) affect treatment outcome, toxicity and survival in Slovenian patients with MPM, treated with PMX.

Patients and methods

Patients

Patients eligible for inclusion in the pharmacogenetic study had histologically proven MPM and were participating in an ongoing prospective randomised phase II clinical trial "Cisplatin with either Alimta or Gemcitabine in long infusion (AGILI) for mesothelioma" (Trial registration ID: NCT01281800) at the Institute of Oncology Ljubljana, Slovenia.[19] Patients that meet the trial's inclusion criteria were randomized in two groups, receiving either PMX or gemcitabine in combination with cisplatin.[19] Patients in which cisplatin was substituted with carboplatin due to poor performance status or renal dysfunction were also included. If disease progression occurred, chemotherapy regimen was switched in second line.

Patients were diagnosed mostly at the University Clinic of Pulmonary and Allergic Diseases in Golnik, Slovenia and treated at the Institute of Oncology Ljubljana, Slovenia. Clinical data were obtained from the medical records or assessed during the clinical interview.

The study was approved by the Slovenian Ethics Committee for Research in Medicine and was carried out according to the Declaration of Helsinki.

Response, survival and toxicity assessment

Tumour response was evaluated using modified Response Evaluation Criteria in Solid Tumours (RECIST).[20] Response rate was defined as the percentage of patients achieving partial or complete response. Progression-free survival (PFS) and overall survival (OS) were evaluated in survival analysis.

Haematological toxicity (anaemia, leucopoenia, neutropenia, and thrombocytopenia), liver toxicity, renal toxicity, and gastrointestinal (GI) toxicity were evaluated according to National Cancer Institute Common Terminology Criteria for Adverse Events, version 4.0.[21]

DNA extraction and genotyping

Peripheral blood samples were collected before the first day of the treatment. Extraction of genomic DNA from frozen whole-blood samples was performed according to the manufacturer's instructions using Qiagen FlexiGene kit (Qiagen, Hilden, Germany).

We genotyped 19 different polymorphisms in five folate pathway and six transporter genes. *MTHFD1* rs2236225 (Arg653Gln), *MTHFR* rs1801133 (Ala222Val) and rs1801131 (Glu429Ala), *SLCO1B1* rs2306283 (Asn130Asp), and *ABCB1* rs1045642 (Ile1145Ile) polymorphisms were determined using TaqMan SNP Genotyping assays according to the manufacturer's instructions (Applied Biosystems, Foster City, CA) as previously described.[22] Genotyping of *MTRR* rs1801394 (Ile22Met), *MTR* rs1805087 (Asp919Gly), *SLC19A1* rs1051266 (Arg27Cys), *SLCO1B1* rs11045879 (intronic), rs4149056 (Val174Ala) and rs2900478 (intronic), *ABCC2* rs717620 (5′ untranslated region (UTR) -24C>T), rs2273697 (Val417Ile) and rs2804402 (5′ UTR -1019A>G), *ABCC4* rs2274407 (Lys304Asn), and *ABCG2* rs2231142 (Gln141Lys) and rs2231137 (Val12Met) polymorphisms was carried out using a fluorescence-based competitive allele-specific (KASPar) assay according to the manufacturer's instructions (KBiosciences, Herts, UK). Determination of promoter *TYMS* rs34743033 (5′ UTR 2R>3R) polymorphism[23] and *ABCB1* rs2032582 (Ala893Ser/Thr) polymorphism was carried out using PCR amplification followed by the analysis of PCR fragments on agarose gel as previously described.[24]

Statistical analyses

Median and range (minimum-maximum) were used to present central tendency and variability. To assess deviation from Hardy–Weinberg equilibrium (HWE), standard chi-square test was used. A dominant genetic model was used in all statistical analyses. The influences of genetic polymorphisms on treatment outcome were examined by univariable logistic regression to calculate odds ratios (ORs) and their 95% confidence intervals (CIs). In

TABLE 2. The influence of investigated polymorphisms on response rate, overall survival (N = 41) and progression-free survival (N = 29) in patients with malignant pleural mesothelioma

Gene	Polymorphism		Response rate[a]		Progression-free survival[b]		Overall survival[b]	
			OR (95 % CI)	p	HR (95 % CI)	p	HR (95 % CI)	p
MTHFR	rs1801133	CC	Reference		Reference		Reference	
		CT+TT	0.63 (0.16-2.39)	0.492	1.82 (0.69-5.04)	0.248	1.11 (0.47-2.64)	0.809
	rs1801131	AA	Reference		Reference		Reference	
		AC+CC	0.76 (0.20-2.85)	0.678	0.93 (0.37-2.34)	0.880	1.15 (0.49-2.74)	0.746
MTHFD1	rs2236225	GG	Reference		Reference		Reference	
		GA+AA	0.12 (0.03-0.54)	**0.005**	3.10 (1.10-8.74)	**0.032**	1.81 (0.72-4.57)	0.207
TYMS	rs34743033	2R/2R	Reference		Reference		Reference	
		2R/3R+3R/3R	0.47 (0.12-1.83)	0.274	0.77 (0.28-2.08)	0.605	0.62 (0.23-1.66)	0.336
MTRR	rs1801394	AA	Reference		Reference		Reference	
		AG+GG	0.91 (0.19-4.39)	0.906	1.14 (0.31-4.20)	0.841	0.57 (0.18-1.78)	0.334
MTR	rs1805087	AA	Reference		Reference		Reference	
		AG+GG	0.97 (0.25-3.73)	0.960	1.38 (0.57-3.32)	0.473	1.57 (0.66-3.72)	0.310
SLC19A1	rs1051266	GG	Reference		Reference		Reference	
		GA+AA	0.90 (0.21-3.78)	0.886	1.05 (0.35-3.17)	0.925	1.45 (0.57-3.69)	0.437
SLCO1B1	rs2306283	AA	Reference		Reference		Reference	
		AG+GG	1.33 (0.29-6.15)	0.712	1.12 (0.44-2.89)	0.809	1.75 (0.65-4.69)	0.265
	rs4149056	TT	Reference		Reference		Reference	
		TC+CC	0.72 (0.19-2.76)	0.633	0.65 (0.27-1.60)	0.348	0.83 (0.35-1.94)	0.664
	rs11045879	TT	Reference		Reference		Reference	
		TC+CC	0.83 (0.22-3.20)	0.790	0.63 (0.26-1.53)	0.306	0.86 (0.37-2.01)	0.724
ABCB1	rs2032582	GG	Reference		Reference		Reference	
		GT+GA+TT+AA	0.49 (0.11-2.25)	0.358	2.89 (0.62-13.44)	0.177	1.47 (0.54-4.01)	0.448
	rs1045642	CC	Reference		Reference		Reference	
		CT+TT	0.92 (0.15-5.78)	0.926	3.19 (0.40-25.62)	0.275	3.90 (0.50-30.26)	0.193
ABCC2	rs2804402	CC	Reference		Reference		Reference	
		CT+TT	1.83 (0.32-10.37)	0.493	0.57 (0.18-1.81)	0.338	0.99 (0.34-2.90)	0.987
	rs717620	GG	Reference		Reference		Reference	
		GA+AA	0.46 (0.10-2.07)	0.314	2.08 (0.75-5.79)	0.159	1.10 (0.46-2.64)	0.826
	rs2273697	GG	Reference		Reference		Reference	
		GA+AA	4.75 (1.15-19.65)	**0.031**	0.57 (0.22-1.49)	0.252	0.88 (0.37-2.08)	0.763
ABCG2	rs2231142	CC	Reference		Reference		Reference	
		CA+AA	2.29 (0.55-9.64)	0.258	2.13 (0.65-6.94)	0.209	1.57 (0.60-4.11)	0.361

[a]calculated using logistic regression; [b]calculated by Cox proportional hazards model and adjusted for C-reactive protein level

survival analysis Cox proportional hazards model was used and the hazard ratio (HR) with the 95% CI was determined. All potential clinical and treatment predictors were also independently analysed for their influence on treatment outcome. All statistical analyses were carried out by Statistical Package for the Social Sciences (SPSS) for Windows, version 19.0 (IBM Corporation, Armonk, NY, USA).

Haplotypes were reconstructed and analysed using Thesias software[25] as described previously.[26]

Only haplotypes with frequencies above 5% were included in the statistical analyses and the most frequent haplotype was used as reference.

All statistical tests were two-sided and the level of significance was set to 0.05. Due to the exploratory nature of the study, no adjustments for multiple comparisons were used.

Results

Patients' characteristics

In our study, we included 41 patients with MPM, participating in the AGILI trial from 2008 to December 2012. In total, 29 patients received PMX as first line of chemotherapy and 12 received PMX as second line. Clinical characteristics of the study group are summarized in Table 1. Twenty (48.8%) patients were smokers and 33 (80.5%) were either occupationally or environmentally exposed to asbestos. Median C-reactive protein (CRP) level at diagnosis was 23 mg/l (range: 1–192 mg/l). The majority of patients (70.7%) received at least 4 cycles of chemotherapy. To the date of the analysis, disease progression occurred in 32 (78.0%) patients and 23 patients (56.1%) had died. There were no significant differences between patients receiving PMX as the first or second line of chemotherapy (Table 1).

Genotyping analysis

All genotype frequencies (Supplemental Table 1) were in agreement with HWE ($p > 0.05$). Three SNPs were excluded from further statistical analyses: *SLCO1B1* rs2900478 was in complete linkage disequilibrium (LD) with *SLCO1B1* rs11045879, while *ABCG2* rs2231137 and *ABCC4* rs2274407 were too rare.

Tumour response analysis

Among 41 patients, one (2.4%) was a complete responder and 12 (29.3%) were partial responders, meaning the overall response rate was 31.7%. Nineteen patients had stable disease and nine had progressive disease. Data on the influence of polymorphisms on response rate are presented in Table 2. Patients with at least one polymorphic *MTHFD1* rs2236225 allele had lower response rate ($p = 0.005$; OR = 0.12; 95% CI = 0.03–0.54) than patients with two wild-type alleles. On the other hand, patients with at least one polymorphic *ABCC2* rs2273697 had significantly better response rate than non-carriers ($p = 0.031$; OR = 4.75; 95% CI = 1.15–19.65).

Higher TNM stage was the only clinical parameter significantly associated with lower response rate ($p = 0.013$; OR = 0.35; 95% CI = 0.15–0.79). After adjustment for TNM stage, *MTHFD1* rs2236225 remained associated with response rate ($p = 0.016$; OR = 0.14; 95% CI = 0.03–0.70), but the effect of *ABCC2* rs2273697 was no longer significant ($p = 0.065$; OR = 4.32; 95% CI = 0.91–20.43).

Toxicity analysis

Several polymorphisms in transporter genes influenced occurrence of treatment-related toxicities. *ABCC2* rs2273697 conferred protection against development of any toxicity ($p = 0.035$; OR = 0.09; 95% CI = 0.01–0.85). Liver toxicity was significantly less frequent in carriers of polymorphic *SLCO1B1* rs11045879 ($p = 0.014$; OR = 0.18; 95% CI = 0.05–0.71) and rs4149056 ($p = 0.028$; OR = 0.23; 95% CI = 0.06–0.85) alleles. *ABCC2* rs2273697 was also associated with decreased liver toxicity ($p = 0.028$; OR = 0.23; 95% CI = 0.06–0.85). On the other hand, GI toxicity was much more common in patients with polymorphic *ABCC2* rs717620 allele ($p = 0.004$; OR = 10.67; 95% CI = 2.15-52.85). The other investigated polymorphisms in transporter and folate pathway genes did not significantly affect occurrence of either overall or specific toxicity (Table 3 and Supplemental Table 2).

Survival analysis

Analysis of OS was performed in the whole cohort of patients, while PFS was only analysed in the group of patients receiving PMX in the first line treatment. Firstly, clinical and treatment characteristics were examined for their influence on PFS or OS. Increased level of CRP before the first day of the treatment was the only parameter associated both with shorter PFS and shorter OS ($p = 0.002$, HR = 1.015, 95% CI = 1.01–1.03 and $p < 0.001$, HR = 1.015, 95% CI = 1.01–1.02, respectively). Patients with sarcomatoid or biphasic MPM had significantly shorter PFS ($p = 0.026$, HR = 4.59, 95% CI = 1.20–17.52). On the other hand, if patients received more chemotherapy cycles, OS was longer ($p = 0.024$, HR = 0.36, 95% CI = 0.15–0.88). However, only CRP remained significant in multivariable model.

The data on the influence of SNPs on survival is presented in Table 2. Among the investigated polymorphisms, only *MTHFD1* rs2236225 signifi-

TABLE 3. The influence of investigated polymorphisms on liver and gastrointestinal (GI) toxicity (N = 41)

Gene	Polymorphism		Liver toxicity[a]			GI toxicity[a]		
			N (%)	OR (95 % CI)	p	N (%)	OR (95 % CI)	p
MTHFR	rs1801133	CC	10 (45.5)	Reference		6 (27.3)	Reference	
		CT+TT	14 (73.7)	3.37 (0.90-12.6)	0.072	5 (26.3)	0.95 (0.24-3.81)	0.945
	rs1801131	AA	10 (58.8)	Reference		5 (29.4)	Reference	
		AC+CC	14 (58.3)	0.98 (0.28-3.46)	0.975	6 (25.0)	0.80 (0.20-3.22)	0.754
MTHFD1	rs2236225	GG	7 (46.7)	Reference		5 (33.3)	Reference	
		GA+AA	17 (65.4)	2.16 (0.59-7.90)	0.245	6 (23.1)	0.60 (0.15-2.46)	0.477
TYMS	rs34743033	2R/2R	7 (50.0)	Reference		2 (14.3)	Reference	
		2R/3R+3R/3R	17 (63.0)	1.7 (0.46-6.28)	0.426	9 (33.3)	3.00 (0.55-16.38)	0.205
MTRR	rs1801394	AA	6 (66.7)	Reference		1 (11.1)	Reference	
		AG+GG	18 (56.3)	0.64 (0.14-3.04)	0.577	10 (31.3)	3.64 (0.40-33.12)	0.252
MTR	rs1805087	AA	15 (60.0)	Reference		5 (20.0)	Reference	
		AG+GG	9 (56.3)	0.86 (0.24-3.06)	0.812	6 (37.5)	2.40 (0.59-9.82)	0.223
SLC19A1	rs1051266	GG	6 (50.0)	Reference		4 (33.3)	Reference	
		GA+AA	18 (62.1)	1.64 (0.42-6.36)	0.477	7 (24.1)	0.64 (0.15-2.77)	0.547
SLCO1B1	rs2306283	AA	9 (81.8)	Reference		3 (27.3)	Reference	
		AG+GG	15 (50.0)	0.22 (0.04-1.21)	0.081	8 (26.7)	0.97 (0.21-4.59)	0.696
	rs4149056	TT	17 (73.9)	Reference		4 (17.4)	Reference	
		TC+CC	7 (38.9)	0.23 (0.06-0.85)	**0.028**	7 (38.9)	3.02 (0.72-12.70)	0.131
	rs11045879	TT	18 (75.0)	Reference		5 (20.8)	Reference	
		TC+CC	6 (35.3)	0.18 (0.05-0.71)	**0.014**	6 (35.3)	2.07 (0.51-8.41)	0.308
ABCB1	rs2032582	GG	5 (55.6)	Reference		2 (22.2)	Reference	
		GT+GA+TT+AA	19 (59.4)	1.17 (0.26-5.20)	0.837	9 (28.1)	1.37 (0.24-7.88)	0.725
	rs1045642	CC	6 (66.7)	Reference		0 (0.0)	Reference	
		CT+TT	20 (57.1)	0.67 (0.11-4.13)	0.663	11 (31.4)	/	0.167[b]
ABCC2	rs2804402	CC	8 (88.9)	Reference		3 (33.3)	Reference	
		CT+TT	16 (50.0)	0.13 (0.01-1.12)	0.063	8 (25.0)	0.67 (0.14-3.30)	0.619
	rs717620	GG	15 (55.6)	Reference		3 (11.1)	Reference	
		GA+AA	9 (64.3)	1.44 (0.38-5.45)	0.591	8 (57.1)	10.67 (2.15-52.85)	**0.004**
	rs2273697	GG	17 (73.9)	Reference		6 (26.31)	Reference	
		GA+AA	7 (38.9)	0.23 (0.06-0.85)	**0.028**	5 (27.8)	1.09 (0.27-4.37)	0.903
ABCG2	rs2231142	CC	17 (56.7)	Reference		10 (33.3)	Reference	
		CA+AA	7 (63.6)	1.34 (0.32-5.56)	0.689	1 (9.1)	0.20 (0.02-1.79)	0.150

[a]calculated using logistic regression; [b]calculated using Fisher's exact test as there were no patients in one group

cantly influenced PFS (p = 0.032; HR = 3.10; 95% CI = 1.10–8.74) after adjustment for CRP level (Figure 1). MPM patients with at least one polymorphic *MTHFD1* allele and high CRP level had shorter survival than patients with two wild-type alleles and lower CRP level.

Haplotype analysis

Haplotype analysis was performed to assess the combined effect of SNPs within one gene. Three *SLCO1B1* haplotypes (ATT, GCC, and GTT) had frequencies above 5% and covered approximately 98% of variability within this gene (Table 4). Liver toxicity was less common in patients with GCC haplotype. This haplotype included all the polymorphic alleles, associated with decreased liver toxicity in single SNP analysis, compared with the reference ATT haplotype (p = 0.048; OR = 0.17; 95% CI = 0.03–0.98).

Four *ABCC2* haplotypes (CGG, CAG, TGG and TGA) covered all the variability within this gene (Table 4). GI toxicity was significantly more common in patients with CAG haplotype (p = 0.006; OR = 5.67; 95% CI = 1.64–19.66) with polymorphic rs717620 allele, associated with increased GI toxicity in single SNP analysis.

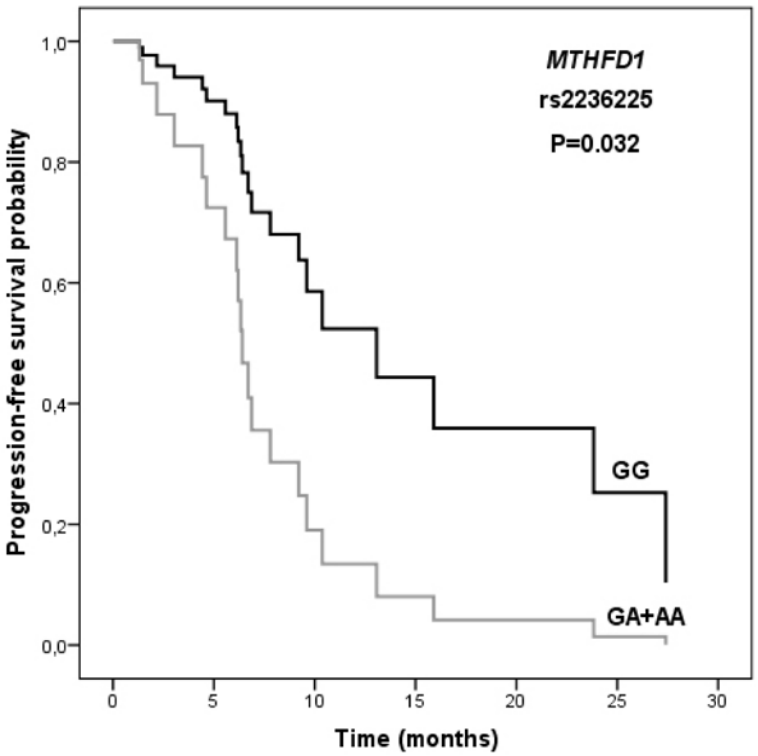

FIGURE 1. The influence of *MTHFD1* rs2236225 polymorphism on progression-free survival in patients with malignant pleural mesothelioma. *P*-value was calculated using Cox regression and adjusted for C-reactive protein level.

Discussion

Patients with MPM participating in a prospective randomized clinical trial were investigated for the influence of folate pathway and transporter polymorphisms on PMX treatment response. Among folate pathway genes only *MTHFD1* was associated with response rate and survival, while transporters mainly influenced PMX-related toxicity.

Only few pharmacogenetic studies on PMX treatment have been published so far. The only study in MPM focused on *TYMS* rs34743033, a tandem repeat of 28 base pairs in the 5′ UTR promoter region that changes TYMS mRNA and protein expression.[18] Consistent with our results, no association of this polymorphism with treatment outcome was observed, even though both mRNA and protein expression significantly affected survival.[18,27,28] Similar results were obtained in NSCLC.[17,29-32]

In our study, the carriers of the polymorphic *MTHFD1* rs2236225 allele had a significantly shorter PFS and were less likely to achieve complete or partial response, even after adjustment for TNM stage. MTHFD1 is essential for the generation of methylene-THF required for thymidylate synthesis and *MTHFD1* rs2236225 (Arg653Gln) was shown to reduce the enzyme activity[33], leading to increased levels of methylene-THF and reducing cytotoxic effects of PMX.[23,34] To our knowledge, no previous studies investigated the role of *MTHFD1* SNPs in treatment with PMX. However, in some, but not all studies on methotrexate treatment in acute lymphoblastic leukaemia (ALL), the variant allele was associated with shorter event-free survival.[23,34]

In our MPM patients PMX treatment outcome was not influenced by other investigated folate pathway SNPs. Most of them have not been studied yet in PMX treated MPM patients, however in NSCLC polymorphic *MTHFR* rs1801133 allele conferred to increased survival in a recessive model.[17,31]

To our knowledge, this is the first study investigating folate transporter gene polymorphisms regarding treatment outcome in MPM. Patients with at least one polymorphic *ABCC2* rs2273697 allele had better response rate and less overall and liver toxicity than non-carriers, while polymorphic *ABCC2* rs717620 allele and *ABCC2* CAG haplotype conferred to increased GI toxicity. *ABCC2* encodes one of the multidrug resistance associated transporters, involved in transport of both natural folates and antifolate agents.[35] The knowledge about the func-

TABLE 4. The influence of *SLCO1B1* and *ABCC2* haplotypes on response rate, gastrointestinal (GI), and liver toxicity (N = 41)

Gene	Haplotype	Estimated frequency	Response rate		GI toxicity		Liver toxicity	
			OR (95 % CI)	*p*	OR (95 % CI)	*p*	OR (95 % CI)	*p*
SLCO1B1	ATT	0.47	Reference		Reference		Reference	
	GCC	0.22	0.98 (0.24-4.04)	0.973	2.63 (0.61-11.37)	0.195	0.17 (0.03-0.98)	**0.048**
	GTT	0.29	1.94 (0.66-5.74)	0.229	0.37 (0.07-1.93)	0.237	0.46 (0.13-1.63)	0.230
ABCC2	CGG	0.28	Reference		Reference		Reference	
	CAG	0.20	0.30 (0.05-1.71)	0.175	5.67 (1.64-19.66)	**0.006**	1.06 (0.21-5.05)	0.941
	TGG	0.28	0.29 (0.06-1.46)	0.133	0.33 (0.07-1.61)	0.171	0.74 (0.18-3.07)	0.680
	TGA	0.24	1.59 (0.39-6.43)	0.519	0.88 (0.23-3.39)	0.847	0.29 (0.06-1.27)	0.099

tional significance of *ABCC2* SNPs is limited, but rs717620 was associated with decreased promoter activity and mRNA expression of *ABCC2*, possibly affecting the accumulation of PMX in cells.[15,36] However, *ABCC2* is also involved in transport of platinum compounds and this could contribute to its effect on treatment response. Indeed, some studies have shown that rs717620 affects treatment with platinum agents in lung cancer.[37,38]

In the present study, polymorphic *SLCO1B1* rs11045879 and rs4149056 alleles were significantly associated with liver toxicity both in single SNP and haplotype analysis. *SLCO1B1* encodes one of the main influx transporters expressed on the basolateral membrane of hepatocytes involved in uptake and clearance of many endogenous compounds and drugs, such as methotrexate.[39] *SLCO1B1* rs4149056 and rs2306283 were associated with decreased membrane expression and activity of the transporter.[39,40] Rs11045879 was identified in a genome-wide association study as the most important genetic factor associated with lower methotrexate clearance in patients with ALL. In later studies, a similar association with methotrexate clearance was observed for rs4149056.[40,41]

Although *SLC19A1* is the predominant uptake transporter for antifolates, we observed no impact of rs1051266 on PMX treatment. Our results are consistent with studies on NSCLC[17,31], although one study reported several other *SLC19A1* SNPs associated with OS.[16]

Our study represents the first comprehensive pharmacogenetic study of treatment with PMX in MPM patients participating in a prospective randomized trial. As MPM is a rare cancer, some potential limitations of our study arise from its small sample size, such as low statistical power. However, the strength of our study was that all patients were from a homogenous population[42], included in phase II clinical trial with well-defined inclusion criteria and clinical protocol, and treated in the same facility, thus minimizing the impact of other variables. We also evaluated the influence of potentially important clinical parameters and included haplotype analysis to evaluate the combined influence of more SNPs in one gene.

Both PMX and gemcitabine have shown comparable efficacy in MPM treatment.[3,4] In previous studies, we have identified some polymorphisms that influence MPM treatment with gemcitabine and cisplatin.[26,43,44] Our present results show for the first time that *MTHFD1*, *ABCC2*, and *SLCO1B1* polymorphisms may play an important role in PMX treatment response in patients with MPM. These SNPs could serve as biomarkers for more personalized treatment and in the future, selection of treatment based on genetic factors may contribute to better treatment outcomes in patients with MPM.

Supplementary files

Supplemental Table 1. Distribution of genotype frequencies in patients with malignant pleural mesothelioma (N = 41). Available from: http://www.degruyter.com/view/j/raon.2014.48.issue-2/raon-2013-0086/suppl/raon-2013-0086_supp1.pdf
Supplemental Table 2 The influence of selected polymorphisms on overall toxicity, hematological and renal toxicity. Available from: http://www.degruyter.com/view/j/raon.2014.48.issue-2/raon-2013-0086/suppl/raon-2013-0086_supp2.pdf

Acknowledgements

The authors thank Barbara Možina, M.Sc., head of the Biochemistry Laboratory, Institute of Oncology

Ljubljana, Slovenia, for her help with blood sample collections and handling. They also wish to acknowledge Nina Erčulj, Ph.D. for the initial help with data acquisition. The authors thank the staff from the University Clinic of Allergic and Pulmonary Disease Golnik, Slovenia for their help with diagnosis and treatment of malignant mesothelioma patients, particularly Izidor Kern, M.D. for performing the histopathological diagnosis and Prof. Tanja Čufer, M.D., Ph.D. and Nadja Triller, M.D. for providing first line treatment for one patient each. We wish to acknowledge Prof. Andrej Debeljak, M.D., Ph.D., Aleš Rozman, M.D., M.Sc., Matjaž Torel, M.D., M.Sc. and Prof. Anton Crnjac, M.D., Ph.D., for performing the invasive diagnostic procedures. We are also grateful to the team for lung cancer treatment at the Institute of Oncology Ljubljana, Slovenia for their help with patient treatment.

This work was financially supported by The Slovenian Research Agency (Grants L3-3648 and P1-0170).

References

1. Podobnik J, Kocijancic I, Kovac V, Sersa I. 3T MRI in evaluation of asbestos-related thoracic diseases – preliminary results. *Radiol Oncol* 2010; **44:** 92-6.
2. Mineo TC, Ambrogi V. Malignant pleural mesothelioma: factors influencing the prognosis. *Oncology (Williston Park)* 2012; **26:** 1164-75.
3. Kovac V, Zwitter M, Zagar T. Improved survival after introduction of chemotherapy for malignant pleural mesothelioma in Slovenia: Population-based survey of 444 patients. *Radiol Oncol* 2012; **46:** 136-44.
4. Lee CW, Murray N, Anderson H, Rao SC, Bishop W. Outcomes with first-line platinum-based combination chemotherapy for malignant pleural mesothelioma: a review of practice in British Columbia. *Lung Cancer* 2009; **64:** 308-13.
5. Raeisi E, Aghamiri SMR, Bandi A, Rahmatpour N, Firoozabadi SM, Kafi-Abad SA, Mir LM. The antitumor efficiency of combined electrochemotherapy and single dose irradiation on a breast cancer tumor model. *Radiol Oncol* 2012; **46:** 226-32.
6. Jeromen A, Oblak I, Anderluh F, Velenik V, Vidmar MS, Ratoša I. Results of postoperative radiochemotherapy of the patients with resectable gastroesophageal junction adenocarcinoma in Slovenia. *Radiol Oncol* 2012; **46:** 337-45.
7. Vogelzang NJ, Rusthoven JJ, Symanowski J, Denham C, Kaukel E, Ruffie P, et al. Phase III study of pemetrexed in combination with cisplatin versus cisplatin alone in patients with malignant pleural mesothelioma. *J Clin Oncol* 2003; **21:** 2636-44.
8. Berk S, Dogan OT, Kilickap S, Epozturk K, Akkurt I, Seyfikli Z. Clinical characteristics, treatment and survival outcomes in malignant mesothelioma: eighteen years' experience in Turkey. *Asian Pac J Cancer Prev* 2012; **13:** 5735-9.
9. Helland A, Solberg S, Brustugun OT. Incidence and survival of malignant pleural mesothelioma in norway: a population-based study of 1686 cases. *J Thorac Oncol* 2012; **7:** 1858-61.
10. Kovac V, Zwitter M, Rajer M, Marin A, Debeljak A, Smrdel U, et al. A phase II trial of low-dose gemcitabine in a prolonged infusion and cisplatin for malignant pleural mesothelioma. *Anticancer Drugs* 2012; **23:** 230-8.
11. Kao SC, Phan VH, Clarke SJ. Predictive markers for haematological toxicity of pemetrexed. *Curr Drug Targets* 2010; **11:** 48-57.
12. Berger SH, Pittman DL, Wyatt MD. Uracil in DNA: consequences for carcinogenesis and chemotherapy. *Biochem Pharmacol* 2008; **76:** 697-706.
13. Franke RM, Sparreboom A. Drug transporters: recent advances and therapeutic applications. *Clin Pharmacol Ther* 2010; **87:** 3-7.
14. Chattopadhyay S, Moran RG, Goldman ID. Pemetrexed: biochemical and cellular pharmacology, mechanisms, and clinical applications. *Mol Cancer Ther* 2007; **6:** 404-17.
15. Silverton L, Dean M, Moitra K. Variation and evolution of the ABC transporter genes ABCB1, ABCC1, ABCG2, ABCG5 and ABCG8: implication for pharmacogenetics and disease. *Drug Metabol Drug Interact* 2011; **26:** 169-79.
16. Adjei AA, Salavaggione OE, Mandrekar SJ, Dy GK, Ziegler KL, Endo C, et al. Correlation between polymorphisms of the reduced folate carrier gene (SLC19A1) and survival after pemetrexed-based therapy in non-small cell lung cancer: a North Central Cancer Treatment Group-based exploratory study. *J Thorac Oncol* 2010; **5:** 1346-53.
17. Tiseo M, Giovannetti E, Tibaldi C, Camerini A, Di Costanzo F, Barbieri F, et al. Pharmacogenetic study of patients with advanced non-small cell lung cancer (NSCLC) treated with second-line pemetrexed or pemetrexed-carboplatin. *Lung Cancer* 2012; **78:** 92-9.
18. Zucali PA, Giovannetti E, Destro A, Mencoboni M, Ceresoli GL, Gianoncelli L, et al. Thymidylate synthase and excision repair cross-complementing group-1 as predictors of responsiveness in mesothelioma patients treated with pemetrexed/carboplatin. *Clin Cancer Res* 2011; **17:** 2581-90.
19. Kovac V, Zwitter M. Cisplatin with Alimta or gemcitabine in long infusion for mesothelioma (AGILI). Available at: http://clinicaltrials.gov/ct2/show/NCT01281800. Accessed January 16, 2013.
20. Byrne MJ, Nowak AK. Modified RECIST criteria for assessment of response in malignant pleural mesothelioma. *Ann Oncol* 2004; **15:** 257-60.
21. *National Cancer Institute Common Terminology Criteria for Adverse Events, version 4.0.* Available at: http://ctep.cancer.gov/protocolDevelopment/electronic_applications/ctc.htm. Accessed February 15, 2012
22. Erculj N, Kotnik BF, Debeljak M, Jazbec J, Dolzan V. The influence of folate pathway polymorphisms on high-dose methotrexate related toxicity and survival in children with non-Hodgkin malignant lymphoma. *Radiol Oncol* 2013; doi:10.2478/raon-2013-0076. 2013.10.26. [Epub ahead of print]
23. Erculj N, Kotnik BF, Debeljak M, Jazbec J, Dolzan V. Influence of folate pathway polymorphisms on high-dose methotrexate-related toxicity and survival in childhood acute lymphoblastic leukemia. *Leuk Lymphoma* 2012; **53:** 1096-104.
24. Kastelic M, Koprivsek J, Plesnicar BK, Serretti A, Mandelli L, Locatelli I, et al. MDR1 gene polymorphisms and response to acute risperidone treatment. *Prog Neuropsychopharmacol Biol Psychiatry* 2010; **34:** 387-92.
25. Tregouet DA, Garelle V. A new JAVA interface implementation of THESIAS: testing haplotype effects in association studies. *Bioinformatics* 2007; **23:** 1038-9.
26. Erculj N, Kovac V, Hmeljak J, Franko A, Dodic-Fikfak M, Dolzan V. The influence of gemcitabine pathway polymorphisms on treatment outcome in patients with malignant mesothelioma. *Pharmacogenet Genomics* 2012; **22:** 58-68.
27. Righi L, Papotti MG, Ceppi P, Bille A, Bacillo E, Molinaro L, et al. Thymidylate synthase but not excision repair cross-complementation group 1 tumor expression predicts outcome in patients with malignant pleural mesothelioma treated with pemetrexed-based chemotherapy. *J Clin Oncol* 2010; **28:** 1534-9.
28. Christoph DC, Asuncion BR, Mascaux C, Tran C, Lu X, Wynes MW, et al. Folylpoly-glutamate synthetase expression is associated with tumor response and outcome from pemetrexed-based chemotherapy in malignant pleural mesothelioma. *J Thorac Oncol* 2012; **7:** 1440-8.
29. Christoph DC, Asuncion BR, Hassan B, Tran C, Maltzman JD, O'Shannessy DJ, et al. Significance of folate receptor alpha and thymidylate synthase protein expression in patients with non-small-cell lung cancer treated with pemetrexed. *J Thorac Oncol* 2013; **8:** 19-30.
30. Sun JM, Han J, Ahn JS, Park K, Ahn MJ. Significance of thymidylate synthase and thyroid transcription factor 1 expression in patients with nonsquamous non-small cell lung cancer treated with pemetrexed-based chemotherapy. *J Thorac Oncol* 2011; **6:** 1392-9.

31. Smit EF, Burgers SA, Biesma B, Smit HJ, Eppinga P, Dingemans AM, et al. Randomized phase II and pharmacogenetic study of pemetrexed compared with pemetrexed plus carboplatin in pretreated patients with advanced non-small-cell lung cancer. *J Clin Oncol* 2009; **27:** 2038-45.

32. Hu Q, Li X, Su C, Chen X, Gao G, Zhang J, et al. Correlation between thymidylate synthase gene polymorphisms and efficacy of pemetrexed in advanced non-small cell lung cancer. *Exp Ther Med* 2012; **4:** 1010-6.

33. Christensen KE, Rohlicek CV, Andelfinger GU, Michaud J, Bigras JL, Richter A, et al. The MTHFD1 p.Arg653Gln variant alters enzyme function and increases risk for congenital heart defects. *Hum Mutat* 2009; **30:** 212-20.

34. Krajinovic M, Lemieux-Blanchard E, Chiasson S, Primeau M, Costea I, Moghrabi A. Role of polymorphisms in MTHFR and MTHFD1 genes in the outcome of childhood acute lymphoblastic leukemia. *Pharmacogenomics J* 2004; **4:** 66-72.

35. Ranganathan P, Culverhouse R, Marsh S, Mody A, Scott-Horton TJ, Brasington R, et al. Methotrexate (MTX) pathway gene polymorphisms and their effects on MTX toxicity in Caucasian and African American patients with rheumatoid arthritis. *J Rheumatol* 2008; **35:** 572-9.

36. Sai K, Saito Y, Itoda M, Fukushima-Uesaka H, Nishimaki-Mogami T, Ozawa S, et al. Genetic variations and haplotypes of ABCC2 encoding MRP2 in a Japanese population. *Drug Metab Pharmacokinet* 2008; **23:** 139-47.

37. Sun N, Sun X, Chen B, Cheng H, Feng J, Cheng L, et al. MRP2 and GSTP1 polymorphisms and chemotherapy response in advanced non-small cell lung cancer. *Cancer Chemother Pharmacol* 2010; **65:** 437-46.

38. Campa D, Muller P, Edler L, Knoefel L, Barale R, Heussel CP, et al. A comprehensive study of polymorphisms in ABCB1, ABCC2 and ABCG2 and lung cancer chemotherapy response and prognosis. *Int J Cancer* 2012; **131:** 2920-8.

39. Niemi M, Pasanen MK, Neuvonen PJ. Organic anion transporting polypeptide 1B1: a genetically polymorphic transporter of major importance for hepatic drug uptake. *Pharmacol Rev* 2011; **63:** 157-81.

40. Trevino LR, Shimasaki N, Yang W, Panetta JC, Cheng C, Pei D, et al. Germline genetic variation in an organic anion transporter polypeptide associated with methotrexate pharmacokinetics and clinical effects. *J Clin Oncol* 2009; **27:** 5972-8.

41. Ramsey LB, Bruun GH, Yang W, Trevino LR, Vattathil S, Scheet P, et al. Rare versus common variants in pharmacogenetics: SLCO1B1 variation and methotrexate disposition. *Genome Res* 2012; **22:** 1-8.

42. Vidan-Jeras B, Jurca B, Dolzan V, Jeras M, Breskvar K, Bohinjec M. Slovenian Caucasian normal. In: Gjertson D, Terasaki P, editors. *HLA 1998*. Kansas: American society for histocompatibility and immunogenetics, Lenexa; 1998. p. 180-1.

43. Erculj N, Kovac V, Hmeljak J, Dolzan V. The influence of platinum pathway polymorphisms on the outcome in patients with malignant mesothelioma. *Ann Oncol* 2012; **23:** 961-7.

44. Erculj N, Kovac V, Hmeljak J, Franko A, Dodic-Fikfak M, Dolzan V. DNA repair polymorphisms and treatment outcomes of patients with malignant mesothelioma treated with gemcitabine-platinum combination chemotherapy. *J Thorac Oncol* 2012; **7:** 1609-17.

research article

Brain metastases in lung adenocarcinoma: impact of EGFR mutation status on incidence and survival

Karmen Stanic[1], Matjaz Zwitter[1,2] , Nina Turnsek Hitij[3] , Izidor Kern[3], Aleksander Sadikov[4], Tanja Cufer[3]

[1] Department of Radiotherapy, Institute of Oncology Ljubljana, Ljubljana, Slovenia
[2] Faculty of Medicine, University of Maribor, Slovenia
[3] University Clinic Golnik, Slovenia
[4] Faculty of Computer and Information Science, University of Ljubljana, Slovenia

Radiol Oncol 2014; 48(2): 173-183.

Received 24 December 2013
Accepted 3 March 2014

Correspondence to: Karmen Stanič, M.D., M.Sc., Institute of Oncology Ljubljana, Zaloška 2, 1000 Ljubljana, Slovenia. Phone: +386 1 5879 502; Fax: +386 1 5879 400; E-mail: kstanic@onko-i.si

Disclosure: The authors declare no conflict of interest.

Background. The brain represents a frequent progression site in lung adenocarcinoma. This study was designed to analyse the association between the epidermal growth factor receptor (EGFR) mutation status and the frequency of brain metastases (BM) and survival in routine clinical practice.

Patients and methods. We retrospectively analysed the medical records of 629 patients with adenocarcinoma in Slovenia who were tested for EGFR mutations in order to analyse the cumulative incidence of BM, the time from the diagnosis to the development of BM (TDBM), the time from BM to death (TTD) and the median survival.

Results. Out of 629 patients, 168 (27%) had BM, 90 patients already at the time of diagnosis. Additional 78 patients developed BM after a median interval of 14.3 months; 25.8 months in EGFR positive and 11.8 months in EGFR negative patients, respectively (p = 0.002). EGFR mutations were present in 47 (28%) patients with BM. The curves for cumulative incidence of BM in EGFR positive and negative patients demonstrate a trend for a higher incidence of BM in EGFR mutant patients at diagnosis (19% *vs.* 13%, p = 0.078), but no difference later during the course of the disease. The patients with BM at diagnosis had a statistically longer TTD (7.3 months) than patients who developed BM later (3.1 months). The TTD in EGFR positive patients with BM at diagnosis was longer than in EGFR negative patients (12.6 *vs.* 6.8, p = 0.005), while there was no impact of EGFR status on the TTD of patients who developed BM later.

Conclusions. Except for a non-significant increase of frequency of BM at diagnosis in EGFR positive patients, EGFR status had no influence upon the cumulative incidence of BM. EGFR positive patients had a longer time to CNS progression. While EGFR positive patients with BM at diagnosis had a longer survival, EGFR status had no influence on TTD in patients who developed BM later during the course of disease.

Key words: brain metastases; lung adenocarcinoma; EGFR mutations

Introduction

The brain represents a frequent progression site in lung adenocarcinoma.[1,2] The incidence of BM is increasing, probably due to a better treatment and prolonged survival as well as due to better imaging techniques.[3] This condition is often disabling and reduces the patients' quality of life.

The survival, even after aggressive multimodality treatment, remains poor.[4] Therefore new subgroups that might benefit from new treatments are being identified.[5,6] In the last few years, much effort and research in lung cancer has been oriented to molecular targets, *e.g.* EGFR activating mutations. Although a substantial proportion of patients with EGFR mutated tumours develop BM, the preva-

TABLE 1. Patients characteristics

Characteristics	Total patient number all	(%)	EGFR wild type	(%)	EGFR mutant	(%)	p
EGFR status	**n = 629**	**100**	**492**	**78.2**	**137**	**21.8**	
Age (years)							
median	64		63		66		
range	25–88		25–87		36–88		
Gender							< 0.001
male	326	51.8	282	57.3	44	32.1	
female	303	48.2	210	42.7	93	67.9	
Smoking status							< 0.001
current	272	43.2	255	51.8	17	12.4	
former	181	28.8	152	30.9	29	21.2	
never	147	23.4	64	13.0	83	60.6	
no data	29	4.6	21	4.3	8	5.8	
Performance status (WHO)							0.513
PS0	84	13.4	63	12.8	21	15.3	
PS1	379	60.3	301	61.2	78	56.9	
PS2	97	15.4	72	14.6	25	18.2	
PS3	41	6.5	34	6.9	7	5.1	
PS4	4	0.6	2	0.4	2	1.5	
no data	24	3.8	20	4.1	4	2.9	
Weight loss							0.511
yes	183	29.2	141	28.7	42	30.6	
no	380	60.4	302	61.3	78	56.9	
unknown	66	10.4	49	10.0	17	12.5	
Stage							0.070
I–III	245	38.9	203	41.2	42	30.6	
IV	379	60.2	286	58.1	93	67.8	
undetermined	5	< 1	4	< 1	1	< 1	

EGFR = epidermal growth factor receptor

lence and the best treatment options for progression to the central nervous system (CNS) have not yet been finally determined.

Prospective trials for progression to CNS are challenging to conduct, therefore retrospective analyses and meta-analyses remain useful and important research tools.

The aim of our retrospective study was to determine the frequency of BM at diagnosis and during the course of disease, the time to the development of BM and the survival after the diagnosis of BM in relation to EGFR mutation status.

Patients and methods

Patients

Between December 2009 and January 2012, 804 patients with lung cancer in Slovenia were tested for EGFR mutations. After excluding cases with other histologic types, 629 patients with primary lung adenocarcinoma and with a definitive report on the mutation status were selected for this analysis.

The patients included in this analysis had a specific oncological treatment at the Institute of Oncology, the University Clinic Golnik and the

TABLE 2. Baseline characteristics of patients with brain metastases

	Patients with BM at diagnosis							Patients who developed BM later						
Characteristics	**Total patient number all**	**(%)**	**EGFR wild type**	**(%)**	**EGFR mutant**	**(%)**	**p**	**Total patient number (BM)**	**(%)**	**EGFR wild type**	**(%)**	**EGFR mutant**	**(%)**	**p**
EGFR status	**n = 90**	**100**	**64**	**71.1**	**26**	**28.9**		**n = 78**	**100**	**57**	**73**	**21**	**27**	
Age (years)														
median	61.5		60		66		0.346	59		59		59		0.154
range	38–87		38–81		40–87			(36–81)		(43–81)		(36–74)		
Gender														
male	39	43.3	31	48.4	8	30.8	0.127	41	52.6	31	54.4	10	47.6	0.598
female	51	56.7	33	51.6	18	69.2		37	47.4	26	45.6	11	52.4	
Stage														
I–III	NA		NA		NA		NA	45	57.6	40	70.1	5	23.8	0.000
IV	90	100	64	71.1	26	28.9		32	42.4	17	29.9	16	76.2	
Metastatic sites														
brain only	25	27.8	22	34.4	3	11.5	0.029	50	64.1	38	66.7	12	57.1	0.440
multiple sites	65	72.2	42	65.6	23	88.5		28	35.9	19	33.3	9	42.9	

BM = brain metastases; EGFR = epidermal growth factor receptor

University Clinic Maribor. The testing was performed either as a routine procedure of adenocarcinoma at the time of diagnosis or, upon a special request of the treating oncologist, in patients who were diagnosed in the past or were candidates for the treatment with TKI at relapse. The medical records of patients were reviewed retrospectively.

The TNM staging is based on 7th Edition. All patients diagnosed before 2010 were restaged according to the new classification.[7]

The presence of BM was diagnosed with computed tomography (CT) or brain magnetic resonance imaging (MRI) either within the initial diagnostic staging of lung cancer or when patients became symptomatic.

The following parameters were recorded: demographic and clinical characteristics, the date of diagnosis, TNM classification, treatment characteristics, the date of first progression after primary treatment, the date of first BM; extracranial sites of disease activity at the time of BM diagnosis or any progression, the treatment of BM, the time of death or the last follow up. The smoking status was categorised as follows: nonsmokers (< 100 cigarettes in their lifetime), former smokers (stopped > 1 year before diagnosis of lung cancer), or current smokers. Performance status (PS) ranged from 0 to 4 according to Eastern Cooperative Oncology Group (ECOG) criteria. Weight loss of more than 2 kilograms per month before diagnosis of lung cancer was considered important. The follow up took place through 7th October 2013.

EGFR testing

There was no extra testing performed only for the purpose of this retrospective analysis. Pathological expertize and results of molecular testing were used for analysis. The samples used to extract genomic DNA were either from formalin-fixed, paraffin-embedded tissue sections or cytological slide preparations. The quantification of extracted DNA was done on Qubit Fluorometer (Invitrogen, Carlsbad, USA). To detect EGFR gene activating mutations, the samples were tested with TheraScreen EGFR29 Mutation Kit (DxS Diagnostics, Qiagen, Manchester, UK).

Statistical analysis

The primary endpoints in this analysis were the cumulative incidence of BM, the time to the development of brain metastases (TDBM) and the survival after the diagnosis of BM representing the time to death (TTD). The TDBM was calculated from the time of the diagnosis to the time of the development of BM for all patients who had no BM at diagnosis. The TTD was calculated from the date of BM to the date of death from any cause or the date of the last follow-up; censored observations represent patients alive at the time of the last follow-up. The second-

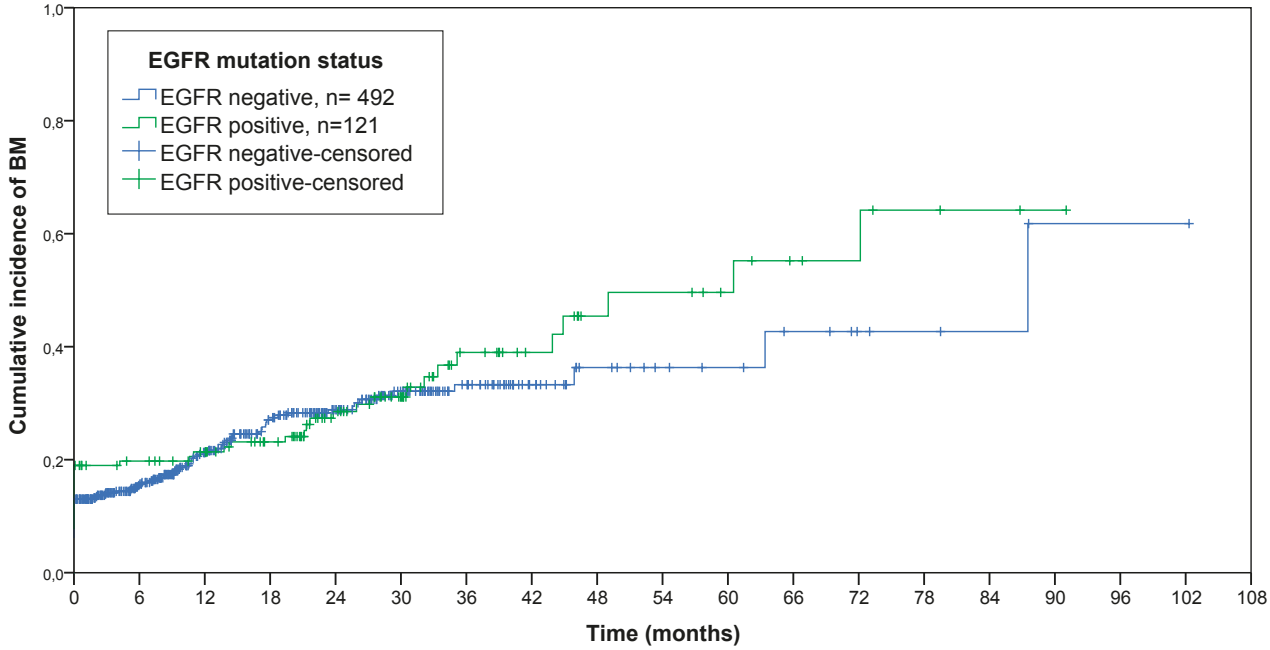

N. at risk																		
EGFR +	111	109	96	87	60	53	27	27	17	12	8	8	4	4	2	1	0	0
EGFR -	428	320	229	175	120	86	56	30	18	13	11	8	5	4	3	2	1	0

Cumulative incidence																		
EGFR +	26	26	29	31	36	38	42	42	44	45	46	46	47	47	47	47	47	47
EGFR -	64	75	93	107	111	116	117	118	119	119	119	120	120	120	120	121	121	121

FIGURE 1. Cumulative incidence of BM in all adenocarcinoma patients by EGFR status.

ary endpoint of this analysis was the overall survival (OS) calculated from the date of diagnosis to the date of death due to any cause. The Kaplan-Meier (KM) method and the log rank test were used to test for the difference between EGFR positive and negative patients. The cumulative incidence was calculated using 1-KM, using progression to CNS as an event. The association between the EGFR mutation status and the clinico-pathological characteristics of patients were tested using the Mann-Whitney U (MW-U) or the Kruskal Wallis H (KW-H) test. All p values reported were based on the two-sided hypothesis. The statistical analysis was computed using SPSS v.20 statistical package.

This survey was approved by the National Ethics Committee on 18.10.2011, No.143/1.

Results

Patient characteristics

The baseline characteristics of all 629 adenocarcinoma patients are presented in Table 1. The series included 326 (52%) men and 303 (48%) women with a median age of 64 years (range from 25 to 88). All patients were Caucasians. A statistically significant higher proportion of EGFR positive patients was among women (67.9% *vs.* 32.1%), $p < 0.001$ and nonsmokers (60.6% *vs.* 33.6%), $p < 0.001$. Out of 629 patients included in the analysis, 379 (60%) had a metastatic disease. Ninety patients had brain metastases already at the time of diagnosis, representing 14.3% of all and 33% of metastatic patients. EGFR mutations were present in 26 (29%) patients with BM.

We identified 168 patients who had BM at any time during their course of disease. Of these, 90 patients had metastases in CNS already at the time of diagnosis and 78 patients progressed to CNS during the treatment and the course of the disease. Out of 168 patients with BM, 47 had EGFR activating mutations (28%). The median follow-up time was 53 months. The data on the basic characteristics of this subgroup of patients (separately for those with BM at diagnosis and for those who developed BM later) are presented in Table 2**.** The median age at

diagnosis for patients with BM at diagnosis was 61.5 years and did not differ due to EGFR status. The proportion of women was higher among EGFR positive patients (69.2%), yet this was not statistically significant compared to EGFR negative patients (MW-U test, p = 0.127). At diagnosis, only 3 patients (11.5%) with EGFR mutated tumours had BM as the only metastatic site, while there were 22 (34%) such patients in EGFR wild type tumours (p = 0.029). No such difference was seen in patients who had BM later during the course of the disease (p = 0.440). EGFR wild type patients in stage I-III progressed to CNS more often than EGFR mutant patients, p < 0.001.

Cumulative incidence of BM

The cumulative incidence of BM for all 629 patients analysed is presented in Figure 1. The incidence of BM did not differ among EGFR groups, the log rank p = 0.47. While more EGFR positive than negative patients had BM already at diagnosis (19% *vs.* 13%), the difference was only marginally significant (MW-U, p = 0.078).

Metastases developed after a median time of 14.3 months (CI 13.2 – 15.4) in 78 patients who had no BM at diagnosis. This group was not homogenous with regard to stage, there were 45 non-metastatic and 33 metastatic patients, but this did not influence the TDBM. The median time to CNS progression for EGFR mutated patients was much longer than for EGFR wild type patients, 25.8 *vs.* 11.8 months (log rank, p = 0.002).

Specific oncological treatment before the development of BM

All 78 patients without BM at diagnosis had a specific oncological treatment of primary tumour. The patients with non-metastatic disease at diagnosis (45 patients) received various combinations of surgery, radiotherapy and chemotherapy. According to guidelines, none received TKI as a primary treatment. Ten patients (3 EGFR positive) had only a surgical treatment of the primary tumour and CNS was the first site of disease progression in 5 patients, none of them EGFR positive. Six patients were treated with radiotherapy only, among them only one was EGFR mutant and received an intermittent treatment with chemotherapy and TKI at the first progression, which was not to CNS, and developed BM while on maintenance treatment with TKI. Thirty patients had a multimodality treatment, two were EGFR mutant. Metastatic patients received systemic treatment, either chemotherapy or TKI. In fact, 12 (80%) of all 15 EGFR positive patients received TKI already as a first line treatment.

In summary, all 21 EGFR positive patients without BM at diagnosis actually received treatment with TKI either as an initial or one of subsequent therapies, all before the development of BM.

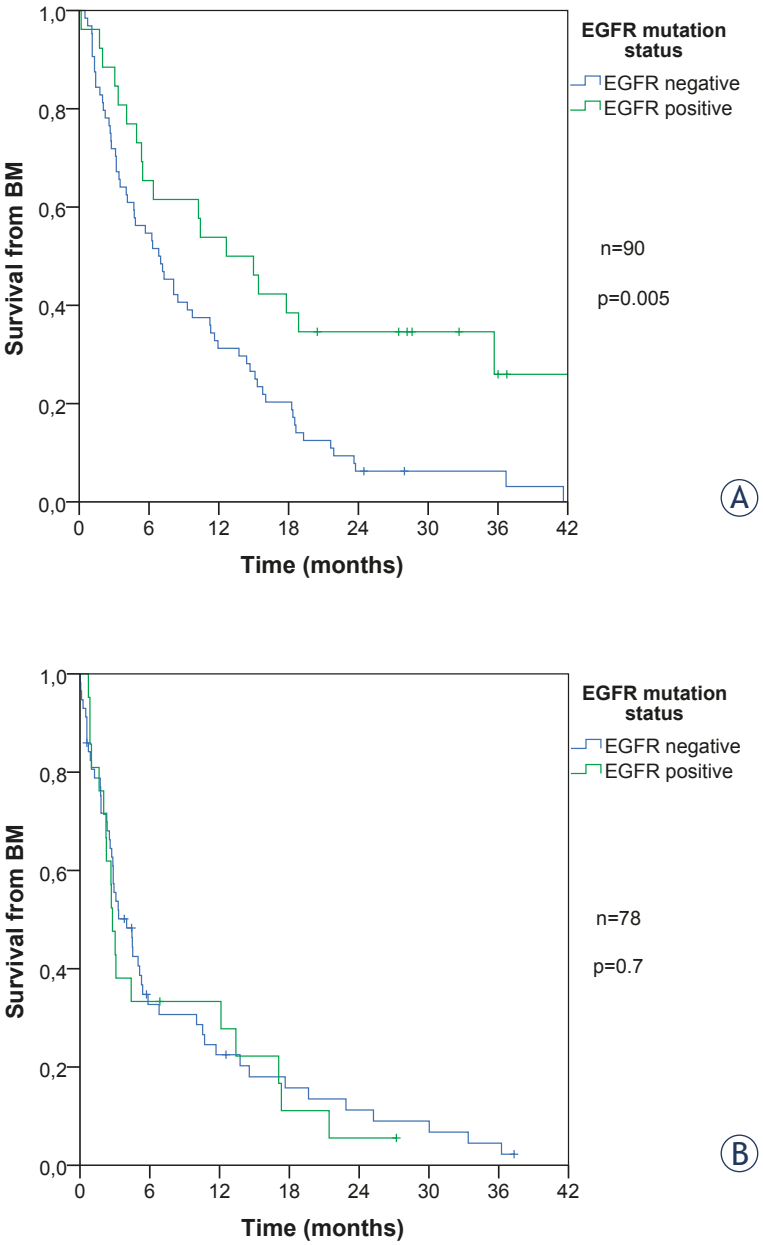

FIGURE 2. Survival from diagnosis of BM according to EGFR status: **(A)** for patients with BM at diagnosis and **(B)** for patients who developed BM later during the course of the disease.

TABLE 3. Univariate and multivariate analysis

	TTD 90 7.3 months (CI 4.1–10.5)			TTD 78 3.1 months (CI 1.7–4.4)		
	Univariate	Multivariate		Univariate	Multivariate	
	p-value	p-value	HR (95% CI)	p-value	p-value	HR (95% CI)
Gender (female/ male)	0.24	-		0.81	-	
Age (< 61 / > 61)	0.15	0.09	ns	0.05	0.15	NS
Smoking (never/ever)	0.33	-		0.64	-	
Weight loss (no/yes)	0.04	0.09	NS	N/A	-	
PS (0-1/2-4)	0.00	0.01	1.96 (1.16–3.30)	N/A	-	
EGFR (negative/ positive)	0.00	0.00	0.37 (0.18–0.77)	0.70	-	
Systemic treatment (yes/no)	0.00	0.00	4.32 (2.39–7.82)	0.00	0.00	2.16 (1.22–3.82)
WBRT (yes/no)	0.07	0.04	0.53 (0.28–0.99)	0.92	-	NS

EGFR = epidermal growth factor receptor; HR = hazard ratio; NS = not significant; PS = performance status; WBRT = whole brain radiotherapy

Specific oncological treatment after the diagnosis of BM

Out of 90 patients with BM at diagnosis, 66 (73%) patients started their treatment with whole brain radiotherapy (WBRT). After WBRT, all 17 EGFR positive patients received TKI treatment. Among 49 EGFR negative patients, 4 were also given TKI, chemotherapy was administered to 25 patients and best supportive care (BSC) to 20 patients. In the group of 24 patients who never had cranial irradiation, there were 9 EGFR positive patients, 7 received TKI and 2 BSC only. EGFR wild type patients in the group without WBRT received chemotherapy (7), TKI (1) and BSC (7). Altogether, no systemic therapy was delivered to 29 (32%) patients (2 EGFR positive) who had BM already at the diagnosis.

Within the group of 78 patients who developed BM later, 63 (80%) had WBRT and afterwards 40 patients (63%) received no systemic treatment, including 7 EGFR positive patients. Of the remaining 10 EGFR positive patients, 9 received TKI and 1 had chemotherapy. Among 15 patients without irradiation, BSC was given to 13 patients and TKI to 2 EGFR positive patients.

In summary, WBRT was delivered to 128 (76%) out of 168 patients with BM, while 40 patients had no irradiation of CNS. In comparison to EGFR wild type patients, those with EGFR mutations treated with WBRT had a longer TTD, 6.9 *vs.* 2.6 months (log rank, p = 0.005). Among all, 11 patients had a brain metastases resection followed by irradiation. We grouped patients into 3 categories regarding the dose of WBRT delivered (< 20 Gy, 21–30 Gy or > 30 Gy). The patients receiving a higher dose had a statistically significant longer TTD (log rank, p = 0.005). This difference was even more pronounced within each dose group for EGFR positive patients; however, no statistic was computed due to the small number of cases in some groups. Patients without WBRT had a statistically lower TTD (log rank, p = 0.002).

The systemic treatment resulted in a longer survival after BM compared to no systemic treatment, though only one half of the patients (52%) received one. The curves for TKI and chemotherapy overlap and show no meaningful difference. Treatment with TKI after the diagnosis of BM was administered to 49 patients (71% were EGFR positive) and chemotherapy to 37 (97% EGFR negative) patients.

Median survival time from diagnosis of BM (TTD)

The TTD for all 168 patients with BM was 5.3 months (CI 3.9–6.6). EGFR positive patients had a longer TTD as compared to EGFR negative patients, 6.3 *vs.* 4.8 months, respectively (log rank, p = 0.026). This difference is entirely due to a better survival of EGFR positive patients who had BM at

initial diagnosis (12.6 months for EGFR positive and 6.8 for EGFR negative patients, p = 0.005). In those patients who developed BM later, the TTD was significantly shorter (3.1 months) and there was no significant difference between EGFR positive and negative patients (p = 0.7) (Figure 2).

Table 3 presents the results of univariate and multivariate analysis of survival from the date of BM (TTD) for patients with BM at diagnosis and those who developed BM later. The TTD for patients with BM at diagnosis (90 patients) was influenced by the EGFR status, age, weight loss, PS, WBRT and systemic treatment according to univariate analysis. The multivariate analysis showed that beside EGFR status also PS, WBRT and systemic treatment were significant.

In the TTD for patients who developed BM later (78 patients) age, systemic treatment and WBRT were significant in univariate, but only systemic treatment in multivariate Cox analysis. The EGFR status showed no significance in patients who developed BM during their course of disease.

Overall survival time

The overall survival of patients with EGFR activating mutations among all 629 adenocarcinomas was significantly longer regardless of metastatic status, log rank p < 0.001 (Figure 3). The median survival time for stage I–III was 59 months for EGFR positive and 36 months for EGFR negative patients. Metastatic patients had a shorter median survival, 20.6 months for EGFR mutant and 8.3 months for EGFR wild type.

The presence of BM at the diagnosis of metastatic disease was a clear negative prognostic factor. The patients who had a metastatic disease at diagnosis, yet not to CNS, had a longer median survival compared to the patients with a metastatic disease to CNS at diagnosis (10.7 *vs.* 7.3 months). The difference within those two subgroups also persists in accordance with the EGFR status. The survival was twice longer in EGFR mutated (24.1 *vs.* 12.6 months) than in wild type patients (8.6 *vs.* 6.8 months) (Figure 4).

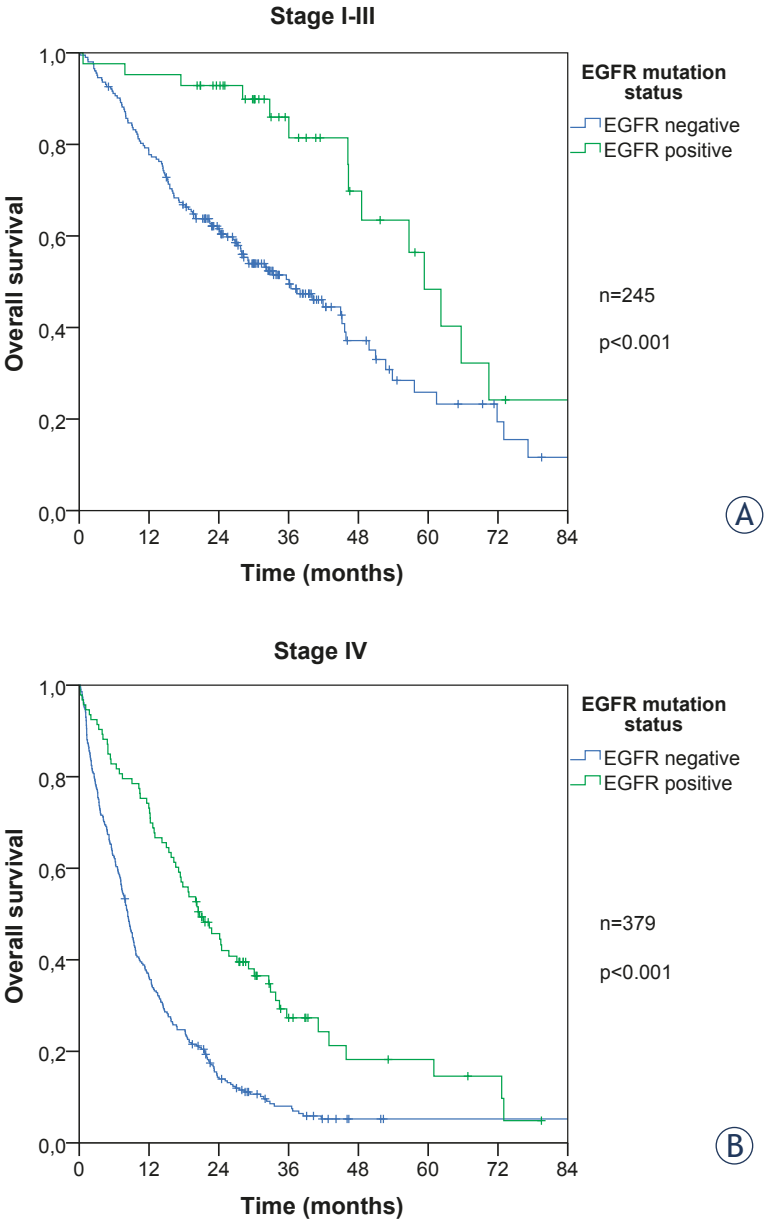

FIGURE 3. Overall survival for EGFR positive and negative patients in stages I-III **(A)** and IV **(B)**.

Discussion

Our retrospective analysis belongs to the largest reports on nationally-based lung adenocarcinoma tested for EGFR mutations. We found that 28% of adenocarcinoma patients developed BM at any time during their course of disease. The majority of papers report a frequency of BM from 25 to over 50% for NSCLC, emphasizing a higher incidence in non-squamous histology.[1,2,8-13] There are also some reports focusing exclusively on adenocarcinoma, yet the number of patients in these studies is low.[14-16]

The publications in recent years also include information on the EGFR status. Due to the increased prevalence of EGFR mutations in Asian population (30–40%) as compared to Caucasians (10–20%), the papers including a substantial proportion of Asian patients should be interpreted with caution since

it has been reported that the incidence of BM is influenced by the EGFR status.[15-23] Saad *et al*. reported no increased risk for development of BM with EGFR expression.[24] All patients in our analyses were Caucasians.

The proportion of women in our analysis is high (52%) and does not reflect the epidemiological data (31%).[25] The reason is a selection bias. The treating oncologists more often ordered EGFR testing at relapse for women and non-smokers, since all publications report a higher probability of EGFR mutations in those subgroups of patients.

In our analysis, the BM were present in 90 (14%) patients already at diagnosis. The same proportion was reported by Sekine *et al.* for 174 analysed Asian patients of whom 40% were EGFR mutated.[20] The proportion of our patients with BM at diagnosis among all EGFR positive ones compared to all EGFR negative ones was higher, yet it did not reach statistical significance (19% *vs.* 13%, log rank, p = 0.078). Fujiwara reported this proportion to be 32% in the EGFR positive and 27% in the EGFR negative group among 141 analysed Asian patients.[15]

In our series, the BM was the only metastatic site for 25 patients at diagnosis, of whom only 3 were EGFR positive (p = 0.029). Significantly more isolated BM in EGFR negative patients was also found in the study of Eichler *et al*., 31% *vs.* 7% (p = 0.03).[25] On the contrary, Lee *et al*. found a higher incidence of isolated BM in EGFR mutated patients from a series of 117 resected tumours (24% *vs.* 9%), which, however, was not statistically significant.[21] This finding indicates a different biology of the disease. It is therefore possible that patients with EGFR mutations are more prone to metastasing, including CNS, or they produce more often asymptomatic metastases and, consequently, patients are diagnosed at a later stage. One can also speculate that women nonsmokers (the majority of EGFR positive patients), although having medical and breathing problems, are not considered being at risk of having lung cancer in spite of seeking medical attention relatively early.

As shown in Figure 1, in the first year the curve of cumulative incidence of BM in EGFR mutated patients rises slower than in EGFR wild type, yet after one year the curves of EGFR mutant and EGFR wild type tumours overlap. Our patients without BM at diagnosis progressed to CNS after a median time of 14.3 months. The interval was longer for EGFR positive patients *vs.* EGFR negative ones, 25.9 *vs.* 11.9 months, respectively (p = 0.002). We believe that this observation is entirely due to a longer survival of EGFR mutated patients since a substantial proportion of EGFR wild type patients die already within the first year and never have a chance to develop BM. The time to the development of BM was also longer in EGFR positive patients in the study by Eichler *et al*., 19 *vs.* 14 months, yet this was not statistically significant.[25]

The median survival time from the diagnosis of brain metastases to death (TTD) was 5.3 months for all patients with BM. The EGFR mutation status strongly influenced the median survival time if BM had been discovered already at diagnosis (12.6 *vs.* 6.8 months) with no significant impact on those found later during the course of disease. A difference in accordance with the EGFR status was also found by Eichler *et al*., 14.5 *vs.* 7.6 months (p = 0.09).[25] The TTD for our EGFR positive patients compares favourably to 5.5 months reported by Heon.[26] Another report including 70% of EGFR positive patients found an overall survival from BM onset to be 15 months.[27] A favourable survival of EGFR mutated patients with BM (13.2 *vs.* 6.8 months, p = 0.001) was also reported by Hsiao.[28]

Patients treated with WBRT had a longer TTD than those without it, which was also reported in other studies.[17,29] EGFR positive patients had a longer TTD within the irradiated and the non-irradiated group as compared to EGFR negative patients. Gow *et al.* also reported that patients with EGFR mutations and WBRT had a better survival and response rate in univariate but only a trend in multivariate analysis.[30] Additionally, we found that a higher dose led to longer survival. A combination of BM resection and postoperative WBRT did not result in a better TTD than WBRT alone for EGFR positive *vs.* negative patients, although the numbers are small. A systemic treatment delivered after the diagnosis of BM also increased survival and there was no difference whether patients received TKI or chemotherapy. Our finding is in accordance with a recent publication by Komatsu *et al*., who report a significant improvement in PFS and OS for patients treated with TKI after WBRT.[29]

Surprisingly, WBRT was an independent factor for better survival only in patients who had BM already at the time of diagnosis, while it had no influence on the subgroup of patients who developed BM later during the treatment and the course of disease. On the contrary, systemic treatment with chemotherapy or TKI had a significant influence on the survival of patients with BM of both subgroups. It is possible that the disruption of blood brain barrier by WBRT in patients with BM at diagnosis increased the permeability and penetration of TKI to CNS, leading to a prolonged survival;

the mechanism was proposed by Ceresoli.[31] All 78 patients who developed BM during the treatment and the course of disease in our study had one or more previous treatment lines with TKI before the BM onset. Due to the retrospective nature of our analysis, we could not establish any reliable PS at the time of BM from our medical records, therefore this was not included in the analysis. Usually, patients after several progressions and chemotherapy or TKI lines have a poor performance, which is also reflected in the fact that 63% of the patients only received BSC after WBRT. The reason for the non-effective WBRT might also be a lower total dose with shorter fractionation delivered to the majority of those patients.

EGFR mutated cell lines exposed to ionizing radiation *in vitro* show a 500 to 1000-fold reduced clonogenic survival.[32] On the other hand, there are also *in vitro* reports for increased radioresistance of EGFR cell lines.[33] It is believed that cells with EGFR mutations are radiosensitive and cells with EGFR overexpression are radioresistant.

Tanaka showed a strong *in vitro* effect of enhanced radiation response with gefitinib due to a prolonged double strand break and suppressed cellular DNA repair capability.[34] TKI is considered to be a radiosensitizer, therefore TKI delivered concomitantly with WBRT represents one option of improved response rate (RR) in treating BM. The combination of WBRT and concomitant treatment with TKI remains controversial. While some researchers found no evidence of increased toxicity, others report an excellent RR and an increased OS at the expense of significant toxicity.[35-39] Currently, TKI delivered concomitantly with WBRT is only recommended in clinical trials.

TKI alone was also used to treat asymptomatic BM from lung adenocarcinoma with high response rate of almost 70% in unselected Asian population of nonsmokers.[40-46] In spite of all publications so far, the association between WBRT, the treatment with TKI and EGFR status is still unclear.

On the basis of the above findings, it is not unexpected that some investigators have proposed prophylactic cranial irradiation (PCI) for EGFR positive NSCLC patients.[47] None of the PCI studies in NSCLC has so far demonstrated an improved OS, therefore this is not a routine practice as in small-cell lung cancer, although studies have been able to show a reduced incidence and delayed appearance of BM by 50%. There have been no reports of EGFR status impact on those parameters.[48-51] Therefore we are eagerly awaiting the results of a prospective clinical trial going on in Germany; an outline

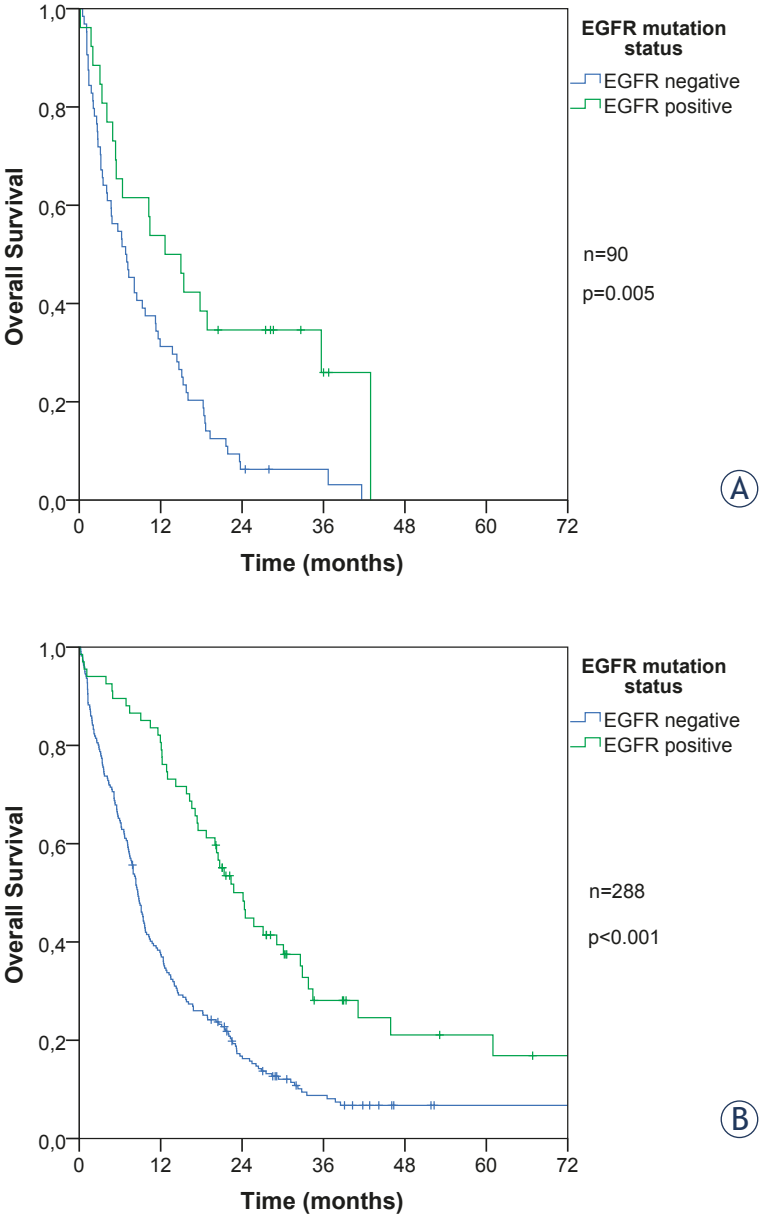

FIGURE 4. Overall survival by EGFR status for metastatic patients with brain metastases at diagnosis **(A)** and those without them **(B)**.

was presented at ASCO 2012.[52] Ongoing clinical trials are already focusing on new molecular targets, therefore retrospective real life analyses, although without possibility to omit all disadvantages of retrospective studies, could add to understanding this complex and disabling medical condition.

Conclusions

Our results show that EGFR positive patients have a higher frequency of BM already at diagnosis,

although not a statistically significant one, and a longer median survival than EGFR wild type patients. They develop BM later than EGFR negative patients, regardless of the stage and the previous treatment. The median survival of patients who develop BM during their course of disease is not different with regard to their EGFR status. Systemic treatment (either chemotherapy or TKI) was the only independent factor increasing the survival after the development of BM.

References

1. Bajard A, Westeel V, Dubiez A, Jacoulet P, Pernet D, Dalphin JC, et al. Multivariate analysis of factors predictive of brain metastases in localised non-small cell lung carcinoma. *Lung Cancer* 2004; **45:** 317-23.
2. Sørensen JB, Hansen HH, Hansen M, Dombernowsky P. Brain metastases in adenocarcinoma of the lung: frequency, risk groups, and prognosis. *J Clin Oncol* 1988; **6:** 1474-80.
3. Burel-Vandenbos F, Ambrosetti D, Coutts M, Pedeutour F. EGFR mutation status in brain metastases of non-small cell lung carcinoma. *J Neurooncol* 2013; **111:** 1-10.
4. Ali A, Goffin JR, Arnold A, Ellis PM. Survival of patients with non-small-cell lung cancer after a diagnosis of brain metastases. *Curr Oncol* 2013; **20:** e300-6.
5. Berger LA, Riesenberg H, Bokemeyer C, Atanackovic D. CNS metastases in non-small-cell lung cancer: Current role of EGFR-TKI therapy and future perspectives. *Lung Cancer* 2013; **80:** 242-8.
6. Linnert M, Iversen HK, Gehl J. Multiple brain metastases - current management and perspectives for treatment with electrochemotherapy. *Radiol Oncol* 2012; **46:** 271-8.
7. Rami-Porta R, Crowley JJ, Goldstraw P. The revised TNM staging system for lung cancer. *Ann Thorac Cardiovasc Surg* 2009; **15:** 4-9.
8. Wang S-Y, Ye X, Ou W, Lin Y-B, Zhang B-B, Yang H. Risk of cerebral metastases for postoperative locally advanced non-small-cell lung cancer. *Lung Cancer* 2009; **64:** 238-43.
9. Robnett TJ, Machtay M, Stevenson JP, Algazy KM, Hahn SM. Factors affecting the risk of brain metastases after definitive chemoradiation for locally advanced non-small-cell lung carcinoma. *J Clin Oncol* 2001; **19:** 1344-9.
10. Mamon HJ, Yeap BY, Jänne PA, Reblando J, Shrager S, Jaklitsch MT, et al. High risk of brain metastases in surgically staged IIIA non-small-cell lung cancer patients treated with surgery, chemotherapy, and radiation. *J Clin Oncol* 2005; **23:** 1530-7.
11. Smrdel U, Zwitter M, Kovač V. Brain metastases in lung cancer. Impact of prognostic factors on patient survival. *Radiol Oncol* 2003; **37:** 213-6.
12. Gaspar LE, Chansky K, Albain KS, Vallieres E, Rusch V, Crowley JJ, et al. Time from treatment to subsequent diagnosis of brain metastases in stage III non-small-cell lung cancer: a retrospective review by the Southwest Oncology Group. *J Clin Oncol* 2005; **23:** 2955-61.
13. Ceresoli GL, Reni M, Chiesa G, Carretta A, Schipani S, Passoni P, et al. Brain metastases in locally advanced nonsmall cell lung carcinoma after multimodality treatment: risk factors analysis. *Cancer* 2002; **95:** 605-12.
14. Matsumoto S, Takahashi K, Iwakawa R, Matsuno Y, Nakanishi Y, Kohno T, et al. Frequent EGFR mutations in brain metastases of lung adenocarcinoma. *Int J Cancer* 2006; **119:** 1491-4.
15. Fujiwara S, Murakami H, Shukuya T, Ono A, Tsuye A, Nakamura Y, et al. Clinical significance of EGFR on progression of brain meta. *J Thorac Oncol* 2011; **6(Suppl 2):** S1214.
16. Sekine A, Kato T, Hagiwara E, Shinohara T, Komagata T, Iwasawa T, et al. Metastatic brain tumors from non-small cell lung cancer with EGFR mutations: distinguishing influence of exon 19 deletion on radiographic features. *Lung Cancer* 2012; **77:** 64-9.
17. Zhou Wei CD. East meets West:ethnic differences in epidemiology and clinical behaviours of lung cancer between East Asian and Caucasians. *Chin J Cancer* 2011; **30:** 287-92.
18. de Mello RA, Pires FS, Marques DS, Oliveira J, Rodrigues A, Soares M, et al. EGFR exon mutation distribution and outcome in non-small-cell lung cancer: a Portuguese retrospective study. *Tumor Biol* 2012; **33:** 2061-8.
19. Li Z, Lu J, Zhao Y, Guo H. The retrospective analysis of the frequency of EGFR mutations and the efficacy of gefitinib in NSCLC patients with brain metastasis. *J Clin Oncol* 2011; **29:** e18065.
20. Sekine A. Characteristics of metastatic brain tumor in patients with lung adenocarcinoma with mutation of epidermal growth factor receptor gene. *Am J Respir Crit Care Med* 2010; **181:** A5147
21. Lee YJ, Park IK, Park M-S, Choi HJ, Cho BC, Chung KY, et al. Activating mutations within the EGFR kinase domain: a molecular predictor of disease-free survival in resected pulmonary adenocarcinoma. *J Cancer Res Clin Oncol* 2009; **135:** 1647-54.
22. Porta R, Sánchez-Torres JM, Paz-Ares L, Massutí B, Reguart N, Mayo C, et al. Brain metastases from lung cancer responding to erlotinib: the importance of EGFR mutation. *Eur Respir J* 2011; **37:** 624-31.
23. Na II, Park JH, Choe DH, Lee JK, Koh JS. Association of epidermal growth factor receptor mutations with metastatic presentations in non-small cell lung cancer. *ISRN Oncol* 2011; **2011:** 756265.
24. Saad AG, Yeap BY, Thunnissen FBJM, Pinkus GS, Pinkus JL, Loda M, et al. Immunohistochemical markers associated with brain metastases in patients with nonsmall cell lung carcinoma. *Cancer* 2008; **113:** 2129-38.
25. *Cancer in Slovenia 2010*. Ljubljana: Institute of Oncology Ljubljana, Epidemiology and Cancer Registry, Cancer Registry of Republic of Slovenia; 2013.
26. Eichler AF, Kahle KT, Wang DL, Joshi VA, Willers H, Engelman JA, et al. EGFR mutation status and survival after diagnosis of brain metastasis in nonsmall cell lung cancer. *Neuro Oncol* 2010; **12:** 1193-9.
27. Heon S, Yeap BY, Britt GJ, Costa DB, Rabin MS, Jackman DM, et al. Development of central nervous system metastases in patients with advanced non-small cell lung cancer and somatic EGFR mutations treated with gefitinib or erlotinib. *Clin Cancer Res* 2010; **16:** 5873-82.
28. Lee HL, Chung TS, Ting LL, Tsai JT, Chen SW, Chiou JF, et al. EGFR mutations are associated with favorable intracranial response and progression-free survival following brain irradiation in non-small cell lung cancer patients with brain metastases. *Radiat Oncol* 2012; **7:** 181.
29. Hsiao SH. Impact of epidermal growth factor receptor mutations on intracranial treatment response and survival after brain metastases in lung adenocarcinoma patients. *Lung Cancer* 2013; **81:** 455-61.
30. Komatsu T, Kunieda E, Oizumi Y, Tamai Y, Akiba T. Clinical characteristics of brain metastases from lung cancer according to histological type: Pretreatment evaluation and survival following whole-brain radiotherapy. *Mol Clin Oncol* 2011; **1:** 692-8.
31. Gow C-H, Chien C-R, Chang Y-L, Chiu Y-H, Kuo S-H, Shih J-Y, et al. Radiotherapy in lung adenocarcinoma with brain metastases: effects of activating epidermal growth factor receptor mutations on clinical response. *Clin Cancer Res* 2008; **14:** 162-8.
32. Ceresoli GL. Role of EGFR inhibitors in the treatment of central nervous system metastases from non-small cell lung cancer. *Curr Cancer Drug Targets* 2012; **12:** 237-46.
33. Das AK, Sato M, Story MD, Peyton M, Graves R, Redpath S, et al. Non-small-cell lung cancers with kinase domain mutations in the epidermal growth factor receptor are sensitive to ionizing radiation. *Cancer Res* 2006; **66:** 9601-8.
34. Liang K, Ang KK, Milas L, Hunter N, Fan Z. The epidermal growth factor receptor mediates radioresistance. *Int J Radiat Oncol* 2003; **57:** 246-54.
35. Tanaka T, Munshi A, Brooks C, Liu J, Hobbs ML, Meyn RE. Gefitinib radiosensitizes non-small cell lung cancer cells by suppressing cellular DNA repair capacity. *Clin Cancer Res* 2008; **14:** 1266-73.
36. Lind J, Lagerwaard F, Smit E, Senan S. Phase I Study of Concurrent Whole Brain Radiotherapy and Erlotinib for Multiple Brain Metastases From Non-Small-Cell Lung Cancer. *Int J Radiat Oncol Biol Phys* 2009; **74:** 1391-6.

37. Welsh JW, Komaki R, Amini A, Munsell MF, Unger W, Allen PK, et al. Phase II trial of erlotinib plus concurrent whole-brain radiation therapy for patients with brain metastases from non-small-cell lung cancer. *J Clin Oncol* 2013; **31:** 895-902.

38. Ma S, Xu Y, Deng Q, Yu X. Treatment of brain metastasis from non-small cell lung cancer with whole brain radiotherapy and Gefitinib in a Chinese population. *Lung Cancer* 2009; **65:** 198-203.

39. Olmez I, Donahue BR, Butler JS, Huang Y, Rubin P XY. Clinical outcomes in extracranial tumor sites and unusual toxicities with concurrent whole brain radiation (WBRT) and Erlotinib treatment in patients with non-small cell lung cancer (NSCLC) with brain metastasis. *Lung cancer* 2010; **70:** 174-9.

40. Zhuang H, Yuan Z, Wang J, Zhao L, Pang Q, Wang P. Phase II study of whole brain radiotherapy with or without erlotinib in patients with multiple brain metastases from lung adenocarcinoma. *Drug Des Devel Ther* 2013; **7:** 179-86.

41. Togashi Y, Masago K, Fukudo M, Tsuchido Y, Okuda C, Kim YH, et al. Efficacy of increased-dose erlotinib for central nervous system metastases in non-small cell lung cancer patients with epidermal growth factor receptor mutation. *Cancer Chemother Pharmacol* 2011; **68:** 1089-92.

42. Grommes C, Oxnard GR, Kris MG, Miller VA, Pao W, Holodny AI, et al. "Pulsatile" high-dose weekly erlotinib for CNS metastases from EGFR mutant non-small cell lung cancer. *Neuro Oncol* 2011; **13:** 1364-9.

43. Kim ST, Uhm JE, Lee J, Sun J, Sohn I, Kim SW, et al. Randomized phase II study of gefitinib versus erlotinib in patients with advanced non-small cell lung cancer who failed previous chemotherapy. *Lung Cancer* 2012; **75:** 82-8.

44. Shimato S, Mitsudomi T, Kosaka T, Yatabe Y, Wakabayashi T, Mizuno M, et al. EGFR mutations in patients with brain metastases from lung cancer: association with the efficacy of gefitinib. *Neuro Oncol* 2006; **8:** 137-44.

45. Tang W-H, Chen J-H, Ye R-H, Ho C-L. Near Total Regression of Diffuse Brain Metastases in Adenocarcinoma of the Lung with an EGFR Exon 19 Mutation: A Case Report and Review of the Literature. *Case Rep Oncol* 2011; **4:** 445-51.

46. Heon S, Yeap BY, Lindeman NI, Rabin MS, Jackman DJ, Johnson BE. Rates of central nervous system (CNS) metastases in patients with advanced non-small cell lung cancer (NSCLC) and somatic EGFR mutations initially treated with gefitinib or erlotinib versus chemotherapy. *J Clin Oncol* 2011; **29(Suppl 15):** A7607.

47. Ceresoli GL, Cappuzzo F, Gregorc V, Bartolini S, Crinò L, Villa E. Gefitinib in patients with brain metastases from non-small-cell lung cancer: a prospective trial. *Ann Oncol* 2004; **15:** 1042-7.

48. Lee YJ, Choi HJ, Kim SK, Chang J, Moon JW, Park IK, et al. Frequent central nervous system failure after clinical benefit with epidermal growth factor receptor tyrosine kinase inhibitors in Korean patients with nonsmall-cell lung cancer. *Cancer* 2010; **116:** 1336-43.

49. Stuschke BM, Eberhardt W, Po C, Stamatis G, Wilke H, Stu G, et al. Prophylactic cranial irradiation in locally advanced Non Small Cell Lung Cancer after multimodality treatment: Long term follow up and investigation of late neuropsychological effects. *J Clin Oncol* 1999; **17:** 2700-9.

50. Lester JF, MacBeth FR, Coles B. Prophylactic cranial irradiation for preventing brain metastases in patients undergoing radical treatment for non-small-cell lung cancer: a Cochrane Review. *Int J Radiat Oncol Biol Phys* 2005; **63:** 690-4.

51. Topkan E, Yildrim BA, Selek U YM. Cranial Prophylactic Irradiation in Locally Advanced Non-Small Cell Lung Carcinoma: Current Status and Future Perspectives. *Oncology* 2009; **76:** 220-8.

52. Dimitropoulos C, Hillas G, Nikolakopoulou S, Kostara I, Sagris K, Vlastos F, et al. Prophylactic cranial irradiation in non-small cell lung cancer patients: who might be the candidates? *Cancer Manag Res* 2011; **3:** 287-94.

53. Tufman A, Belka C, Kuenel H, Huber RM. Prophylactic cranial irradiation after reaching complete response, partial response, or stable disease in non-small cell lung cancer patients treated with epidermal growth factor receptor tyrosine kinase inhibitors (ProACT). *J Clin Oncol* 2012; **30:** TPS7617.

case report

Long-term remission of a Her2/neu positive primary breast cancer under double monoclonal antibody therapy with trastuzumab and bevacizumab

Robert Königsberg[1,2], Julia Maierhofer[1], Tanja Steininger[1,2], Gabriele Kienzer[1,3], Christian Dittrich[1,2]

[1] Ludwig Boltzmann Institute for Applied Cancer Research (LBI-ACR VIEnna) – LB Cluster Translational Oncology, 3rd Medical Department – Centre for Oncology and Haematology, Kaiser Franz Josef-Spital, Vienna, Austria

[2] Applied Cancer Research – Institution for Translational Research Vienna (ACR –ITR VIEnna), Vienna, Austria

[3] Institute for Radiodiagnostics, Kaiser Franz Josef-Spital, Vienna, Austria

Radiol Oncol 2014; 48(2): 184-188.

Received 27 August 2013
Accepted 18 November 2013

Correspondence to: Robert Königsberg, M.D., ACR-ITR VIEnna, Bernardgasse 24/2, A-1070 Vienna Austria. Phone: +43 699 1 4567827; Fax: +43 1 52335944; Email: robert.koenigsberg@gmx.at

Disclosure: No potential conflicts of interest were disclosed.

Background. The attempt to act on several signalling pathways involved in tumour development simultaneously appears to be more attractive than attacking a single target structure alone. Vascular endothelial growth factor (VEGF) over-expression is frequently observed in human epidermal growth factor receptor 2 (Her2/neu) positive patients with breast cancer and over-expression of the proto-oncogene Her2/neu is associated with an up-regulation of VEGF.

Case report. The case of a Her2/neu positive patient with breast cancer who refused cytotoxic chemotherapy with its potential side effects as well as mastectomy is presented. Our patient has been receiving the combined double administration of bevacizumab and trastuzumab for more than 4 years.

Conclusions. This case report shows that (a) the combined double administration of bevacizumab and trastuzumab was be clinically effective. (b) The combination of bevacizumab and trastuzumab is safe and non-toxic. (c) Bevacizumab and trastuzumab can be used as a long-term application.

Key words: breast cancer; Her2/neu; trastuzumab; bevacizumab; VEGF

Introduction

Vascular endothelial growth factor (VEGF) over-expression is frequently observed in human epidermal growth factor receptor 2 (Her2/neu) positive patients with breast cancer. Over-expression of the proto-oncogene Her2/neu is associated with an up-regulation of VEGF. There is, therefore, a biological rationale for targeting both Her2/neu and VEGF pathways in patients with Her2/neu positive breast cancer. We present the case of a postmenopausal patient with Her2/neu positive breast cancer, who received the combined administration of bevacizumab and trastuzumab over a long period of time.

A 58-year-old woman with a newly diagnosed cancer of the right breast was referred to our department for antineoplastic therapy. In order to better understand and justify our further management, the reader has to know that the patient had a history of a psychiatric disorder with long-standing delusional symptoms. She had discontinued antipsychotic drugs because of subjectively perceived worsening. Overall, the patient is socially well integrated. Other known co-morbidities were chronic impairment of renal function after nephrectomy following pyelo-nephritis and diabetes mellitus type II. The first low quality mammography was performed at the outpatient setting, showed two

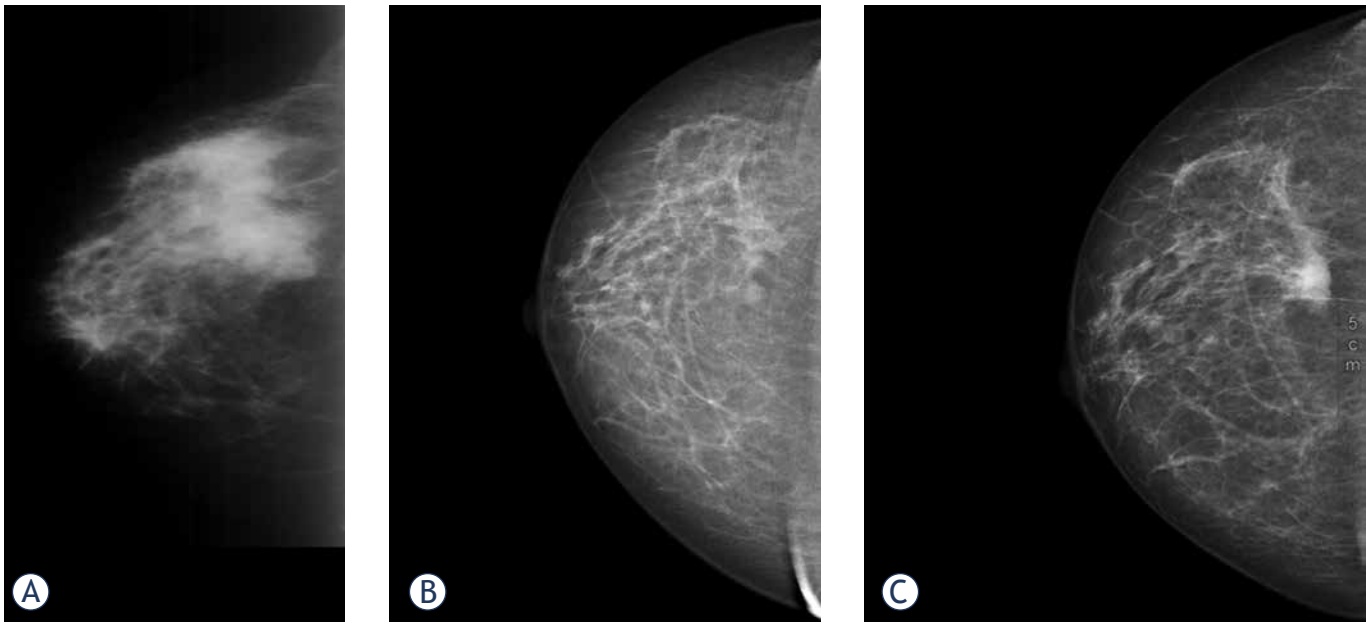

FIGURE 1. A. Low quality mammography showing a polycyclic lesion in the laterocranial quadrant with a diameter of 35 mm and a second lesion with a diameter of 20 mm in the centrocaudal quadrant. **B.** Mammography performed after 25 cycles of trastuzumab and bevacizumab. The former polycyclic lesion in the laterocranial quadrant now has a diameter of 4 mm. The second lesion in the cetntrocaudal quadrant is no more traceable. **C.** Mammography performed after 74 cycles of trastuzumab and bevacizumab. The lesion in the laterocranial quadrant progressed, measuring 20 mm in diameter.

masses in the right breast, one lesion with a diameter of 35 mm and one of 20 mm (Figure 1A). During the diagnostic evaluation process, the patient refused to repeat the mammography. Biopsy revealed a multi-centric, invasive ductal, grade 2 carcinoma with lymphangiosis. Oestrogen receptor status (ER-ICA: SI 3, PP 4 (90%) IRS 12) and Her2/neu receptor status (DAKO lot 30586: 3+) were highly positive, progesterone receptor status was completely negative (PR-ICA: SI 0, PP 0, IRS 0), respectively. Thirty percent of tumor cells had a positive Ki-67 index.

The proposed classical preoperative cytotoxic chemotherapy with its potential side effects as well as mastectomy and axillary lymph node dissection were not reconcilable with the integrity of a female body image, and thus were categorically refused by the patient. Our therapeutic approach therefore focused on the immune-histochemistry data of the Her2/neu positivity and the use of new targeted, non-cytotoxic drugs. As a result, the patient was offered customized, albeit experimental treatment with the humanized monoclonal antibody trastuzumab (Herceptin®) combined with the humanized monoclonal antibody bevacizumab (Avastin®).

Therapy was initiated according to Table 1 and repeated on a three weekly base. For the first four cycles of combined antibody therapy the initial bevacizumab dosage of 10 mg/kg of body weight (BW) was chosen because the patient refused to accept the internationally recommended dosage of 15 mg/kg.

After the fourth cycle, a good partial response was documented by mammography. The second lesion with a diameter of 2 cm was and would be no more traceable throughout the forthcoming mammographies. After 25 cycles of double antibody therapy a further reduction of the tumor mass was observed (Figure 1B). As the patient did not cease refusing surgery categorically, the original treatment was consistently continued. After 8 months of treatment, the bevacizumab dosage was reduced to 7.5 mg/kg due to the patient´s request. After 51 cycles of combined antibody therapy the patient agreed to receive 15 mg/kg of bevacizumab, according to the recommendation for breast cancer treatment, because mammography presented a suspicious enlargement. The mammography performed after 48 months of therapy, confirmed the persistence of a partial remission compared to the initial outpatient mammography. Four years after diagnosis the patient was free of symptoms related to her malignant disease or the respective treatment which let us maintain therapy unchanged. However, after 74 cycles of combined antineoplastic therapy progression of the lesion was documented by mammography (Figure 1C).

TABLE 1. Antineoplastic treatment plan of a patient with estrogen - and Her2/neu receptor positive breast cancer

cycle	week	trastuzumab	bevacizumab	tumor size
1	0	8 mg/kg	-	35 mm
2	3	6 mg/kg	10 mg/kg	
4	9	6 mg/kg	10 mg/kg	10 mm
...	...	...	...	
11	30	6 mg/kg	7.5 mg/kg	
...	...	...	...	
25	75	6 mg/kg	7.5 mg/kg	4 mm
...	...	...	...	
51	151	6 mg/kg	15 mg/kg	12 mm
...	...	...	...	
74	222	6 mg/kg	15 mg/kg	20 mm

Monitoring of potential cardiac abnormalities, including echocardiography and measuring of NT-proBNP levels, have been done repeatedly. Newly diagnosed hypertension was well controlled by ACE inhibitors.

Discussion

VEGF is a well-established key-factor inducing angiogenesis leading to tumour growth and metastasis.[1,2] There exists a significant correlation between tumour microvessel density in breast cancer, the presence of axillary lymph node and distant metastases, respectively.[3] VEGF over-expression is frequently observed in Her2/*neu* positive patients with breast cancer.[4,5] Via multiple intracellular pathways VEGF and Her2/*neu* act at various stages of breast cancer development.[6] Over-expression of the proto-oncogene Her2/*neu* is associated with an up-regulation of VEGF *in vitro* and *in vivo*.[8-9] Transfection of Her2/*neu* over-expression resulted in a rise of VEGF on RNA as well as on protein levels.[8-9] *In vitro* VEGF was reduced by exposure to Her2/neu antibodies such as trastuzumab, especially in cells with Her2/neu over-expression.[7,9,10] Considering VEGF as a possible downstream effector of Her2/*neu*, which might contribute to the more aggressive phenotype of Her2/neu over-expressing breast cancer cells, Konecny *et al*., showed a significant association of Her2/neu over-expression and VEGF up-regulation based on tissue samples of 611 unselected breast cancer patients.[11] In this study, VEGF expression was negatively correlated with survival. These results were concordant with the results of Linderholm *et al*., thus prompting to a re-evaluation of combined treatment strategies targeting both Her2/neu and VEGF.[12] On the other hand a paper recently published by Liu *et al.* showed that in Her2/*neu* positive breast cancer patients VEGF over-expression was not significantly correlated with breast cancer-specific mortality, distant recurrence or overall mortality, respectively.[5] These conflicting retrospective results regarding the possible prognostic and predictive value of VEGF over-expression are demanding prospective clinical studies evaluating the benefit of adding bevacizumab to trastuzumab in patients with Her2/neu positive breast cancer.

So far, in a clinical phase I trial, 9 patients were subjected to combination treatment with bevacizumab, 3.0, 5.0 or 10.0 mg/kg BW, respectively, at intervals of 14 days, and trastuzumab at a loading dose of 4 mg/kg BW, followed by 2 mg/kg BW once a week until progression.[13] Grade 3 and 4 side effects were absent throughout. Grade 1 and 2 side effects consisted of diarrhoea, fatigue and nausea. In addition, one patient developed grade 2 allergic reactions, another one grade 2 hypertension and yet another one grade 2 proteinuria. Left ventricular function did not deteriorate. Bevacizumab combined with trastuzumab was well tolerated. After 6 cycles complete remission was recorded in one, partial remission in 4, stable disease in 2 and disease progression in 2 patients, respectively. Pharmacokinetic studies showed that the administration of the two drugs on the same day did not alter the pharmacokinetic patterns of either drug. According to this study, the dosage recommended for the phase II trials was 10 mg/kg BW every 14

days for bevacizumab and 4 mg/kg BW for loading followed by 2 mg/kg BW once a week for trastuzumab. In this study, one patient had progressed on prior chemotherapy and trastuzumab. Five of 9 patients improved clinically. These data argue in favour of combining anti-Her2/neu and anti-VEGF treatment in patients with Her2/neu-positive breast cancer.

In the very first phase II trial with a combination of these humanized antibodies in breast cancer[14], the clinical efficacy of combination treatment with trastuzumab and bevacizumab as well as safety and toxicity were evaluated. Patients were initially given trastuzumab at a loading dose of 4 mg/kg BW and bevacizumab at a dose of 10 mg/kg BW on day 7. In the further course, trastuzumab was given at a dose of 2 mg/kg BW once weekly combined with bevacizumab, 20 mg/kg BW, at intervals of 2 weeks. Interim analysis of 37 patients treated accordingly showed complete remission in one patient, partial remission in 19 patients, stable disease in 11 and disease progression in 6 patients.

One multicenter phase III trial initiated by the NSABP (BETH Study) will determine the value of adding bevacizumab to chemotherapy plus trastuzumab in patients with resected node-positive or high risk node-negative, Her2/neu-positive breast cance.[15]

To make the regimen more convenient to our patient, we chose a three weekly cycle. This is justifiable nonetheless since bevacizumab displays linear pharmacokinetics, yielding similar exposure with flexible dosage regimens administered on a mg/kg basis such as bi- or three-weekly dosing.[16] Pharmaco-dynamic information collected during clinical trials in phase I to III studies of bevacizumab showed that under treatment with bevacizumab at different dosages, *e.g.* at a dose of 2.5 mg/kg per week in colorectal cancer and at 5.0 mg/kg per week in breast cancer circulating VEGF levels were un-measurable.[17,18]

The initial intention to augment the dosage of bevacizumab to 15 mg/kg three weekly was finally reached because the patient could be convinced that the internationally recommended dosage of bevacizumab might suspend further tumor growth. Due to our patient´s request, she received initially 10 mg/kg bevacizumab. The dosage was reduced after 11 cycles to 7.5 mg/kg. But even with the lower dosage of bevacizumab further reduction of the tumor mass was observed. This observation might support the effectiveness of lower dosages of bevacizumab which is in line with previously published pharmaco-dynamic studies. On the other hand lowering the dosage of bevacizumab with no detrimental effect on the tumor size might indirectly indicate that the addition of bevacizumab to trastuzumab had little or no benefit which would be in line with some comparable phase III studies in metastatic breast cancer. However, the benefit of trastuzumab in Her2/neu positive breast cancer is indisputable. As a single agent in first-line treatment of Her2/neu positive metastatic breast cancer trastuzumab yielded objective response rate up to 26%.[19] Another phase III study (ECOG 1105) currently evaluates this issue studying first-line chemotherapy and trastuzumab to compare how well they work when given with or without bevacizumab in treating patients with metastatic breast cancer that over-expresses Her2/neu.[20]

Currently, the combination of trastuzumab and bevacizumab in the first line treatment of HER2/neu positive breast cancer is not justified since there are other anti-HER2 drug combinations that have shown more striking results at least in the metastatic setting.[21,22]

Conclusions

The attempt to act on several signalling pathways involved in tumor development simultaneously appears to be more attractive than attacking a single target structure alone. The combined double administration of bevacizumab and trastuzumab is easily handled, and represents a safe and non-toxic regimen allowing long-term application in patients with Her2/neu-positive recurrent, metastasizing as well as primary breast cancer. Targeting both Her2/neu and VEGF pathways was effective in our case for a long period of time although we can not say to what extent the benefit is attributed to the addition of bevacizumab and to what extent to trastuzumab solely.

References

1. Hicklin DJ, Ellis LM. Role of the vascular endothelial growth factor pathway in tumor growth and angiogenesis. *J Clin Oncol* 2005; **23:** 1011-27.
2. Rozman A, Silar M, Kosnik M. Angiogenin and vascular endothelial growth factor expression in lungs of lung cancer patients. *Radiol Oncol* 2012; **46:** 354-9.
3. Weidner N, Semple JP, Welch WR, Folkman J. Tumor angiogenesis and metastasis--correlation in invasive breast carcinoma. *N Engl J Med* 1991; **324:** 1-8.
4. Linderholm B, Bergqvist J, Hellborg H, Johansson U, Linderholm M, von Schoultz E, et al. Shorter survival-times following adjuvant endocrine therapy in oestrogen- and progesterone-receptor positive breast cancer overexpressing HER2 and/or with an increased expression of vascular endothelial growth factor. *Med Oncol* 2009; **26:** 480-90.

5. Liu Y, Tamimi RM, Collins LC, Schnitt SJ, Gilmore HL, Connolly JL, et al. The association between vascular endothelial growth factor expression in invasive breast cancer and survival varies with intrinsic subtypes and use of adjuvant systemic therapy: results from the Nurses' Health Study. *Breast Cancer Res Treat* 2011; **129:** 175-84.

6. Matos M, Zakotnik B, Grasic Kuhar C. Effectiveness of adjuvant transtuzmab in daily clinical practice. *Radiol Oncol* 2013; Ahead of print; doi:10.2478/raon-2013-008. Available from: http://www.degruyter.com/view/j/raon.ahead-of-print/raon-2013-0081/raon-2013-0081.xml?format=INT

7. Petit AM, Rak J, Hung MC, Rockwell P, Goldstein N, Fendly B, et al. Neutralizing antibodies against epidermal growth factor and ErbB-2/neu receptor tyrosine kinases down-regulate vascular endothelial growth factor production by tumor cells in vitro and in vivo: angiogenic implications for signal transduction therapy of solid tumors. *Am J Pathol* 1997; **151:** 1523-30.

8. Yen L, You XL, Al Moustafa AE, Batist G, Hynes NE, Mader S, et al. Heregulin selectively upregulates vascular endothelial growth factor secretion in cancer cells and stimulates angiogenesis. *Oncogene* 2000; **19:** 3460-9.

9. Epstein M, Ayala R, Tchekmedyian N, Borgstrom P, Pegram M, Slamon D. HER-2/neu-overexpressing human breast cancer xenografts exhibit increased angiogenic potential mediated by vascular endothelialgrowthfactor(VEGF). [Abstract]. *Breast Cancer Res Treat 2002*; **76(Suppl 1):** S143.

10. Izumi Y, Xu L, di Tomaso E, Fukumura D, Jain RK. Tumour biology: herceptin acts as an anti-angiogenic cocktail. *Nature 2002*; **416:** 279-80.

11. Konecny GE, Meng YG, Untch M, Wang HJ, Bauerfeind I, Epstein M, et al. Association between HER-2/neu and vascular endothelial growth factor expression predicts clinical outcome in primary breast cancer patients. *Clin Cancer Res* 2004; **10:** 1706-16.

12. Linderholm B, Andersson J, Lindh B, Beckman L, Erlanson M, Edin K, et al. Overexpression of c-erbB-2 is related to a higherexpression of vascular endothelial growth factor (VEGF) and constitutes anindependent prognostic factor in primary node-positive breast cancer afteradjuvant systemic treatment. *Eur J Cancer* 2004; **40:** 33-42.

13. Pegram M, Yeon C, Ku N, Gaudreault J, Slamon DJ. Phase I combined biological therapy of breast cancer using two humanized monoclonal antibodies directed against HER2 proto-oncogene and vascular endothelial growth factor (VEGF). [Abstract]. *Breast Cancer Res Treat* 2004; **88(Suppl 1):** S124-5.

14. Pegram M, Chan D, Dichmann R, Tar-Chin E, Yeon C, Duran L, et al. Phase II combined biological therapy targeting the HER2 proto-oncogene and the vascular endothelial growth factor using trastuzumab (T) and bevacizumab (B) as first line therapy of HER2 amplified breast cancer. *Breast Cancer Res Trea*t 2006; **100(Suppl 1):** S28-9.

15. BETH Study: Treatment of HER2 positive breast cancer with chemotherapy plus trastuzumab vs chemotherapy plus trastuzumab plus bevacizumab. Available at http://clinicaltrials.gov/ct2/show/NCT00625898?term=BETH&rank=1

16. Lu JF, Bruno R, Eppler S, Novotny W, Lum B, Gaudreault J. Clinical pharmacokinetics of bevacizumab in patients with solid tumors. *Cancer Chemother Pharmacol* 2008; **62:** 779-86.

17. Kabbinavar F, Hurwitz HI, Fehrenbacher L, Meropol NJ, Novotny WF, Lieberman G, et al. Phase II, randomized trial comparing bevacizumab plus fluorouracil (FU)/leucovorin (LV) with FU/LV alone in patients with metastatic colorectal cancer. *J Clin Oncol* 2003; **21:** 60-5.

18. Giantonio BJ, Catalano PJ, Meropol NJ, O'Dwyer PJ, Mitchell EP, Alberts SR, et al. Bevacizumab in combination with oxaliplatin, fluorouracil, and leucovorin (FOLFOX4) for previously treated metastatic colorectal cancer: results from the Eastern Cooperative Oncology Group Study E3200. *J Clin Oncol* 2007; **25:** 1539-44.

19. Gianni L, Romieu GH, Lichinitser M, Serrano SV, Mansutti M, Pivot X et al. AVEREL: a randomized phase III Trial evaluating bevacizumab in combination with docetaxel and trastuzumab as first-line therapy for HER2-positive locally recurrent/metastatic breast cancer. *J Clin Oncol.* 2013; **10:** 1719-25.

20. ECOG 1105: First-line chemotherapy and trastuzumab with or without bevacizumab in treating patients with metastatic breast cancer that overexpresses HER-2/NEU. Available at: http://clinicaltrials.gov/ct2/results?term=ECOG+1105&Search=Search

21. Baselga J, Cortés J, Kim SB, Im SA, Hegg R, Im YH, et al. CLEOPATRA Study Group. Pertuzumab plus trastuzumab plus docetaxel for metastatic breast cancer. *N Engl J Med*. 2012; **366:** 109-19.

22. Verma S, Miles D, Gianni L, Krop IE, Welslau M, Baselga J, et al. EMILIA Study Group. Trastuzumab emtansine for HER2-positive advanced breast cancer. *N Engl J Med.* 2012; **367:** 1783-91.

research article

Capecitabine in adjuvant radiochemotherapy for gastric adenocarcinoma

Irena Oblak, Marija Skoblar Vidmar, Franc Anderluh, Vaneja Velenik, Ana Jeromen, Jasna But Hadzic

Department of Radiotherapy, Institute of Oncology Ljubljana, Ljubljana, Slovenia

Radiol Oncol 2014; 48(2): 189-196.

Received 28 June 2013
Accepted 13 August 2013

Correspondence to: Assist. Prof. Irena Oblak, M.D., Ph.D., Institute of Oncology Ljubljana, Zaloška 2, SI-1000 Ljubljana, Slovenia. Phone: +386 1 5879 661; Fax: +386 1 5879 304; E-mail: ioblak@onko-i.si

Disclosure: No potential conflicts of interest were disclosed.

Background. In patients with non-metastatic gastric cancer surgery still remains the treatment of choice. Postoperative radiochemotherapy with 5-fluorouracil and leucovorin significantly improves the treatment outcome. The oral fluoropyrimidines, such as capecitabine, mimic continuous 5-fluorouracil infusion, are at least as effective as 5-fluorouracil, and such treatment is more comfortable for the patients.

Patients and methods. In the period from October 2006 to December 2009, 101 patients with gastric cancer in stages Ib–IIIc were treated with postoperative chemoradiation with capecitabine. Distal subtotal resection of the stomach was performed in 46.3%, total resection in 50.5% and multivisceral resection in 3.2% of patients. The main endpoints of this study were loco-regional control (LRC), disease-free survival (DFS), disease-specific survival (DSS) and overall survival (OS). The rates of acute side-effects were also estimated.

Results. Seventy-seven percent of patients completed the treatment according to the protocol. The median follow-up time of all patients was 3.9 years (range: 0.4-6.3 years) and in survivors it was 4.7 years (range: 3.2-6.3 years). No death occurred due to the therapy. Acute toxicity, such as nausea and vomiting, stomatitis, diarrhoea, hand-foot syndrome and infections of grade 3 or 4, occurred in 5%, 1%, 2%, 8.9% and 18.8% of patients, respectively. On the close-out date 63.4% patients were still alive and with no signs of the disease. The 4-years follow-up survey showed that LRC, DFS, DSS and OS were 95.5%, 69.2%, 70.7%, and 66.2%, respectively. Higher pN-stage and splenectomy were found to be independent prognostic factors for all four types of survival and perineural invasion and lower treatment intensity for DFS, DSS and OS.

Conclusions. Postoperative radiochemotherapy with capecitabine is feasible, with low toxicity and the results of such treatment are good.

Key words: gastric cancer; capecitabine; adjuvant therapy; radiochemotherapy; survival; toxicity

Introduction

Although the incidence of gastric cancer has declined in recent years it is still one of the most common causes of cancer death.[1,2] Complete removal of tumour masses with regional lymph nodes (so called R0 surgical resection) represents the treatment of choice in patients with non-metastatic gastric cancer.[2] The standard recommendations for lymphadenectomy are at least D1 resection and the removal of a minimum of 15 lymph nodes.[3,4] Although the R0 surgical resection is performed, patients' survival remain unsatisfactory. During the past few decades, the principle of combined modality treatment has been developed and applied in practice for various solid tumours with gastric cancer not being an exception. One of the landmark studies in adjuvant trials was the Intergroup Study INT-0116, in which a significant improvement in survival with the use of 5-fluorouracil (5-FU) based radiochemotherapy after surgery was reported.[5] After this study radiochemotherapy was established as routine adjuvant treatment in the USA, as well as in several European countries. In

TABLE 1. Pathohistologic characteristics of tumours

Characteristic		No. of patients	%
pT – stage	1a	1	1
	1b	5	5
	2	48	47.5
	3	40	39.5
	4a	2	2
	4b	5	5
pN – stage	0	21	20.8
	1	22	21.8
	2	27	26.7
	3a	18	17.8
	3b	13	12.9
Overall stage	Ib	14	13.9
	IIa	22	21.8
	IIb	20	19.8
	IIIa	25	24.7
	IIIb	17	16.8
	IIIc	3	3
Pathohistological tumour grade	1	5	5
	2	29	28.7
	3	65	64.3
	unknown	2	2
Borrman type	1	0	0
	2	11	10.9
	3	30	29.7
	4	17	16.8
	unknown	43	42.6
Growth type according to Lauren	diffuse	28	27.7
	intestinal	45	44.6
	mixed	19	18.8
	unknown	9	8.9
Perineural invasion	yes	49	48.5
	no	36	35.7
	unknown	16	15.8
Lymphovascular invasion	yes	48	47.6
	no	16	15.8
	unknown	37	36.6
Angioinvasion	yes	21	20.8
	no	52	51.5
	unknown	28	27.7
HP	yes	9	8.9
	No	44	43.6
	unknown	48	47.5

pT = pathological T-stage; pN = pathological N-stage; HP = Helicobacter pylori infection

the Institute of Oncology Ljubljana, the program of combined postoperative treatment of non-metastatic gastric carcinoma with radiochemotherapy was introduced into clinical practice in 2001. The results of that regimen were analysed and presented.[6,7]

It is well known that capecitabine is an oral 5-FU prodrug and we assume that it can replace standard chemotherapy. It has been proven that capecitabine mimics continuous 5-FU infusion[8,9] and is at least as effective as 5-FU10,11, but with less side effects.[9] In addition, treatment with the oral fluoropyrimidines, such as capecitabine, is more comfortable for patients because these drugs can be taken at home, without any invasive procedures (such as application of parenteral infusion of chemotherapy). We speculate that radio sensibilisation with capecitabine could be more effective than with 5-FU, because 5-FU is given only on the first four and last three days of radiotherapy, whereas capecitabine is given through the whole course of the radiotherapy. The aim of this study was to evaluate the efficacy and toxicity of adjuvant radiochemotherapy with capecitabine.

Patients and methods

Patients

In the period from October 2006 to December 2009, 101 patients (66 males and 35 females, aged 26-78 years, mean age 58.9 years) were treated for non-metastatic adenocarcinoma of non-cardial gastric cancer with postoperative concomitant chemoradiation with capecitabine at the Institute of Oncology, Ljubljana, Slovenia. All patients had locally and/or regionally advanced disease without distant metastases (stages Ib–IIIc).[12] Before the start of the treatment 62 (61.4%) patients suffered from epigastrial pain and 25 (24.8%) patients complained of early satiety. Anaemia was found in 28 (27.7%) patients, melena in 17 (16.8%) patients and weight loss in 57 (56.4%) patients.

Surgical treatment

Of the 101 patients, 83 (82.1%) were operated on in two major surgical centres in Slovenia (at the University Medical Centre Ljubljana or Maribor) and the remaining 18 (17.1%) patients in one of five Slovenian regional hospitals. Distal subtotal resection of the stomach was performed in 47 (46.5%) patients, total resection of the stomach in 51 (50.5%) patients and multivisceral resection in three (3%) patients, respectively. Radical resection (R0) of the

stomach was performed in 97 (96%) patients and the remaining four (4%) patients underwent non-radical surgery (R1) with no possibility of reoperation. At least 15 lymph nodes were removed and histologically examined in 70 (69.3%) patients and less than 15 lymph nodes were examined in 31 (30.7%) patients.

Tumour characteristics

Primary tumours originated in the antrum in 49 (48.5%) patients, in the corpus in 38 (37.6%) patients, in the lesser curvature in 10 (9.9%) and in the greater curvature in four (4%) patients. In 47 (46.5%) patients, the tumour was staged as pT3 or pT4, and 80 (79.2%) patients had N+ disease. Sixty-five (64.4%) tumours were poorly differentiated (G3) (Table 1).

Investigations before and during therapy

After surgery, all patients with the disease in pathological stage Ib or more were presented to a multidisciplinary advisory team, consisting of a surgeon, radiation oncologist and medical oncologist, in order to assess the prospects of eventual adjuvant treatment. Patients had to fulfil the following criteria: histologically confirmed adenocarcionoma of the stomach, cancer removed with R0 or R1 resection, age greater than 18 and below 80 years, a performance status of 1 or lower according to the World Health Organization (WHO), adequate function of major organs (including cardiac, bone marrow, renal and hepatic function), no difficulty in swallowing tablets and adequate collaboration during treatment. All patients underwent a general clinical examination and blood counts. The investigations, such as X-ray, ultrasound (US), and/or computer tomography (CT) of the thorax or abdomen, performed before surgery to rule out metastatic disease, were repeated only in the patients in whom the progression of the disease was clinically suspected. During the therapy, the patients were clinically examined and referred to haematology and biochemistry blood tests once a week. The therapy-related local and systemic toxicity was assessed according to the National Cancer Institute Common Toxicity Criteria (NCI-CTC) version 2.0.[13] The performance status of patients was determined and their body weight was measured on a weekly basis.

Postoperative radiochemotherapy

Adjuvant treatment was initiated within 6-8 weeks after surgery and consisted of concomitantly applied chemo- and radiotherapy. Chemotherapy started with peroral capecitabine 1250 mg/m^2 twice daily (bid) on days 1-14, with a one week break. Concurrently with irradiation, continuous capecitabine 825 mg/m^2 bid was administered, without weekend breaks. After the completion of radiotherapy with two weeks break, the patients received three more cycles of capecitabine 1250 mg/m^2 bid on days 1-14, with a one week break between each cycle.

Patients were irradiated on linear accelerator with 15 MV photon beams for five days per week, at a daily dose of 1.8 Gy. Radiotherapy planning was performed using simulator with CT option and 3-D treatment planning computer software. The total irradiation dose was 45 Gy delivered in five weeks. The clinical target volume (CTV) was defined using preoperative CT, endoscopic findings, surgical clips and findings during operation. In CTV tumour bed, anastomosis site, duodenal stump, remnant stomach and regional lymph nodes were enclosed, and it extended 2.5 cm beyond the proximal and distal margins of resection. The irradiation dose was specified according to the International Commission on Radiation Units (ICRU) recommendations.

In case of severe therapy-related toxicity, irradiation and/or chemotherapy doses were modified and adapted to the patient's physical condition or laboratory tests. When necessary, chemotherapy application was delayed or radiotherapy was temporarily interrupted or terminated.

Statistics

Statistical analysis was performed using personal computer and software statistical package SPSS, version 15 (SPSS Inc., USA). The main endpoints of this study were as follows: locoregional control (LRC; the event was local and/or regional recurrence), disease-free survival (DFS; the event was local, regional or systemic recurrence), disease-specific survival (DSS; the event was death due to gastric adenocarcinoma) and overall survival (OS; the event was death from any cause).

The survival of patients was computed from the date of the surgery to January 1st, 2013 (close-out date). Survival probability was calculated using the Kaplan-Meier estimate[14], and log rank test[15] was used to evaluate the differences between individual groups of patients. Independent prognostic values of variables that appeared as statistically significant on univariate analysis were tested by multivariate Cox regression analysis model.[16] Two-

TABLE 2. Toxicity of adjuvant radiochemotherapy

Toxicity	NCI grade (%)					
	0	1	2	3	4	Total
Nausea, vomiting	**56.4**	**34.6**	**4**	**5**	**0**	**100**
Stomatitis	90.1	7.9	1	1	0	100
Diarrhoea	86.1	10.9	2	1	0	100
Hand-foot syndrome	73.3	10.9	6.9	8.9	0	100
Dysphagia	73.3	25.7	1	0	0	100
Acute coronary syndrome	96	4	0	0	0	100
Alopecia	97	3	0	0	0	100
Infection	43.6	8.9	28.7	17.8	1	100
Leucocyte count	25.8	36.6	30.7	5.9	1	100
Haemoglobin level	28.7	62.4	8.9	0	0	100
Platelet count	52.4	42.6	4.	1	0	100

sided tests were used and differences of $p < 0.05$ were considered as statistically significant.

Results

Toxicity of adjuvant radiochemotherapy

Postoperative chemotherapy started 2.6–11.2 weeks after surgery (median 6 weeks). Total postoperative treatment time ranged from 4.3 to 29.3 weeks (median 17.1 weeks), whereas the median duration of the radiotherapy part of the protocol was 4.7 weeks. Seventy-seven percent of patients completed the treatment according to the protocol. Ninety-seven (96%) patients reached the total radiation dose of 45 Gy, whereas in four patients (4%) the total dose was lower (two patients received 9 Gy, one 32.4 Gy and one 34.2 Gy, respectively). The other 19 (18.8%) patients who did not complete the treatment according to the protocol did not receive all cycles of chemotherapy (one patient received two cycles, 7 patients three cycles and 11 patients four cycles). No death occurred due to the therapy. Acute toxicity, such as nausea and vomiting, stomatitis, diarrhoea, hand-foot syndrome and infections of grade 3 or 4, occurred in 5%, 1%, 2%, 8.9% and 18.8% of patients, respectively (Table 2). Despite intensive nutritional support, only in two patients an increase of body weight was recorded during the therapy. Forty (39.6%) patients maintained constant weight, whereas the remaining 59 (58.4%) patients lost their weight compared to the weight they had at the beginning of treatment. The body weight loss was 1-17 kg (median 5 kg).

Outcome

The median follow-up time of all 101 patients was 3.9 years (range: 0.4-6.3 years), whereas in survivors it was 4.7 years (range: 3.2-6.3 years). On the close-out date, 64 (63.4%) patients were still alive, all of them being with no signs of the disease. Thirty (29.6%) patients died from gastric carcinoma, five (5%) patients died from other causes and in two (2%) patients the cause of death could not be determined. After adjuvant radiochemotherapy, recurrence was observed in 32 (31.7%) patients. Local and/or regional recurrence developed in five (5%) patients after a median period of time of 1.1 year (range: 0.6-1.3 years). Systemic disease alone developed in 27 (26.7%) patients in the median period of time of 0.9 year (range: 0.2-3 years). The 4-years follow-up survey showed that LRC, DFS, DSS and OS were 95.5%, 69.2%, 70.7%, and 66.2%, respectively (Figures 1 and 2).

Prognostic factors

On a univariate analysis of survival, the patients with pN3-stage, low pretreatment haemoglobin (Hb) concentration ≤ 120 g/l and age above 70 years had lower locoregional control and survival in comparison to their counterparts in all four survival endpoints. In addition, poorer treatment outcome correlated also with locally advanced disease (pT3-4), overall disease stage III, perineural invasion, lower treatment intensity (patients who did not complete the treatment according to the protocol and patients who started with adjuvant radiochemotherapy in more than 6 weeks after surgery), low

TABLE 3. Multivariate analysis of survival

Prognostic factors	Locoregional control			Disease-free survival			Disease-specific survival			Overall survival		
	HR	95% CI	P-value	HR	95% CI	P-value	HR	95% CI	P-value	HR	95% CI	P-value
pN- stage: - 0+1+2 - 3	17.97	1.32-244.69	0.03	7.38	2.93-18.59	<0.0001	9.67	3.54-26.36	<0.0001	7.40	3.08-17.78	<0.0001
Perineural invasion: - Yes - No	0.57	0.07-4.90	NS	2.89	1.07-7.77	0.036	3.45	1.16-10.27	0.026	2.55	1.08-6.02	0.032
Splenectomy: - Yes - No	22.42	1.20-417.44	0.037	3.07	1.12-8.48	0.03	4.37	1.50-12.71	0.007	5.59	2.27-13.81	<0.0001
Treatment according to the protocol: - Yes - No	0.19	0.02-1.88	NS	0.30	0.11-0.80	0.016	0.27	0.10-0.78	0.015	0.28	0.12-0.66	0.004

HR = hazard ratio; CI = confidence interval; NS = not significant

Hb (< 110 g/l) during radiochemotherapy and with splenectomy performed. The multivariate analysis identified the more advanced pN-stage and splenectomy as independent prognostic factors for all four types of survival. Independent prognostic factors for DFS, DSS and OS were perineural invasion and lower treatment intensity (Table 3).

Discussion

For gastric cancer, complete resection is the only curative therapy. Unfortunately, more than 50% of patients are diagnosed with unresectable disease.[17] In patients who underwent radical resection the 5-years survival rate is lower than 30%[18] with the rate of locoregional recurrence up to 50-80%.[19,20] For this reason, patients with gastric adenocarcinoma in many countries receive postoperative radiochemotherapy with 5-FU in combination with leucovorin (LV), because it has been proven that it significantly improves the survival of these patients.[4,5,20-25]

An updated analysis of INT 0116 study of 556 patients with resectable adenocarcinoma of the stomach or gastroesophageal junction showed that postoperative radiochemotherapy with 5-FU and LV improves 5-years overall survival (40% vs. 22%) and local recurrence rate (19% vs. 22%) compared with surgery alone.[22] However, this study was criticized by some due to poorly performed surgery. In 54% of patients only D0 lymphadenectomy instead of the recommended D2 lymphadenectomy was performed. When comparing these results with those of Kim´s study in which all patients

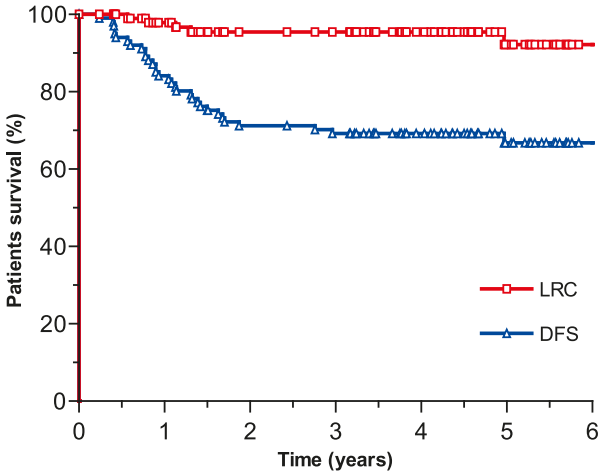

FIGURE 1. Locoregional control (LRC) and disease-free survival (DFS).

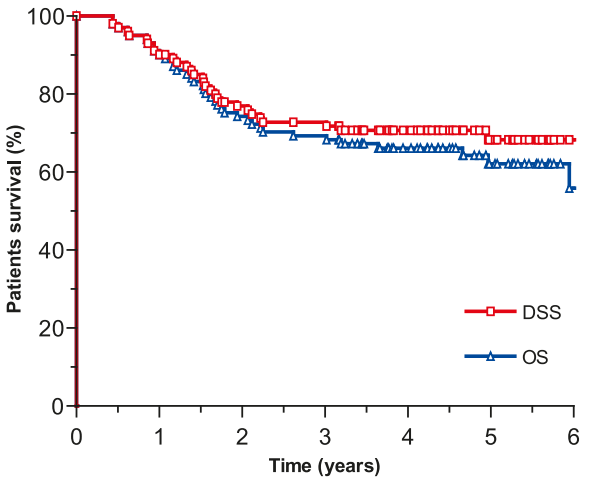

FIGURE 2. Disease-specific survival (DSS) and overall survival (OS).

underwent D2 lymphadenectomy, the 5-years survival rate was 57.1% in the radiochemotherapy arm and 51% in the surgery only group.[21] In the study of Park *et al.* in all patients D2 lymphadenectomy was performed and the results were similar with the 5-years survival rate of 60%.[20] As the same adjuvant regimen was used in both studies, it seems that the reason for better outcome in both studies is a more extensive lymphadenectomy. This thinking seems to be confirmed also in the Dutch study, where there was only a little benefit from adjuvant radiochemotherapy in patients with D2 lymphadenectomy in comparison to those with D1 limphadenectomy.[23] The ARTIST trial, in which patients after radical resection of gastric cancer were randomized in the group treated with capecitabine and cisplatin and in the group treated with the same regiment of chemotherapy plus radiotherapy, reported that in the group treated with postoperative radiochemotherapy a statistical trend towards better DFS was observed. The benefit of postoperative radiochemotherapy was even higher in the subgroup of patients with positive lymph nodes.[24] In a similarly designed trial, Chinese experts concluded that adjuvant radiochemotherapy with intensity-modulated radiotherapy (IMRT) significantly improves 5-years DFS in comparison with postoperative chemotherapy in the whole patient population, not only in those with positive lymph nodes.[25] In the above two trials and in the trial of Yu *et al.*[26] it has been noticed that adjuvant radiochemotherapy in the patients with gastric cancer gives higher benefit in more advanced stages of the disease (but without distant metastases). The survival benefit noted in patients who were treated with radiochemotherapy was entirely due to an improvement in local control with less effect on distant metastases, which suggests that the chemotherapy with 5-FU and LV is producing its effect through radiosenzitisation.[4]

In our study the surgeons were obliged to follow the protocol and to perform routinely at least D1 lymphadenectomy. Fifteen or more lymph nodes were removed and histologically examined in 70 (69.3%) patients and less than 15 lymph nodes were examined in 31 (30.7%) patients. In only 4 patients the resection was estimated as R1 and reoperation in the opinion of surgeons was not possible.

In our previous report, long term results of adjuvant radiochemotherapy with 5-FU and LV in patients with gastric cancer were analyzed with the 5-years LRC, DFS, DSS and OS of 81%, 48.3%, 50.4% and 48.4%, respectively.[7] In the reports of Macdonald *et al.*[5], Kim *et al.*[21] and ours, chemotherapy with 5-FU and LV was given concomitantly during radiotherapy only in the first four and last three days. In our current study with administration of capecitabine on each day of radiotherapy, we hoped for better radiosensitization effects and a better treatment outcome. Jansen *et al.* designed the phase I-II study with postoperative radiochemotherapy with capecitabine and they reported that such treatment is feasible with low toxicity.[26] The estimated 5-years follow-up survey in our study showed that LRC, DFS, DSS and OS were 92.2%, 66.8%, 68.3%, and 62.1%, respectively. These results were better in comparison to other data[5,20-23] which can be attributed to the fact that chemotherapy with capecitabine instead of 5-FU and LV was used. On the other hand, these good results could be due to careful selection of patients because we excluded all the patients with tumours located in the cardia (known to have a worse treatment outcome), patients who were not able to take capecitabine (difficulty in swallowing tablets or unable to comply) and patients with significant co-morbidities.

The other criticism of the American intergroup study was referred to the high percentage of patients (36%) who did not conclude the therapy according to the protocol.[5,22] In Kim´s study, 24.8% of enrolled patients with radiochemotharapy did not complete the treatment as planned.[21] They also reported that, due to chemotherapy related toxicity, the dose of the drugs had to be reduced in 48.9%, whereas in 24.5% of patients the application of chemotherapeutics had to be delayed. All above mentioned authors nevertheless believe that the INT 0116 protocol is safe and acceptable for clinical use and we also support this opinion.[7] In our study, in which radiochemotherapy with capecitabine was used, only 19 (18.8%) patients did not complete the treatment according to the protocol which is more favourable than the other authors´ reports for radiochemotherapy with 5-FU and LV.[5,20] In our previous study with radiochemotherapy with 5-FU and LV, we obtained the same results with only 18% of patients who were not able to complete the treatment. We believe that in our case, this favourable experience may be due to the fact that we insisted on extensive advising of our patients on all potential side-effects of chemo- and radiotherapy. Furthermore, all of the patients received intensive supportive care, including intensive nutritional support.

If we look at acute toxicity more precisely, we can conclude that it is low and feasible. Nausea and vomiting, stomatitis, diarrhoea, hand-foot

syndrome and infections of grade 3 or 4 in our current study occurred in 5%, 1%, 2%, 8.9% and 18.8% of patients. In our previous study, where radiochemotherapy with 5-FU and LV was used, nausea and vomiting, stomatitis, diarrhoea and infections of grade 3 or 4, occurred in 18.7%, 26%, 8.9% and 12.2% of patients, respectively.[6] In Macdonald´s study the gastrointestinal type of toxic effects of grade 3 or more occurred in 33% of patients, infection in 6% and there were three deaths due to the therapy.[5] In our study we did not have any death related to the treatment. In the study of Park *et al.* nausea, stomatitis and diarrhoea of grade 3 or more occurred in 12%, 15% and in 11% of patients, respectively.[20] In the study of Lee *et al.*[24] and Zhu *et al.*25 the toxicity profile was a bit better with nausea in 12.3 and 2.7% and vomiting in 3.1% and 1.6% of patients. In Zhu's study diarrhoea was present in 1.6% and in Lee's study hand-foot syndrome was present in 3.1% of patients. Jansen *et al.* who used capecitabine in doses of 650 mg/m^2, 800 mg/m^2, 900 mg/m^2 and 1000 mg/m^2 with radiotherapy, did not notice any grade 3 or more side effects such as nausea, vomiting, diarrhoea and hand-foot syndrome.[27]

From our analysis of prognostic factors, we may conclude that the patients with more advanced pN-stage and/or underwent splenectomy and/or had perineural invasion and/or lower treatment intensity have lower survival in comparison to their counterparts. More advanced pN-stage is considered to be well established negative prognostic factor for patients with gastric cancer and is also usually mentioned as such in pertinent literature.[28-32] Some researchers noted that splenectomy has an adverse effect on patients' survival.[5,33] This has been shown in our study, too. Splenectomy is recommended only for patients with direct tumour invasion in the spleen or in the advanced gastric cancer located in the proximal part of the stomach, when there is evidence of macroscopic invasion into serosal surface and with regional lymph node metastasis.[34,35] Otherwise its negative effect on postoperative morbidity and mortality is too strong and it prevails over treatment benefit. Perineural invasion has already been established as an important negative prognostic factor in our previous study of adjuvant radiochemotherapy with 5-FU and leucovorin.[6] It is well known that the intensity of therapy can have an influence on treatment outcome in many neoplasms.[6,7,31,36]

In conclusion, we emphasize that multidisciplinary approach is mandatory for taking the decision about the treatment of patients with gastric cancer. Adjuvant radiochemotherapy with capecitabine is acceptable for clinical use, because it gives encouraging results regarding patients' survival and low toxicity. However, because the local control with the existing treatment is excellent, in our opinion, to improve the outcome for these patients and reduce the rate of distant metastases, the new generation of systemic therapy combinations which could be used with the irradiation is needed.

References

1. *Cancer in Slovenia 2009.* Ljubljana: Institute of Oncology Ljubljana, Epidemiology and Cancer Registry, Cancer Registry of Republic of Slovenia; 2013.
2. Buyukasik O, Hasdemir AO, Gulnerman Y, Col C, Ikiz O. Second primary cancers in patients with gastric cancer. *Radiol Oncol* 2010; **44:** 239-43.
3. Rajev L. Treatment options for surgically resectable gastric cancer. *Curr Treat Options Oncol* 2010; **11:** 14-23.
4. Buergy D, Lohn F, Baack T, Siebenlist K, Haneder S, Michaely H, *et al.* Radiotherapy for tumors of the stomach and gastoesophageal junction - a review of its role in multimodal therapy. *Radiat Oncol* 2012; **7:** 192.
5. Macdonald JS, Smalley SR, Benedetti J, Hundahl SA, Estes NC, Stemmermann GN, *et al.* Chemoradiotherapy after surgery compared with surgery alone for adenocarcinoma of the stomach or gastroesophageal junction. *N Engl J Med* 2001; **345:** 725-30.
6. Oblak I, Velenik V, Anderluh F, Strojan P. Results of adjuvant radiochemotherapy for gastric adenocarcinoma in Slovenia. *Eur J Surg Oncol* 2007; **33:** 982-7.
7. Oblak I, Anderluh F, Velenik V**.** Postoperative radiochemotherapy for gastric adenocarcinoma: long term results. *Radiol Oncol* 2009; **43:** 274-81.
8. Rossi D, Alessandroni P, Catalano V, Giordani P, Fedeli A, Baldelli AM, *et al.* Safety profile and activity of lower capecitabine dose in patients with metastatic breast cancer. *Clin Breast Cancer* 2007; **7:** 857-60.
9. Walko CM, Lindley C. Capecitabine: a review. *Clin Ther* 2005; **27:** 23-44.
10. Ocvirk J, Rebersek M, Skof E, Hlebanja Z, Boc M. Randomized prospective phase II study to compare the combination chemotherapy regiment epirubicin, cisplatin and 5-fluorouracil with epirubicin, cisplatin and capecitabine in patients with advanced or metastatic gastric cancer. *Am J Clin Oncol* 2012; **35:** 237-41.
11. Twelves C, Scheithauer W, McKendrick J, Seitz JF, Van Hazel G, Wrong A, *et al.* Capecitabine versus 5-fluorouracil/folinic acid as adjuvant therapy for stage III colon cancer: final results from the X-ACT trial with analysis by age and preliminary evidence of a pharmacodynamic marker of efficacy. *Ann Oncol* 2012; **23:** 1190-7.
12. American Joint Committee on Cancer. *AJCC cancer staging manual.* 7th edition. New York: Springer-Verlag; 2009.
13. Ajani JA, Welch SR, Raber MN, Fiels WS, Krakoff IM. Comprehensive criteria for assessing therapy-induced toxicity. Cancer Invest 1990; **8:** 147-59.
14. Kaplan EL, Meier P. Nonparametric estimation from incomplete observations. *J Am Stat Assoc* 1958; **53:** 457-81.
15. Peto R, Pike MC, Armitage P, Breslow NE, Cox DR, Howard SV, *et al.* Design and analysis of randomized clinical trials requiring prolonged observation of each patient. II. Analysis and examples. *Br J Cancer* 1977; **35:** 1-39.
16. Cox DR. Regression models and life-tables. *J R Stat Soc Bull* 1972; **34:** 187-220.
17. Greenlee RT, Murray T, Bolden S, Wingo PA. Cancer statistics 2000. *Ca Cancer J Clin* 2000; **50:** 7-33.
18. Ajani JA. Chemotherapy for gastric carcinoma: new and old options. *Oncology (Huntingt)* 1998; **12 (10 Suppl 7):** 44-7.

19. Gunderson LL. Gastric cancer: patterns of relapse after surgical resection. *Semin Radiat Oncol* 2002; **12:** 150-61.

20. Park SH, Kim DY, Heo JS, Lim DH, Park CK, Lee KW, *et al.* Postoperative chemotherapy for gastric cancer. *Ann Oncol* 2003; **14:** 1373-7.

21. Kim S, Lim DH, Lee J, Kang WK, McDonald JS, Park CH, *et al.* An observation study suggesting clinical benefit for adjuvant postoperative chemoradiation in a population of over 500 cases after gastric resection with D2 nodal dissection for adenocarcinoma of the stomach. *Int J Radiat Oncol Biol Phys* 2005; **63:** 1279-85.

22. Smalley SR, Benedetti JK, Haller DG, Hundahl SA, Estes NC, Ajani Ja, *et al.* Updated analysis of SWOG-directed intergroup study 0116: a phase III trial of adjuvant radiochemotherapy versus observation after curative gastric cancer resection. *J Clin Oncol* 2012; **30:** 2327-33.

23. Dikken JL, Jansen EP, Cats A, Bakker B, Hartgrink HH, Kranenbarg EM, *et al.* Impact of the extent of surgery and postoperative chemoradiotherapy on recurrence patterns in gastric cancer. *J Clin Oncol* 2010; **28:** 2430-6.

24. Lee J, Lim do H, Kim S, Park SH, Park JO, Park YS, *et al.* Phase III trial comparing capecitabine plus cisplatin versus capecitabine plus cisplatin with concurrent capecitabine radiotherapy in completely resected gastric cancer with D2 lymph node dissection: the ARTIST trial. *J Clin Oncol* 2012; **30:** 268-73.

25. Zhu WG, Xua DF, Pu J, Zong CD, Li T, Tao GZ, *et al.* A randomized, controlled, multicenter study comparing intensity-modulated radiotherapy plus concurrent chemotherapy with chemotherapy alone in gastric cancer patients with D2 resection. *Radiother Oncol* 2012; **104:** 361-6.

26. Yu C, Yu R, Zhu W, Song Y, Li T. Intensity-modulated radiotherapy combined with chemotherapy for the treatment of gastric cancer patients after standard D1/D2 surgery. *J Cancer Res Clin Oncol* 2012; **138:** 255-9.

27. Jansen EP, Boot H, Saunders MP, Crosby TD, Dubbelman R, Bartelink H, *et al.* A phase I-II study of postoperative capecitabine-based chemoradiotherapy in gastric cancer. *Int J Radiat Oncol Biol Phys* 2007; **69**: 1424-8.

28. Kim JP, Lee JH, Kim SJ, Yu HJ, Yang HK. Clinicopathologic characteristics and prognostic factors in 10783 patients with gastric cancer. *Gastric Cancer* 1998; **1:** 125-33.

29. Orditura M, De Vita F, Muto P, Vitiello F, Murino P, Lieto E, *et al.* Adjuvant chemotherapy in patients with stage III or IV radically resected gastric cancer. *Arch Surg* 2010; **145:** 233-8.

30. Yao JC, Mansfield PF, Pisters PWT, Feig BW, Janjan NA, Crane C, *et al.* Combined modality therapy for gastric cancer. *Semin Surg Oncol* 2003; **21:** 223-7.

31. Avital I, Pisters PWT, Kelsen DP, Willett CG. Cancer of the stomach. In: DeVita VT, Lawrence TS, Rosenberg SA, editors. *Cancer; principles & practice of oncology.* 9th edition. Philadelphia: Lippincott-Williams &Wilkins; 2004. p. 924-54.

32. Willett CG, Gunderson LL. Stomach. In: Halperin EC, Perez CA, Brady LW, editors. *Principles and practice of radiation oncology.* 5th edition. Philadelphia: Lippincott-Williams &Wilkins; 2008. p. 1318-35.

33. Chua YJ, Cunningham D. The UK NCRI MAGIC trial of perioperative chemotherapy in resectable gastric cancer: implications for clinical practice. *Ann Surg Oncol* 2007; **14:** 2687-90.

34. Ikeguchi M, Kaibara N. Lymph node metastasis at the splenic hilum in proximal gastric cancer. *Am Surg* 2004; **70:** 645-8.

35. Huang CM, Wang JB, Lu HS, Zheng CH, Li P, Wie JW, *et al.* Prognostic impact of splenectomy on advanced proximal gastric cancer with No.10 lymph node metastasis. *Chin Medl J* 2009; **122:** 2757-62.

case report

Xp 11.2 translocation renal carcinoma in young adults; recently classified distinct subtype

Andrej Kmetec[1], Jera Jeruc[2]

[1] Urologic Clinical Department, University Medical Centre Ljubljana, Ljubljana, Slovenia
[2] Institute of Pathology, Medical Faculty, University of Ljubljana, Ljubljana, Slovenia

Radiol Oncol 2014; 48(2): 197-202.

Received 5 October 2012
Accepted 2 December 2012

Correspondence to: Prof. Andrej Kmetec, M.D., Ph.D., University Medical Center Ljubljana, Zaloška cesta 7, 1000 Ljubljana, Slovenia. Phone: +386 1 522 3212; E-mail: andrej.kmetec@kclj.si

Disclosure: No potential conflicts of interest were disclosed.

Background. XP11.2 renal translocation carcinomas are often encountered in paediatric group of patients where they are believed to be rather indolent. They are rare but more aggressive in young adults. They are slow growing, sometimes without characteristic symptoms and their biologic behaviour is uncertain.

Case report. We report two cases of this type of tumour in Slovenian young adult males with long and unusual history. Tumours were confirmed imunohistologically by positive reaction for CD10, P504S and TFE3.

Conclusions. According to the indications in the literature prognosis of these tumours in young adults depends upon the stage. It seems that cysts, haematomas and necrosis around the kidney are often encountered in these tumours. In advanced stage with lymph nodes involvement or distant metastases, the prognosis is poor. Surgery seems to be basic mode of therapy.

Key words: renal tumours; translocation renal cell carcinoma; histology

Introduction

Renal cell carcinoma (RCC) represents 2.9% of all carcinomas in Slovenia. The crude incidence was increasing in males from 10.6/100000 and females 6.1/100000 in the period 1993-97 to 20.4/100000 in males and 10.5/100000 in females during the period 2005-2009.[1-3] Cancer originates in the epithelium of the proximal convoluted tubule filtering the blood and it accounts for more than 90% of all renal malignancies occurring in adults. The 2004 World Health Organisation (WHO) classification distinguishes three main histologic types: clear cell, papillary and chromophobe renal cell carcinoma.[4] Lately, the use of new imunohistologic and molecular techniques, has recognised some rare, uncommon unclassified types of tumours, *e.g.* Bellini duct carcinoma, medullary carcinoma, Xp11.2 translocation carcinoma, mucinous tubular and spindle cell carcinoma.[5,6] These new entities comprise only 10-15% of renal tumours, but they have important implication on the outcome. Yet for some subtypes the prognosis and the optimal way of treatment is still not well defined.[6]

Xp11.2 translocation carcinoma has been recently recognised as a distinct subtype of renal carcinoma. Xp11.2 renal cell carcinomas are defined by at lest six different translocations involving Xp11.2 chromosome, all of which result in a gene fusion involving the TFE3 (transcription factor E3) gene.[7-16] This subtype of renal cell tumour occurs predominantly in the paediatric group where it accounts for 20-40% of paediatric renal cell carcinoma. It is very rare in adults, the incidence has been reported to be 1-1.6% of all renal tumours, but its actual incidence remains underestimated.[8,9] Meta-analyses of cases in the literature found that 50% or even 65% of patients with Xp11.2 translocation renal cell carcinoma presented with high-stage tumours, namely in stage III and IV.[9] Classification is the same as for all renal cell tumours (Table 1). Complete surgical removal of the tumour mass including the kidney is the preferred therapy in patients with lower stage tumours. In patients with metastatic or relapsed

TABLE 1. Classification of renal cell tumours (adapted from EAU guidelines 2013)

Stage I, T1N0M0	Tumour is < 7 cm, confined to kidney
Stage II, T2N0M0	Tumour is > 7 cm, confined to kidney
Stage III, T1-3N0-1M0	Tumour of any size, growing into major vein, into tissue around the kidney not beyond Gerota's fascia, spread to lymph nodes
Stage IV, T4N1-2,M1	Tumour of any size, growing beyond Gerota's fascia, spread to nearby or distant lymph nodes, spread to organs (bones, lungs, liver)

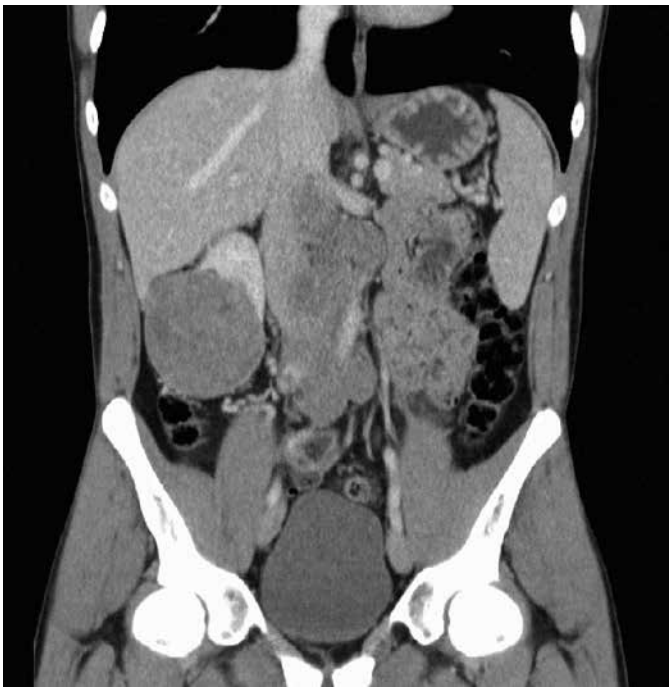

1

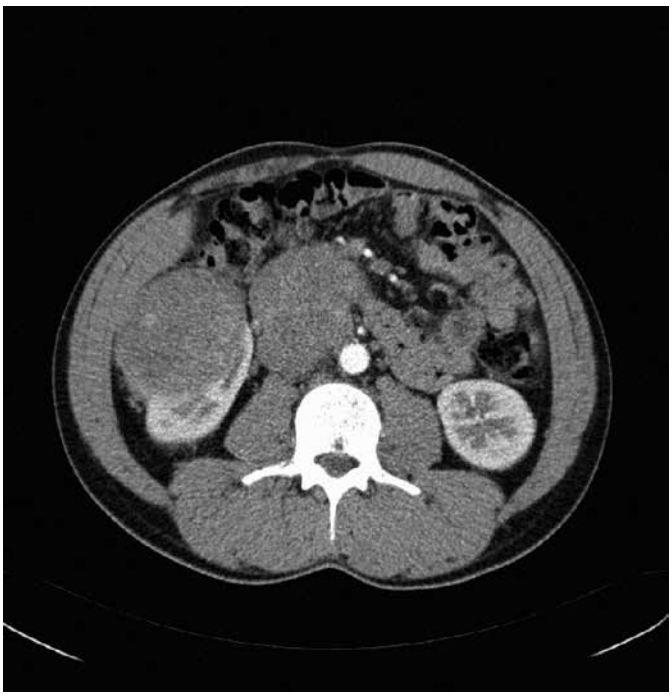

2

FIGURES 1, 2. Abdominal CT scan of 27 year adult male.

carcinoma targeted agents are used such as sunitinib and mTOR inhibitors, while chemotherapy is not effective.[9] Malouf *et al.* in his study concluded that Xp11 translation renal cell carcinoma targeted therapy achieve objective responses and prolonged progression-free survival.[9] Prognosis of patients in higher stages is poor, most of them die within a year after the surgery, while the prognosis of patients with low stage disease is variable because the exact biologic behaviour of tumours and impact of current treatment modalities remains uncertain.[10] Prognosis depends also on the age: in children tumour can be rather indolent, but in patients aged 16 or older Xp11.2 translocation carcinoma has a more aggressive clinical course.[11,12]

Cases presentation

We present the first two cases of Xp11.2 translocation renal cell carcinomas confirmed in Slovenia in two young males admitted to the urological department in the period of three months. The first one, aged 27, was accepted urgently due to an unbearable pain and a palpable tumour in the abdominal and lumbar region. CT scan revealed a huge solid tumour mass measuring 7.6 x 8.2 x 8.1 cm located in the lower and lateral part of right kidney with metastatic tumours of similar size in the retroperitoneal region, over and under the vena cava, between the aorta and the vena cava extending up to the liver and down to the aortal bifurcation.

Four years prior the last hospitalisation, he was admitted to hospital also due to a pain in the lumbar region. At the time CT scan and ultrasound examination revealed a septal haematoma with a thick wall measuring 10 cm in diameter on the anterior side of the right kidney and an angiomyolipoma-like change on the lower pole of the same kidney measuring 3.5 x 2.5 cm. The cause of the haematoma was not clearly identified, bleeding from angiomyolipoma or trauma was suspected. Furthermore, CT scan showed a solid mass near the kidney haematoma that was not further investigated or been even overlooked. Months later,

the ultrasound investigation confirmed that haematoma decreased and showed the persistent angiomyolipoma of the same size without any solid mass around the kidney. Because the patient was asymptomatic, he did not attend regular controls until lumbar and abdominal pain re-emerged after four years. Tumour biopsy verified a solid renal tumour. Due to the persistent pain and haematuria, embolization of the kidney and tumour mass was performed. Using a transabdominal surgical approach we managed to remove the kidney with the tumour and the haematoma and well delineated retroperitoneal metastases along vena cava. Tumour burden was removed radically, but eight months later local recurrence and distant lymph nodes were established. The patient refused additional surgical intervention and he preferred treatment at department for oncology. He was given sunitinib as the first line therapy, but no objective response was achieved. Treatment changed to mTOR inhibitor (everolimus), also without any objective response. Despite specific therapy the disease progressed and later only symptomatic treatment was introduced. A year after the surgery the patient died because of massive cancer involvement (Figures 1 and 2).

The second patient, aged 31, experienced sudden respiratory distress and was admitted to the pulmonary department where pulmonary embolism was confirmed and treated. The CT scan revealed a huge cystic formation measuring 28 x 21 x 16 cm embracing the left kidney with a solid mass near compressed kidney. The formation distended to the abdominal wall. As the patient thought he has been gaining weight, has been practising slimming diets for over a year. Otherwise the patient felt no pain; his only complaint was shortness of breath. Prior the surgery cava filter was inserted into the lower vena cava. Surgical procedure was done using lumbar approach, a huge cystic cavity was isolated and 3.5 l of cloudy liquid was evacuated. A compressed kidney with adjacent tumour was removed along with the entire tumour mass. Lymph nodes were negative and tumour extension over cystic margins was not detected. Ten months after surgery the patient is still asymptomatic (Figures 3 and 4)

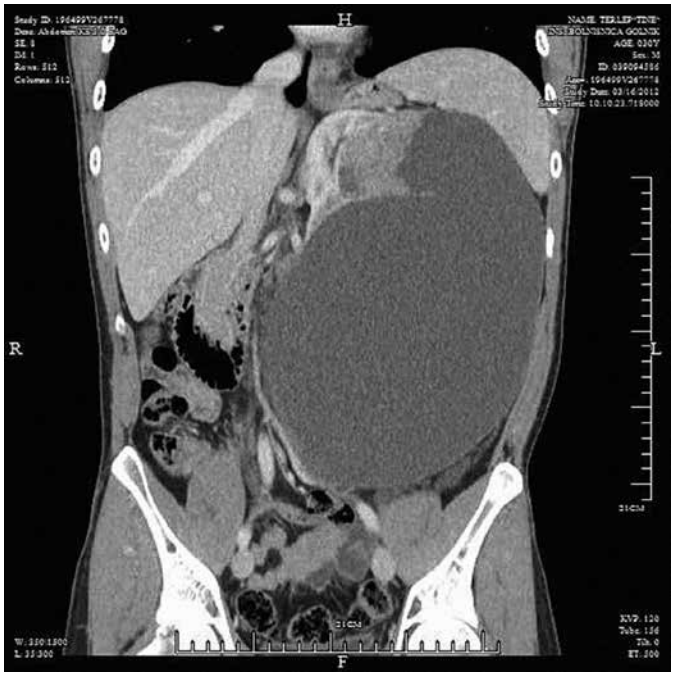

3

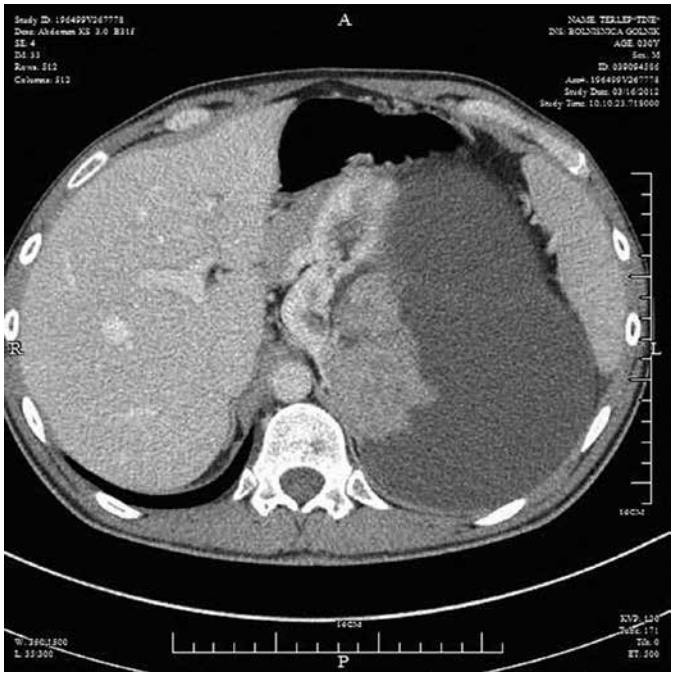

4

FIGURE 3, 4. CT scan of the 31 year adult male with cystic mass.

Histology

In the first case the kidney contained a well circumscribed solid, yellowish tumour with a central haemorrhage and necrosis, measuring 6.5 x 5.3 cm and grossly confined by the renal capsule. The uninvolved renal parenchyma was pale with dark brown spots, consistent with postembolization changes. There were five additional tumour nodules, weighing 292 g in total, all well circumscribed, some with adherent fat. On the cut surface, the tumours appeared multilobulated, soft, tan-pink, with tissue organised into papillary structures. Histologically the tumour was composed of

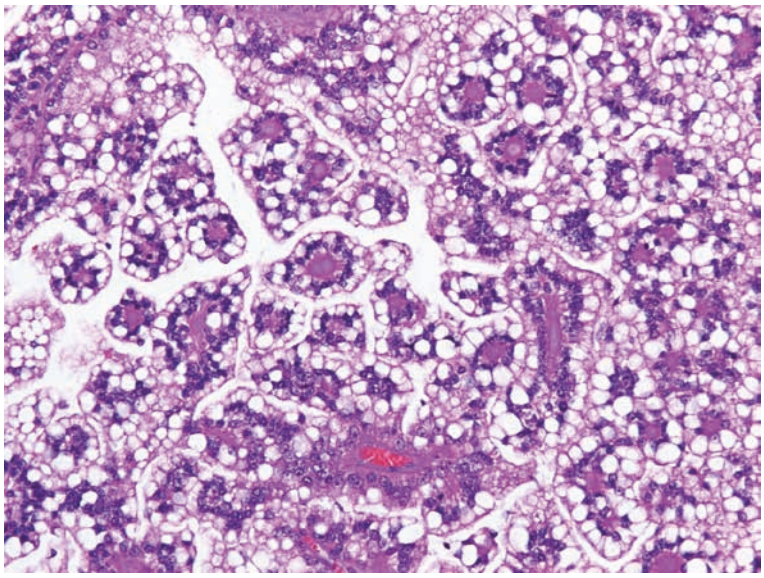

FIGURE 5. Translocation renal cell carcinoma composed of clear cells with voluminous cytoplasm and distinct cell borders showing typical papillary architecture and hyalinised fibrovascular cords.

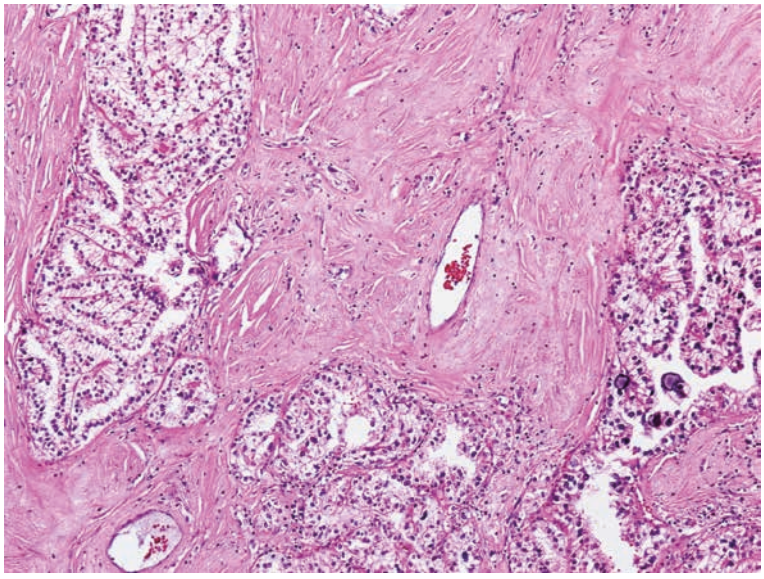

FIGURE 6. Translocation renal cell carcinoma composed of clear cells arranged in tubule-alveolar pattern laying in hyalinised stroma. There are some psammoma bodies in the lower right corner.

cells arranged mostly papillary and focally in solid/alveolar patterns. The tumour cells were large with sharply defined borders and mostly clear, in some areas they had finely granular eosinophilic cytoplasm. Fibrovascular cords in some areas of the papillae were strongly hyalinised. Psammomatous calcifications were present in the stroma and in the capsule surrounding the tumour nodules. There were extensive areas of necrosis and haemorrhage surrounded by hemosiderin-laden macrophages. The neoplastic cells were diffusely immunoreactive for RCC antigen and racemase, focally for CD10 and negative for CK7, EMA, HMB45 and Melan A (Figure 5)

In the second case the tumour was cystic, the solid part of the yellowish-gray tumour with necrotic and haemorrhagic areas measured 9.4 x 7.1 cm. Microscopic examination revealed a clear cell papillary tumour with abundant hyalinised stroma. Tumour cells showed partially clear and partially eosinophilic cytoplasm and enlarged hyperchromatic nuclei. There were numerous psammoma bodies, larger calcifications and some hyaline globules. The neoplastic cells were diffusely immunoreactive for RCC antigen, racemase, CD 10 and vimentin and negative for CK7 and EMA. Angiomyolipoma was not found in the resected specimen (Figure 6)

In both cases the tumour cells showed diffuse strong nuclear immunopositivity for transcription factor for immunoglobulin heavy-chain enhancer 3 (TFE3) confirming the diagnosis of Xp11.2 translocation renal cell carcinoma (Figure 7)

Discussion

We report the first two documented cases of Xp11.2 translocation/TFE3 fusion renal cell carcinomas in Slovenia in young adult males with a long and unusual history. This is a rare subtype of RCC that we were probably not sufficiently aware of since it was included in the WHO classification of RCC for the first time in 2004. Its incidence is higher in children and young adults.[9,10]

Morphologically Xp11.2 translocation RCCs are quite heterogeneous. The most consistent histologic appearance is a carcinoma with mixed papillary and nested/alveolar architecture, composed of cells with clear and/or eosinophilic, granular, voluminous cytoplasm, discrete borders and the presence of extensive psammoma bodies. These features are partially consistent with clear cell RCC and partially with papillary RCC, therefore we believe, that in the past these tumour were misdiagnosed as one of this more common subtypes of RCC. The diagnosis of Xp11.2 translocation RCC is suspected based on clinical information, histology and immunochemical features, however, it is confirmed by the detection of chromosome translocation involving TFE3 gene at Xp11.2 using different methods.[13] In this regard nuclear immunoreactivity for TFE3 protein

by routine immunohistochemistry is a highly sensitive and specific marker.[14,15] The anti-TFE3 antibody has only recently become available in our pathology department.

The biologic behaviour of Xp11.2 translocation RCC and its response to treatment is still not well defined. As described in literature, Xp11.2 translocation renal cell carcinomas are usually large tumours with focal cystic areas, haemorrhage and necrosis that present in advanced stage.[16] Nevertheless, the prognosis in young children seems to be rather good, while in adults it seems to behave in more aggressive fashion. Prior exposure to chemotherapy is the only known risk factor for the development of these tumours.[17] But, neither of our patients had a history of previous chemotherapy. Both of them were young adults, and presented with long-term history of complaints, so it is possible that the tumours had developed when they were younger or even in childhood, but had not been detected until reaching the dimension of a large mass or an advanced stage. Another possibility is that the Xp11.2 translocation renal cell carcinoma is more aggressive when it occurs in adults than when it occurs in children.[18,19]

In our cases late diagnosis was established on one hand because the diagnosis of Xp11 translocation RCC may have been previously underestimated in young adults. Initial symptoms were not clear and diagnostic evaluation and imagines were underestimated too. Cysts, haematomas, necrotic tissue in or around the kidney or even extensive psammomatous calcification evident radiographically can be misinterpreted as some traumatic injury or harmless developmental abnormality in young adults. Therefore, it is necessary to diagnose this tumour entity accurately taking into consideration all available diagnostic tools to clarify unusual pains and problems in young adults.

Conclusions

Because of the small number of Xp11.2 translocation renal cell carcinoma described in the literature, the exact biologic behaviour and impact of current treatment modalities remain to be uncertain. Increased awareness among urologists, pathologists, and oncologist is necessary in order to help identifying more cases of this phenotype in the future. Treatment is primarily surgical; in advanced-stage target agents should be a treatment of choice but with doubtful success. When dealing with younger patients we must be aware that haematomas, cysts or necrotic tissue in/around the kidneys could represent an initial stage of translocation renal cell carcinoma. In such cases we must use appropriate imaging studies to exclude reliably malignant tumour or angimyolipoma. Lesion biopsy and the use of antibodies against TFE3 in all RCC, with emphasis on young adults, may be necessary to determine the biologic nature and incidence of this tumour.

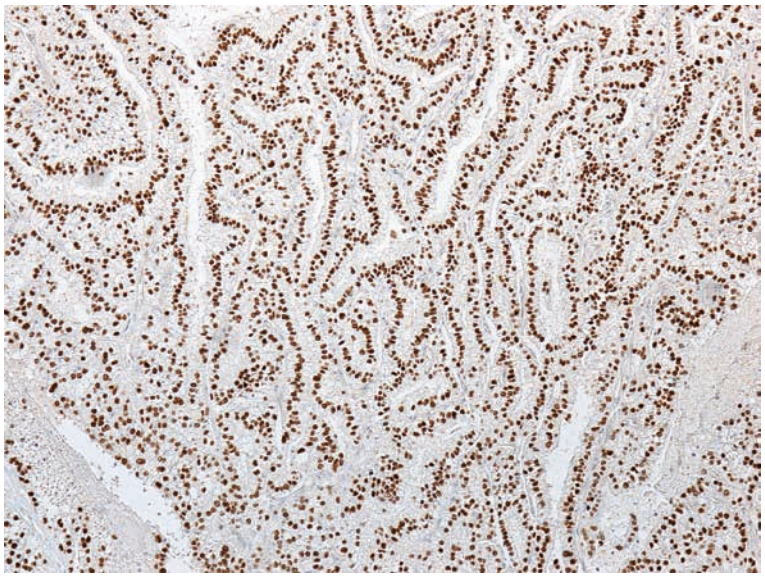

FIGURE 7. Strong diffuse nuclear transcription factor for immunoglobulin heavy-chain enhancer 3 (TFE3) immunostaining.

References

1. *Cancer in Slovenia 2007*. Ljubljana: Institute of Oncology Ljubljana, Epidemiology and Cancer Registry, Cancer Registry of Republic of Slovenia; 2010.
2. *SLORA. Slovenija in rak*. Ljubljana: Register raka RS, Onkološki inštitut Ljubljana. Available from: http://www.slora.si. Accessed on 1 december 2012.
3. Karim-Kos HE, deVries E, Soerjomataramam I, Iemmens V, Siesling S, Coebergh JW. Recent trends of cancer in Europe: acombined approach of incidence, survival and mortality for 17 cancer sites since the 1990s. *Eur J Cancer* 2008; **44:** 1345-89.
4. Eble JN, Togashi K, Pisani P. Renal cell carcinoma. In: Eble JN, Sauter G, Epstein JI, Sesterhenn IA, editors. *Pathology and genetics of tumours of the urinary system and male genital organs. World Health Organisation Classification of Tumors.* Lyon: IARC Press; 2004, p. 12-43.
5. Lopez-Beltran A, Scarpelli M, Montironi R, Kirkali Z. 2004 WHO classification of the renal tumors of the adults. *Eur Urol* 2006; **49:** 798-805.
6. Ljungberg B, Cowan N, Hanbuty DC, Hora M, Kucyk MA, Merseburger AS, et al. *Guidelines on renal cancer.* European association of Urology; 2012. p. 18-22.
7. Argani P. The evolving story of renal translocation carcinomas. *Am J Clin Pathol* 2006; **126:** 332-4.
8. Komai Y, Fujiwara M, Fujii Y, Mukai H, Yonese J, Kawakami S, et al. Adult Xp11 translocation renal cell carcinoma diagnosed by cytogenetics and immunohistochemistry. *Clin Cancer Res* 2009; **15:** 1170-6.

9. Malouf GG, Camparo P, Oudard S, Schleiermacher G, Theodore C, Rustine A, et al. Targeted agents in metastatic Xp11 translocation/TFE3 gene fusion renal cell carcinoma (RCC): a report from the Juvenile RCC Network. *Ann Oncol* 2010; **21:** 1834-8.

10. Camparo P, Vasiliu V, Molinie V, Couturier J, Dykema KJ, Petilio D. Renal translocation carcinomas: clinicopathologic, immunohistological and gene expression profiling analysis of 31 cases with a review of the literature. *Am J Surg Patho*l 2008; **32:** 656-70.

11. Meyer PN, Clark JI, Flanigan RC, Picken MM. Xp11.2 translocation renal cell carcinoma with very aggressive course in five adults. *Am J Clin Pathol* 2007; **128:** 70-9.

12. Klatte T, Streubel B, Wrba F, Remzi M, Krammer B, de Martino M, et al. Renal cell carcinoma associated with transcription factor E3 expression and Xp11.2 translocation: incidence, characteristics, and prognosis. *Am J Clin Pathol* 2012; **137:** 761-8.

13. Armah HB, Parwani AV. Xp11.2 translocation renal cell carcinoma. *Arch Pathol Lab Med* 2010; **134:** 124-9.

14. Argani P, Lal P, Hutchinson B, Lui MY, Reuter VE, Ladanyi M. Aberrant nuclear immunoreactivity for TFE3 in neoplasms with TFE3 gene fusions: a sensitive and specific immunohistochemical assay. *Am J Surg Pathol* 2003; **27:** 750-61.

15. Kuroda N, Mikami S, Pan CC, Cohen RJ, Hes O, Michal M, et al. Review of renal carcinoma associated with Xp11.2 translocations/TFE3 gene fusions with focus on pathobiological aspect. *Histol Histopathol* 2012; **27:** 133-40.

16. Zhong M, De Angelo P, Osborne L, Paniz-Mondolfi AE, Geller M, Yang Y, et al. Translocation renal cell carcinomas in adults: a single-institution experience. *Am J Surg Pathol* 2012; **36:** 654-62.

17. Argani P, Laé M, Ballard ET, Amin M, Manivel C, Hutchinson B, et al. Translocation carcinomas of the kidney after chemotherapy in childhood. *J Clin Oncol* 2006; **24:** 1529-34.

18. Argani P, Olgac S, Tickoo SK, Goldfischer M, Moch H, Chan DY, et al. Xp11 translocation renal cell carcinoma in adults: expanded clinical, pathologic, and genetic spectrum. *Am J Surg Pathol* 2007; **31:** 1149-60.

19. Klatte T, Streubel B, Wrba F, Remzi M, Krammer B, de Martino M, et al. Renal cell carcinoma associated with transcription factor E3 expression and Xp11.2 translocation: incidence, characteristics, and prognosis. *Am J Clin Pathol* 2012; **137:** 761-8.

research article

Inter-application displacement of brachytherapy dose received by the bladder and rectum of the patients with inoperable cervical cancer

Goran Marosevic[1], Dzenita Ljuca[2], Hasan Osmic[3], Semir Fazlic[3], Oliver Arsovski[1], Dusan Mileusnic[1]

[1] Centre for Radiotherapy, International Medical Centre Banja Luka, Banja Luka, Bosnia and Herzegovina
[2] Gynaecology and Obstetrics Clinic, University Clinical Centre Tuzla, Tuzla, Bosnia and Herzegovina
[3] Department for Radiotherapy, University Clinical Centre Tuzla, Tuzla, Bosnia and Herzegovina

Radiol Oncol 2014; 48(2): 203-209.

Received 19 April 2013
Accepted 16 October 2013

Correspondence to: Goran Marosević; Center for Radiotherapy, International Medical Centre Banja Luka, 78000 Banja Luka, Bosnia and Herzegovina. Phone: +387 63 116 431; Fax: +387 51 340 510; E-mail: goran.marosevic@euromedic.ba

Disclosure: No potential conflicts of interest were disclosed.

Background. The aim of the study was to examine on the CT basis the inter-application displacement of the positions $D_{0.1cc}$, D_{1cc} and D_{2cc} of the brachytherapy dose applied to the bladder and rectum of the patients with inoperable cervical cancer.

Patients and methods. This prospective study included 30 patients with cervical cancer who were treated by concomitant chemo-radiotherapy. HDR intracavitary brachytherapy was made by the applicators type Fletcher tandem and ovoids. For each brachytherapy application the position $D_{0.1cc}$ was determined of the bladder and rectum that receive a brachytherapty dose. Then, based on the X, Y, and Z axis displacement, inter-application mean X, Y, and Z axis displacements were calculated as well as their displacement vectors (R). It has been analyzed whether there is statistically significant difference in inter-application displacement of the position of the brachytherapy dose $D_{0.1cc}$, D_{1cc} and D_{2cc} of the bladder and rectum. The ANOVA test and post-hoc analysis by Tukey method were used for testing statistical importance of differences among the groups analyzed. The difference among the groups analyzed was considered significant if $p < 0.05$.

Results. There are significant inter-application displacements of the position of the brachytherapy dose $D_{0.1cc}$, D_{1cc} and D_{2cc} of the bladder and rectum.

Conclusions. When we calculate the cumulative brachytherapy dose by summing up $D_{0.1cc}$, D_{1cc} and D_{2cc} of the organs at risk for all the applications, we must bear in mind their inter-application displacement, and the fact that it is less likely that the worst scenario would indeed happen.

Key words: inter-application variations; brachytherapy; inoperable cervical cancer

Introduction

Intra-cavitary brachytherapy has for decades been an obligatory type of the treatment of the locally advanced cervical cancer. The basic principles of brachytherapy are based in the traditional schools (Paris, Manchester, Stockholm, Fletcher, etc.); any are still dominant in planning the brachytherapy for the cervical cancer.[1,2] Verification of the applicator position, as well as of the organs at risk (the bladder and rectum, as well as the sigmoid for 3D brachytherapy) is done with the aim of optimizing the brachytherapy dose in order to achieve a complete distribution of the dose around the target volume, with maximum sparing of the organs at risk. The prescribing of the dose is made

by the standard Manchester system of the dose to the point A.[3] Nowadays, especially in the developed countries, CT (computer tomography) and MR (magnetic resonance) based brachytherapy is becoming standard in treating gynaecological tumours, particularly those locally advanced.[4-8] 3D MRI could potentially replace multiplanar 2D MRI in cervix cancer IGABT (image guided adaptive MRI based brachytherapy), shortening the overall MRI scanning time and facilitating the contouring process, thus making this treatment method more widely employed.[9] Intracavitary brachytherapy of cervical cancer consists of multiple applications, usually four to five. As recommended by the GEC-ESTRO work group, it is important for the 3D image guided adaptive MRI based brachytherapy of cervical cancer to verify what is the minimum dose received by the most irradiated 0.1 cm^3, 1 cm^3 and 2 cm^3 ($D_{0.1cc}$, D_{1cc} and D_{2cc}, respectively) of the bladder and rectum volume.[10] The doses received by organs at risk for all brachytherapy applications are summed up together with the external dose, and by using the linear-quadratic model, the total cumulative dose is determined.[11] In planning brachytherapy CT does not give us the possibility to precisely delineate tumour and plan the distribution of the therapy dose to the tumour (as is the case with MR planning). However, it is possible to obtain precise data on the contribution of the brachytherapy dose to the organs at risk.[12,13] Georg *et al.*, correlated the level of complications with the dose received by the above mentioned referential volumes of the organs at risk.[14] Recently, Hollowey *et al.* published the results including the application related variation of the dose received by the sigmoid, under the conditions that the same volume of sigma always receives the brachytherapy dose.[15] However, provided that there are inter-application displacements of $D_{0.1cc}$, D_{1cc} and D_{2cc} of the organs at risk, the question is how much of and which volume of the organs at risk receives the calculated cumulative dose for all the fractions? Does the worst case scenario exist at all?

The aim of our study was to examine on the CT basis the inter-application displacement of the positions $D_{0.1cc}$, D_{1cc} and D_{2cc} of the brachytherapy dose applied to the bladder and rectum of the patients with inoperable cervical cancer.

Patients and methods

This prospective study included the patients with cervical cancer FIGO IIb-IVa stage, who were treated by concomitant chemo-radiotherapy at the University Clinical Centre Tuzla, at the Department for Radiotherapy of the Clinic for Oncology, Haematology and Radiotherapy. The study was conducted on a consecutive sample of 30 patients treated in the period April 2010 – May 2012. The inclusion criteria were non-operated patients; brachytherapy was made with an intra-uterus applicator and two vaginal ovoids. The investigators followed recommendations of the Helsinki Declaration. The study protocol was approved by the ethic committees of the University Clinical Centre Tuzla.

The patients were treated by the external radiotherapy to the pelvis by the tumour dose (TD) 45 Gy in 25 fractions along with the concomitant chemotherapy with cisplatin with the dose of 40 mg/m^2. External radiotherapy was applied by the linear accelerator ElektaSinergy® and the energy of 15 MV. After 10 to 13 fractions of the external radiotherapy, intracavitary brachytherapy was started. The intracavitary brachytherapy was applied by the applicators type Fletcher tandem and ovoids, once a week at the high dose rate (HDR) regime with Iridium (^{192}Ir) on Flexitron®. Protocols for the rectum and bladder filling required that the patients took 20 mg bisacodyl laxative suppositories (Dulcolax®) 12 hours prior to every brachytherapy application and that they urinated immediately before every brachytherapy application. During every application, a tamponade towards the urinary bladder and rectum was made by the gauze soaked in the lopromide (Ultravist®) contrast liquid which was in 4 to 1 ratio with the physiological solution. The therapy dose of (TD 7 Gy) was determined in accordance to the Manchester system to the A point.

After each brachytherapy application (five in total), computer tomography of the pelvis was made. During every CT scan, on the previously marked referential spots needed for the external radiotherapy, 3-mm diameter small lead balls were fixated, and the patients were positioned in such a way that the referential marks corresponded to the laser coordinate system of the CT scanner. This way, patient's geometry was connected to the geometry of the CT scanner, fulfilling the condition that during each computer tomography scan the patient is in the same position.

After every computer tomography the delineation of organs at risk (the bladder and rectum) was made. The bladder and rectum delineation was made on every CT slice: for the rectum at 1 cm from the anus to the recto-sigmoid transition

TABLE 1. Patient demographics

Characteristics	Mean ± SD
Age	52 ± 11
Cancer stage FIGO	
IIb	24 (80%)
IIIb	5 (16.7%)
IVa	1 (3.3%)

FIGO = International Federation of Gynecology and Obstetrics; SD = standard deviation

through the entire thickness of the organ wall, and for the bladder following the outer contour of the entire organ volume. The planning of brachytherapy dose distribution for each application was made on the basis of computer tomography with the software system for planning Flexiplan Isodose Control®.

For each application $D_{0.1cc}$, D_{1cc} and D_{2cc} for the bladder and rectum were calculated. The above-mentioned planning system was used for the formation of co-ordinate system whose axes X (lateral), Y (antero-posterior), and Z (cranial-caudal) were lying on the referential marks (small lead balls), since they have a constant value and represent the pelvis as one co-ordinate system. In this co-ordinate system, for each application the position $D_{0.1cc}$ was determined for bladder and rectum. Considering the fact that $D_{0.1cc}$ is located in D_{1cc} and D_{2cc}, it therefore represents their position as well. Then, on the basis of X, Y, and Z axis displacements, the mean inter-application X, Y, and Z displacements were calculated, as well as their absolute displacements, that is displacement vectors (R). We analyzed whether there is a statistically significant difference in the inter-application displacement of the position of the brachytherapy dose $D_{0.1cc}$, D_{1cc} and D_{2cc} for the bladder and rectum between the planning for all applications in relation to the first application. A post-hoc analysis was made of the position displacement from one application to another.

In the statistical processing of the results, standard methods of descriptive statistics have been used (arithmetic mean with the standard deviation and the numerical range from minimum to maximum value). For testing the statistical significance of differences among the examined groups ANOVA test was used as well as the post-hoc analysis by Tukey. Statistical hypotheses were tested at the significance level of $\alpha = 0.05$, *i.e.* the difference p

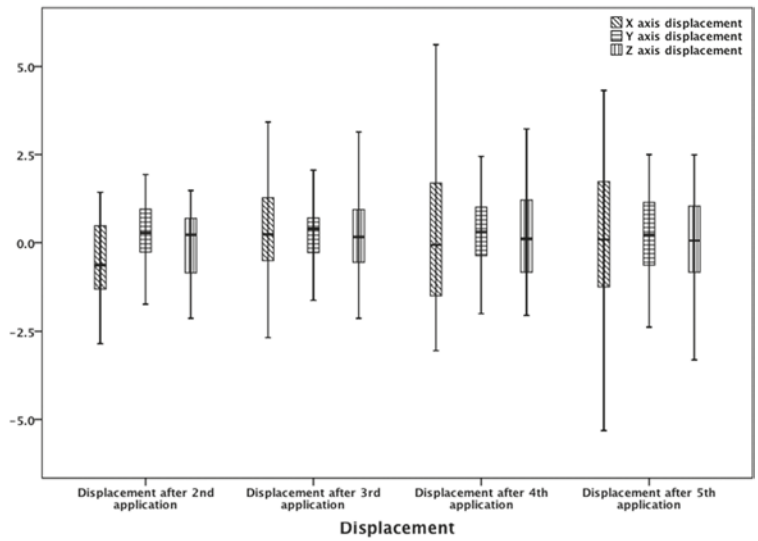

FIGURE 1. The mean values of the inter-application X, Y, and Z axis displacements of the brachytherapy dose on the bladder for each application in relation to the first one. Also, the figure shows the differences between every fraction individually. The results are given in centimetres (cm).

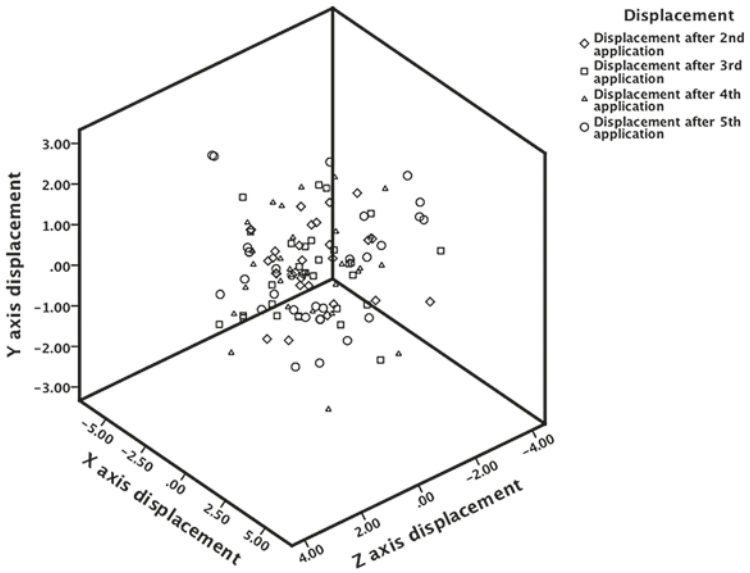

FIGURE 2. Absolute displacements, that is the vector of inter fraction displacements of the brachytherapy dose on the bladder given in centimetres for every fraction in relation to the first one, which is presented by the centre of the co-ordinate system.

< 0.05 was considered statistically significant. SPSS 17.0 (SPSS Inc, Chicago, IL) statistics software was used for the data analysis.

Results

Thirty patients were included in the study. A total of 150 brachytherapy applications were made.

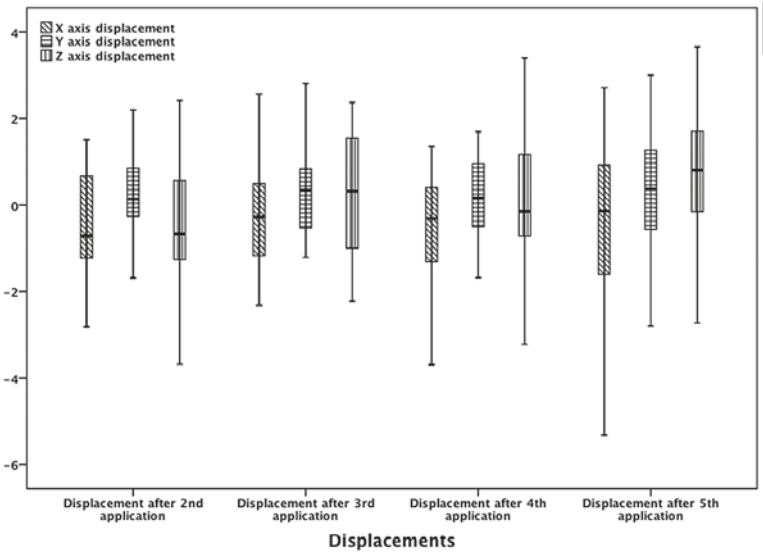

FIGURE 3. The mean values of the inter-application X, Y, and Z axis displacements of the brachytherapy dose on the rectum for each application in relation to the first one. Also, the figure shows the differences between every fraction individually. The results are given in centimetres (cm).

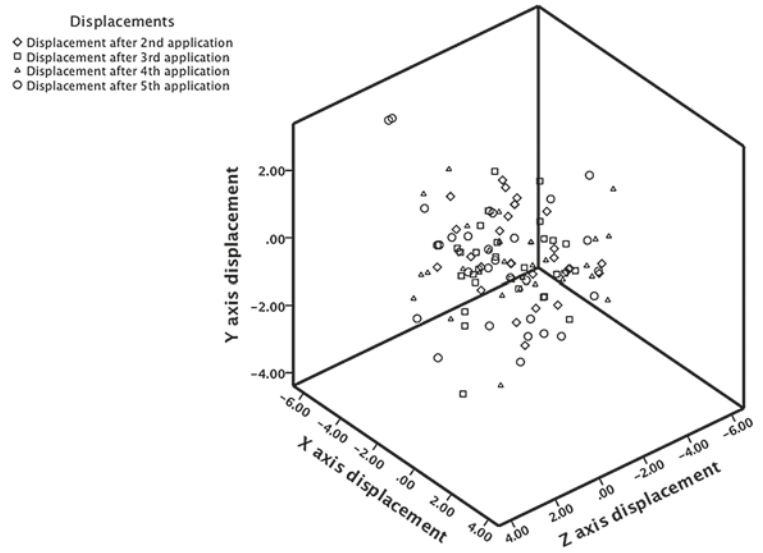

FIGURE 4. Absolute displacement that is the vector of interfraction displacements of the brachytherapy dose on the rectum given in centimetres for every fraction in relation to the first one, which is presented by the centre of the co-ordinate system.

Table 1 shows the patient demographics. The average age of the patients at the time of the treatment was 52, a most of them were at FIGO IIb stage of planocelular cervical cancer.

The results of the mean values of inter-application X, Y, and Z axis displacements of the brachytherapy dose on the urinary bladder for each application in relation to the first one are given in Figure 1 and Table 2. The absolute displacements, that is, their displacement vector is represented in a three-dimensional figure (Figure 2). The range of vector magnitude of the brachytherapy dose received by the referential volumes of the bladder was 1.95 to 2.83 cm. The post-hoc analysis by Tukey shows for the absolute displacement that the significant difference by ANOVA analysis is due to a statistically significant difference among absolute displacements after applications II and V; $p = 0.018$ (Table 2).

The results of the mean values of the inter-application X, Y, and Z axis displacements of the brachytherapy dose to the rectum for each application in relation to the first one are given in Figure 3 and Table 3, while the absolute displacements, that are their displacement vector, are shown in a three-dimensional figure (Figure 4). The range of vector magnitude of the brachytherapy dose received by the referential volumes of the rectum was 2.05 to 2.78 cm. The post-hoc analysis by Tukey shows for the absolute displacement that the significant difference by ANOVA analysis is due to a statistically significant difference among absolute displacements after applications II and V; $p = 0.038$ and applications III and V; $p = 0.023$ (Table 3).

Discussion

No publications currently available showing displacement of the brachytherapy dose received by the referential volumes of organs at risk from one application to another, for patients treated against inoperable cervical cancer. By analyzing the results of the average values of inter-application X, Y, and Z axis displacements of the brachytherapy dose on the bladder, which are shown in Figure 1 and Table 2, it can be noticed that the mean values of displacements are not of statistical significance. However, one should pay attention to minimum and maximum variations that are not irrelevant, especially on the X axis. Considering that the displacement of irregular three-dimensional volumes is analyzed in three-dimensional space, it is important to show the results of the absolute displacement, that is their vectors, in three-dimensional space.

Figure 2 shows a three-dimensional co-ordinate system which presents inter-application displacement vectors of the brachytherapy dose received by the referential volumes of the bladders. Besides the fact that it is evident that the vectors of the volumes analyzed do not overlap at a single point (and even if they did, they would probably not be-

TABLE 2. The mean values, standard deviation, and minimum and maximum X, Y, and Z axis displacement of the brachytherapy dose received by the referential volumes of the bladder, and their absolute displacement / intensity of the vector (R) are shown for all applications in relation to the first one. The values are given in centimetres

		Mean	SD	Minimum	Maximum
[1]X axis displacement	II-I applications	-.29	1.78	-2.85	5.38
	III-I applications	.42	1.71	-2.68	4.26
	IV-I applications	-.04	2.11	-3.05	5.62
	V-I applications	-.07	2.45	-5.32	4.32
[2]Yaxis displacement	II-I applications	.29	.80	-1.73	1.93
	III-I applications	.29	.99	-1.62	2.43
	IV-I applications	.29	1.10	-2.00	2.45
	V-I applications	.20	1.28	-2.38	2.50
[3]Zaxis displacement	II-I applications	-.05	1.00	-2.13	1.48
	III-I applications	.34	1.35	-2.13	3.14
	IV-I applications	.20	1.42	-2.05	3.23
	V-I applications	-.09	1.52	-3.31	2.49
[4]Vector magnitude (R)	II-I applications	1.95	1.03	.68	5.52
	III-I applications	2.18	1.10	.72	4.88
	IV-I applications	2.53	1.09	.74	5.63
	V-I applications	2.83	1.32	.74	5.63

SD = standard deviation; [1]p = 0.59; [2]p = 0.98; [3]p = 0.54; [4]p = 0.02

long to the same patient), this figure also shows the position of the referential volumes of the bladder in relation to the first application which represents the centre of the co-ordinate system, as well as the positions of volumes from one application to another. By observing the three-dimensional vectors of all the applications, the impression is that in the entire space they have a form of a ball. Statistically, a significant difference has been shown in inter-application displacements of the referential volumes of the bladder that receive the brachytherapy dose, and the difference between the second and fifth application is especially important (Table 2).

The displacements of the bladder during the transcutaneous radiotherapy have already been proved in the study by Ahmad R *et al.*, although the patients were in a prone position and immobilized by a belly board.[16]

The recommendations by the Gynaecological (GYN) GEC-ESTRO Working Group (IV) for MR imaging within the frame of image based adaptive cervix cancer brachytherapy suggest that prior to MR imaging a folley catheter is inserted, the urinary bladder is emptied, 50 ml of salt solution is injected, and then the procedure is repeated immediately before the very delivery of the brachytherapy dose.[17] During the preparation of the patients for brachytherapy in this study, a folley catheter was not inserted into the urinary bladder. The planning was not made on MRI basis, and the urinary bladder wall was clearly visible, especially the back side wall, as the gauze soaked in the Ultravist® contrast liquid clearly demarked the front vaginal fornix from the back wall of the bladder. The results of the mean values of inter-application X, Y, and Z axis displacements of the brachytherapy dose on the rectum, presented in Figure 3 and Table 3, show that there is no statistical significance. However, there are also extreme minimum and maximum values for all the axes, while the statistical significance for Z axis is at the level of P = 0.08. These extreme values of the displacements of the brachytherapy dose received by the referential volumes of the urinary bladder and the rectum which are obtained in this study are not that incomprehensible.

Namely, the measurements of the brachytherapy dose position are determined in relation to the centre of the co-ordinate system (whose axes lie on lead marks), which was positioned in the virtual centre of the pelvis, and not in relation to the brachytherapy applicator. This methodology was chosen with the aim to determine the real inter-ap-

TABLE 3. The mean values, standard deviation, and minimum and maximum X, Y, and Z axis displacement of the brachytherapy dose received by the referential volumes of the rectum, and their absolute displacement / intensity of the vector (R) are shown for all applications in relation to the first one. The values are given in centimetres

		Mean	SD	Minimum	Maximum
[1]X axis displacement	II-I applications	-.46	1.17	-2.82	1.51
	III-I applications	-.15	1.11	-2.32	2.56
	IV-I applications	-.39	1.67	-3.69	3.36
	V-I applications	-.44	2.07	-5.32	2.71
[2]Yaxis displacement	II-I applications	.24	1.01	-1.99	2.20
	III-I applications	.20	1.10	-3.13	2.81
	IV-I applications	.12	1.05	-2.71	1.69
	V-I applications	.37	1.48	-2.80	3.00
[3]Zaxis displacement	II-I applications	-.51	1.42	-3.68	2.41
	III-I applications	.18	1.50	-2.23	2.37
	IV-I applications	-.22	1.99	-4.55	3.40
	V-I applications	.52	1.55	-2.73	3.66
[4]Vector magnitude(R)	II-I applications	2.05	.77	.55	3.78
	III-I applications	2.01	.69	.23	3.74
	IV-I applications	2.48	1.31	.46	5.06
	V-I applications	2.78	1.22	.54	6.17

SD = standard deviation; [1]p = 0.87; [2]p = 0.87; [3]p = 0.08; [4]p = 0.012

plication displacements of the brachytherapy dose, given by all the possible factors combined. These factors include: inter-application displacements of the applicator position, inter-application displacements of the cervix and tumour, different degree of tamponing the vaginal fornicis, physiological movements, and changes in the volume of the rectum and bladder.

Figure 4 shows a three-dimensional co-ordinate system for the rectum, in which inter-application displacements are visible of the vector of the maximum brachytherapy dose received by the referential volumes. Statistically significant difference exists here, especially between the second and fifth application and the third and fifth application (Table 3). It is difficult to explain with certainty why the inter-application displacements of the brachytherapy dose received by the referential volume of the rectum are more frequent than those of the bladder volume. The reason may lie in the fact that the volume of the rectum, as the organ which can potentially receive a maximum brachytherapy dose, is bigger. Also, the rectum has a higher possibility of drastically changing its volume due to gases. Haripotepornkul *et al.* analyzed both inter and intra-fraction displacements of the cervix during the IMRT, and, as one of the reasons for the cervix displacement they stated the gases, which at a certain point lead to a higher exposure of the rectum to the therapy dose.[18] Other authors noticed this problem as well, but they also concluded that it is not easy to solve, as the application of laxatives is not efficient since it only decreases the solid matter in the rectum.[19,20]

Physiological movements of the intestines, that is, peristaltic, can be one of the factors which, during the brachytherapy treatment, lead to the displacement of the brachytherapy dose on the rectum wall. Physiological movements of the intestines can be reduced by the application of intravenous and intramuscular drugs, as in the preparation of the MRI based "image guided" adaptive brachytherapy of the cervical cancer.[16] However, it has not been examined to what extent it affects the inter-application displacement of the brachytherapy dose on the front wall of the rectum.

The disadvantage of this study is that the displacement of $D_{0,1cc}$ represented the displacement D_{1cc} and D_{2cc}. However, $D_{1cc,}$ and especially D_{2cc} are extremely irregular volumes that change their shape from one application to another. Right now, the literature does not contain a published meth-

odology that might analyze this problem in a more appropriate way in terms of three-dimensional view. Therefore, to analyze them as dotted structures ($D_{0,1cc}$) is currently closest to the truth for this type of research.

Conclusions

During the brachytherapy of the inoperable cervical cancer, there is a significant inter-application displacement of the positions$D_{0.1cc}$, D_{1cc} and D_{2cc} of the bladder and rectum. When we calculate the cumulative brachytherapy dose by summing up $D_{0.1cc}$, D_{1cc} and D_{2cc} of the organs at risk for all the applications, we must bear in mind their inter-application displacement, as well as the fact that it is less likely that these volumes indeed received the calculated dose. That means that it is less likely that the worst case scenario shall indeed happen. Planning the brachytherapy of the inoperable cervical cancer on the basis of computer tomography is required for every application during the brachytherapy treatment.

Acknowledgments

Thank Dr. Umesh Mahantshetty for internal review of the manuscript.

References

1. Jürgenliemk-Schulz IM, Lang S, Tanderup K, de Leeuw A, Kirisits C, Lindegaard J, et al. Gyn GEC ESTRO network. Variation of treatment planning parameters (D90 HR-CTV, D 2cc for OAR) for cervical cancer tandem ring brachytherapy in a multicentre setting: comparisonof standard planningand 3D image guided optimisation based on a joint protocol for dose-volume constraints. *Radiother Oncol* 2010; **94:** 339-45.
2. Segedin B, Gugic J, Petric P. Uterine perforation – 5-year experience in 3-D image guided gynaecological brachytherapy at Institute of Oncology Ljubljana. *Radiol Oncol* 2013; **47:** 154-60.
3. Perez CA, Kavanagh BD. Uterine cervix. In: Halperin EC, Perez CA, Brady LW, editors. *Principles et practice of radiation oncology.* 5th edition, Philadelphia: Lippincott Williams & Wilkins; 2008. p. 1532-609.
4. Gerbaulet A, Pötter R, Haie-Meder C. Cervix cancer. In: Gerbaulet A, Pötter R, Mazeron JJ, Meertens H, Van Limbergen E, editors. *GECESTRO handbook of brachytherapy*. Brussels: ESTRO; 2002. p. 301-63.
5. Weitmann HD, Pötter R, Waldhäusl C, Nechvile E, Kirisits C, Knocke TH. Pilot study in the treatment of endometrial carcinoma with 3D image-based high-dose-rate brachytherapy using modified Heyman packing: clinical experience and dose-volume histogram analysis. *Int J Radiat Oncol Biol Phys* 2005; **62:** 468-78.
6. Lindegaard JC, Tanderup K, Nielsen SK, Haack S, Gelineck J. MRI-guided 3D optimization significantly improves DVH parameters of pulsed-dose-rate brachytherapy in locally advanced cervical cancer. *Int J Radiat Oncol Biol Phys* 2008; **71:** 756-64.
7. Rogelj P, Hudej R, Petric P. Distance deviation measure of contouring variability. *Radiol Oncol* 2013; **47:** 86-96.
8. De Brabandere M, Mousa AG, Nulens A, Swinnen A, Van Limbergen E. Potential of dose optimisation in MRI-based PDR brachytherapy of cervix carcinoma. *Radiother Oncol* 2008; **88:** 217-26.
9. Petric P, Hudej R, Rogelj P, Blas M, Segedin B, Logar HB, Dimopoulos JC. Comparison of 3D MRI with high sampling efficiency and 2D multiplanar MRI forcontouring in cervix cancer brachytherapy. *Radiol Oncol* 2012; **46:** 242-51.
10. Pötter R, Haie-Meder C, Van Limbergen E, Barillot I, De Brabandere M, Dimopoulos J, et al. GEC ESTRO Working Group. Recommendations from gynaecological (GYN) GEC ESTRO working group (II): concepts and terms in 3D image-based treatment planning in cervix cancer brachytherapy-3D dose volume parameters and aspects of 3D image-based anatomy, radiation physics, radiobiology. *Radiother Oncol* 2006; **78:** 67-77.
11. Lang S, Kirisits C, Dimopoulos J, Georg D, Pötter R. Treatment planning for MRI assisted brachytherapy of gynecologic malignancies based on total dose constraints. *Int J Radiat Oncol Biol Phys* 2007; **69:** 619-27.
12. Datta NR. From 'points' to 'profiles' in intracavitary brachytherapy of cervical cancer. *Curr Opin Obstet Gynecol* 2005; **17:** 35-41.
13. Viswanathan AN, Dimopoulos J, Kirisits C, Berger D, Potter R. Computed tomography versus magnetic resonance imaging-based contouring in cervical cancer brachytherapy: results of a prospective trial and preliminary guidelines for standardized contours. *Int J Radiat Oncol Biolo Phys* 2007; **69:** 963-4.
14. Georg P, Kirisits C, Goldner G, Dorr W, Hammer J, Potzi R, et al. Correlation of dose-volume parameters, endoscopic and clinical rectal side effects in cervix cancer patients treated with definitive radiotherapy including MRI-based brachytherapy. *Radiother Oncol* 2009; **91:** 173-80.
15. Holloway CL, Racine ML, Cormack RA, O'Farrell DA, Viswanathan AN. Sigmoid dose using 3D imaging in cervical-cancer brachytherapy. *Radiother Oncol* 2009; **93:** 307-10.
16. Ahmad R, Hoogeman MS, Quint S, Mens JW, de Pree I, Heijmen BJ. Interfraction bladder filling variations and time trends for cervical cancer patients assesed with portabile 3-dimensional ultrasound bladder scanner. *Radiother Oncol* 2008; **89:** 172-9.
17. Dimopoulos JC, Petrow P, Tanderup K, Petric P, Berger D, Kirisits C, et al. Recommendations from Gynaecological (GYN) GEC-ESTRO Working Group (IV): Basic principles and parameters for MR imaging within the frame of image based adaptive cervix cancer brachytherapy. *Radiother Oncol* 2012; **103:** 113-22.
18. Haripotepornkul NH, Nath SK, Scanderbeg D, Saenz C, Yashar CM. Evaluation of intra- and inter-fraction movement of the cervix during intensity modulated radiation therapy. *Radiother Oncol* 2011; **98:** 347-51.
19. Lim K, Kelly V, Stewart J, Xie J, Cho YB, Moseley J, et al. Pelvic radiotherapy for cancer of the cervix: is what you plan actually what you deliver? *Int J Radiat Oncol Biol Phys* 2009; **74:** 304-12.
20. van de Bunt L, van der Heide UA, Ketelaars M, de Kort GA, Jürgenliemk-Schulz IM. Conventional, conformal, and intensity-modulated radiation therapy treatment planning of external beam radiotherapy for cervical cancer: The impact of tumor regression. *Int J Radiat Oncol Biol Phys* 2006; **64:** 189-96.

research article

Preoperative radiotherapy for rectal cancer: a comparative study of quality control adherence at two cancer hospitals in Spain and Poland

Magdalena Fundowicz[1], Miguel Macia[2], Susanna Marin[2], Marta Bogusz-Czerniewicz[3], Ewelina Konstanty[4], Ignaci Modolel[5], Julian Malicki[4,6], Ferran Guedea[2]

[1] Department of Radiotherapy, Greater Poland Cancer Centre, Poznan, Poland
[2] Department of Radiotherapy, Catalan Institute of Oncology, L'Hospitalet de Llobregat, Spain
[3] Department of Training, Scientific Cooperation and Quality Assurance, Greater Poland Cancer Centre, Poznan, Poland
[4] Department of Medical Physics, Greater Poland Cancer Centre, Poznan, Poland
[5] Department of Catalan Institute of Oncology, L'Hospitalet de Llobregat, Spain
[6] Department of Electroradiology, University of Medical Sciences, Poznan, Poland

Radiol Oncol 2014; 48(2): 210-218.

Received 18 November, 2013
Accepted 14 February, 2014

Correspondence to: Magdalena Fundowicz, M.D., Department of Radiotherapy, Greater Poland Cancer Centre, Garbary15, 60-866 Poznan, Poland. E-mail: magdalena.fundowicz@gmail.com

Disclosure: No potential conflicts of interest were disclosed.

Background. We performed a clinical audit of preoperative rectal cancer treatment at two European radiotherapy centres (Poland and Spain). The aim was to independently verify adherence to a selection of indicators of treatment quality and to identify any notable inter-institutional differences.

Methods. A total of 162 patients, in Catalan Institute of Oncology (ICO) 68 and in Greater Poland Cancer Centre (GPCC) 94, diagnosed with locally advanced rectal cancer and treated with preoperative radiotherapy or radiochemotherapy were included in retrospective study. A total of 7 quality control measures were evaluated: waiting time, multidisciplinary treatment approach, portal verification, *in vivo* dosimetry, informed consent, guidelines for diagnostics and therapy, and patient monitoring during treatment.

Results. Several differences were observed. Waiting time from pathomorphological diagnosis to initial consultation was 31 (ICO) *vs.* 8 (GPCC) days. Waiting time from the first visit to the beginning of the treatment was twice as long at the ICO. At the ICO, 82% of patient experienced treatment interruptions. The protocol for portal verification was the same at both institutions. *In vivo* dosimetry is not used for this treatment localization at the ICO. The ICO utilizes locally-developed guidelines for diagnostics and therapy, while the GPCC is currently developing its own guidelines.

Conclusions. An independent external clinical audit is an excellent approach to identifying and resolving deficiencies in quality control procedures. We identified several procedures amenable to improvement. Both institutions have since implemented changes to improve quality standards. We believe that all radiotherapy centres should perform a comprehensive clinical audit to identify and rectify deficiencies.

Key words: clinical audit; quality control; preoperative radiotherapy

Introduction

In recent years, interest in improving the quality and efficiency of cancer care delivery has become increasingly urgent as health care costs have surged along with increased demand from an aging population. In 1999, a report entitled "Ensuring Quality Cancer Care" published by the Institute of Medicine in the United States described numerous quality control issues in cancer care.[1] A major recommendation of the report was the need to establish a system to measure and monitor quality of care through the use of core set of indicators. In Europe, the European Union published a directive

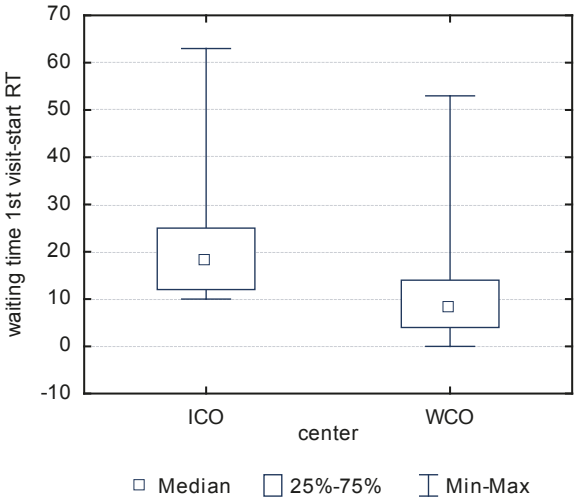

FIGURE 1. Waiting time from the first visit to start the treatment. RT = radiotherapy

requiring that the implementation of clinical audits to improve quality in radiation medicine.[2,3] Quality assessment through a system of indicators is still a relatively recent practice in radiotherapy and there is limited published research in this area. However, two recent studies in Italy, one by Cionini *et al*. and another by *the Instituto Superiore di Sanità* have attempted to establish quality indicators for radiotherapy.[4,5]

Given the relative paucity of quality control studies in radiotherapy, we decided to carry out a clinical audit of preoperative rectal cancer treatment at our two institutions, the Greater Poland Cancer Centre (GPCC) in Poland and the Catalan Institute of Oncology (ICO) in Spain.

The aim of this study was to select a set of relevant quality control measures and then determine institutional adherence to these standards in order to improve quality at our own institutions.

Methods

We elected to use colorectal cancer to perform this clinical audit for 3 reasons: 1) In Europe, colorectal cancer is among the most common cancers, accounting for 436,000 cases (13.6% of the total) [6]; 2) Both institutions in this study treat large numbers of patients for this disease; 3) Given the high incidence and mortality rates for rectal cancer, any improvements in our quality control procedures would have a large positive impact on a large numbers of patients. All of these factors made rectal cancer treatment an ideal process for comparison.

TABLE 1. Quality control indicators evaluated

#1: Waiting time and compliance
1.1 Time from pathological diagnosis to initial consultation.
1.2 Time from the first visit to start the treatment
1.3. Existence of protocol for unplanned curative treatment interruptions
1.4 Compliance to the prescribed overall treatment time.
#2: Existence of a multidisciplinary treatment approach
#3: Portal Verification
3.1 Existence of protocol for periodic verification of treatment fields
3.2. Number of portal verifications per preoperative course of radiotherapy
#4: Informed consent
4.1 Existence of signed consent form in patient records
4.2 Availability of detailed information about treatment & side-effects
#5. In vivo dosimetry
5.1 Existence of protocol and recommendations for checking the entrance dose
5.2 Number of in vivo dosimetric verifications per preoperative course of radiotherapy.
#6: Guidelines used for diagnostics and therapy.
#7. Monitoring & review of rectal cancer patients during the treatment period.

Selection of quality indicators and standards

The aim of any quality assessment is to provide feedback on meaningful and interpretable measures, including cost-effectiveness.[7,8] Cionini *et al.* recently performed a review of the scientific literature, including guidelines and national regulations, to select quality indicators based on the scientific literature to assure the highest strength of evidence. For this reason, we selected from the quality control indicators described by Cionini, choosing those most relevant to colorectal cancer. The following indicators were selected: 1) waiting times; 2) multidisciplinary treatment approach; 3) portal verification; 4) informed consent; 5) *in vivo* dosimetry; 6) diagnostic & therapeutic guidelines; and 7) monitoring & review of patient during treatment. Table 1 provides a description of these indicators.

Clinical audit

The clinical audit was performed as a 5-step process. First, each institution selected a multidisciplinary quality evaluation team consisting of departmental staff with experience in quality assurance. The 4-person GPCC team was composed of 1 radiation oncologist, 2 medical physicists, and 1 quality manager. The 4-person ICO team included 2 radiation oncologists (one of whom was assigned

the role of "quality manager"), 1 medical physicist, and 1 statistician.

We used the International Atomic Energy Association (IAEA) QUATRO questionnaire as a model for our own modified survey.[6] A checklist was created to organize the audit program and to ensure coverage of all relevant topics. To ensure objectivity, the 2-day on-site clinical audits were performed exclusively by the visiting institution's team, who collected all necessary data on current local practices. All clinical audits were performed in the year 2008 by a 2- or 3-person team consisting of one radiation oncologist (two in the case of the ICO) and a medical physicist. The working language of the audit was English.

The clinical audit was performed as follows: a) audit preparation (appointment of auditing team, review of the background information prepared by the institution to be audited, and preparation of the audit program); b) entrance briefing: to introduce the auditors to the various staff members and to discuss the methods, objectives and details of the audit; and c) assessment: on-site clinical audit.

During the audit, staff members were interviewed about work practices and approaches, the facilities were inspected and all procedures and relevant documentation (including treatment records of the rectal cancer patients included in the study) were reviewed. In addition, the auditors observed directly the practical implementation of working procedures during the 2-day audit, including as many aspects of the patient treatment process (initial patient examination, diagnosis, evaluation, staging, treatment planning and delivery, and follow up) as feasible. An exit briefing was performed to give the host institution preliminary feedback.

Patients and treatments

Patient inclusion criteria were as follows: locally advanced cancer of the middle and lower rectum diagnosed and treated with preoperative radiotherapy or radiochemotherapy during the year 2008. A total of 162 patients were evaluated (ICO=68; GPCC=94). All patients at the ICO underwent preoperative radiochemotherapy, as did 9 of the 94 patients from the GPCC; the remaining 85 GPCC patients received preoperative radiotherapy alone. All patients at both institutions were clinical stage T3/4 N-/+.

Preoperative radiotherapy was delivered using a high-energy linear accelerator (18 or 20 MV) with multileaf collimators and 3D treatment planning. All patients were treated in prone position with full bladder. At the GPCC, most patients were treated with a belly board for small bowel displacement. Three field technique to 25 Gy (5 Gy per day) at the GPCC or 45 Gy in 25 fractions (1.8 Gy per day) followed by a boost of 5.4 Gy in 3 fractions at the ICO and GPCC (9 patients).

Surgery was performed 6-8 weeks after completion of combined radiochemotherapy (ICO) or during the first week after completion of preoperative radiotherapy (GPCC). The definitive surgical technique included low anterior resection, abdominal-perineal resection (Miles technique), Hartmann resection or tumour excision. Most patients at both institutions underwent surgery following completion of radiotherapy.

Portal imaging was performed on the first day of treatment at both institutions. Following protocol, in most cases (85 patients) treated at the Polish centre, only one portal check was necessary due to the short duration of radiotherapy (5 days). In patients who underwent combined radiochemotherapy, portal checks were performed every 10 days (and prior to the boost) at both institutions due to the longer treatment duration.

Clinical protocols at both institutions call for a deviation no greater than 5 mm. If deviations were considered excessive, corrections were made and the portal repeated. ICO performs either electronic or film portal depending on the accelerator, whereas only electronic portal imaging is available at the GPCC. The portal images are evaluated by a physician at the ICO while either a physicist or technician performs this function at the GPCC. Documentation from portal verification is available on the hospital network at the ICO or in the patient treatment chart (GPCC).

In vivo dosimetry was offered only at the GPCC, where it is performed in all cases before the first session, in the middle of the radiotherapy course, after treatment plan change, or on request of physician or physicist. Deviations between measured and expected dose were considered acceptable when they were less than 5% for open fields and 7% for wedged fields.

Indicators

We evaluated seven different indicators (some with sub-indicators), described in Table 1.

Statistical analysis

This was primarily a descriptive study. Quantitative data were analyzed using the Statistica PL 8.0

TABLE 2. Portal imaging

	Acceptable N (%)	Unacceptable N (%)	Not performed N (%)
ICO	35 (51%)	31 (46%)	2 (3%)
GPCC	78 (83%)	15 (16%)	1 (1%)

N = number; ICO = Catalan Institute of Oncology; GPCC = Greater Poland Cancer Centre

TABLE 3. Percent of patient medical records containing a signed informed consent form

	ICO		GPCC	
Informed consent	Pts	[%]	Pts	[%]
Yes	61	89.7	94	100
No	7	10.3	0	0

ICO = Catalan Institute of Oncology; GPCC = Greater Poland Cancer Centre; Pts = patients

Statistical Software Package (StatSoft, Poland). Since numerical variables did not follow normal distribution, comparison between the two groups was performed using the Mann-Whitney U-test. The results of numerical data were expressed as median and range. Qualitative data were analyzed using Chi-square test of independence or, in cases in which zero observed frequencies occurred, the Fisher exact test. Statistical significance was established at $p<0.05$ in all the analyses.

Results

Indicator #1. Waiting times and compliance to treatment duration

Waiting time from pathomprphological diagnosis to initial consultation.

The average length of waiting time for this indicator was 31 days at the ICO *vs*. 8 days for the GPCC, a significant difference (p<0.0001) Medians and range were 28.5 [87] and 5 [36] for ICO and GPCC, respectively.

Waiting time from the first visit to start the treatment. The average waiting time at the ICO is twice that (18 [53] *vs*. 8 [53]) of the GPCC, a significant inter-institutional difference (p<0.0001).

Existence of protocol for unplanned curative treatment interruptions. At the time of the audit, only the ICO had a protocol in place to compensate for unplanned interruptions of curative radiotherapy. The GPCC had no guidelines and compensation was *ad hoc* on a case by case basis.

Compliance to the prescribed overall treatment time: treatment interruptions. Most (85 of 94) GPCC patients underwent radiotherapy alone (without chemotherapy). As a result, the total radiotherapy treatment duration was 5 days (1 fraction/day), and no interruptions were recorded in these 85 patients. In contrast, treatment delivery time was considerably longer in the patients who underwent combined chemoradiotherapy (all 68 patients at the ICO and 9 patients at the GPCC). In these cases, radiotherapy consisted of 25 or 28 fractions delivered over a 33-day period. Of the 68 ICO patients who underwent combined chemoradiotherapy, 56 (82%) experienced treatment interruptions (mainly due to toxicity, machine malfunctions, holidays or unplanned quality control checks) versus 0 out of 9 cases (0%) at the GPCC. This large difference (82% *vs*. 0%) is notable but should not be considered significant given the small sample size (only 9 cases) at the GPCC.

Indicator #2. Existence of a multidisciplinary treatment approach

At the time of study, the ICO had an established protocol for reviewing complex cases at a weekly interdisciplinary tumour board. No such protocol was in place at the GPCC. As per the ICO protocol, cases considered standard were not referred to the tumour board. Of the 68 patients at the ICO, 44 were referred to the interdisciplinary tumor board, while 24 (35%) were not.

Indicator #3. Portal verification

Existence of protocol/recommendations for periodic verification of treatment fields. Both institutions had a protocol in place at the time of the study. Portal imaging is performed at both institutions on the first day of treatment. In the 85 patients who underwent radiotherapy alone at the GPCC, only one portal check was performed due to the short treatment time (1 fraction/day for 5 days). Portal checks for patients undergoing chemoradiotherapy were performed every 10 days at both institutions due to the longer treatment duration (25 fractions over 33 days). Portal checks were also performed before the boost.

Number of portal verifications per preoperative course of radiotherapy. Table 2 shows the number

of patients for whom portal images were considered acceptable, unacceptable, or not performed. If deemed unacceptable due to deviations greater than those set by the protocol, the image was corrected and portal verification was repeated.

Indicator #4. Informed consent & additional explanatory material

Informed consent. After verifying patient records, we found that the informed consent form was available for all GPCC patients whereas at the ICO, the signed forms were missing in 7 cases, a significant inter-institutional difference (p=0.0019).

Existence of a form, booklets, films and other supporting materials. Both institutions provided additional, detailed information. In the case of the ICO, detailed, specific information about the treatment was included in the informed consent form. At the GPCC, the patients were given a brochure with general information and a video with more detailed information.

Indicator #5. In vivo dosimetry

Existence of a protocol and its content/recommendations for checking the entrance dose. At the time of study, only the GPCC had a protocol in place (as required by Polish law). *In vivo* dosimetry is not used for rectal cancer at the ICO.

Number of verifications (in vivo dosimetry) per preoperative course of radiotherapy. In vivo dosimetry was performed on the 2nd or 3rd day of the treatment at the GPCC. Of the 94 patients at the GPCC, *in vivo* dosimetry was considered acceptable in 80 cases and unacceptable in 14. In these 14 cases, the dosimetry was recalculated to reach acceptable levels.

Indicator #6. Guidelines for diagnostics and therapy

The GPCC follows the National Comprehensive Cancer Network (NCCN) guidelines for diagnosis and treatment of colorectal cancer.[9] In contrast, the ICO uses locally-developed guidelines based largely on international guidelines (including the NCCN), but with some modifications as established by the hospital tumor board.

At both institutions, patients undergo digital rectal exam to determine eligibility for surgery. Subsequent assessment may include (depending on the institutional protocol) the following: colonoscopy with tumour biopsy, physical examination, chest and abdominal-pelvic CT, chest X-ray, pelvic MRI, endoscopic ultrasound, and blood tests. All GPCC patients underwent x-ray examination versus 50% of patients at the ICO.

Indicator #7. Review of rectal cancer patients during the treatment

At both institutions, patients receiving radiotherapy are reviewed once a week by a radiation oncologist. If problems are found, additional examinations/reviews are possible. This review process is governed by the protocols in place at both institutions.

Discussion

The results of this study reveal that both institutions had some deficiencies in adherence to the quality indicators chosen for preoperative radiotherapy for rectal cancer. These findings confirm the need for independent audits in radiotherapy to identify deviations from good practice and to harmonize and determine what good practice is. In the paragraphs that follow, we contextualize our findings for each of the 7 indicators evaluated.

Waiting times

Waiting times at the ICO were significantly longer for both variables (time from pathological diagnosis to first visit, and time from first visit to treatment). The wait from the first visit with the radiation oncologist to treatment at the ICO was double that of the GPCC. The reasons for these variations are many, but we suspect that main difference is that the sources of patient referrals to the ICO are much more heterogeneous than at the GPCC. In Spain, staging is performed by the radiation oncologist so that if any additional tests need to be requested, the start of treatment will be delayed. In many countries (including Poland), staging is performed before the patient is referred to the radiation oncologist; as a result, treatment can begin sooner.

Waiting times are perhaps among the most important quality variables and it is well-known that excessive waits can impact the results of treatment.[10-12] Clearly, the main risk of increased waiting times is the possibility of tumour growth and metastasis.

TABLE 4. Type of examination (%)

	Digital rectal exam	Colonoscopy	Ultrasound		Computed Tomography			MRI
			Abdomen	Transrectal	Pelvis	Abdomen	Chest	
ICO	100%	100	0	85.3	98.5	98.5	64.7	89.7
GPCC	100%	100	100	3.2	12.8	23.4	0	21.3

MRI = magnetic resonance imaging; ICO = Catalan Institute of Oncology; GPCC = Greater Poland Cancer Centre

Although no standard waiting times have yet been established, the National Health Service of the United Kingdom published a cancer plan that called for waits of no more than 1 month between referral by the general practitioner to the start of treatment.[13] We believe, based on our experience and a literature review, that an optimal maximum waiting time should not exceed 21 days from first visit to start of treatment. Using these guidelines, both the ICO and the GPCC treated the patients in a timely manner, despite the large differences between the two institutions.

Treatment interruptions

Treatment interruptions are another important indicator of quality that can have a marked effect on outcomes.[14-16] The usual causes of interruptions include machine malfunction or maintenance, toxicity, holidays, or unplanned quality control checks. In such cases, it is essential to have a protocol in place to compensate for the interruption. At the time of our study, the ICO had a well-established comprehensive protocol to guide compensation for unplanned interruptions of curative radiotherapy. The GPCC had no established protocol at the time of the audit, although that has since been remedied.

We found important differences between the two hospitals in treatment interruptions, mainly because there were none at the GPCC. The GPCC patients received a short-course of radiotherapy (5 fractions in 5 days), while all 68 of the ICO patients (and only 9 GPCC patients) underwent an extended course of 25 fractions delivered in 33 days. For this reason, we can only reasonably compare results from the two groups who underwent a similar radiotherapy schedule. Unfortunately, the number of GPCC patients who received this schedule was too small (9 patients) for meaningful comparisons. Nevertheless, it is important to note that 82% of patients at the ICO experienced a treatment interruption. We know that treatment interruptions are a common occurrence in radiotherapy. This indicates an important quality control issue (poor record-keeping) that needs to be resolved.

In terms of this indicator, both institutions were found wanting: the GPCC for lack of a written protocol, and the ICO for failing to record the cause and responses to interruptions.

Multidisciplinary approach

In recent years, more and more medical societies and institutions have come to accept the importance of using a multidisciplinary approach in cancer care to provide patients with optimal treatment for their specific characteristics.[17-20] In this audit, we found that 35% of patients at the ICO were not presented to the board. However, this does not necessarily indicate a quality failure because the in-house protocol states that only unusual or complicated cases need to be brought to the board. Therefore, we must assume that those 35% of patients were considered standard cases (i.e., no unusual conditions). However, steps must be taken to assure, in the future, that this information is added to the patient records.

The GPCC was considered deficient in this category because no interdisciplinary treatment board was in place at the time of this audit. Fortunately, in this case the audit served its purpose, as the GPCC instituted a multidisciplinary approach in 2009.

Portal verification

Portal Film or EPID (Electronic Portal Imaging Detection) is commonly used to evaluate the accuracy of the patient's set up and of the field shape and geometry with respect to the treatment plan. Repeated verifications during treatments are aimed at controlling the stability and the reproducibility of treatment conditions. The relevance of this procedure varies for different treatments and consequently it is suggested to stratify the standard in relation to the treatment objective.

Our results showed that 3 patients at the ICO did not have a portal verification. The reason for

this is not clear, but may be simply due to a failure to record the values in the patient records. However, this is a clear quality control failure that must be rectified. In contrast, all GPCC patients had the necessary verifications and adjustments when necessary.

Informed consent

At the ICO, there were 7 cases in which we were unable to locate the informed consent form (versus no cases at the GPCC). While it is possible that these forms were never collected, we suspect that they were simply misplaced or lost.

In both countries the law requires that patients receive and sign an informed consent form prior to treatment. This is a basic patient protection method used in most countries.[21] However, the fact that a patient signs the form does not necessarily mean he/she understands the treatment, as many patients will readily sign any document presented by the physician. One particularly shocking example of this was described by Byrne *et al*., who found that of 100 patients who underwent surgery, 27 did not know which organ had been treated.[22] For this reason, we believe that patients should be given the information in a variety of formats, in addition to the legally required informed consent form. Aside from the informed consent form and a verbal explanation from the physician and/or nurse, we recommend that patients be given user-friendly brochures and videos that explain the treatment in an easy to understand way. We believe that our institutions should attempt to standardize the provision of information to patients, especially in providing written, treatment-specific information about the procedure and its expected outcomes and side-effects.

In vivo dosimetry

In vivo dosimetry is a technique that uses semiconductors to ensure the calculated and measured doses are similar. It is used mainly for complex techniques and is useful for detecting rare cases of over- or underdosing.[23,24] Although the routine use of *in vivo* dosimetry to prevent dosing errors may seem to be an obvious quality control measure, many centres do not use it. At present, *in vivo* dosimetry is not considered standard because there are doubts about its costs, time requirements, and clinical role, particularly in certain cancer localizations.[25-27] For this reason, many centers prefer not to use it for routine procedures, especially because modern linear accelerators are believed to be more reliable and accurate than older ones. However, several authors continue to insist on the importance of *in vivo* dosimetry, notably Williams and McKenzie, who wrote an impassioned plea for its generalized use.[28] However, we agree with the conclusions of a study by the Royal College of Radiologists in the UK, which stated that while *in vivo* dosimetry should be used at the beginning of treatment for most patients, each department should develop its own protocol.[29] For the moment, the differences observed between protocols at our two institutions serve to illustrate the debate about the benefits of *in vivo* dosimetry for this localization and technique.

Guidelines for diagnostics and therapy

Few would argue about the value of clinical guidelines provided that these have been prepared by expert groups and based on the best available evidence and practices. The benefit are many, as guidelines serve to standardize best practices, guide less-experienced physicians, and use evidence-based strategies.[30,31] The ICO prefers to use locally-developed guidelines, which are based on and similar to international guidelines such as the NCCN. After performing this audit and seeing the merits of using guidelines tailored for a specific population and resources, staff at the GPCC began to develop their own local guidelines.

Feedback to project partners

We performed this audit with a number of objectives in mind. The first and most important was to improve quality at our institutions. By identifying deficiencies in our processes, we hoped to eliminate these and so improve our results. We also wanted to contribute to the establishment of quality control indicators for radiotherapy and for a standard audit process.

Upon completion of the audit, both audit teams drafted a report of their findings. The results were discussed at a joint meeting, during which we discussed the deficiencies and agreed on joint standards based on the results of our clinical audit and a literature review.

To close the audit cycle, each institution began the process of implementing the newly-agreed standards. The intention is to perform a second audit in the future to verify the actual results of this process and to determine the effectiveness and usefulness of the new standards and improvements.

This was a retrospective study with a relatively small sample. Moreover, for both institutions, this was our first experience in performing a clinical audit for quality control.

Conclusions

We believe that external audit programs such as ours can help to improve both patient safety and quality of care and this is why the IAEA has called for the development of comprehensive quality control programs for radiotherapy.[32-35] However, there is still a glaring lack of experience in radiotherapy.

Performing a clinical audit is a time-consuming and labour-intensive process. However, despite the time and expense involved, the results have more than compensated the efforts. As a result of this study, both institutions have benefitted as we have identified numerous areas to target for improvement, which we hope will lead to better quality treatments and results. Moreover, the procedures developed here for rectal cancer can be adapted to improve treatment of other tumour localizations.

Our experience has also shown us that the road ahead will not be easy. Even in colorectal cancer, in which treatment is generally quite standardized, we still found a large gap between two similarly structured European hospitals. We believe that an independent external clinical audit is an excellent method of identifying and rectifying deficiencies in quality control procedures.

Acknowledgements

We would like to recognize help of Bradley Londres in editing the article.

The study was supported by the grant provided by the Greater Poland Cancer Centrem (ref. # 19/05/2009/ZFM/GPCC/0004).

References

1. Smith TJ, Hillner BE. Ensuring quality cancer care by the use of clinical practice guidelines and critical pathways. *J Clin Oncol* 2001; **19:** 2886-97.
2. Shortt K, Davidsson L, Hendry J, Dondi M, Andreo P. International perspectives on quality assurance and new techniques in radiation medicine: outcomes of an IAEA conference. *Int J Radiat Oncol Biol Phys* 2008; **71:** S80-4.
3. Cerezo L, Ciria JP, Arbea L, Linan O, Cafiero S, Valentini V, et al. Current treatment of rectal cancer adapted to the individual patient. *Rep Pract Oncol Radiother* 2013; **18:** 353-62.
4. Cionini L, Gardani G, Gabriele P, Magri S, Morosini PL, Rosi A, et al. Quality indicators in radiotherapy. *Radiother Oncol* 2007; **82:** 191-200.
5. Working Group "Assicurazione di Qualità in Radioterapia" of the Istituto Superiore di Sanità, editor. *[Indications for quality assurance in conformal radiotherapy in Italy].* [Italian]. Rapporti ISTISAN 04/34. 2004. p. 54.
6. Ferlay J, Parkin DM, Steliarova-Foucher E. Estimates of cancer incidence and mortality in Europe in 2008. *Eur J Cancer* 2010; **46:** 765-81.
7. Malicki J, Litoborski M, Bogusz-Czerniewicz M, Swiezewski A. Cost-effectiveness of the modifications in the quality assurance system in radiotherapy in the example of in-vivo dosimetry. *Phys Med* 2009; **25:** 201-6.
8. Mainz J. Defining and classifying clinical indicators for quality improvement. *Int J Qual Health Care* 2003; **15:** 523-30.
9. Engstrom PF, Arnoletti JP, Benson AB 3rd, Chen Y-J, Choti MA, Cooper HS, et al. NCCN Clinical Practice Guidelines in Oncology: rectal cancer. *J Natl Compr Canc Netw* 2009; **7:** 838-81.
10. Fortin A, Bairati I, Albert M, Moore L, Allard J, Couture C. Effect of treatment delay on outcome of patients with early-stage head-and-neck carcinoma receiving radical radiotherapy. *Int J Radiat Oncol Biol Phys* 2002; **52:** 929-36.
11. Chen Z, King W, Pearcey R, Kerba M, Mackillop WJ. The relationship between waiting time for radiotherapy and clinical outcomes: a systematic review of the literature. *Radiother Oncol* 2008; **87:** 3-16.
12. Korsgaard M, Pedersen L, Laurberg S. Delay of diagnosis and treatment of colorectal cancer: a population-based Danish study. *Cancer Detect Prev* 2008; **32:** 45-51.
13. Duff SE, Wood C, McCredie V, Levine E, Saunders MP, O'Dwyer ST. Waiting times for treatment of rectal cancer in North West England. *J R Soc Med* 2004; **97:** 117-8.
14. Fesinmeyer MD, Mehta V, Blough D, Tock L, Ramsey SD. Effect of radiotherapy interruptions on survival in medicare enrollees with local and regional head-and-neck cancer. *Int J Radiat Oncol Biol Phys* 2010; **78:** 675-81.
15. Bese NS, Hendry J, Jeremic B. Effects of prolongation of overall treatment time due to unplanned interruptions during radiotherapy of different tumor sites and practical methods for compensation. *Int J Radiat Oncol Biol Phys* 2007; **68:** 654-61.
16. Conde S, Borrego M, Teixeira T, Teixeira R, Sa A, Soares P. Neoadjuvant oral vs. infusional chemoradiotherapy on locally advanced rectal cancer: prognostic factors. *Rep Pract Oncol Radiother* 2013; **18:** 67-75.
17. Tremblay D, Roberge D, Cazale L, Touati N, Maunsell E, Latreille J, et al. Evaluation of the impact of interdisciplinarity in cancer care. *BMC Health Serv Res* 2011; **11:** 144.
18. Jones WE 3rd, Thomas CR Jr, Herman JM, Abdel-Wahab M, Azad N, Blackstock W, et al. ACR appropriateness criteria: resectable rectal cancer. *Radiat Oncol* 2012; **7:** 161.
19. Mihaylova I, Parvanova V, Velikova C, Kurteva G, Ivanova D. Degree of tumor regression after preoperative chemo-radiotherapy in locally advanced rectal cancer-Preliminary results. *Rep Pract Oncol Radiother* 2011, **16:** 233-8.
20. Molinari C, Ballardini M, Teodorani N, Giannini M, Zoli W, et al. Genomic alterations in rectal cancer tumors and response to neoadjuvant chemioradiotherapy; an exploratory study. *Radiat Oncol* 2011; **6:** 161.
21. Bogusz-Osawa M, Osawa T. The influence of the European and Polish acts of law, regulations and standards on the forms and the contents of the informed consent for oncological treatments. *Rep Pract Oncol Radiother* 2005; **10:** 1-10.
22. Byrne DJ, Napier A, Cuschieri A. How informed is signed consent? *Br Med J (Clin Res Ed)* 1988; **296:** 839-40.
23. Malicki J. The importance of accurate treatment planning, delivery, and dose verification. *Rep Pract Oncol Radiother* 2012; **17:** 63-5.
24. Richetti A, Fogliatta A, Clivo A, Nicolin G, Pesce G, et al. Neo-adjuvant chemo-radiation of rectal cancer with volumetric modulated arc therapy: summary of technical and dosimetric features and early clinical experience. *Radiat Oncol* 2010; **5:** 14.
25. Saminathan S, Chandraraj S, Sridhar CH, Manickam R. Comparison of individual and composite field analysis using array detector for Intensity Mosulated Radiotherapy dose verification. *Rep Pract Oncol Radiother* 2012; **17:** 157-62.
26. Edwards CR, Mountford PJ. Characteristics of in vivo radiotherapy dosimetry. *Br J Radiol* 2009; **82:** 881-3.

27. Edwards CR, Hamer E, Mountford PJ, Moloney AJ. An update survey of UK in vivo radiotherapy dosimetry practice. *Br J Radiol* 2007; **80:** 1011-4.

28. Williams MV, McKenzie A. Can we afford not to implement in vivo dosimetry? *Br J Radiol* 2008; **81:** 681-4.

29. The Royal College of Radiologists. *Towards safer radiotherapy.* BFCO(08). London: Royal College of Radiologists; 2008. Available from: https://www.rcr.ac.uk/docs/oncology/pdf/Towards_saferRT_final.pdf.

30. Woolf SH, Grol R, Hutchinson A, Eccles M, Grimshaw J. Potential benefits, limitations, and harms of clinical guidelines. *BMJ* 1999; **318:** 527-30.

31. Guedea F, Malicki J. Quality indicators in radiation oncology: in regard to Albert and Das. *Int J Radiat Oncol Biol Phys* 2013; **87:** 432.

32. Ishikura S. Quality assurance of radiotherapy in cancer treatment: toward improvement of patient safety and quality of care. *Jpn J Clin Oncol* 2008; **38:** 723-9.

33. Savatta SG, Temple L. Quality of life in patients treated for curable rectal cancer. *Semin Colon Rectal Surg* 2005; **16:** 170-80.

34. International Atomic Energy Agency. *International basic safety standards for protection against ionizing radiation and for the safety of radiation sources.* IAEA Safety Series No. 115. Vienna: IAEA; 1996.

35. Di Genesio Paglica M, Turri L, Munoz F, Melano A, Bacigalupo A, Franzone P, et al. Patterns of practice in the radiation therapy management of rectal cáncer: survey of the Interregional Group Piedmont, Valle d'Aosta and Liguria of the "Associazione Italiana di Radioterapia Oncologica (AIRO). *Tumori* 2013; **99:** 61-7.

Radiol Oncol 2014; 48(2): 99-104.
doi:10.2478/raon-2013-0035

Prevalenca in tveganje za rak debelega črevesa in danke ob žariščnem kopičenju pri preiskavah ^{18}F-FDG-PET ali PET/CT: metaanaliza

Treglia G, Taralli S, Salsano M, Muoio B, Sadegi R, Giovanella L

Izhodišča. Namen članka je z metaanalizo objavljenih podatkov ugotoviti prevalenco in nevarnost maligne transformacije žariščnega incidentaloma debelega črevesa in danke, diagnosticiranega z fluor-18-fluorodeoksiglukozo pozitronsko emisijsko tomografijo (^{18}F-FDG-PET) ali pozitronsko emisijsko tomografijo / računačniško tomografijo (PET/CT).

Metode. Izvedli smo natančen pregled objavljene literature o žariščnem incidentalomu debelega črevesa in danke v času do 31. julija 2012, diagnosticiranega z ^{18}F-FDG-PET ali PET/CT. Izračunali smo prevalenco bolnikov in njihovo verjetnost za maligno transformacijo na osnovi kolonoskopije in histopatološke verifikacije tkiva. Poleg tega smo izračunali geografsko porazdelitev primerov. Predstavili smo tudi povprečne vrednosti standardnega prevzema (SUV) izotopa za maligne, premaligne in benigne žariščne incidentalome debelega črevesa in danke.

Rezultati. V metaanalizo smo vključili 32 objavljenih raziskav, ki so vsebovale 89.061 bolnikov obravnavanih z ^{18}F-FDG-PET ali PET/CT. Prevalenca žariščnih incidentalomov, ki so jih odkrili z ^{18}F-FDG-PET ali PET/CT, je bila 3,6% (95% interval zaupanja [CI]: 2,6-4,7%). Z ^{18}F-FDG-PET ali PET/CT so odkrili 1.044 žariščnih incidentalomov debelega črevesa in danke, pri katerih so naredili tudi kolonoskopijo ali histološko verfikacijo tkiva. Skupno tveganje za premaligno ali maligno spremembo je bilo 68% (95% CI: 60-75%). Tveganje za premaligno ali maligno spremembo je bilo večje v Aziji in Ocenaiji kot v Evropi ali Ameriki. Ugotovili smo precejšnje prekrivanje med SUV malignih, premalignih in benignih žariščnih incidentalomov debelega črevesa in danke.

Zaključki. Preiskava z ^{18}F-FDG-PET ali PET/CT lahko odkrije veliko bolnikov z žariščnim incidentalomom debelega črevesa in danke, ki imajo visoko tveganje za premaligne ali maligne spremembe. SUV ni zanesljivo merilo za ločevanje med malignimi, premalignimi in benignimi spremembami. Če z ^{18}F-FDG-PET ali PET/CT odkrijemo žariščni incidentalom debelega črevesa in danke, so potrebne še nadaljnje preiskave, da potrdimo vrsto bolezni.

Radiol Oncol 2014; 48(2): 105-112.
doi:10.2478/raon-2013-0040

Kardiotoksičnost sočasnega zdravljenja z radioterapijo in trastuzumabom pri bolnicah z zgodnjim rakom dojke

Marinko T, Dolenc J, Bilban-Jakopin C

Izhodišča. Zdravljenje s trastuzumabom je zaradi pomembnega vpliva na preživetje del standardnega sistemskega dopolnilnega zdravljenja bolnic, pri katerih smo dokazali rak dojke z receptorjem-2 za humani epidermalni rastni dejavnik (HER2). Bolnice, ki so na dopolnilnem obsevanju dojke ali prsne stene, prejemajo trastuzumab sočasno z obsevanjem. Pri majhnem deležu bolnic trastuzumab povzroča kardiotoksičnost. Predklinični izsledki kažejo na radiosenzibilizirajoči učinek trastuzumaba na celice raka dojke, ni pa še jasno, ali radiosenzibilizira tudi zdrave celice.

Zaključki. Pri obsevanju leve dojke ali leve mamarne regije je potrebna previdnost, saj dolgoročni učinki sočasnega zdravljenja s trastuzumabom in obsevanjem zdaj še niso znani. Ker se preživetje bolnic z rakom dojke izboljšuje, je zgodnje odkrivanje posledic onkološkega zdravljenja na srcu vedno bolj pomembno.

Radiol Oncol 2014; 48(2): 113-119.
doi:10.2478/raon-2013-0060

Scintigrafija pljuč v diagnostičnem procesu pri pljučni emboliji. Sodobne metode in interpretacijski kriteriji v klinični praksi

Skarlovnik A, Hrastnik D, Fettich J, Grmek M

Izhodišča. V klinični praksi uporabljamo scintigrafijao pljuč, predvsem kadar želimo izključiti akutno pljučno embolijo, če na njo posumimo. Uveljavljajo se novejše scintigrafske metode npr. enofotonska emisijska tomografija (SPECT), spreminjajo se tudi kriteriji, ki jih uporabljamo pri odčitavanju planarnih scintigramov.

Bolniki in metode. Retrospektivno smo zbrali podatke bolnikov iz Oddelka za internistično prvo pomoč. Pri 98 bolnikih smo naredili planarno ventilacijsko in perfuzijsko (V/P) scintigrafijo pljuč, 49 bolnikom pa ventilacijski in perfuzijski SPECT. Planarne ventilacijske in perfuzijske scintigrame smo ocenjevali skladno z revidiranimi kriteriji PIOPED II in kriteriji temelječimi na 0,5 segmenta neujemanja. Perfuzijske scintigrame smo ocenjevali skladno s kriteriji PISA-PED. Scintigrame ventilacijskega in perfuzijskega SPECT-a pljuč smo interpretirali po kriterijih, ki so bili predlagani v smernicah EANM. Končno diagnozo pljučne embolije smo postavili glede na klinično odločitev lečečega zdravnika po 12-mesečnem sledenju bolnika.

Rezultati. Planarna ventilacijska in perfuzijska scintigrafija pljuč je bila ob uporabi kriterija 0.5 segmenta neujemanja diagnostična pri 93% bolnikov, ob uporabi PIOPED kriterijev pa pri 84% bolnikov. Če smo upoštevali zgolj rezultate preiskav, ki so bile diagnostične, je bila specifičnost izvidov ob uporabi kriterija 0.5 segmenta neujemanja 98%, ob uporabi PIOPED kriterijev pa 99%. Ventilacijska in perfuzijska SPECT metoda je imela 100% senzitivnost in 98% specifičnost ter nobenega nediagnostičnega izvida. Ventilacijska in perfuzijska scintigrafija pljuč je bila pri bolnikih z nizko predtestno verjetnostjo ob uporabi kriterija 0.5 segmenta neujemanja diagnostična v 92%. Pri uporabi PIOPED kriterijev je bila preiskava diagnostična v 85%, zgolj perfuzijska scintigrafija pljuč ob uporabi PISA-PED kriterijev pa v 80%.

Zaključki. Scintigrafija pljuč je primerna metoda za izključevanje pljučne embolije pri bolnikih napotenih na preiskavo iz ambulante za nujno medicinsko pomoč. Ventilacijski in perfuzijski SPECT je imel odlično senzitivnost in specifičnost, nismo pa ugotovili nediagnostičnih izvidov. Pri planarni scintigrafiji, ko smo uporabili kriterij 0,5 segmenta neujemanja, je bil odstotek nediagnostičnih rezultatov manjši kot, če smo uporabili revidirane kriterije PIOPED. Diagnostična vrednost perfuzijske scintigrafije pljuč, ovrednotene po kriterijih PISA-PED, je manjša glede na diagnostično vrednost ventilacijske in perfuzijske scintigrafije pljuč. Razlika je očitna predvsem pri bolnikih, pri katerih je verjetnost pljučne embolije majhna.

Radiol Oncol 2014; 48(2): 120-126.
doi: doi:10.2478/raon-2014-0012

Odkrivanje nevroendokrinih tumorjev v tankem črevesu z uporabo kontrastnega večfaznega Ga-68 DOTATOC PET/CT. Možna vloga arterijske hiperperfuzije

Schreiter NF, Maurer M, Pape UF, Hamm B, Brenner W, Froeling V

Izhodišča. Interpretacija nevroendokrinih tumorjev tankega črevesa (NET) z Ga-68 DOTATOC PET/CT je lahko težavna. Ocenili smo možno vlogo arterijske hiperperfuzije v odkrivanju NET.

Metode. V letih od 2006 do 2009 smo naredili 320 preiskav z Ga-68 DOTATOC PET/CT za odkrivanje NET. Pri 25 bolnikih smo ugotovili 40 za NET sumljivih lezij. Prepoznali smo dve skupini lezij: epigastrične lezije, evaluabilne v arterijski in venski fazi slikanja s CT-jem (skupina 1) in hipogastrične lezije, evaluabilne samo v venski fazi slikanja s CT-jem (skupina 2). Lezije smo skupaj ocenili dva radiologa in specialist nuklearne medicine. Ugotavljali smo največje vrednosti standardnega privzema (SUVmax) v lezijah in ozadju. Ugotovitve smo primerjali s histološkim izvidom (dosegljiv za 28 lezij) ali pregledi ob sledenju bolnika (srednji čas sledenja 22,9 mesecev).

Rezultati. S PET-om smo zaznali vse sumljive lezije, vendar so bile 3 lažno pozitivne. V skupini 1 je bilo arterijsko slikanje statistično značilno bolj učinkovito kot vensko slikanje ($p = 0,008$). Uspešnost diagnostike je bila večja v skupini 1 kot v skupini 2 ($p < 0,001$). SUVmax pravilno pozitivnih lezij je bil statistično značilno višji kot SUVmax ozadja ($p < 0,001$) in SUVmax lažno pozitivnih lezij ($p = 0,005$).

Zaključki. Arterijska faza večfaznega Ga-68 DOTATOC PET/CT lahko izboljša lokalizacijo črevesnih NET in izboljša diagnostično natančnost. Preiskava omogoča dodatne informacije o perfuziji lezij, ki sicer ni na voljo, kadar je narejena le venska faza slikanja s CT-jem.

Radiol Oncol 2014; 48(2): 127-136.
doi:10.2478/raon-2014-0004

Celostne spremenljivke, pridobljene z difuzijskim tenzorskim slikanjem, lahko razločijo glioblastom od normalnega možganskega tkiva s pomočjo razločitvene analize. Nova diagnostična obravnava celotnih možgan

Roldan-Valadez E, Rios C, Cortez-Conradis D, Favila R, Moreno-Jimenez S

Izhodišča. Histološke značilnosti glioblastoma kažejo na prednost celostne ocene pred področno oceno. Celosten (nanašajoč se na celotne možgane) izračun spremenljivk, pridobljenih z difuzijskim tenzorskim slikanjem (DTI), omogoča oceno integritete struktur bele možganovine in hkrati infiltrirane dele možganov, ki jih konvencionalne preiskovalne metode ne razpoznajo kot take. V raziskavi smo s pomočjo celostnih napetostnih spremenljivk izdelali napovedni model za infiltracijo možganov pri bol nikih z glioblastomom.

Metode. Naredili smo retrospektivno raziskavo primerov s kontrolami. Pri 27 bolnikih z glioblastomom in pri 34 kontrolnih preiskovancih smo izračunali 11 celostnih z DTI pridobljenih napetostnih spremenljivk: povprečno difuzivnost, delno anizotropijo, čisto anizotropijo, čisto anizotropno difuzijo, skupno vrednost difuzijske napetosti, linearno napetost, ravninsko napetost, sferično napetost, relativno anizotropijo, osno difuzivnost in radialno difuzivnost. Naredili smo multivariatno razločitveno analizo teh spremenljivk (vključno s starostjo ptriskovancev) in ocenili diagnostične preiskave.

Rezultati. S sočasno analizo 732 meritev 12 zveznih spremenljivk pri 61 osebah smo naredili razločitveni model, s katerim smo značilno razločili normalne dele možganov od možganovine z glioblastomom: Wilks-ov $\lambda = 0{,}324$; $\chi 2\ (3) = 38{,}907$; $p < 0{,}001$. Celokupna napovedna natančnost je bila 92,7 %.

Zaključki. Predstavljamo nov celosten pristop za oceno infiltracije možganov z uporabo bioloških kazalcev prizadetosti možganov. S končnim napovednim modelom smo izbrali samo tri pomembne vrednosti: osno difuzivnost, sferično napetost in linearno napetost. Te vrednosti lahko uporabimo tudi za diagnosticiranje, sledenje in raziskovanje drugih nevroloških bolezni.

Radiol Oncol 2014; 48(2): 137-141.
doi:10.2478/raon-2013-0013

Magnetnoresonančna spektroskopija (MRS) kot dodatna metoda za ocenjevanje agresivnosti hemangiomu podobnih sprememb v hrbtenici

Jeromel M, Podobnik J

Izhodišča. Večina hemangiomov v vretencih je asimptomatskih in jih odkrijemo slučajno. V redkih primerih kažejo radiografske znake agresivnosti in posnemajo druge agresivne patološke spremembe, kot n. pr. pri solitarnem plazmocitomu.

Prikaz primera. Predstavljava primer bolnice z veliko, agresivnemu hemangiomu podobno patološko spremembo v dvanajstem prsnem vretencu. Za natančnejšo diagnostično opredelitev sva uporabila magnetnoresonančno spektroskopijo (MRS), s katero sva analizirala sestavo (delež maščobe) v patološki spremembi. V patološki spremembi sva ugotovila nizko vsebnost maščobe (33% maščobni delež). Maščobni delež v sosednjem zdravem vretencu je bil za starost pričakovan (68%). Na podlagi MRS podatkov sva patološko spremembo opredelila kot agresivni hemangiom. Pravilnost diagnoze je potrdila patohistološka analiza vzorca, odvzetega med terapevtskim posegom - perkutano vertebroplastiko.

Zaključki. Opisan primer bolnice potrjuje uporabnost MRS kot dodatne diagnostične metode za oceno agresivnosti hemangiomu podobnih patoloških sprememb v hrbtenici.

Radiol Oncol 2014; 48(2): 142-154.
doi:10.2478/raon-2013-0087

Proteomska analiza učinkov obsevanja z žarki x in težkimi ioni na celicah HeLa

Bing Z, Yang G, Zhang Y, Wang F, Ye C, Sun J, Zhou G, Yang L

Izhodišča. Zdravljenje raka z ogljikovimi ioni naj bi bilo bolj uspešno kot z žarki x (fotoni). Biološke prednosti žarkovnega snopa ogljikovih ionov v primerjavi z žarki x smo preučevali na celicah HeLa, ki niso občutljive na sevanje. Spremembe v bioloških procesih smo določali eno uro po obsevanju s klinično ustrezno dozo (2 Gy žarkov X in 2 Gy žarkov ogljikovih ionov). Biološke učinke smo analizirali za proteine, ki so se različno izražali po obsevanjih.

Materiali in metode. Raziskavo smo naredili na celicah HeLa, ki niso občutljive na sevanje. Uporabili smo metodo označevanja aminokislin s stabilnimi izotopi skupaj z masno spektroskopijo 2D-LC-LTQ Orbitrap za identifikacijo in kvantifikacijo različnega izražanja proteinov po obsevanju. Z metodo prenosa po Westernu smo validirali dobljene podatke.

Rezultati. Eno uro po obsevanju z 2 Gy ogljikovih ionov je bilo značilno spremenjenih 123 proteinov, po obsevanju z 2 Gy žarkov X pa 155. Z metodo genskega ontološkega obogatenja (*Gene Ontology [GO] enrichment)* smo ugotovili, da so ti deregulirani proteini vpleteni predvsem v različne metabolne procese, ki pa se razlikujejo med obema vrstama obsevanja.

Zaključki. Neobčutljivost rakavih celic na obsevanje z 2 Gy žarkov x je v veliki meri odvisna od povečanja glikolize, medtem ko je povečano uničevanje celic po obsevanju z 2 Gy ogljikovih ionov posledica nespremenjene glikolize in zmanjšanega metabolizma aminokislin.

Radiol Oncol 2014; 48(2): 155-162.
doi:10.2478/raon-2013-0072

Določanje klonalnosti limfoidnih proliferacij s standardizirano metodo BIOMED-2 na Onkološkem inštitutu Ljubljana

Koković I, Jezeršek Novaković B, Cerkovnik P, Novaković S

Izhodišča. Določanje klonalnosti limfoidnih proliferacij z molekularnimi metodami ima pomembno vlogo v diagnostiki limfoidnih neoplazem, saj omogoča razlikovanje med reaktivnimi in malignimi procesi. Namen raziskave je bil oceniti uporabno vrednost standardizirane metode BIOMED-2 za določanje klonalnosti pri različnih limfoidnih proliferacijah.

Materiali in metode. Retrospektivno smo analizirali 121 vzorcev 91 bolnikov s sumom na limfom, ki smo jih prejeli v preiskavo na Oddelku za molekularno diagnostiko Onkološkega inštituta Ljubljana v letu 2011. Glede na končno diagnozo je bila naša študijska skupina sestavljena iz 32 primerov B-celičnih limfomov, 38 primerov T-celičnih limfomov in 51 primerov reaktivnih lezij. Analizo klonalnosti smo izvedli s standardizirano metodo BIOMED-2.

Rezultati. Občutljivost metode TCR za določanje klonalnosti celic T je bila 91,9 %, občutljivost metode IGH za določanje klonalnosti celic B pa 74,2 %. Specifičnost metode IGH je bila 73,3 % v skupini limfomov in 87,2 % v skupini reaktivnih vzorcev. Specifičnost metode TCR je bila 62,5 % v skupini limfomov ter 54,3% pri reaktivnih vzorcih.

Zaključki. V raziskavi smo potrdili uporabnost standardizirane metode BIOMED-2 za določanje klonalnosti limfoidnih proliferacij v rutinski diagnostiki. Reakcije za detekcijo dokončnih preureditev v genu *IGH* in reakcije za detekcijo preureditev v genih za *TCR* so uporabne za določanje klonalnosti široke palete limfoidnih proliferacij iz različnih bioloških vzorcev. Nasprotno pa reakcije za dokazovanje delnih preureditev v genu *IGH* po naših izkušnjah nimajo dodatne uporabne vrednosti.

Radiol Oncol 2014; 48(2): 163-172.
doi:10.2478/raon-2013-0086

Polimorfizmi v folatni poti in odgovor na zdravljenje s pemetreksedom pri bolnikih z malignim plevralnim mezoteliomom

Goričar K, Kovač V, Dolžan V

Izhodišča. Pri bolnikih z malignim plevralnim mezoteliomom zdravljenje s kombinacijo pemetrekseda in cisplatina izboljša preživetje, vendar pa se med bolniki kažejo razlike v odgovoru na zdravljenje. V naši raziskavi smo želeli opredeliti vpliv polimorfizmov v genih za encime folatne poti in prenašalce folata na izid zdravljenja pri slovenskih bolnikih z malignim plevralnim mezoteliomom.

Bolniki in metode. Pri bolnikih z malignim plevralnim mezoteliomom, vključenih v prospektivno randomizirano klinično raziskavo, smo določili 19 polimorfizmov v 5 genih folatne poti in v 6 genih za prenašalce folata. Vpliv polimorfizmov na učinkovitost in toksičnost zdravljenja smo preverili z logistično regresijo, vpliv na preživetje pa s Coxovo regresijo.

Rezultati. Bolniki z vsaj enim polimorfnim alelom *MTHFD1* rs2236225 so imeli statistično značilno slabši odgovor na zdravljenje (p = 0,005; razmerje obetov [OR] = 0,12; 95 % interval zaupanja [CI] = 0,03−0,54) in krajši čas do napredovanja bolezni (p = 0,032; razmerje tveganj [HR] = 3,10; 95 % CI = 1,10−8,74). Polimorfizmi v genih za prenašalce niso vplivali na preživetje, so pa bili povezani s toksičnostjo. Hepatotoksičnost je bila manj pogosta pri nosilcih polimorfnih alelov *ABCC2* rs2273697 (p = 0,028; OR = 0,23; 95 % CI = 0,06−0,85), *SLCO1B1* rs4149056 (p = 0,028; OR = 0,23; 95 % CI = 0,06−0,85) in rs11045879 (p = 0,014; OR = 0,18; 95 % CI = 0,05−0,71) ter pri bolnikih s haplotipom *SLCO1B1* GCAC (p = 0,048; OR = 0,17; 95 % CI = 0,03−0,98). Gastrointestinalna toksičnost je bila bolj pogosta pri bolnikih z vsaj enim polimorfnim alelom *ABCC2* rs717620 (p = 0,004; OR = 10,7; 95 % CI = 2,2−52,9) in haplotipom *ABCC2* CAG (p = 0,006; OR = 5,67; 95 % CI = 1,64−19,66).

Zaključki. Polimorfizem *MTHFD1* je vplival na odgovor na zdravljenje in preživetje, medtem ko so bili polimorfizmi genov za prenašalce *ABCC2* in *SLCO1B1* povezani s tveganjem za pojav neželenih učinkov. Ti polimorfizmi bi zato lahko služili kot označevalci odgovora na zdravljenje s pemetreksedom pri bolnikih z malignim mezoteliomom.

Radiol Oncol 2014; 48(2): 173-183.
doi:10.2478/raon-2014-0016

Možganski zasevki pri žleznem raku pljuč. Vpliv mutacij EGFR na incidenco in preživetje

Stanič K, Zwitter M, Turnšek Hitij N, Kern I, Sadikov A, Čufer T

Izhodišča. Žlezni rak pljuč pogosto zaseva v možgane. Retrospektivno raziskavo smo zasnovali, da bi pokazali povezavo med mutacijami receptorja za epidermalni rastni faktor (EGFR) in pogostostjo možganskih zasevkov ter preživetjem v vsakodnevni klinični praksi.

Bolniki in metode. Pregledali smo podatke 629 slovenskih bolnikov z žleznim rakom pljuč, ki smo jih od decembra 2009 do januarja 2012 testirali na prisotnost mutacij EGFR. Ugotavljali smo incidenco možganskih zasevkov, čas od diagnoze bolezni do nastanka možganskih zasevkov, čas od diagnoze možganskih zasevkov do smrti in srednje preživetje.

Rezultati. Med 629 bolniki smo odkrili 168 (27 %) bolnikov z možganskimi zasevki, 90 je imelo možganske zasevke že ob diagnozi. Pri 78 bolnikih so možganski zasevki nastali po srednjem času 14,3 mesecev, po 25,8 mesecih pri EGFR pozitivnih in 11,8 mesecih pri EGFR negativnih bolnikih (p = 0,002). Mutacije EGFR so bile prisotne pri 47 (28 %) bolnikih z možganskimi zasevki. Krivulji kumulatvnih incidenc možganskih zasevkov za EGFR pozitivne in negativne bolnike kažeta težnjo večje incidence za EGFR mutirane bolnike ob diagnozi (19 % vs. 13 %, p = 0,078). Kasneje, med potekom bolezni pa te razlike nismo ugotovili. Bolniki z možganskimi zasevki ob diagnozi raka pljuč so imeli značilno daljše preživetje od diagnoze možganskih zasevkov do smrti (7,3 mesece) kot bolniki, pri katerih so se možganski zasevki razvili kasneje (3,1 mesecev). Pri EGFR pozitivnih bolnikih, ki so imeli možganske zasevke že ob diagnozi, je bil čas od možganskih zasevkov do smrti daljši kot pri EGFR negativnih bolnikih (12,6 vs. 6,8 mesecev, p = 0,005), medtem ko ni bilo razlik glede na EGFR status pri tistih bolnikih, kjer so se možganski zasevki pojavili kasneje, med potekom bolezni.

Zaključki. Bolniki z mutacijami EGFR so imeli ob diagnozi neznačilno višjo incidenco možganskih zasevkov kot tisti brez mutacij. Med potekom bolezni so počasneje razvili možganske zasevke in so imeli značilno daljše srednje preživetje. Status EGFR ni imel vpliva na čas od nastanka možganskih zasevkov do smrti pri tistih bolnikih, ki so bili brez možganskih zasevkov ob diagnozi in so jih razvili med potekom bolezni oz. med zdravljenjem.

Radiol Oncol 2014; 48(2):184-188.
doi:10.2478/raon-2013-0083

Dolgotrajna remisija Her2/neu pozitivnega primarnega raka dojke po zdravljenju z dvema monoklonskima protitelesoma - transtuzumabom in bevaciumabom

Königsberg R, Maierhofer J, Steininger T, Kienzer G, Dittrich C

Izhodišča. Istočasno delovanje na več signalnih poti, ki so vključene v razvoj raka, se zdi pomembneje kot delovanje na eno samo tarčno signalno molekulo. Pogosto je povečano izražanje žilnega epidermalnega rastnega dejavnika (VEGF) prisotno pri bolnicah s pozitivnim humanim epidermalnim rastnim dejavnikom (2Her2/neu) raka dojke. Povečano izražanje protoonkogena Her2/neu pa je obenem združeno z povečanim izražanjem VEGF.

Prikaz primera. Predstavljamo primer bolnice s pozitivnim HER2/neu rakom dojke, ki je zaradi možnih stranskih učinkov zavrnila operativno odstranitev dojke in citotoksično kemoterapijo. Zato je bolnica več kot štiri leta prejemala kombinirano dvojno zdravljenje z bevacizumabom in transtuzumabom.

Zaključki. Primer kaže, da (a) bi lahko bilo kombinirano dvojno zdravljenje z bevacizumabom in transtuzumabom klinično učinkovita; (b) je kombinacija bevacizumaba in transtuzumaba varna in netoksična; (c) bi lahko uporabljali bevacizumab in transtuzumab tudi pri dolgotrajni terapiji.

Radiol Oncol 2014; 48(2):189-196.
doi:10.2478/raon-2013-0065

Pooperativna radiokemoterapija s kapecitabinom pri bolnikih z žleznim rakom želodca

Oblak I, Skoblar Vidmar M, Anderluh F, Velenik V, Jeromen A, But Hadžić J

Izhodišča. Pri bolnikih z nemetastatskim rakom želodca je še vedno osnovno zdravljenje operacija. Pooperativna radiokemoterapija s 5-fluorouracilom in levkovorinom statistično značilno izboljša rezultate zdravljenja. Oralni fluoropirimidini, kot npr. kapecitabin, posnemajo neprekinjeno infuzijo s 5-fluorouracilom in so vsaj enako učinkoviti, poleg tega pa je zdravljenje z njimi za bolnike udobnejše.

Bolniki in metode. V obdobju med oktobrom 2006 in decembrom 2009 smo s pooperativno radiokemoterapijo s kapecitabinom zdravili 101 bolnikov z žleznim rakom želodca v stadiju Ib-IIIc. Predhodno so pri 46,3 % bolnikov naredili distalno subtotalno resekcijo želodca, pri 50,5 % totalno resekcijo in pri 3,2 % bolnikov multivisceralno resekcijo. V raziskavi smo ugotavljali lokoregionalno kontrolo bolezni, preživetje brez bolezni, bolezensko specifično preživetje in celokupno preživetje. Prav tako smo ocenjevali stopnjo akutnih stranskih sopojavov zdravljenja.

Rezultati. 77 % bolnikov je zdravljenje zaključilo v skladu s protokolom. Srednji čas sledenja je bil za vse bolnike 3,9 let (razpon 0,4-6,3 let), za še žive v času analize pa 4,7 let (razpon: 3,2-6,3 let). Zaradi pooperativnega zdravljenja ni umrl noben bolnik. Ugotovili smo naslednje deleže akutne toksičnosti stopnje 3 in 4: slabost in bruhanje pri 5 % bolnikov, stomatitis pri 1 %, drisko pri 2 %, sindrom roka-noga pri 8,9 % in okužbo pri 18,8 % bolnikov. V času analize je bilo živih 63,4 % bolnikov in vsi so bili brez znakov ponovitve bolezni. Štiri-letna lokoregionalna kontrola bolezni, preživetje brez bolezni, bolezensko specifično preživetje in celokupno preživetje so bili 95,5 %, 69,2 %, 70,7 % in 66, 2 %. Višji stadij pN in splenektomija sta bila neodvisna napovedna dejavnika za vsa analizirana preživetja, perinevralna invazija in nižja intenziteta zdravljenja pa za preživetje brez bolezni, bolezensko specifično preživetje in celokupno preživetje.

Zaključki. Pooperativna radiokemoterapija s kapecitabinom je primeren način zdravljenja z malo stranskimi učinki, rezultati tovrstnega zdravljenja pa so dobri.

Radiol Oncol 2014; 48(2): 197-202.
doi:10.2478/raon-2013-0077

Rak ledvičnih celic s translokacijo Xp11.2 pri mlajših odraslih bolnikih. Nedavno nov podtip ledvičnega raka

Kmetec A, Jeruc J

Izhodišča. Rak ledvičnih celic s translokacijo Xp11.2 je pogostejši pri otrocih. Pri njih je napoved poteka bolezni sorazmerno dobra. Redek in bolj agresiven pa je ta rak pri mlajših odraslih. Raste bolj počasi, brez značilnih simptomov, njegov biološki potencial je negotov.

Prikaz primera. Predstavljamo prva dva bolnika s takšnim podtipom ledvičnega raka, ki smo ju ugotovili v Sloveniji pri mlajših moških. Imela sta dolg in nenavaden potek bolezni. Tumorja sta bila potrjena histološko in imunohistokemično s pozitivno reakcijo na CD10, P504S in TFE3.

Zaključki. Po navedbah iz literature je potek bolezni odvisen od njenega stadija. Pri napredovali obliki bolezni in pri zajetih bezgavkah je napoved slaba. Pogosto najdemo ciste, hematom in nekrozo okoli ledvice, kar daje neznačilno sliko na slikovnih preiskavah. Zdravljenje je predvsem kirurško.

Radiol Oncol 2014; 48(2): 203-209.
doi:10.2478/raon-2013-0082

Medaplikacijski premik brahiterapevtske doze, ki jo prejmeta mehur in rektum pri bolnicah z inoperabilnim rakom maternične vratu

Marošević G, Ljuca D, Osmić H, Fazlić S, Arsovski O, Mileusnić D

Izhodišča. Namen raziskave je bil s pomočjo računalniške tomografije preučiti medaplikacijski premik brahiterapevtskih doz $D_{0,1cc}$, D_{1cc} in D_{2cc} na sečni mehur in rektum bolnic, ki smo jih zdravili zaradi inoperabilnega raka maternične vratu.

Bolniki in metode. V prospektivno raziskavo smo vključili 30 bolnic z rakom maternične vratu, ki smo jih sočasno zdravili s kemo- in radioterapijo. Intrakavitarno brahiterapijo z visoko hitrostjo doze smo izvajali s Flatcherjevim tandemom in ovoidi. Ob vsaki aplikaciji brahiterapije smo določili položaj $D_{0,1cc}$ mehurja in rektuma. Na osnovi premikov osi X, Y, in Z smo določili srednje vrednosti teh premikov in njihovih vektorjev (R). Uporabili smo test ANOVA in analizo *post hoc* z metodo Tukey za analizo statistično značilnih razlik med skupinami. Razlike med skupinami so veljale za statistično značilne, če je bil $p < 0,05$.

Rezultati. Ugotovili smo statistično značilne razlike pri medaplikacijskih premikih brahiterapevtskih doz $D_{0,1cc}$, D_{1cc} in D_{2cc}, ki sta jih prejela mehur in rektum.

Zaključki. Pri preračunavanju kumulativne brahiterapevtske doze z vsoto $D_{0,1cc}$, D_{1cc} in D_{2cc} rizičnih organov pri vseh aplikacijah je potrebno upoštevati medaplikacijski premik. Tako je malo verjetno, da bi se v najslabšem primeru doze v resnici seštele.

Radiol Oncol 2014; 48(2): 210-218.
doi:10.2478/raon-2014-0008

Preoperativno obsevanje pri raku danke. Primerjalna raziskava doseganja standardov kakovosti v dveh onkoloških bolnišnicah v Španiji in na Poljskem

Fundowicz M, Macia M, Marin S, Bogusz-Czerniewicz M, Konstanty E, Modolel I, Malicki J, Guedea F

Izhodišča. Naredili smo pregled preoperativnega zdravljenja raka danke v dveh evropskih radioterapevtskih centrih, v Španiji in na Poljskem. Namen raziskave je bil neodvisno preveriti doseganje izbranih kazalcev kakovosti zdravljenja in prepoznanje kakršnih koli pomembnih razlik med ustanovama.

Metode. V retrospektivno raziskavo smo vključili 162 bolnikov, 68 bolnikov iz Katalanskega onkološkega inštituta (ICO) in 94 bolnikov iz Velikega poljskega onkološkega centra (GPCC). Vsi bolniki so imeli diagnozo lokalno napredovalega raka danke in smo jih zdravili s preoperativno radioterapijo ali radiokemoterapijo. Ocenjevali smo skupaj 7 kazalcev kontrole kakovosti: smernice za diagnostiko in zdravljenje, čakalno dobo, multidisciplinarno obravnavo bolnikov, ozaveščen pristanek, portalno preverjanje obsevanja, in vivo dozimetrijo, ter spremljanje bolnikov med zdravljenjem.

Rezultati. Ugotovili smo več razlik. Čas od patomorfološke diagnoze do prvega posveta o zdravljenju je bil 31 (ICO) proti 8 (GPCC) dni. Čas od prvega obiska do začetka zdravljenja je bil dvakrat daljši v ICO. V ICO je 82 % bolnikov prekinilo zdravljenje. Protokol za portalno preverjanje obsevanja je bil enak v obeh ustanovah. V ICO za to lokalizacijo raka ne uporabljamo in vivo dozimetrije. V ICO uporabljamo lastne smernice za diagnostiko in zdravljenje, medtem ko jih v GPCC ravnokar oblikujemo.

Zaključki. Neodvisen zunanji pregled je odličen način, s katerim prepoznavamo in odpravljamo pomanjkljivosti v postopkih kontrole kakovosti. Prepoznali smo številne postopke, ki jih lahko izboljšamo. V obeh ustanovah smo po pregledu uvedli spremembe za izboljšanje standardov kakovosti. Prepričani smo, da bi morali vsi radioterapevtski centri izpeljati obsežen pregled za prepoznavo in odpravo pomanjkljivosti.

Fundacija "Docent dr. J. Cholewa"
je neprofitno, neinstitucionalno in nestrankarsko
združenje posameznikov, ustanov in organizacij, ki želijo
materialno spodbujati in poglabljati raziskovalno
dejavnost v onkologiji.

Dunajska 106
1000 Ljubljana

ŽR: 02033-0017879431

Activity of "Dr. J. Cholewa" Foundation for Cancer Research and Education – a report for the first quarter of 2014

The Dr. J. Cholewa Foundation for Cancer Research and Education is a non-profit, non-political and non-government organisation that unites medical professionals, medical institutions and other individuals and organisations in their support of cancer research, education, treatment and prevention. It provides financial support for all qualified individuals and organisations interested in problems associated with cancer, resulting in a number of successful initiatives, publications and projects.

The symposium to honour the 20th anniversary of the Dr. J. Cholewa Foundation for Cancer Research and Education took place on December 13th, 2013, in Ljubljana, Slovenia, and was considered a success by organizers and participants alike. Preliminary discussions are being held to organise a similar Symposium in 2014 and to establish enough support to organise such symposia on a regular basis in the future.

The Foundation continues to provide regular financial support to "Radiology and Oncology", an international scientific journal that is edited, published and also printed in Ljubljana, Slovenia. "Radiology and Oncology" publishes scientific research articles, reviews, case reports, short reports and letters to the editor about research and studies in experimental and clinical oncology, supportive therapy, experimental and clinical research in radiology, radiophyics, prevention and early diagnostics of different types of cancer. It is an open access journal available in pdf format and with an important Science Citation Index Impact factor. All the abstracts in "Radiology and Oncology" are translated in Slovenian and the journal can thus provide sufficient scientific information from various fields of high quality cancer research to interested lay public in Slovenia.

The Dr. J. Cholewa Foundation for Cancer Research and Education is evaluating ways to intensify financial and other means of support to all in Slovenia interested in the fight against cancer. Efforts to help to organise scientific and other meetings of specific interest in different fields of cancer research and education are thus perhaps the first step in expanding Foundation's activities in the future.

Borut Štabuc, MD, PhD
Tomaž Benulič, MD
Viljem Kovač, MD, PhD
Andrej Plesničar, MD, MSc

TANTUM VERDE®

Lajšanje bolečine in oteklin pri vnetju v ustni votlini in žrelu, ki nastanejo zaradi okužb in stanj po operaciji in kot posledica radioterapije (t.i. radiomukozitis).

CSC ANGELINI

Imetnik dovoljenja za promet
CSC Pharma d.o.o.
Jana Husa 1a
1000 Ljubljana

www.tantum-verde.si

Tantum Verde 1,5 mg/ml oralno pršilo, raztopina

Kakovostna in količinska sestava
1 ml raztopine vsebuje 1,5 mg benzidaminijevega klorida, kar ustreza 1,34 mg benzidamina. V enem razpršku je 0,17 ml raztopine. En razpršek vsebuje 0,255 mg benzidaminijevega klorida, kar ustreza 0,2278 mg benzidamina. En razpršek vsebuje 13,6 mg 96 odstotnega etanola, kar ustreza 12,728 mg 100 odstotnega etanola, in 0,17 mg metilparahidroksibenzoata (E218).

Terapevtske indikacije
Samozdravljenje: lajšanje bolečine in oteklin pri vnetju v ustni votlini in žrelu, ki so lahko posledica okužb in stanj po operaciji. Po nasvetu in navodilu zdravnika: lajšanje bolečine in oteklin v ustni votlini in žrelu, ki so posledica radiomukozitisa.

Odmerjanje in način uporabe
Uporaba 2- do 6-krat na dan (vsake 1,5 do 3 ure). Odrasli: 4 do 8 razprškov 2- do 6-krat na dan. Otroci od 6 do 12 let: 4 razprški 2- do 6-krat na dan. Otroci, mlajši od 6 let: 1 razpršek na 4 kg telesne mase; do največ 4 razprške 2 do 6-krat na dan.

Kontraindikacije
Znana preobčutljivost za zdravilno učinkovino ali katerokoli pomožno snov.

Posebna opozorila in previdnostni ukrepi
Pri manjšini bolnikov lahko resne bolezni povzročijo ustne/žrelne ulceracije. Če se simptomi v treh dneh ne izboljšajo, se mora bolnik posvetovati z zdravnikom ali zobozdravnikom, kot je primerno. Zdravilo vsebuje aspartam (E951) (vir fenilalanina), ki je lahko škodljiv za bolnike s fenilketonurijo. Zdravilo vsebuje izomalt (E953) (sinonim: izomaltitol (E953)). Bolniki z redko dedno intoleranco za fruktozo ne smejo jemati tega zdravila. Uporaba benzidamina ni priporočljiva za bolnike s preobčutljivostjo za salicilno kislino ali druga nesteroidna protivnetna zdravila. Pri bolnikih, ki imajo ali so imeli bronhialno astmo, lahko pride do bronhospazma. Pri takih bolnikih je potrebna previdnost.

Medsebojno delovanje z drugimi zdravili in druge oblike interakcij
Pri ljudeh raziskav o interakcijah niso opravljali.

Nosečnost in dojenje
Tantum Verde z okusom mentola 3 mg pastile se med nosečnostjo in dojenjem ne smejo uporabljati.

Vpliv na sposobnost vožnje in upravljanja s stroji
Uporaba benzidamina lokalno v priporočenem odmerku ne vpliva na sposobnost vožnje in upravljanja s stroji.

Neželeni učinki
Bolezni prebavil Redki: pekoč občutek v ustih, suha usta.
Bolezni imunskega sistema Redki: preobčutljivostna reakcija.
Bolezni dihal, prsnega koša in mediastinalnega prostora Zelo redki: laringospazem.
Bolezni kože in podkožja Občasni: fotosenzitivnost. Zelo redki: angioedem.

Rok uporabnosti
4 leta. Zdravila ne smete uporabljati po datumu izteka roka uporabnosti, ki je naveden na ovojnini. Posebna navodila za shranjevanje Za shranjevanje pastil niso potrebna posebna navodila. Plastenko z raztopino shranjujte v zunanji ovojnini za zagotovitev zaščite pred svetlobo. Shranjujte pri temperaturi do 25°C. Shranjujte v originalni ovojnini in nedosegljivo otrokom.

Neulasta®:
Zaščitite bolnike, optimizirajte zdravljenje s citostatiki

NEULASTA® 6 mg raztopina za injiciranje (pegfilgrastim) – SKRAJŠAN POVZETEK GLAVNIH ZNAČILNOSTI ZDRAVILA
Samo za strokovno javnost. Pred predpisovanjem si preberite povzetek glavnih značilnosti zdravila.
SESTAVA ZDRAVILA: Ena napolnjena injekcijska brizga vsebuje 6 mg pegfilgrastima v 0,6 ml (10 mg/ml) raztopine za injiciranje. **TERAPEVTSKE INDIKACIJE:** Skrajšanje trajanja nevtropenije in zmanjšanje incidence febrilne nevtropenije pri odraslih bolnikih, zdravljenih s citotoksično kemoterapijo za maligne bolezni (z izjemo kronične mieloidne levkemije in mielodisplastičnih sindromov). **ODMERJANJE IN NAČIN UPORABE:** Za vsak cikel kemoterapije priporočajo en 6 mg odmerek (eno napolnjeno injekcijsko brizgo) zdravila Neulasta®, ki je dana v obliki subkutane injekcije približno 24 ur po citotoksični kemoterapiji. Varnost in učinkovitost zdravila Neulasta® pri otrocih še nista bili dokazani in priporočil o odmerjanju ni mogoče dati. Pri bolnikih z okvaro ledvic in s končno odpovedjo ledvic odmerka ni treba spreminjati. **KONTRAINDIKACIJE**: Preobčutljivost za zdravilno učinkovino ali katerokoli pomožno snov. **POSEBNA OPOZORILA IN PREVIDNOSTNI UKREPI**: Pri bolnikih z *de novo* akutno mieloično levkemijo omejeni klinični podatki kažejo primerljiv učinek pegfilgrastima in filgrastima na čas do okrevanja po hudi nevtropeniji. Dolgoročni učinki zdravila Neulasta® pri akutni mieloični levkemiji niso ugotovljeni, zato ga je treba pri tej populaciji bolnikov uporabljati previdno. Varnost in učinkovitost zdravila Neulasta® nista raziskani pri bolnikih z mielodisplastičnim sindromom, s kronično mielogeno levkemijo in s sekundarno akutno mieloično levkemijo (AML), zato ga pri takšnih bolnikih ne smete uporabljati. Posebno pozornost je treba nameniti razlikovanju diagnoze blastne transformacije kronične mieloične levkemije od akutne mieloične levkemije. Varnost in učinkovitost uporabe zdravila Neulasta® pri bolnikih z *de novo* AML, mlajših od 55 let in s citogenetiko t(15;17), nista ugotovljeni. Varnosti in učinkovitosti zdravila Neulasta® niso raziskovali pri bolnikih, ki prejemajo kemoterapijo v velikih odmerkih. Tega zdravila ne smete uporabljati za zvečevanje odmerka citotoksične kemoterapije preko uveljavljenih shem odmerjanja. Pojav pljučnih znakov, kot so kašelj, zvišana telesna temperatura in dispneja v povezavi z radiološkimi znaki pljučnih infiltratov, in poslabšanje pljučne funkcije skupaj z zvečanim številom nevtrofilcev utegnejo biti preliminarni znaki sindroma dihalne stiske odraslih (ARDS -'*Adult Respiratory Distress Syndrome*'). V takih primerih je treba zdravilo Neulasta® po presoji zdravnika prenehati dajati in poskrbeti za ustrezno zdravljenje. Bolnike, ki se jim pojavijo simptomi sindroma kapilarne prepustnosti, je treba natančno kontrolirati in deležni morajo biti standardnega simptomatskega zdravljenja, ki lahko vključuje potrebo po intenzivni negi. Skrbno je treba spremljati velikost vranice (s kliničnim pregledom, ultrazvokom). Na diagnozo rupture vranice moramo misliti pri bolnikih, ki poročajo o bolečini v zgornjem levem delu trebuha ali v predelu lopatice. Zdravljenje s samim zdravilom Neulasta® ne prepreči trombocitopenije in anemije, ker se hkrati vzdržuje mielosupresivna kemoterapija s polnimi odmerki po predpisani shemi. Priporočajo redno spremljanje števila trombocitov in hematokrita. Posebna previdnost je potrebna med uporabo posameznih kemoterapevtikov ali njihovih kombinacij, za katere je znano, da povzročajo hudo trombocitopenijo. Pri bolnikih s srpasto anemijo je bila uporaba pegfilgrastima povezana s srpastocelično krizo, zato se mora pri teh bolnikih zdravilo Neulasta® dajati previdno in spremljati ustrezne klinične parametre in laboratorijski status in biti pozoren na morebitno povezavo tega zdravila z zvečanjem vranice in vazookluzivno krizo. Zaradi kliničnih učinkov zdravila Neulasta® in zaradi možnosti levkocitoze je treba med zdravljenjem redno kontrolirati število belih krvničk. Če število levkocitov po pričakovanem najmanjšem številu preseže 50 x 109/l, je treba nemudoma prenehati z zdravljenjem s tem zdravilom. V primeru resne alergijske reakcije je treba poskrbeti za ustrezno zdravljenje in pazljivo spremljanje bolnika še nekaj dni. Pri bolnikih, pri katerih je prišlo do resne alergijske reakcije, je treba z zdravljenjem z zdravilom Neulasta® dokončno prenehati. Varnosti in učinkovitosti zdravila Neulasta® za mobilizacijo matičnih krvotvornih celic pri bolnikih ali zdravih dajalcih niso primerno ovrednotili. Pokrovček igle pri napolnjeni injekcijski brizgi vsebuje suho naravno gumo (derivat lateksa), ki lahko povzroča alergične reakcije. Povečana hemopoetična aktivnost kostnega mozga zaradi zdravljenja z rastnimi dejavniki je bila povezana s prehodnimi pozitivnimi izvidi pri slikanju kosti, kar je treba upoštevati pri interpretaciji izvidov na podlagi slikanja kosti. Zdravilo Neulasta® vsebuje sorbitol. Bolniki z redko prirojeno motnjo intolerance za fruktozo ne smejo dobiti tega zdravila. Zdravilo Neulasta® vsebuje manj kot 1 mmol (23 mg) natrija na 6 mg odmerek, kar v bistvu pomeni ″brez natrija″. Za izboljšanje sledljivosti granulocitne kolonije spodbujajočih faktorjev (G-CSF) je treba v bolnikovi dokumentaciji jasno zabeležiti zaščiteno ime uporabljenega zdravila. **MEDSEBOJNO DELOVANJE ZDRAVIL IN DRUGE OBLIKE INTERAKCIJ**: Zaradi možne občutljivosti hitro se delečih mieloidnih celic za citotoksično kemoterapijo je treba zdravilo Neulasta® dati približno 24 ur po aplikaciji citotoksične kemoterapije. Sočasne uporabe zdravila Neulasta® s katerimkoli kemoterapevtskim zdravilom pri bolnikih niso ovrednotili. **NEŽELENI UČINKI:** Podatki opisujejo neželene učinke, zabeležene v kliničnih preskušanjih in med spontanim poročanjem. Zelo pogosti (≥ 1/10): glavobol, navzea, bolečina v kosteh, mišično-skeletna bolečina (mialgija, artralgija, bolečina v okončini, bolečina v hrbtu, mišično-skeletna bolečina, bolečina v vratu). Pogosti (≥ 1/100 do < 1/10): trombocitopenija, reakcija na mestu injiciranja (vključno z bolečino na mestu injiciranja). Občasni (≥ 1/1.000 do < 1/100): srpastocelična kriza, levkocitoza, preobčutljivostne reakcije, anafilaksija, zvišanje sečne kisline, sindrom dihalne stiske odraslih, pljučne neželene reakcije (intersticijska pljučnica, pljučni edem, pljučni infiltrati in pljučna fibroza), splenomegalija, ruptura vranice, Sweetov sindrom (akutna febrilna dermatoza), kožni vaskulitis, bolečina v prsih, ki ne izvira od srca, zvišanje laktat-dehidrogenaze in alkalne fosfataze, prehodno zvišanje jetrnih funkcijskih testov za ALT ali AST. Redki (≥ 1/10.000 do < 1/1.000): sindrom kapilarne prepustnosti. **FARMACEVTSKI PODATKI:** Shranjujte v hladilniku (2 °C – 8 °C). Ne zamrzujte. Zdravilo Neulasta® sme biti izpostavljeno sobni temperaturi (ne nad 30 °C) za enkratno obdobje, ki ne sme preseči 72 ur. Zdravilo Neulasta® ni kompatibilno z raztopinami natrijevega klorida. **NAČIN IN REŽIM PREDPISOVANJA TER IZDAJE ZDRAVILA**: Predpisovanje in izdaja zdravila je le na recept s posebnim režimom – H/Rp. **IMETNIK DOVOLJENJA ZA PROMET:** Amgen Europe B.V., 4817 ZK Breda, Nizozemska. Dodatna pojasnila lahko dobite v lokalni pisarni: **Amgen zdravila d.o.o., Šmartinska 140, SI-1000 Ljubljana. DATUM ZADNJE REVIZIJE BESEDILA:** 21. november 2013 **DATUM PRIPRAVE INFORMACIJE:** April 2014. Podrobni podatki o tem zdravilu so na voljo na spletni strani Evropske agencije za zdravila http://www.ema.europa.eu/.

Neulasta®
(pegfilgrastim)

Zaščitite bolnike, optimizirajte zdravljenje s citostatiki.

SLO-FF-AMG-001-2014-APR

Skrajšan povzetek glavnih značilnosti zdravila ZELBORAF

Samo za strokovno javnost.

▼ Za to zdravilo se izvaja dodatno spremljanje varnosti. Tako bodo hitreje na voljo nove informacije o njegovi varnosti. Zdravstvene delavce naprošamo, da poročajo o katerem koli domnevnem neželenem učinku zdravila.

Ime zdravila: Zelboraf 240 mg filmsko obložene tablete
Kakovostna in količinska sestava: Ena tableta vsebuje 240 mg vemurafeniba (v obliki precipitata vemurafeniba in hipromeloze acetat sukcinata). **Terapevtske indikacije:** Vemurafenib je indiciran za samostojno zdravljenje odraslih bolnikov z neresektabilnim ali metastatskim melanomom, s pozitivno mutacijo BRAF V600. **Odmerjanje in način uporabe:** Zdravljenje z vemurafenibom mora uvesti in nadzorovati usposobljen zdravnik, ki ima izkušnje z uporabo zdravil za zdravljenje raka. Odmerjanje: Priporočeni odmerek vemurafeniba je 960 mg (4 tablete po 240 mg) dvakrat na dan (to ustreza celotnemu dnevnemu odmerku 1920 mg). Vemurafenib lahko vzamemo s hrano ali brez nje, izogibati pa se moramo stalnemu jemanju obeh dnevnih odmerkov na prazen želodec. Zdravljenje z vemurafenibom moramo nadaljevati do napredovanja bolezni ali pojava nesprejemljive toksičnosti. Če bolnik izpusti odmerek, ga lahko vzame do 4 ure pred naslednjim odmerkom za ohranitev sheme dvakrat na dan. Obeh odmerkov pa ne sme vzeti hkrati. Če bolnik po zaužitju vemurafeniba bruha, ne sme vzeti dodatnega odmerka zdravila, ampak mora z zdravljenjem normalno nadaljevati. Prilagoditve odmerjanja: Za obvladovanje neželenih učinkov ali ob podaljšanju intervala QTc je potrebno zmanjšanje odmerka, začasna prekinitev in/ali dokončno prenehanje zdravljenja (za podrobnosti o prilagoditvi odmerka, prosimo glejte SmPC zdravila). Zmanjšanje odmerka pod 480 mg dvakrat na dan ni priporočljivo. Če se pri bolniku pojavi ploščatocelični karcinom kože, priporočamo nadaljevanje zdravljenja brez zmanjšanja odmerka vemurafeniba. *Posebne populacije*: Za bolnike, starejše od 65 let, prilagajanje odmerka ni potrebno. O bolnikih z okvaro ledvic ali jeter je na voljo malo podatkov. Bolnike s hudo okvaro ledvic ali z zmerno do hudo okvaro jeter je treba pozorno spremljati. Varnost in učinkovitost vemurafeniba pri otrocih in mladostnikih, mlajših od 18 let, še nista bili dokazani. Podatkov ni na voljo. Način uporabe: Tablete vemurafeniba je treba zaužiti cele, z vodo. Ne sme se jih žvečiti ali zdrobiti. **Kontraindikacije:** Preobčutljivost na zdravilno učinkovino ali katerokoli pomožno snov. **Posebna opozorila in previdnostni ukrepi:** Pred uporabo vemurafeniba je treba z validirano preiskavo potrditi, da ima bolnik tumor s pozitivno mutacijo BRAF V600. Dokazi o učinkovitosti in varnosti vemurafeniba pri bolnikih s tumorji z izraženo redko BRAF V600 mutacijo, ki ni V600E ali V600K, niso prepričljivi. Vemurafeniba se ne sme uporabljati pri bolnikih z malignim melanomom, ki ima divji tip BRAF. *Preobčutljivostne reakcije:* V povezavi z vemurafenibom so bile opisane resne preobčutljivostne reakcije, vključno z anafilaksijo. Hude preobčutljivostne reakcije lahko vključujejo Stevens-Johnsonov sindrom, generaliziran izpuščaj, eritem ali hipotenzijo. Pri bolnikih, pri katerih se pojavijo resne preobčutljivostne reakcije, je treba zdravljenje z vemurafenibom dokončno opustiti. *Kožne reakcije:* Pri bolnikih, ki so prejemali vemurafenib, so v ključnem kliničnem preskušanju poročali o hudih kožnih reakcijah, vključno z redkim Stevens-Johnsonovim sindromom in toksično epidermalno nekrolizo. Po prihodu vemurafeniba na trg so v povezavi z njim poročali o reakciji na zdravilo z eozinofilijo in sistemskimi simptomi (DRESS, *Drug Reaction with Eosinophilia and Systemic Symptoms*). Pri bolnikih, pri katerih se pojavi huda kožna reakcija, je treba zdravljenje z vemurafenibom dokončno opustiti. *Podaljšanje intervala QT:* V nekontrolirani, odprti študiji faze II pri predhodno zdravljenih bolnikih z metastatskim melanomom, so opazili podaljšanje intervala QT, odvisnega od izpostavljenosti vemurafenibu. Podaljšanje intervala QT lahko poveča tveganje za ventrikularne aritmije, vključno s t. i. *Torsade de Pointes*. Z vemurafenibom ni priporočljivo zdraviti bolnikov z elektrolitskimi motnjami (vključno z magnezijem), ki jih ni mogoče odpraviti, bolnikov s sindromom dolgega intervala QT in bolnikov, zdravljenih z zdravili, ki podaljšajo interval QT. Pred zdravljenjem z vemurafenibom, en mesec po zdravljenju in po spremembi odmerka je treba pri vseh bolnikih posneti elektrokardiogram (EKG) in kontrolirati elektrolite (vključno z magnezijem). Nadaljnje kontrole so priporočljive predvsem pri bolnikih z zmerno do hudo jetrno okvaro, in sicer mesečno prve 3 mesece zdravljenja, potem pa na 3 mesece oziroma pogosteje, če je to klinično indicirano. Zdravljenja z vemurafenibom ni priporočljivo uvesti pri bolnikih, ki imajo interval QTc > 500 milisekund (ms). *Bolezni oči:* Poročali so o resnih neželenih učinkih na očeh, vključno z uveitisom, iritisom in zaporo mrežnične vene. Bolnikom je treba oči redno kontrolirati glede morebitnih neželenih učinkov na očeh. *Ploščatocelični karcinom kože*: Pri bolnikih, zdravljenih z vemurafenibom, so bili opisani primeri ploščatoceličnega karcinoma kože, vključno s ploščatoceličnim karcinomom, opredeljenim kot keratoakantom ali mešani keratoakantom. Priporočljivo je, da vsi bolniki pred uvedbo zdravljenja opravijo dermatološki pregled in da so med zdravljenjem deležni rednih kontrol. Vsako sumljivo spremembo je treba izrezati, poslati na histopatološko oceno in jo zdraviti v skladu z lokalnimi smernicami. Med zdravljenjem in do šest mesecev po zdravljenju ploščatoceličnega karcinoma mora zdravnik enkrat mesečno pregledati bolnika. Pri bolnikih, ki se jim pojavi ploščatocelični karcinom kože, je priporočljivo nadaljevati zdravljenje brez zmanjšanja odmerka. Nadzor se mora nadaljevati še 6 mesecev po prenehanju zdravljenja z vemurafenibom ali do uvedbe drugega antineoplastičnega zdravljenja. Bolnikom je treba naročiti, naj svojega zdravnika obvestijo o pojavu kakršnih koli sprememb na koži. *Ploščatocelični karcinom, ki se ne nahaja na koži:* Pri bolnikih, ki so prejemali vemurafenib v kliničnih preskušanjih, so poročali o primerih ploščatoceličnega karcinoma, ki se ne nahaja na koži. Bolnikom je treba pred uvedbo zdravljenja in na 3 mesece med zdravljenjem pregledati glavo in vrat (pregled mora obsegati vsaj ogled ustne sluznice in palpacijo bezgavk). Poleg tega morajo bolniki pred zdravljenjem in na 6 mesecev med zdravljenjem opraviti računalniško tomografijo (CT) prsnega koša. Pred in po končanem zdravljenju ali kadar je klinično indicirano, je priporočljivo opraviti pregled zadnjika in ginekološki pregled (pri ženskah). Po prenehanju zdravljenja z vemurafenibom se mora nadzor glede ploščatoceličnega karcinoma, ki se ne nahaja na koži, nadaljevati še 6 mesecev ali do uvedbe drugega antineoplastičnega zdravljenja. Nenormalne spremembe je treba obravnavati v skladu s klinično prakso. *Novi primarni melanom:* V kliničnih preskušanjih so poročali o novih primarnih melanomih. Bolnike s takšnimi primeri so zdravili z ekscizijo, bolniki pa so nadaljevali z zdravljenjem brez prilagoditve odmerka. Nadzor nad pojavom kožnih lezij je treba izvajati, kot je navedeno zgoraj pri ploščatoceličnem karcinomu kože. *Druge malignosti:* Glede na mehanizem delovanja lahko vemurafenib povzroči napredovanje rakov, povezanih z mutacijo RAS. Pred dajanjem vemurafeniba bolnikom, ki so imeli ali imajo raka, povezanega z mutacijo RAS, skrbno razmislite o koristih in tveganjih. *Poškodbe jeter:* Med uporabo vemurafeniba se lahko pojavijo jetrne laboratorijske nepravilnosti (zvišanje GGT, ALT, alkalne fosfataze, bilirubina, AST). Pred uvedbo zdravljenja in mesečno med zdravljenjem oz. kot je klinično indicirano, je treba kontrolirati jetrne encime (transaminaze in alkalno fosfatazo) ter bilirubin. Laboratorijske nepravilnosti je treba obvladati z zmanjšanjem odmerka, prekinitvijo zdravljenja ali prenehanjem zdravljenja (za podrobnosti o prilagoditvi odmerka, prosimo glejte SmPC zdravila). *Jetrna okvara:* Bolnikom z jetrno okvaro začetnih odmerkov ni treba prilagajati. Bolnike, ki imajo zaradi metastaz v jetrih blago jetrno okvaro in nimajo hiperbilirubinemije, se lahko nadzoruje v skladu s splošnimi priporočili. Podatkov o bolnikih z zmerno do hudo jetrno okvaro je le malo; pri takih bolnikih je izpostavljenost lahko večja. Tako je posebej po prvih tednih zdravljenja potreben skrben nadzor, saj lahko po daljšem obdobju (več tednih) pride do kopičenja. *Ledvična okvara:* Bolnikom z blago ali zmerno ledvično okvaro začetnih odmerkov ni treba prilagajati. Pri bolnikih z hudo ledvično okvaro je treba vemurafenib uporabljati previdno ter jih pozorno spremljati. *Fotosenzibilnost:* Pri bolnikih, ki so v kliničnih študijah prejemali vemurafenib, je bila opisana blaga do huda fotosenzibilnost. Vsem bolnikom je treba naročiti, naj se med jemanjem vemurafeniba ne izpostavljajo soncu. V primeru fotosenzibilnosti stopnje 2 (neprenosljivo) ali več so priporočljive prilagoditve odmerka. *Ženske v rodni dobi* morajo med zdravljenjem in vsaj še 6 mesecev po zdravljenju uporabljati učinkovito kontracepcijsko zaščito. Vemurafenib lahko zmanjša učinkovitost hormonskih kontraceptivov. *Sočasno dajanje ipilimumaba* Pri sočasni uporabi ipilimumaba in vemurafeniba so v preskušanju faze I poročali o asimptomatskih zvišanjih transaminaz in bilirubina stopnje 3. Glede na te preliminarne podatke sočasna uporaba ipilimumaba in vemurafeniba ni priporočljiva. **Medsebojno delovanje z drugimi zdravili in druge oblike interakcij:** *Vplivi vemurafeniba na substrate CYP* Vemurafenib lahko poveča izpostavljenost v plazmi tistih snovi, ki se presnavljajo pretežno s CYP1A2; v takem primeru je treba razmisliti o prilagoditvi odmerka. Vemurafenib lahko zmanjša plazemsko izpostavljenost zdravilom, ki se presnavljajo pretežno s CYP3A4. Tako je lahko učinkovitost kontracepcijskih tablet, ki se presnavljajo s CYP3A4 in se uporabljajo sočasno z vemurafenibom, zmanjšana. Pri substratih CYP3A4, ki imajo ozko terapevtsko okno, je treba razmisliti o prilagoditvi odmerka. Zaenkrat še ni znano ali lahko vemurafenib pri 100 µM koncentraciji v plazmi, ki je bila opažena pri bolnikih v stanju dinamičnega ravnovesja (približno 50 µg/ml), zmanjša plazemske koncentracije sočasno dajanih substratov CYP2B6, kot je bupropion. Kadar se vemurafenib pri bolnikih z melanonom uporabi hkrati z varfarinom (CYP2C9), je potrebna previdnost. Tveganja za klinično pomemben učinek na sočasno uporabljene učinkovine, ki so substrati CYP2C8, pa ni mogoče izključiti. Zaradi dolge razpolovne dobe vemurafeniba je mogoče, da popolnega inhibitornega učinka vemurafeniba na sočasno dajano zdravilo ne opazimo, dokler ne mine 8 dni zdravljenja z vemurafenibom. Po končanem zdravljenju z vemurafenibom bo morda potreben 8-dnevni premor, da se izognemo interakcijam z nadaljnjim zdravljenjem. *Vpliv vemurafeniba na transportne sisteme zdravil* Možnosti, da vemurafenib morda poveča izpostavljenost drugih zdravil, ki se prenašajo s P-gp, ni mogoče izključiti. Možen vpliv vemurafeniba na druge prenašalce trenutno ni znan. *Vplivi sočasno uporabljenih zdravil na vemurafenib* Študije *in vitro* kažejo, da sta presnova s CYP3A4 in glukuronidacija odgovorni za presnovo vemurafeniba. Zdi se, da je tudi izločanje z žolčem pomembna pot izločanja. Vemurafenib je treba uporabljati previdno v kombinaciji z močnimi inhibitorji CYP3A4, glukuronidacije in/ali prenašalnih beljakovin (npr. ritonavirjem, sakvinavirjem, telitromicinom, ketokonazolom, itrakonazolom, vorikonazolom, posakonazolom, nefazodonom, atazanavirjem). Sočasna uporaba močnih induktorjev P-gp, glukuronidacije, in/ali CYP3A4 (npr. rifampicina, rifabutina, karbamazepina, fenitoina ali šentjanževke [Hypericum perforatum]) lahko vodi v suboptimalno izpostavljenost vemurafenibu in se ji je treba izogibati. Študije *in vitro* so pokazale, da je vemurafenib substrat sekretornih prenašalcev, P-gp in BCRP. Vplivi induktorjev in inhibitorjev P-gp in BCRP na izpostavljenost vemurafenibu niso znani. Ne moremo pa izključiti možnosti, da imajo lahko zdravila, ki vplivajo na P-gp (npr. verapamil, ciklosporin, ritonavir, kinidin, itrakonazol) ali BCRP (npr. ciklosporin, gefitinib), vpliv na farmakokinetiko vemurafeniba. Za zdaj ni znano, ali je vemurafenib substrat tudi za druge beljakovinske prenašalce.
Neželeni učinki: Med najpogostejšimi neželenimi učinki (> 30 %), o katerih so poročali v zvezi z vemurafenibom, so artralgija, utrujenost, kožni izpuščaj, fotosenzibilnostna reakcija, navzea, alopecija in srbenje. Zelo pogosto je bil opisan ploščatocelični karcinom kože. Sledijo najpogostejši neželeni učinki, ki so se pojavili pri bolnikih, zdravljenih z vemurafenibom v študiji faze II in III in dogodki iz varnostnih poročil vseh preskušanj in obdobja po prihodu zdravila na trg. *Zelo pogosti:* ploščatocelični karcinom kože, seboroična keratoza, kožni papilom, zmanjšanje teka, glavobol, disgevzija, kašelj, driska, bruhanje, slabost, zaprtost, fotosenzibilna reakcija, aktinična keratoza, kožni izpuščaj, makulo-papulozen izpuščaj, papulozen izpuščaj, srbenje, hiperkeratoza, eritem, alopecija, suha koža, sončne opekline, artralgija, mialgija, bolečina v okončini, mišično-skeletne bolečine, bolečine v hrbtu, utrujenost, pireksija, periferni edem, astenija, zvišanje GGT. *Pogosti:* folikulitis, bazalnocelični karcinom, novi primarni melanom, ohromelost sedmega živca, omotica, uveitis, sindrom palmarno-plantarne eritrodisestezije, panikulitis (vključno z nodoznim eritemom), pilarna keratoza, artritis, zvišanje ALT, alkalne fosfataze, bilirubina in izguba telesne mase, podaljšanje QT. *Posebne populacije*: Pri starejših bolnikih (≥ 65 let) je možna večja verjetnost neželenih učinkov, vključno s ploščatoceličnim karcinomom kože, zmanjšanjem teka in motnjami srčnega ritma. Med neželene učinke stopnje 3, ki so bili med kliničnimi preskušanji vemurafeniba pri ženskah opisani pogosteje kot pri moških, spadajo kožni izpuščaj, artralgija in fotosenzibilnost. Poročanje o domnevnih neželenih učinkih: Prosimo, da o neželenih učinkih, ki jih opazite pri zdravljenju z zdravilom Zelboraf, poročate v skladu s Pravilnikom o farmakovigilanci (uradni list RS, št. 53/06 in 16/11), na obrazcu za poročanje, ki je objavljen na spletni strani www.jazmp.si. Prosimo, da izpolnjen obrazec pošljete Univerzitetnemu kliničnemu centru Ljubljana, Interna klinika, Center za zastrupitve, Zaloška cesta 2, SI-1000 Ljubljana, faks: + 386 (0)1 434 76 46, ali na elektronski naslov: farmakovigilanca@kclj.si, lahko pa tudi Javni agenciji RS za zdravila in medicinske pripomočke (JAZMP), Sektor za farmakovigilanco, Ptujska ulica 21, SI- 1000 Ljubljana, faks: + 386 (0)8 2000 510, ali na elektronski naslov: h-farmakovigilanca@jazmp.si.
Režim izdaje zdravila: Rp/Spec
Imetnik dovoljenja za promet: Roche Registration Limited, 6 Falcon Way, Shire Park, Welwyn Garden City, AL7 1TW, Velika Britanija
Verzija: 2.0/14
Informacija pripravljena: april 2014

DODATNE INFORMACIJE SO NA VOLJO PRI:
Roche farmacevtska družba d.o.o., Vodovodna cesta 109, 1000 Ljubljana
Povzetek glavnih značilnosti zdravila je dosegljiv na www.roche.si

PG-19-14-ZEL-TG

Zelboraf®
vemurafenib

Vsak bolnik z metastatskim melanomom je drugačen.

S pravilnim izborom za tarčno zdravljenje z zdravilom ZELBORAF® se bolnikom z neresektabilnim ali metastatskim melanomom s potrjeno mutacijo $BRAF^{V600}$ lahko bistveno izboljša odgovor na zdravljenje in celokupno preživetje v primerjavi z dakarbazinom. Neželeni učinki zdravljenja z zdravilom ZELBORAF® so obvladljivi.[1]

Zelboraf®
vemurafenib

1 Povzetek glavnih značilnosti zdravila Zelboraf® 20.2.2014.

ERBITUX®
CETUXIMAB

See the difference

Individualizirano zdravljenje za bolnike z metastatskim kolorektalnim rakom

Merck Serono Onkologija | *Ključ je v kombinaciji*

Erbitux 5 mg/ml raztopina za infundiranje
Skrajšan povzetek glavnih značilnosti zdravila

Sestava: En ml raztopine za infundiranje vsebuje 5 mg cetuksimaba in pomožne snovi. Cetuksimab je himerno monoklonsko IgG_1 protitelo. **Terapevtske indikacije:** Zdravilo Erbitux je indicirano za zdravljenje bolnikov z metastatskim kolorektalnim rakom z ekspresijo receptorjev EGFR in nemutiranim tipom RAS v kombinaciji s kemoterapijo na osnovi irinotekana, kot primarno zdravljenje v kombinaciji s FOLFOX in kot samostojno zdravilo pri bolnikih, pri katerih zdravljenje z oksaliplatinom in zdravljenje na osnovi irinotekana ni bilo uspešno in pri bolnikih, ki ne prenašajo irinotekana. Zdravilo Erbitux je indicirano za zdravljenje bolnikov z rakom skvamoznih celic glave in vratu v kombinaciji z radioterapijo za lokalno napredovalo bolezen in v kombinaciji s kemoterapijo na osnovi platine za ponavljajočo se in/ali metastatsko bolezen. **Odmerjanje in način uporabe:** Zdravilo Erbitux pri vseh indikacijah infundirajte enkrat na teden. Pred prvo infuzijo mora bolnik prejeti premedikacijo z antihistaminikom in kortikosteroidom najmanj 1 uro pred uporabo cetuksimaba. Začetni odmerek je 400 mg cetuksimaba na m^2 telesne površine. Vsi naslednji tedenski odmerki so vsak po 250 mg/m^2. **Kontraindikacije:** Zdravilo Erbitux je kontraindicirano pri bolnikih z znano hudo preobčutljivostno reakcijo (3. ali 4. stopnje) na cetuksimab. Kombinacija zdravila Erbitux s kemoterapijo, ki vsebuje oksaliplatin, je kontraindicirana pri bolnikih z metastatskim kolorektalnim rakom z mutiranim tipom RAS ali kadar status RAS ni znan. **Posebna opozorila in previdnostni ukrepi:** Pojav hude reakcije, povezane z infundiranjem, zahteva takojšnjo in stalno ukinitev terapije s cetuksimabom. Če pri bolniku nastopi blaga ali zmerna reakcija, povezana z infundiranjem, lahko zmanjšate hitrost infundiranja. Priporočljivo je, da ostane hitrost infundiranja na nižji vrednosti tudi pri vseh naslednjih infuzijah. Če se pri bolniku pojavi kožna reakcija, ki je ne more prenašati, ali huda kožna reakcija (≥ 3. stopnje po kriterijih CTCAE), morate prekiniti terapijo s cetuksimabom. Z zdravljenjem smete nadaljevati le, če se je reakcija izboljšala do 2. stopnje. Če ugotovite intersticijsko bolezen pljuč, morate zdravljenje s cetuksimabom prekiniti, in bolnika ustrezno zdraviti. Zaradi možnosti pojava znižanja nivoja elektrolitov v serumu se pred in periodično med zdravljenjem s cetuksimabom priporoča določanje koncentracije elektrolitov v serumu. Pri bolnikih, ki prejemajo cetuksimab v kombinaciji s kemoterapijo na osnovi platine, obstaja večje tveganje za pojav hude nevtropenije. Takšne bolnike je potrebno skrbno nadzorovati. Pri predpisovanju cetuksimaba je treba upoštevati kardiovaskularno stanje in indeks zmogljivosti bolnika in sočasno dajanje kardiotoksičnih učinkovin kot so fluoropirimidini. Če je diagnoza ulcerativnega keratitisa potrjena, je treba zdravljenje s cetuksimabom prekiniti ali ukiniti. Cetuksimab je treba uporabljati previdno pri bolnikih z anamnezo keratitisa, ulcerativnega keratitisa ali zelo suhih oči. Cetuksimaba ne uporabljajte za zdravljenje bolnikov s kolorektalnim rakom, če imajo tumorje z mutacijo RAS ali pri katerih je tumorski status RAS neznan. **Interakcije:** Pri kombinaciji s fluoropirimidini se je v primerjavi z uporabo fluoropirimidinov, kot monoterapije, povečala pogostnost srčne ishemije, vključno z miokardnim infarktom in kongestivno srčno odpovedjo ter pogostnost sindroma dlani in stopal. V kombinaciji s kemoterapijo na osnovi platine se lahko poveča pogostnost hude levkopenije ali hude nevtropenije. V kombinaciji s kapecitabinom in oksaliplatinom (XELOX) se lahko poveča pogostnost hude driske. **Neželeni učinki:** Zelo pogosti (≥ 1/10): hipomagneziemija, povečanje ravni jetrnih encimov, kožne reakcije, blage ali zmerne reakcije povezane z infundiranjem, mukozitis, v nekaterih primerih resen. Pogosti (≥ 1/100 do < 1/10): dehidracija, hipokalciemija, anoreksija, glavobol, konjunktivitis, driska, navzeja, bruhanje, hude reakcije povezane z infundiranjem, utrujenost. **Posebna navodila za shranjevanje:** Shranjujte v hladilniku (2 °C - 8 °C). **Pakiranje:** 1 viala z 20 ml ali 100 ml raztopine. **Način in režim izdaje:** Izdaja zdravila je le na recept-H. **Imetnik dovoljenja za promet:** Merck KGaA, 64271 Darmstadt, Nemčija.

Datum zadnje revizije besedila: december 2013.

Pred predpisovanjem zdravila natančno preberite celoten Povzetek glavnih značilnosti zdravila.

Samo za strokovno javnost.

Podrobnejše informacije so na voljo pri predstavniku imetnika dovoljenja za promet z zdravilom:
Merck d.o.o., Ameriška ulica 8, 1000 Ljubljana, tel.: 01 560 3810, faks: 01 560 3830, el. pošta: info@merck.si

www.merckserono.net
www.Erbitux-international.com

PM-ONC-01/14/28.01.2014

Merck Serono

Merck Serono is a division of Merck

MERCK

kapsule
SUTENT®
sunitinibijev malat

Vsak dan šteje

za bolnike z napredovalim karcinomom ledvičnih celic

28. september	15. december	**30. april**	2. avgust
Jesenski festival	Zimske počitnice	**Družinsko srečanje**	Začetek kuharskega tečaja

BISTVENI PODATKI IZ POVZETKA GLAVNIH ZNAČILNOSTI ZDRAVILA

SUTENT 12,5 mg, 25 mg, 37,5 mg, 50 mg trde kapsule
Sestava in oblika zdravila: Ena kapsula vsebuje 12,5 mg, 25 mg, 37,5 mg ali 50 mg sunitiniba (v obliki sunitinibijevega malata). **Indikacije:** Zdravljenje neizrezljivega in/ali metastatskega malignega gastrointestinalnega stromalnega tumorja (GIST) pri odraslih, če zdravljenje z imatinibom zaradi odpornosti ali neprenašanja ni bilo uspešno. Zdravljenje napredovalega/metastatskega karcinoma ledvičnih celic (MRCC) pri odraslih. Zdravljenje neizrezljivih ali metastatskih, dobro diferenciranih nevroendokrinih tumorjev trebušne slinavke (pNET), kadar gre za napredovanje bolezni pri odraslih (izkušnje z zdravilom Sutent kot zdravilom prve izbire so omejene). **Odmerjanje in način uporabe:** Terapijo mora uvesti zdravnik, ki ima izkušnje z uporabo zdravil za zdravljenje rakavih bolezni. *GIST in MRCC:* Priporočeni odmerek je 50 mg peroralno enkrat na dan, 4 tedne zapored; temu sledi 2-tedenski premor (Shema 4/2), tako da celotni ciklus traja 6 tednov. *pNET:* Priporočeni odmerek je 37,5 mg peroralno enkrat na dan, brez načrtovanega premora. *Prilagajanje odmerka*: Odmerek je mogoče prilagajati v povečanjih po 12,5 mg, upoštevaje individualno varnost in prenašanje. Pri GIST in MRCC dnevni odmerek ne sme preseči 75 mg in ne sme biti manjši od 25 mg; pri pNET je največji odmerek 50 mg na dan, z možnimi prekinitvami zdravljenja. Pri sočasni uporabi z močnimi zaviralci ali induktorji CYP3A4 je treba odmerek ustrezno prilagoditi. *Pediatrična populacija:* Uporaba sunitiniba ni priporočljiva. *Starejši bolniki (≥ 65 let):* Med starejšimi in mlajšimi bolniki niso opazili pomembnih razlik v varnosti in učinkovitosti. *Okvara jeter:* Pri bolnikih z jetrno okvaro razreda A in B po Child-Pughu prilagoditev odmerka ni potrebna; pri bolnikih z okvaro razreda C sunitinib ni bil preizkušen, zato njegova uporaba ni priporočljiva. *Okvara ledvic:* Prilagajanje začetnega odmerka ni potrebno, nadaljnje prilagajanje odmerka naj temelji na varnosti in prenašanju pri posameznem bolniku. *Način uporabe:* Zdravilo Sutent se uporablja peroralno, bolnik ga lahko vzame s hrano ali brez nje. Če pozabi vzeti odmerek, ne sme dobiti dodatnega, temveč naj vzame običajni predpisani odmerek naslednji dan. **Kontraindikacije:** Preobčutljivost na zdravilno učinkovino ali katerokoli pomožno snov. **Posebna opozorila in previdnostni ukrepi:** *Bolezni kože in tkiv:* obarvanje kože, gangrenozna pioderma (običajno izgine po prekinitvi zdravljenja), hude kožne reakcije (multiformni eritem (EM), Stevens-Johnsonov sindrom (SJS) in toksična epidermalna nekroliza (TEN)). Če so prisotni znaki EM, SJS ali TEN, je treba zdravljenje prekiniti. *Krvavitve* v prebavilih, dihalih, sečilih, možganih; najpogosteje epistaksa; krvavitve tumorja, včasih s smrtnim izidom. Pri bolnikih, ki se sočasno zdravijo z antikoagulanti, se lahko redno spremlja celotna krvna slika (trombociti), koagulacijski faktorji (PT / INR) in opravi telesni pregled. *Bolezni prebavil:* poleg diareje, navzee/bruhanja, bolečine v trebuhu, dispepsije, stomatitisa/bolečine v ustih in ezofagitisa tudi hudi zapleti (včasih s smrtnim izidom), vključno z gastrointestinalno perforacijo. *Hipertenzija:* pri bolnikih s hudo hipertenzijo, ki je ni mogoče urediti z zdravili, je priporočljivo začasno prenehanje zdravljenja. *Hematološke bolezni:* zmanjšanje števila nevtrofilcev, trombocitov, anemija. *Bolezni srca in ožilja:* srčno-žilni dogodki, vključno s srčnim popuščanjem, kardiomiopatijo in motnjami v delovanju miokarda, v nekaterih primerih s smrtnim izidom. Sunitinib povečuje tveganje za pojav kardiomiopatije. *Podaljšanje intervala QT:* previdna uporaba pri bolnikih z znano anamnezo podaljšanja intervala QT, tistih, ki jemljejo antiaritmike, in tistih z relevantno, že obstoječo srčno boleznijo, bradikardijo ali elektrolitskimi motnjami. *Venski in arterijski trombembolični dogodki*; arterijski včasih s smrtnim izidom. *Dogodki na dihalih:* dispneja, plevralni izliv, pljučna embolija ali pljučni edem; redki primeri s smrtnim izidom. *Moteno delovanje ščitnice:* bolnike je treba med zdravljenjem rutinsko spremljati glede delovanja ščitnice vsake 3 mesece. *Pankreatitis*, tudi resni primeri s smrtnim izidom. *Hepatotoksičnost*, nekateri primeri s smrtnim izidom. *H*olecistitis, vključno z akalkuloznim in emfizemskim holecistitisom. *Delovanje ledvic:* primeri zmanjšanega delovanja ledvic, odpovedi ledvic in/ali akutne odpovedi ledvic, v nekaterih primerih s smrtnim izidom. *Fistula:* če nastane fistula, je treba zdravljenje s sunitinibom prekiniti. *Oteženo celjenje ran:* pri bolnikih, pri katerih naj bi bil opravljen večji kirurški poseg, je priporočljiva začasna prekinitev zdravljenja s sunitinibom. *Osteonekroza čeljustnic:* pri sočasnem ali zaporednem dajanju zdravila Sutent in intravenskih bisfosfonatov je potrebna previdnost; invazivni zobozdravstveni posegi predstavljajo dodatni dejavnik tveganja. *Preobčutljivost/angioedem. Motnje okušanja. Konvulzije:* obstajajo poročila, nekatera s smrtnim izidom, o preiskovancih s konvulzijami in radiološkimi znaki sindroma reverzibilne posteriorne levkoencefalopatije. *Sindrom lize tumorja*, v nekaterih primerih s smrtnim izidom. *Okužbe:* hude okužbe z ali brez nevtropenije (okužbe dihal, sečil, kože in sepsa), vključno z nekaterimi s smrtnim izidom; redki primeri nekrotizitajočega fasciitisa, vključno s prizadetostjo presredka, ki so bili včasih smrtni. **Medsebojno delovanje z drugimi zdravili:** (Študije so izvedli le pri odraslih.) Zdravila, ki lahko zvečajo koncentracijo sunitiniba v plazmi (ketokonazol, ritonavir, itrakonazol, eritromicin, klaritromicin ali sok grenivke). Zdravila, ki lahko zmanjšajo koncentracijo sunitiniba v plazmi (deksametazon, fenitoin, karbamazepin, rifampin, fenobarbital, *Hypericum perforatum* oz. šentjanževka). **Plodnost, nosečnost in dojenje:** Zdravila Sutent ne smemo uporabljati med nosečnostjo in tudi ne pri ženskah, ki ne uporabljajo ustrezne kontracepcije, razen če možna korist odtehta možno tveganje za plod. Ženske v rodni dobi naj med zdravljenjem z zdravilom Sutent ne zanosijo. Ženske, ki jemljejo zdravilo Sutent, ne smejo dojiti. Nekliničnі izsledki kažejo, da lahko zdravljenje s sunitinibom poslabša plodnost samcev in samic. **Vpliv na sposobnost vožnje in upravljanja s stroji:** Sutent lahko povzroči omotico. **Neželeni učinki:** Najbolj resni neželeni učinki (nekateri s smrtnim izidom) so: odpoved ledvic, srčno popuščanje, pljučna embolija, gastrointestinalna perforacija in krvavitve (npr. v dihalih, prebavilih, tumorju, sečilih in možganih). Najpogostejši neželeni učinki (ki so se pojavili pri vsaj 20 % bolnikov v registracijskih preskušanjih) so: zmanjšan apetit, motnje okušanja, hipertenzija, utrujenost, prebavne motnje (npr. driska, slabost, stomatitis, dispepsija in bruhanje), sprememba barve kože in sindrom palmarno-plantarne eritrodisestezije. Med najbolj pogostimi neželenimi učinki so hematološke motnje (nevtropenija, trombocitopenija in anemija). Ostali zelo pogosti (≥ 1/10) neželeni učinki so: virusne okužbe, hipotiroidizem, nespečnost, omotica, glavobol, dispneja, epistaksa, ustno-žrelna bolečina, kašelj, bolečina v trebuhu, glosodinija, bolečine v ustih, zaprtje, flatulenca, suha usta, gastroezofagealna refluksna bolezen, motnje pigmentacije, izpuščaj, eritem, alopecija, spremembe barve las, suha koža, bolečine v udih, mialgija, artralgija, mišično-skeletna bolečina, mišični krči, bolečine v hrbtu, bolečina v prsnem košu, vnetje sluznice, edem, pireksija, mrzlica, zmanjšan iztisni delež, zmanjšanje telesne mase. **Način in režim izdaje:** Predpisovanje in zdaja zdravila je le na recept, zdravilo pa se uporablja samo v bolnišnicah. Izjemoma se lahko uporablja pri nadaljevanju zdravljenja na domu ob odpustu iz bolnišnice in nadaljnjem zdravljenju. **Imetnik dovoljenja za promet:** Pfizer Limited, Ramsgate Road, Sandwich, Kent, CT13 9NJ, Velika Britanija. **Datum zadnje revizije besedila:** 23. 1. 2014
Pred predpisovanjem se seznanite s celotnim povzetkom glavnih značilnosti zdravila.

SUT-04-14 Samo za strokovno javnost

Pfizer Luxembourg SARL, GRAND DUCHY OF LUXEMBOURG 51, Avenue J.F. Kennedy, L-1855
PFIZER, Podružnica Ljubljana, Letališka cesta 3c, 1000 Ljubljana, Slovenija

Radiology and Oncology | Ljubljana | Slovenia | www.degruyter.com/view/j/raon

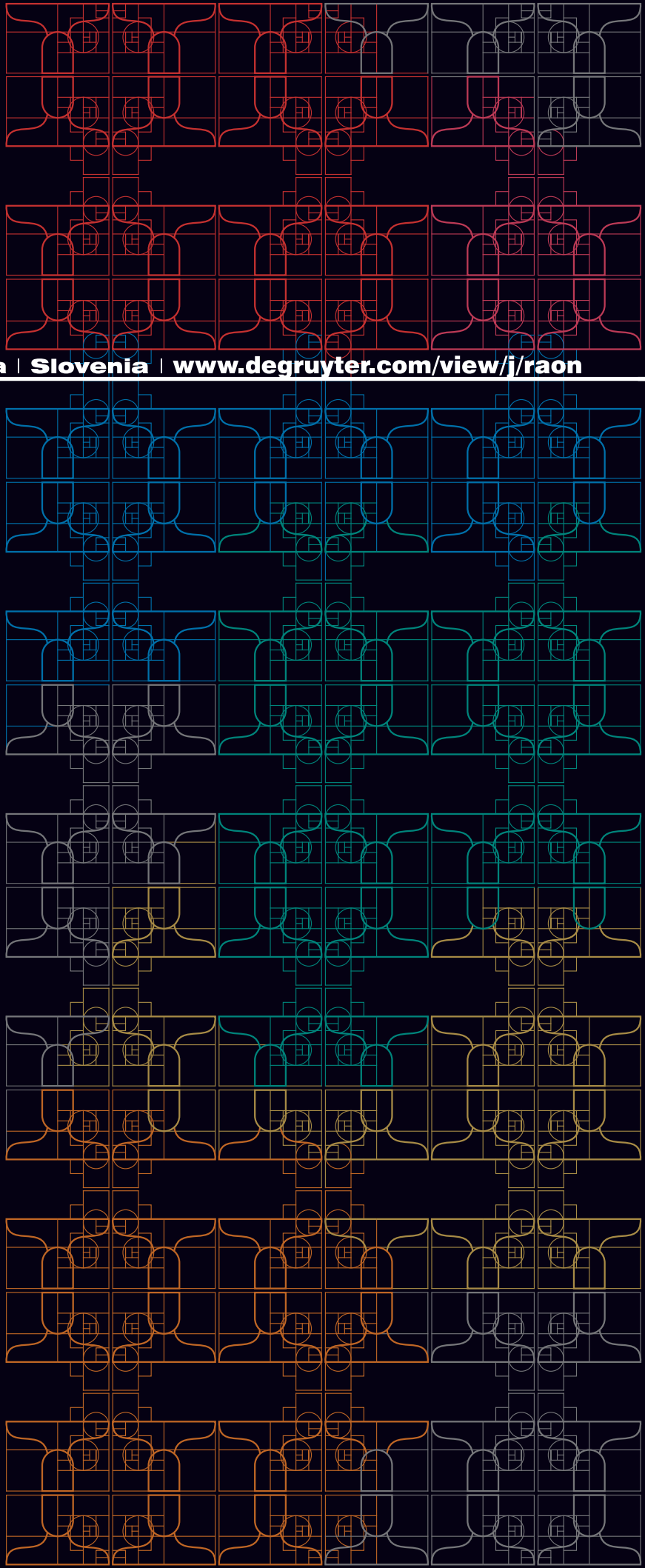

ISSN 1318 - 2099